Open Research Online

The Open University's repository of research publications
and other research outputs

Analysis of the Production and Composition of Outer Membrane Vesicles in the Pathogenic Bacterium *Neisseria menengitidis* for Improved Vaccine Production

Thesis

How to cite:

Bullen, Anwen Alice (2011). Analysis of the Production and Composition of Outer Membrane Vesicles in the Pathogenic Bacterium Neisseria menengitidis for Improved Vaccine Production. PhD thesis The Open University.

For guidance on citations see FAQs.

© 2011 The Author

https://creativecommons.org/licenses/by-nc-nd/4.0/

Version: Version of Record

Link(s) to article on publisher's website:
http://dx.doi.org/doi:10.21954/ou.ro.0000f1f5

Copyright and Moral Rights for the articles on this site are retained by the individual authors and/or other copyright owners. For more information on Open Research Online's data policy on reuse of materials please consult the policies page.

oro.open.ac.uk

UNRESTRICTED

Analysis of the Production and Composition of Outer Membrane Vesicles in the Pathogenic Bacterium *Neisseria meningitidis* for Improved Vaccine Production

Anwen Bullen BSc, MSc

Thesis submitted in fulfilment of the requirements for the degree of:

Doctor of Philosophy in Life and Biomolecular sciences

National Institute for Biological Standards and Control

September 2010

DATE OF SUBMISSION : 24 SEP 2010

DATE OF AWARD : 31 MAY 2011

ProQuest Number: 13837632

All rights reserved

INFORMATION TO ALL USERS
The quality of this reproduction is dependent upon the quality of the copy submitted.

In the unlikely event that the author did not send a complete manuscript
and there are missing pages, these will be noted. Also, if material had to be removed,
a note will indicate the deletion.

ProQuest 13837632

Published by ProQuest LLC (2019). Copyright of the Dissertation is held by the Author.

All rights reserved.
This work is protected against unauthorized copying under Title 17, United States Code
Microform Edition © ProQuest LLC.

ProQuest LLC.
789 East Eisenhower Parkway
P.O. Box 1346
Ann Arbor, MI 48106 – 1346

Abstract

Extraction of outer membrane vesicles (OMVs) from *Neisseria meningitidis* for vaccine production relies exclusively on the use of detergent. Broader protection is induced from naturally formed vesicles but insufficient quantities are generated. Little is known about the mechanisms governing the release, morphology and composition of the OMVs. To identify factors involved in these processes two *N. meningitidis* proteins, GNA33 and RmpM, were examined. In addition the *tol-pal* genes from *Escherichia coli,* a complex which stabilises the outer membrane, were expressed in *N. meningitidis.* Increased vesicle release could be induced by deletion or mutation of RmpM, the structural protein binding the outer membrane to the peptidoglycan. Regulation of size and shape of vesicles was perturbed by the deletion of the GNA33 protein and by the expression of the Tol-Pal proteins. Together these observations indicated a model of vesicle release controlled by selective disconnection of RmpM resulting in separation of the peptidoglycan from the outer membrane. Vesicle size is maintained by the even distribution of proteins that anchored the outer membrane to the peptidoglycan, including GNA33. A strain containing a mutated RmpM protein that lacked only the C-terminal peptidoglycan binding domain demonstrated the greatest increase in vesicle production. In addition, due to the presence of the RmpM N-terminal domain, this mutant maintained interaction with outer membrane proteins and produced vesicles enriched for the immunodominant protein PorA. This combination of PorA enrichment and increased vesicle release makes this strain an excellent candidate for vaccine production.

Acknowledgements

I would like to thank everyone who has helped in the completion of this thesis. My supervisors Dr Rory Care and Professor Ian Feavers for their knowledge, support and boundless patience. Barbara Bolgiano for her help with the production of native vesicles and Kirsty MacLellan and Roland Fleck for their help and expertise in electron microscopy. Hannah Chan, Caroline Vipond, Claire Mattick Raine, Anne-Marie Wilkes, Rachel Bigwood, Hema Patel and Holly Sanders for all their help, advice and support.

Dedication

To my parents, sister and brother for supporting me in every way I could possibly think of. To everyone from Crouch End to Chingford and beyond who has put up with me and helped me through this in ways you probably never even realised. Finally, to Gareth, who has been a constant source of love, support, scripts, software, and when all else failed, chocolate. I love you all.

Contents

Figures and Tables

Abbreviations used in this thesis

APS	Ammonium persulphate
ATP	Adenosine triphosphate
BCA	Bicinchoninic acid
BN	Blue native
Bp	Base Pair
BSA	Bovine serum albumin
CCCP	carbonyl cyanide m-chlorophenylhydrazone
CEMOVIS	Cryo-electron microscopy of vitreous sections
CFU	Colony forming units
CPS	Capsular Polysaccharide
Cryo-TEM	Cryo transmission electron microscopy
CSPD	chloro-5-substituted adamantyl-1,2-dioxetane
DAB	3,3 diaminobenzene
D-ala	D-alanine
dATP	deoxyadenosine triphosphate
dCTP	deoxycytidine triphosphate
dGTP	deoxyguanosine triphosphate
DIG	Digoxygenin
DLS	Dynamic light scattering
DNA	Deoxyribonucleic acid
dNTP	deoxynucleotide triphosphate
DOC	Deoxycholate
dTTP	deoxythymidine triphosphate
dUTP	deoxyuridine triphosphate
dUTP-DIG	deoxyuridine triphosphate linked to digoxygenin
EDTA	ethylenediaminetetraacetic acid
fHbp	Factor H binding protein
FPLC	Fast protein liquid chromatography
GC	guanosine-cytosine
gna33	Genome derived neisserial antigen 33
HMM	High molecular mass
HPA-MLS	Health Protection Agency Manchester Laboratory Services
HRP	Horseradish Peroxidase
IM	Inner membrane
IPTG	Isopropyl β-D-1-thiogalactopyranoside
Kb	Kilobase
LB	Luria Lysogeny broth
LOS	Lipooligosaccharide
LPS	Lipopolysaccharide
m-DAP	meso-diaminopimelate
MIC	Minimum Inhibitory Concentration
MLST	Multi-Locus sequence type
mRNA	messenger ribonucleic acid

Mw	Molecular weight
NadA	Neisserial adhesin A
NAG	N-acetylglucosamine
NAM	N-acetylmuramic acid
NHBA	Neisserial heparin binding antigen
NIBSC	National Institute of Biological Standards and Control
NIPH	Norwegian Institute of public health
OD_{600}	Optical density at 600nm
OM	Outer Membrane
OMP	Outer membrane protein
OmpA	Outer membrane protein A
OMV	Outer membrane vesicles
OU	Oxford University
PBP	Penicillin binding protein
PBS	Phosphate buffered saline
PCR	Polymerase chain reaction
PMF	Proton motive force
PVDF	polyvinylidine fluoride
RI	Refractive index
RmpM	Reduction modified protein M
RNA	Ribonucleic acid
ROI	Region of interest
rRNA	Ribosomal ribonucleic acid
RT	Reverse transcription
RT-PCR	Reverse transcriptase PCR
SD	Standard deviation
SDS	sodium dodecyl sulphate
SDS PAGE	sodium dodecyl sulphate polyacrylamide gel electrophoresis
SEM	Standard error of the mean
SOC	Super optimal broth with catabolite repression
SSC	Saline sodium citrate buffer
ST	Sequence type
TAE	Tris-Acetic acid EDTA buffer
TBS	Tris-buffered saline
TE	Tris-EDTA buffer
TEMED	N,N,N';N'-tetra-methyl-ethylenediamine
TM	Transmembrane
Tris	Tris(hydroxymethyl)aminomethane
UDP	Uridine diphosphate
UMP	Uridine monophosphate
UV	Ultraviolet
VTF	Vitreous thin film
X-gal	bromo-chloro-indolyl-galactopyranoside

Chapter 1- Introduction

It is a truth universally acknowledged that an infectious disease, that is serious and potentially life threatening, must be in want of a vaccine. The production of vaccines against disease caused by the pathogenic bacterium *Neisseria meningitidis* has been successful in eliciting protection against some forms of the disease, but neither individual vaccines against all forms nor a comprehensive vaccine have been achieved. With the failure of traditional methods of vaccine design to produce a global *N. meningitidis* vaccine, novel designs and delivery systems for vaccine antigens must be considered. This in turn requires greater understanding of underlying processes that occur in the cell wall and outer membrane. It is one of these processes, the release of membrane vesicles, which is examined by this thesis.

1.1 Organism

N. meningitidis is a Gram negative diplococcal bacterium not known to have any environmental niche other than humans. The bacterium can cause clusters, endemic cases and epidemics of meningitis and septicaemia (135). *N. meningitidis* was first described in 1887 by Weischelbaum, who found Gram negative diplococcal bacteria in samples from six acute cases of cerebrospinal meningitis (28,33). The role of *N. meningitidis* as the causative agent of acute meningitis was described in a report of the Massachusetts medical board in 1898, commensal carriage of the organism was also described in this document (28). The organism colonises the nasal pharynx and is a commensal bacterium in 8-25% of the population (48). Among carriers, length of infection can vary from extended periods in about 25% of individuals, be intermittent in around 35% and transient in 40% (136).

N. meningitidis has been classified into twelve separate serogroups based on the capsular polysaccharide (CPS). Of these serogroups, six have been identified as the main causative agents of disease; serogroups A, B, C, W-135, X and Y. These serogroups are responsible for 90% of cases of meningococcal meningitis and septicaemia (48). The bacteria can also be classified by using

monoclonal antibodies against the variable antigens of the porin proteins PorA (variable regions 1 and 2) and PorB and the outer membrane protein (OMP) FetA (41,171). Classification was further refined by the use of multi-locus sequence typing (MLST) which used regions of seven housekeeping genes to divide the bacteria into sequence types (ST) (86). Bacteria are now classed by the serogroup, PorA variable regions, FetA variable region (and PorB variable region if required) ST and clonal complex of the organism (66).

1.2 Disease

Disease prevalence of the different serogroups varies across the world; serogroups B and C are responsible for up to 90% of infections in developed countries, whereas in Africa disease is predominantly caused by serogroup A (48,100). In an area of sub-Saharan Africa known as the Meningitis belt meningococcal disease reoccurs as epidemics every 5-10 years (137). Infection is less common in developed countries. However, in the UK acute infection by *N. meningitidis* can result in fatality rates of up to 11% (50). Survivors of meningococcal disease can also suffer amputations and develop conditions such as epilepsy or deafness as a result of damage caused by the infection.

Among asymptomatic carriers of *N. meningitidis* progression to acute infection is rare; this may be due to immunity developed in these individuals. Invasion by the bacteria of the epithelial and endothelial cells and crossing over into the circulation can lead to clinical disease. A component of the Gram negative cell wall, Lipooligosaccharide (LOS) is important for the recognition of *N. meningitidis* by the innate immune system. Toll-like receptors 2 and 4 have been implicated as acting as receptors for LOS (77). The adaptive immune response is also important in the immune response to *N. meningitidis* by activation of the complement system of bactericidal killing. The importance of complement in meningococcal infections is highlighted by individuals deficient in components of the complement pathway, who have an increased risk of meningococcal infection (77). It has been hypothesised that *N. meningitidis* is an 'accidental' pathogen. The bacteria are adapted to live

commensally in humans and symptomatic infection is detrimental to the organism's survival (105). The rapid onset and high fatality rate in untreated meningococcal infections indicate that it is not favourable to the bacteria to cause disease, as it prevents transmission of the organism.

Although it is possible to treat meningococcal infection with antibiotics, the rapid progression of disease means vaccination provides the best approach for controlling meningococcal infection. Vaccines to *N. meningitidis* can be produced using the CPS of the organism. CPS will provoke an immune response, however in order to produce a T-cell dependent response it is necessary to conjugate the CPS to protein carrier molecules such as diphtheria or tetanus toxoid. This approach has been successful in producing vaccines to serogroups A, C, W-135 and Y, but vaccines for serogroup B produced in this way do not elicit an effective immune response. This is thought to be due to the similarity of the serogroup B CPS to a human cell surface molecule, involved in neural cell adhesion. An immune response to the CPS is not induced in order to prevent autoimmunity (96). Alternative approaches have been used for the development of a vaccine to serogroup B meningococcus. Reverse vaccinology was used to identify new components of potential vaccines, and identified 29 proteins that induced bactericidal antibodies. This included the proteins Neisserial adhesin A (NadA), Factor H binding protein (fHbp) (GNA1870) and Neisserial heparin binding antigen (NHBA) (GNA2132), all of which have been considered as potential vaccine antigens (27,29,108,127).

1.3 The cell wall

N. meningitidis strains can be either encapsulated or unencapsulated, but all invasive (disease causing) strains express capsule (135). The *N. meningitidis* cell wall shares the typical structure of Gram negative bacteria; the outer membrane (OM) lies above a layer of peptidoglycan and below this lies the inner (cytoplasmic) membrane (IM). The areas between the OM and peptidoglycan and the IM and peptidoglycan are called the periplasmic space (or periplasm). The capsule resides outside the outer membrane. *N. meningitidis* is capable of exchanging the genes responsible for capsule

production with other meningococci, leading to a process of capsule switching and resulting change in the serogroup of the organism (117). The outer membrane, peptidoglycan and inner membrane form a semi-permeable barrier around the cell, controlling the influx and efflux of molecules as well as the shape and size of the bacteria.

1.3.1 Peptidoglycan

Peptidoglycan is a network of glycan strands, containing chains of N-acetylglucosamine (NAG) and N-acetylmuramic acid (NAM) acid molecules linked by 1,4-β-glycosidic bonds. The chains are cross-linked by short peptides (usually pentapeptides) attached to the NAM residues (160). Modelling has demonstrated that the peptidoglycan forms a honeycomb like structure (94). The structure forms a rigid wall around the cell required to withstand the osmotic pressures of the cell and maintain cell shape. In *E. coli* the peptidoglycan is 2.5-7nm thick and has elastic properties due to movement allowed by the peptide bonds linking the glycan strands (160). The structure of peptidoglycan varies somewhat between Gram negative bacterial species. The peptidoglycan of *N. meningitidis* contains NAG-NAM chains crosslinked predominantly by tetrapeptides (4). Several antibiotics target peptidoglycan synthesis, as inhibition causes eventual lysis of the bacterial cells.

1.3.1.1 Peptidoglycan synthesis

Peptidoglycan synthesis (fig.1) begins in the cytoplasm. A NAM molecule linked to uridine diphosphate (UDP) is linked to amino acids by a series of enzymes called the Mur ligases. This forms short peptide chains (16). These peptides contain both L-amino acids and D-amino acids and include meso-diaminopimelate (m-DAP). Bacteria use racemase enzymes to convert L-amino acids to the D-amino acid form. D-alanine, which is important for the formation of the bond that links glycan strands, is produced using the enzyme D-alanine (D-ala) racemase. Once formed the D-ala residues are linked by the enzyme D-ala D-ala ligase. The racemase and ligase enzymes are both inhibited by the antibiotic D-cycloserine (point 1 fig. 1) (78,165).

Once completed the NAM-peptide molecule must be transported to the penicillin binding protein, which is positioned on the outer face of the inner membrane. The molecules are linked to a carrier lipid undecaprenyl phosphate which cycles between the inner and outer faces of the membrane. The pyrophosphate form (with two phosphates) of the lipid is dephosphorylated and linked to the NAM-peptide molecule in a reaction that requires UDP and releases uridine monophosphate (UMP). The NAG molecule is then added to the lipid-NAM-peptide. The carrier protein is 'flipped' to the outside face of the membrane and the NAG-NAM-peptide molecule is passed to the penicillin binding protein through a mechanism that has yet to be elucidated. The undecaprenyl pyrophosphate is recycled back to the inner face of the membrane (16,78).

The penicillin binding proteins (PBP) are multifunctional enzymes that catalyse the polymerization of the growing glycan chain through a transglycosylase activity, and the crosslinking of adjacent glycan strands through a transpeptidase activity. There are several different forms of PBP protein; the high molecular mass (HMM) proteins are those responsible for the incorporation of new glycan strands into the cell wall (124). *N. meningitidis* contains the PBP proteins PBP1 and PBP2 transcribed from the genes *ponA* and *penA* respectively (4,115). Penicillin resistance in *N. meningitidis* is linked to recombination of the *penA* gene with orthologues from commensal species (18). The transglycosylase function of the penicillin binding protein is blocked by glycopeptides including vancomycin (point 2 fig. 1). Glycopeptides bind to the NAM-NAG-peptide precursor at the D-alanyl-D-alanine portion and the bulky glycopeptide molecules prevent the transglycosylase having access to the precursor. Vancomycin is thought to act at the outer face of the inner membrane, but other glycopeptides cross this membrane and act at the point of transfer of the precursor to the penicillin binding protein (78).

After transglycosylation glycan strands are passed to the transpeptidase site of the penicillin binding protein. Here the strands are crosslinked by forming a peptide bond between the D-ala residue of one glycan chain and the m-DAP residue of an adjacent one. The energy required for this reaction is released by the cleavage of the peptide bond linking the terminal D-ala residue to the peptide (78).

The cross-linking reaction is inhibited by the penicillin family of antibiotics (point 3 fig. 1). The penicillins bind to the transpeptidase site and are cleaved by the enzyme. However the product of this cleavage remains bound to the transpeptidase and the complex has a half life of the order of 10 minutes. This prevents the transpeptidase from catalyzing any further cross-linking reactions (78,172).

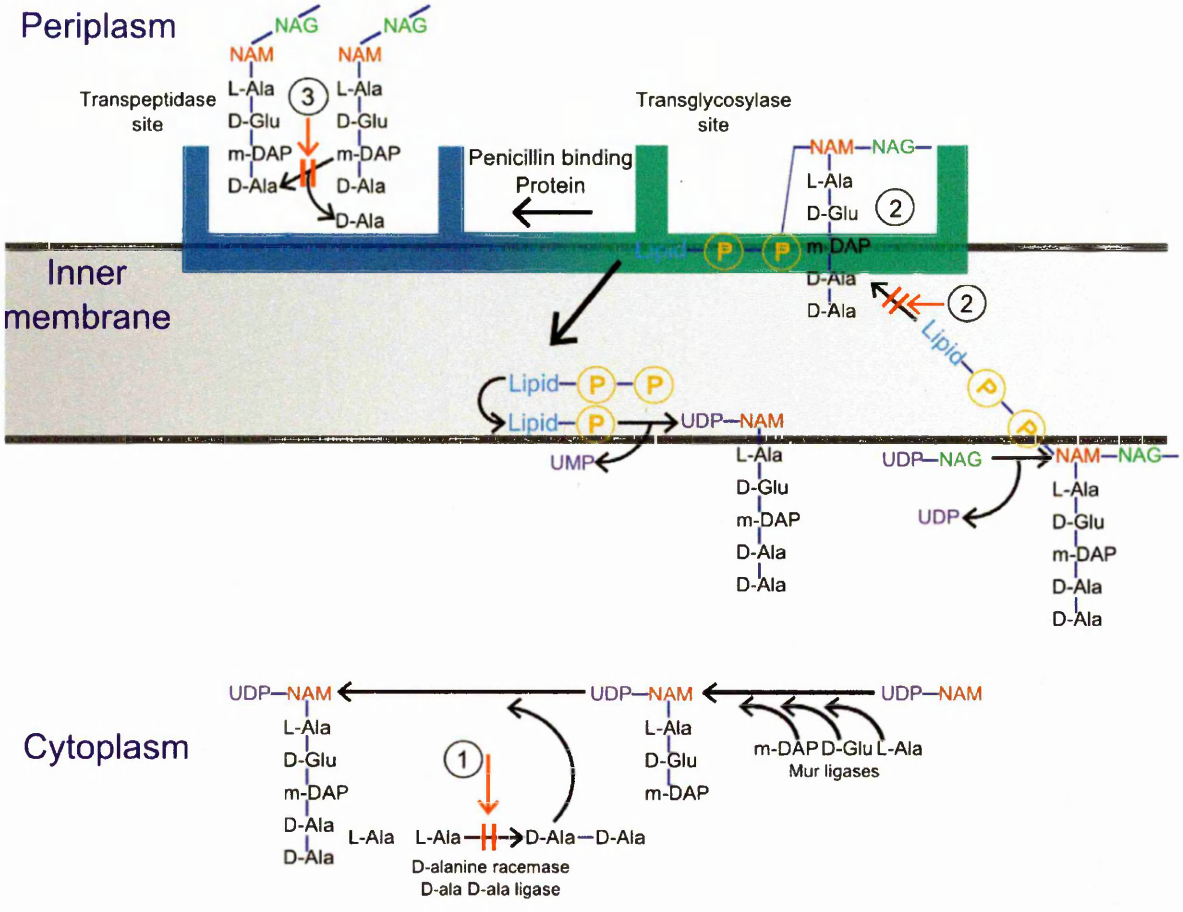

Figure 1. Synthesis of peptidoglycan and action of antibiotics that inhibit peptidoglycan synthesis. The synthesis of peptidoglycan from the cytoplasm to assembly in the periplasm. The inhibitory action of the antibiotics D-cycloserine, glycopeptides and penicillins are indicated at points 1, 2, and 3 respectively.

1.3.1.2 Maintenance and degradation of the peptidoglycan

The peptidoglycan is maintained by the PBP proteins driving peptidoglycan synthesis and murein hydrolases which cleave peptidoglycan for degradation, cell division and remodelling of the cell wall. There are a large number of peptidoglycan cleavage enzymes, which are divided into three main

groups. The *N*-Acetylmuramyl-L-alanine amidases cleave the bond between the NAM molecule and L-alanine. Carboxypeptidases and endopeptidases cleave the peptide bonds in the amino acid linkages; carboxypeptidases remove the C-terminal amino acid whereas endopeptidases cleave within the amino acid chain. The peptidases are further categorised as LD (cleaving between an L amino acid and a D amino acid) or DD (cleaving between two D amino acids). Glycan strand cleaving enzymes are divided into three further groups; lysozymes, lytic transglycosylases and *N*-acetylglucosamidases. *N*-acetylglucosamidases hydrolyse glycosidic bonds in a variety of substrates including peptidoglycan, N-glycans and chitins. The lysozyme and lytic transglycosylase enzymes cleave the same β-1,4-glycosidic bond between NAG and NAM, however lytic transglycosylase enzymes also catalyse a transglycosylase reaction that forms a 1,6-anhydromuramic acid at the NAM residue. This reaction may conserve the energy from the cleavage of the β-1,4-glycosidic bond, making it available for further rearrangement reactions (63,161). Gram negative bacteria usually contain multiple peptidoglycan hydrolases (161). In *N. meningitidis* only the lytic transglycosylase GNA33 has been positively identified (65). The hydrolases of *Neisseria gonorrhoeae* are better studied and in this species a family of lytic transglycosylases similar to those of *E. coli* have been discovered. *N. gonorrhoeae* produces cytotoxic peptidoglycan monomers using some of these enzymes. Although these enzymes (with the exception of GNA33) have not been positively identified, homologues to the genes encoding lytic transglycosylases are present in the *N. meningitidis* genome (26). In addition to the lytic transglycosylases, *N. gonorrhoeae* also contains other peptidoglycan hydrolases including the carboxypeptidase and endopeptidase enzymes PBP3 and PBP4 (134) as well as the amidase enzyme AmiC (44).

Enlargement and remodelling of the peptidoglycan requires the action of several peptidoglycan hydrolases. Work in *E. coli* has shown that lytic transglycosylases facilitate the breaking of bonds to allow the insertion of new peptidoglycan strands, whilst excess pentapeptides are trimmed from new peptidoglycan by DD-carboxypeptidases. Both these processes regulate cell wall growth (161). In cell

division, amidases, lytic transglycosylases and endopeptidases have all been implicated in the separation of the daughter cells in *E. coli* by deletion analysis (161). The amidase AmiC is not required for cell separation in *N. gonorrhoeae* (44). Remodelling of the peptidoglycan is also required to allow large transmembrane complexes such as pili and flagella to pass through the cell wall (161). In *N. gonorrhoeae* the assembly of a type IV secretion system involved in the secretion of deoxyribonucleic acid (DNA) requires the presence of two lytic transglycosylase enzymes, AtlA and LtgX. The genes for both of these proteins are contained in the gene cluster of the type IV secretion system. It is thought that both enzymes produce breaks in the peptidoglycan allowing different proteins of the type IV system to interact with each other (72).

There is strong evidence that the proteins involved in murein synthesis and degradation in *E. coli* may form a multienzyme complex that controls peptidoglycan turnover and the shape of the organism. This complex would contain penicillin binding proteins, endopeptidases and lytic transglycosylases (61,62). Although the control of bacterial shape is different in *E. coli* and *N. meningitidis* (rod shaped bacteria and cocci respectively) the formation of complexes of the GNA33 protein with penicillin binding proteins implies a similar mechanism may be present in *N. meningitidis* (65).

1.3.2 The outer membrane

The outer membrane is considered to be the outermost layer of the cell envelope and as such must provide a selectively permeable barrier between the cell and the external environment. This membrane is a complex structure, composed of integral membrane proteins, lipoproteins, phospholipids and LOS (10). In order to be permeable to certain compounds, the OM contains protein channels to allow the influx and efflux of solutes that would normally be unable to cross the lipid bilayer; these are formed by integral OMPs containing β-barrel structures. The correct folding and insertion of β-barrel OMPs in *N. meningitidis* requires the Omp85 protein complex (162,163). There is no energizing proton gradient across the outer membrane (unlike the inner membrane) and there is

also no access to adenosine triphosphate (ATP) in the periplasm. Therefore transport processes are either passive, or rely on energy transduction from proteins in the inner membrane using the proton motive force that can be generated there (14).

1.3.2.1 Transport through the outer membrane

Passive transport occurs via non-specific protein channels, formed by the porin proteins (102). In *N. meningitidis* the porin proteins PorA and PorB are the most abundant proteins in the Neisserial OM. Although PorA shows a strong antigenic response, the response to PorB is much lower. PorA therefore, has been recognised as an important antigenic target for vaccine development (98). The porin proteins form complexes, with each other and with other OMPs including reduction modified protein M (RmpM). Although complex formation has been observed with several OMPs, recent evidence demonstrates that PorA, PorB and RmpM are the main proteins involved in porin complex formation in the outer membrane (89,119,121). In *N. meningitidis* and other Gram negative species, the TonB system provides active transport across the outer membrane. Transport is energized by a proton motive force generated in the inner membrane by the proteins ExbB and ExbD (57). This energy is transduced across the outer membrane by the TonB protein which binds to transporters in the outer membrane through an N-terminal motif on the transporter proteins called the Ton-box (19). The TonB system has been linked to the transport of iron and other molecules in *N. meningitidis* and proteins shown to bind to TonB include the iron acquisition proteins HmbR and TbpA (107). In *E. coli* and other Gram negative bacteria a second transport system with a high level of similarity in the inner membrane proteins to the TonB system has been identified (57,111). This complex, the Tol-Pal complex, is not present in *N. meningitidis*.

1.3.2.2 Lipooligosaccharide

LOS forms the major part of the outer surface of the outer membrane and *N. meningitidis* expresses 12 immunologically distinct LOS types (69). LOS consists of a lipid molecule, lipid A, linked to an

oligosaccharide core region. In some Gram negative bacteria the core region is linked to polysaccharide, producing lipopolysaccharide (LPS), but this is not the case in *N. meningitidis* (14). LOS is an important virulence factor for *N. meningitidis*. Mutation of genes involved in the assembly of LOS affects the adhesion of bacteria to epithelial cells and their invasion as well as the survival of the bacteria in the blood (110). LOS is an endotoxin and in the host exposure leads to the up-regulation of pro-inflammatory cytokines through pathways including those linked to Toll like receptor 4. The response of Toll like receptor 4 differs between *N. meningitidis* strains, probably due to variation in Lipid A (113). Inflammation caused by LOS is a major factor in the pathogenesis of meningococcal disease. LOS is also bound by the complement factor C4b and O-acetylation in the core oligosaccharide is thought to disrupt this binding in some LOS types (69). LOS is a good antigen and has been considered as a vaccine candidate, using a peptide antigen that mimics a bactericidal LOS antigen (142). However, the inflammatory properties of LOS make it an undesirable component of vaccine preparations; strains that produce no detectable LOS can be produced in *N. meningitidis* by mutation of the *lpxA* gene, part of the pathway of LOS synthesis (133). This is despite *lpxA* being an essential gene in *E. coli* (42). However, the undetectable levels of LOS in these strains were shown to be caused by the insertion of a second truncated copy of the *lpxA* gene. Deletion of the *lpxA* gene in *N. meningitidis* could not be achieved and the gene may also be essential in *N. meningitidis,* despite the ability to produce mutants with no detectable LOS (174). Reduction of the number of acyloxyacyl linked fatty acids linked to the lipid A molecule, through mutation of the genes *lpxL1* or *lpxL2,* also reduces the endotoxin activity of LOS. However, only LOS produced from the *lpxL1* mutated strains maintained adjuvant activity (154). The mutation of *lpx1* singly, and in combination wtih mutations to the genes *synX* and *lgtA* which prevent the expression of carbohydrate structures similar to those found on human cells as part of the LOS, is being tested as a method of detoxifying LOS for vaccine production (150,176).

1.3.2.3 Organisation of proteins in the outer membrane

Organisation of proteins in the outer membrane is a complex process, involving insertion and assembly of the proteins into the outer membrane. A complex of proteins, named the Omp85 complex, has been identified in *E. coli* and *N. meningitidis* involved in the organization of β-barrel proteins in the outer membrane. The first protein identified in this complex was Omp85 (BamA in *E. coli*) (14). BamA associates with the proteins BamB, BamC, BamD and BamE, although only BamD and BamA are essential. Homologues of the genes for BamC, BamD (previously named ComL) and BamE were found in the *N. meningitidis* MC58 genome. The BamD protein is also essential in *N. meningitidis*; BamC and BamE were both non-essential proteins. In *N. meningitidis* RmpM also associates with the Omp85 complex, stabilizing the protein interactions (162). The importance of the Omp85 protein in correct assembly of OMPs was demonstrated by the aggregation of unfolded OMPs in *N. meningitidis* bacteria depleted for Omp85. The same aggregation of proteins did not occur in *E. coli* (15). This is presumably because the unfolded proteins activate the σ^E stress response pathway which prevents further translation of OMPs and upregulates the transcription of chaperones and protease (1,15) . *N. meningitidis* lacks several of the genes active in this pathway (see table 1. pg. 16) (15).

1.3.2.4 Disruption of the outer membrane

Disruption of the outer membrane can be caused by a variety of agents, including cationic detergents, chelating agents such as ethylenediaminetetraacetic acid (EDTA), large and small polycationic peptides and proteins and calcium and magnesium ions. Most of these agents act by interaction with the LPS or LOS. In the case of the chelating agents, chelation of stabilising divalent cations from the LPS leads to its destabilisation and release. By contrast it is hypothesised that calcium and magnesium ions bind to the LPS and alter the fluidity of the LPS layer. LPS is also disrupted by the binding of cationic peptides and detergents (148). The antibiotic polymyxin B is an example of a detergent like

molecule that functions by disruption of both the outer membrane and inner membrane. Polymyxin B binds first to the LPS in the outer membrane and disrupts the structure, leading to permeabilisation of the outer membrane. The antibiotic is then able to penetrate to the inner membrane, where the disruption of the structure leads to the leakage of the cell contents. This is the lethal action of the antibiotic (78,148). *N. meningitidis* is not susceptible to polymyxin B; this is thought to be due to modifications of the lipid A molecule and is also related to the Mtr efflux pump. The presence of the PorB protein also effects the sensitivity of *N. meningitidis* strains to polymyxin B (146).

1.4. Outer membrane vesicles

A unique feature of Gram negative bacteria is the blebbing of the outer membrane into structures called outer membrane vesicles (OMVs). These structures are 10-300nm in diameter and consist of outer membrane: OMPs; LOS and phospholipids as well as containing constituents of the periplasm (10,35). Although OMVs have been observed from many bacterial species, including *E. coli*, generally only very low amounts are released. In contrast, certain Gram negative bacterial species including *N. meningitidis,* and bacteria in the genera of *Porphyromonas* and *Treponema* produce larger amounts of OMVs during normal growth (58).

In a typical *E. coli* or *Pseudomonas aeruginosa* culture, OMVs constitute about 1% of the total OM material present. In contrast, about 8-12% of the protein and endotoxin content of a typical *N. meningitidis* culture is comprised of OMVs (35). This far greater abundance of OMVs produced by *N. meningitidis* could indicate that different mechanisms are responsible for the release and composition of vesicles in different species. Transmission electron microscopy images of native OMVs (produced without the use of detergent to extract vesicles from the organism) from *N. meningitidis* and other Gram negative species are similar in shape and appearance, although some variation in size and differences in electron density within the vesicles can be observed (6,37,68,92,101). However, without a comprehensive study to compare OMVs from different species using a single methodology

for preparation and examination of the samples, it is difficult to say how much of this difference may be due to differences in preparation methods. The proteomic profiles of natively derived vesicles from high vesicle producing mutants of *N. meningitidis* and *E. coli* have been examined in two studies by Scorza et al. and Ferrari et al. (6,37). Comparison of the two profiles showed that both *E. coli* and *N. meningitidis* vesicles were constituted mainly and possibly exclusively by outer membrane and periplasmic proteins. The similar OMV proteomic profiles of the two species indicated that a common mechanism may be responsible for the release of vesicles in both species (6).

1.4.1 Functions of outer membrane vesicles

The function of OMVs continues to be debated and several different hypotheses have been proposed. Outer membrane vesicles are involved in the transfer of DNA and in its uptake (90), the transfer of proteins and in the delivery of antimicrobial agents. In *P. aeruginosa,* under conditions of restricted nutrition, OMVs can deliver an autolysin (a peptidoglycan hydrolase) to other bacteria of the same species or those with similar peptidoglycan chemotypes and cause lysis (90). Outer membrane vesicles can also modulate virulence in several species, including *Neisseria*. Vesicles may provide a mechanism for the release of virulence factors by several bacteria, which protects such factors from dilution by diffusion and inactivation by host factors (10). In addition *P. aeruginosa* uses OMVs to deliver virulence factors directly to the cytoplasm of host cells. These factors include phospholipase C, proteases and haemolysins and aid invasion of the bacteria (13). In *N. meningitidis* the ADP-ribosyl transferase enzyme NarE (a potential toxin), is present in a subgroup of hypervirulent group B strains. The mechanism for delivery of the toxin to eukaryotic cells has been putatively linked to OMVs (35,91). It is also thought that the OMVs may increase the inflammatory response in meningococcal sepsis, probably due to endotoxin (a virulence factor) contained within the OMV (95). Neisserial OMVs may also modulate the immune response by binding bactericidal factors in serum, preventing them binding to the organism (74). Also meningococcal OMVs may have an immunosuppressive function, inhibiting the proliferation of $CD4^+$ T-cells due to binding of neisserial Opa proteins to the

human coinhibitory receptor carcinoembryonic antigen-related cellular adhesion molecule 1 (79). OMVs are also used as a method of both intra-and inter-species communication and communication between prokaryotes and eukaryotes, such as in the symbiotic relationship between *Rhizobium* species and leguminous plants (90). OMV production in *E. coli* is affected by the disruption of genes in the envelope stress response pathways σ^E and Cpx. Impairing either of these pathways leads to an increase in vesicle production; however vesiculation is not directly controlled by either pathway. There is a relationship between the production of vesicles and the amount of misfolded protein present in the periplasm and it has been hypothesised that vesiculation may be a method of removing this material directly (93). Vesicle release can be activated by agents that produce envelope stress, such as ethanol, and low vesiculation mutants show decreased survival when exposed to these agents. However, the mechanism for activating this response is not clear (93).

1.4.2 Release of outer membrane vesicles

Several mechanisms have been hypothesised for the release of outer membrane vesicles in Gram negative bacteria. In *E. coli* the formation of OMVs is predominantly the result of the mutation of genes involved in the structure of the OM and peptidoglycan or links between them. This indicates that the release of OMVs may be a function of disruption of the connections between the outer membrane and the peptidoglycan. However, OMV release is independent of overall membrane instability (92). Models of vesicle release in Gram negative organisms have indicated that the release of outer membrane vesicles is due to turgor pressure in the periplasmic space leading to bulging and eventual blebbing of the outer membrane. Turgor pressure may be due to muramyl peptides produced from peptidoglycan turnover (175) or from membrane stress caused by misfolded protein present in the outer membrane (93). An alternative explanation for the blebbing of the outer membrane is that the membrane is disconnected from the peptidoglycan due to changes in the density of proteins linking the outer membrane to the peptidoglycan and inner membrane (31).

Several genes affect the release of membrane vesicles in *E. coli* and other Gram negative bacteria, these genes and their potential homologues in the *N. meningitidis* genome are shown in table 1.

Table 1. Genes shown to affect vesicle release in *E.coli* and homologous genes in the *N.meningitidis* MC58 genome. Genes previously shown to affect vesicle release were aligned against the published sequence for the *N.meningitidis* group B strain MC58 using the nucleotide BLAST algorithm blastn. Percentage of sequence identity is shown. Genes involved in stress response pathways are highlighted in blue.

Gene	Function	Effect of deletion on vesiculation	Homology in *N.meningitidis* MC58 genome	Refs.
tol-pal complex	Membrane structure and division machinery	Increase	No	(7,45)
degS	σ^E envelope stress pathway serine protease for RseA	Increase	No	(92)
degP	σ^E envelope stress pathway serine protease	Increase	Homologous protease *htrA*	(92)
rpoE	σ^E envelope stress pathway effector (σ^E)	Lethal	No	(20)
rseA	σ^E envelope stress pathway inhibitor	Increase	No	(92)
cpxR	Cpx envelope stress pathway response regulator	Increase	50% similarity to DNA binding response regulator *NMB0595*	(93)
ydcQ	Putative DNA binding protein. Mutation is a suppressor mutation for *RpoE*	Decrease	No	(20)
ponB	peptidoglycan synthesis	Increase	36% similarity to *ponA*	(92)
tatC	IM secretion apparatus	Increase	50% similarity to *NMB0599*	(92)
Pnp	Polynucleotide phosphorylase	Increase	60% similarity to *pnp*	(92)
glnA	Glutamine synthetase	Decrease	63% similarity to *glnA*	(92)
lysS/herC	Lysyl tRNA synthetase	Decrease	56% similarity to *LysRS*	(92)
pepP	Proline aminopeptidase	Decrease	No	(92)
nlpI	OM lipoprotein	Increase	32% similarity to *NMB1309*	(92)
yieM	Unknown	Increase	No	(92)
ypjA	Unknown	Decrease	No	(92)
nlpA	IM Lipoprotein	Decrease	33% similarity to *GNA1946*	(92)
wzxE	IM translocase	Increase	No	(92)
ompC	OM porin	Increase	30% similarity to *PorB*	(92)
waaG	LPS core biosynthesis glucosyl transferase	Increase/Decrease (depends on location of mutation)	No	(92)

The genes which affect the release of membrane vesicles in Gram negative bacteria are involved in a variety of pathways. Several are involved in envelope stress responses; others are involved in peptidoglycan synthesis and turnover, synthesis of LPS and outer membrane stability. In addition genes encoding lipoproteins have also been implicated in changes to vesicle release. The diverse nature of the gene products involved does not support any one theory of the causes of vesicle release.

1.4.3 Outer membrane vesicle vaccines

Due to the inherent problems of producing a capsular vaccine for serogroup B *N. meningitidis,* other approaches have been sought. One of the most promising of these approaches is using OMVs to produce vaccine based on the antigens displayed on the bacterial outer membrane. Outer membrane vaccines for serogroup B *N. meningitidis* are effective as a method of immunisation against meningitis epidemics. Serogroup B OMV vaccines have been used for control of epidemic strains in New Zealand, Cuba and Norway and the vaccines have been shown to be both safe and immunogenic against these strains (11,17,59,167). The New Zealand vaccine is 80% effective in reducing the risk of infection among children under five years (43)(97). Outer membrane vesicle vaccines are most effective when dealing with clonal outbreaks of disease. In a situation where disease is caused by several different meningococcal strains or where the vaccine strain is not homologous to the epidemic strain, the levels of protection are reduced. This is due to antigenic variation, leading to poor cross reactivity of the antibodies produced. In addition, variation in expression of antigenic proteins, particularly PorA, also affects cross reactivity. Vaccines of this type, therefore, are often referred to as 'tailor made' OMV vaccines. (59,141). Proteomic analysis of the New Zealand vaccine identified forty proteins, including seven proteins thought to be key proteins in the antigenic response: Omp85, FetA, PorA, PorB, RmpM, OpcA and NspA (159). The specificity of OMV vaccines has been attributed to PorA which is the immunodominant antigen both in vitro and in animal models (123) and is the major target for the bactericidal immune response elicited by the New Zealand OMV vaccine (87). The

degree of cross reactive immunity induced by OMV vaccines is predominantly due to the variation of PorA antigens (141). PorA is known to have hyper-variable regions present in the surface exposed parts of the protein. The two variable surface exposed loops, designated VR1 and VR2, can elicit bactericidal antibodies. Evolutionary pressure to escape the immune response has resulted in distinct families of VR1 and VR2 sequences, which need to be represented in any broad spectrum vaccine based on PorA (118). As PorA is the immunodominant target for bactericidal antibodies, attempts have been made to engineer a broader-spectrum OMV vaccine by the inclusion of several different PorA subtypes in a single OMV formulation (153). Vaccines of this kind produce broader protection (106); however the level of bactericidal response varies between different subtypes of the PorA antigen. This difference is probably the result of differing immunogenicity among PorA subtypes. Evidence suggests that the immunogenicity of these PorAs can be improved by using a heterologous prime boost strategy for immunisation (83). Also, although these vaccines induce broader protection, the protection is still limited primarily to the PorA subtypes contained within the vaccine (155).

More recent strategies for design of an OMV vaccine for group B *N. meningitidis* have included three approaches: the combination of multiple PorA subtypes into vesicles, the use of OMVs from the commensal species *Neisseria lactamica,* or the combination of OMVs with purified proteins in a vaccine formulation. The combination of multiple PorA subtypes has been produced in the vaccines HexaMen and NonaMen (six and nine PorA variants, respectively). NonaMen has been predicted to cover 75% of the strains circulating globally. However up to four doses of the vaccine may be required in the primary immunisation to cover some of the least immunogenic PorA subtypes (60). In addition the ability of *N. meningitidis* to rapidly change the subtype or expression levels of PorA is likely to lead to the need to periodically reformulate the vaccine (51). The vesicles of the commensal species *N. lactamica* provided a potentially attractive alternative to *N. meningitidis* vesicles, as *N. lactamica* has been implicated in the development of immunity to *N. meningitidis* in young children. Immunisation with *N. lactamica* vesicles also protected mice against lethal challenge with several *N. meningitidis*

strains (52). A phase I clinical trial of an *N. lactamica* OMV vaccine showed that the vaccine was immunogenic and produced similar antibody levels and bactericidal activity as the Norwegian *N. meningitidis* OMV vaccine against heterologous strains. Results indicated that *N. lactamica* vesicles could be used as an adjuvant or in a combination vaccine with purified proteins, although it was unlikely a successful vaccine candidate could be produced using them alone (51).

Combination vaccines, using both OMV and recombinant purified proteins have also shown success in clinical trials. The Novartis vaccine rMenB has been produced in two formulations, one without OMV (rMenB) and one containing OMVs from the NZ98/254 strain (rMenB-OMV). Both vaccines contain recombinant proteins: fHbp sub-variant 1.1 fused to the lipoprotein GNA2091, NHBA sub-variant 2 fused to GNA1030 and NadA variant 3. The functions of the GNA2091 and GNA1030 proteins are not known, but the fusion proteins increase the stability and immunogenicity of the fHbp and NHBA proteins (38). The OMVs from the NZ98/254 strain included in rMenB-OMV contain PorA subtype P1.7-2,4 (82). Clinical trials have shown that the OMV component increases the immunogenicity of the vaccine; this is thought to be due to an adjuvant effect of the LPS contained in the OMVs or the effects of the presence of other protein antigens in the OMV. In addition the presence of PorA produces a strong immune response to homologous strains (38,130). The rMenB-OMV vaccine shows better potential to produce cross-protection than monovalent OMV vaccines and can also induce immunological memory (38). Although this vaccine needs to be tested against a wider strain panel to fully establish the levels of cross-protection to strains heterologous for the vaccine antigens produced, the combination of purified protein and OMV offers the best option currently for a cross-protective *N. meningitidis* group B vaccine.

1.4.4 Production of outer membrane vesicles

The specificity of the immune response to an OMV vaccine is not solely dependent on the protein composition in the OMV, and can also be affected by the methods used to produce the vaccine. Although *N. meningitidis* produces a greater number of vesicles than most other Gram negative species, producing sufficient OMVs for vaccine production is usually accomplished by detergent extraction using deoxycholate. Deoxycholate extraction also removes much of the endotoxic LOS component of OMVs. The lack of cross reactivity in OMV vaccines may be due in part to this process, as OMVs could become contaminated by proteins from other sub-cellular fractions not found in naturally released 'native' vesicles. Proteomic analysis of detergent extracted compared to natively produced OMVs showed that detergent extracted OMVs contain a number of proteins which localise to the inner membrane and cytoplasm. In contrast native OMVs were composed almost exclusively of OMPs and contained more OMPs. Immunisation with native OMVs also produced a broader range of bactericidal antibodies than immunisation by detergent extracted OMVs from the same strain (37,150). The use of detergent also removes some lipoproteins, including the important protein antigens fHbp and NHBA, and can promote vesicle aggregation (150). To improve the quality of OMV vaccines it is desirable eliminate detergent extraction, in order to minimise the contamination with cytoplasmic proteins, prevent the loss of lipoproteins and improve the consistency of OMV composition between batches of vaccine.

OMV release is likely to be controlled by proteins and structures related to the structure of the cell wall and outer membrane. Three proteins that are involved in vesicle release in *E. coli* and *N. meningitidis* are examined in more detail, the *N. meningitidis* lytic transglycosylase GNA33, the OMP RmpM and the *E. coli* protein complex Tol-Pal.

1.5. GNA33

In the search for suitable vaccine antigens that could be exploited in a vesicle vaccine several candidate proteins were identified (109). Genome derived Neisserial antigen 33 (*gna33*) was derived from the *Neisserial* genome and found to be a potential mimetic antigen, which could elicit an antibody response by mimicking loop 4 of the PorA protein in serotype P1.2 strains. (53). The GNA33 protein shares 41.3% amino acid sequence homology with the lytic transglycosylase MltA in *E. coli*. Despite significant sequence homology with the *E. coli* MltA protein, GNA33 only shares 21.5% structure identity by x-ray crystallography. However the protein also shares significant sequence homology with the LtgC protein of *N. gonorrhoeae* (95% amino acid identity). GNA33 is a lipoprotein of 44.5kDa which attaches to the outer membrane and peptidoglycan and produces degradation products from the murein cleavage reaction which indicate that it is acting as a lytic transglycosylase (65). The structure of the *N. gonorrhoeae* LtgC protein has been mapped by X-ray crystallography and has been shown, like MltA, to contain several domains. The N-terminal domain (domain 1) comprises a β-barrel and domain 2 forms part of the active site of the enzyme, producing a groove between domain 1 and domain 2. Both these domains are equivalent between ltgC (and potentially GNA33) and MltA; however MltA lacks domain 3 which in LtgC is formed by a 66 amino acid insertion into domain 2 forming a small β-barrel. The presence of domain 3 causes the relative positions of domains 1 and 2 to vary between LtgC and MltA, the effect of which is to make the groove between the two domains wider in ltgC than in MltA. The amino acids forming this loop are also present in GNA33. The loop may be of importance as conserved residues and homology between MltA and other lytic transglycosylases indicate that part of the active site of the enzyme is positioned in this groove, thought to be important in binding the glycan strand. However, the two enzymes share conserved residues in the active site and probably share a common reaction mechanism (112).

1.5.1 Deletion of *gna33*

Characterisation of a Δ*gna33* mutant in several strains (MC58, BZ232 and NMB) showed that the bacteria exhibited changes in viability; they produced fewer colonies than the equivalent wildtype strain and growth appeared to be retarded (2). Morphology of the cells was also different. Rather than the normal diplococci, cells grew in clusters where the inner membranes and peptidoglycan were separated, but the outer membrane was continuous. The mutant also released OMPs into the medium and showed decreased virulence, possibly due to increased susceptibility to complement mediated lysis (2). The release of OMPs is due to an abnormally high level of OMV production from Δ*gna33* (37). The predicted function of GNA33 is to anchor to both the outer membrane and the peptidoglycan and the loss of this link may cause the vesicle releasing phenotype.

Compared to the phenotype of MltA mutants of *E. coli,* which show no change in growth or release of OMPs (81), the phenotype of the Δ*gna33* mutant is surprisingly severe. The lack of phenotype in the *ΔmltA* mutant has been hypothesized to be due to functional redundancy. *E. coli* contains seven recognized lytic transglycosylases, the membrane bound enzymes MltA, B, C, D, F and EmtA and the soluble lytic transglycosylase Slt70 (81). *N. meningitidis* contains homologues for all these proteins (65), but apparently does not demonstrate the same level of functional redundancy. The other lytic transglycosylase proteins have not been cloned and assayed, so it is not known if these proteins are functional. In *N. gonorrhoeae*, several lytic transglycosylase genes have also been identified and the mutation of one (*ltgC*, which shares homology with *mltA*) produces a phenotype very similar to that of the *Δgna33* mutant (25). Other lytic transglycosylases *ltgA* (*slt70*) and *ltgD* (*mltB*) have been identified as being involved in the release of peptidoglycan monomers from *N. gonorrhoeae* and lytic transglycosylases of unknown function *ltgB* (*mltC*) and *ltgE* (*mltD*) have also been identified (26). The two *Neisserial* species therefore appear to have a similar functional arrangement in their lytic transglycosylases, a single lytic transglycosylase (GNA33 or LtgC) that is primarily responsible for peptidoglycan processing and turnover and several other lytic transglycosylases that perform other

functions in *N. gonorrhoeae* and for which functions have not been elucidated in *N. meningitidis*. In *E. coli* the family of murein hydrolases, including the lytic transglycosylases are important in diverse functions including murein turnover, autolysis, spore formation, cell elongation and cell division (63). The other lytic transglycosylases in the *N. meningitidis* genome may therefore be found to perform a variety of functions.

1.6. Tol-Pal

Tol-Pal is a complex of proteins spanning the inner and outer membranes and is found in many Gram negative bacteria. Tol-Pal has a variety of functions, including transport of molecules across the cell wall, a structural role and a function in the final separation of the outer membrane during cell division (45,49). Deletion of the *tol-pal* gene cluster in *E. coli* will produce a phenotype which is detergent sensitive, tolerant of filamentous bacteriophages and molecules such as colicin A which use the Tol-Pal complex to cross the membrane, fails to separate during cell division and releases larger numbers of vesicles into the medium (7,45,156). The Tol-Pal complex forms a link between the inner membrane, peptidoglycan and outer membrane and is wide spread among Gram negative bacteria. However, it is lacking in species including: *N. meningitidis*; *N. gonorrhoeae*; *Borrelia burgdorferi*; *Treponema pallidum* and *Porphyromonas gingivalis.* In a phylogenetic tree based on ribosomal ribonucleic acid (rRNA) these bacteria do not have close relationships to each other and are more closely related to bacteria containing the Tol-Pal complex, indicating that the loss of the *tol-pal* cluster was not a single evolutionary event in a cluster of Gram negative bacteria (139). Bacteria that lack the *tol-pal* cluster all produce OMVs at a higher rate than other Gram negative bacteria (12,34,129,175).

1.6.1 Structure of the *tol-pal* operon

The Tol-Pal complex consists of five proteins: TolQ, TolR, TolA, TolB and Pal. The operon which encodes these also contains another two genes; *ybgF* and *ybgC* whose functions do not appear to be

related to the Tol-Pal complex. ybgF is a periplasmic protein of unknown function and ybgC is a cytoplasmic protein with thioesterase activity (49,55). The genes are arranged in an operon with two promoters, the first promoter (P_1) reading from *ybgC* to *ybgF* and the second (P_B) from *tolB* to *ybgF* (Fig.2). Although the first promoter is capable of reading through the entire operon to produce one long polycistronic messenger ribonucleic acid (mRNA) the majority of transcription of *tolB, pal* and *ybgF* is controlled by the P_B promoter (156). Both promoters have Rho-dependent terminators. The translation of *tolR* is dependent on *tolQ* translation; this is due to the *tolR* ribosome binding site being non-functional. In order to translate *tolR* therefore, it is necessary to use the ribosome from *tolQ* translation. (156).

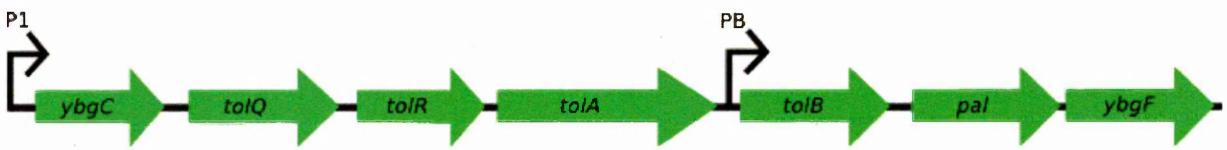

Figure 2: The *tol-pal* operon. The genes of the *tol-pal* complex are arranged in a single 6kb operon along with the two genes of unknown function, *ybgC* and *ybgF*.

1.6.2 Structure of the Tol-Pal complex

The proteins of the Tol-Pal complex are distributed in the inner membrane, the periplasm and the outer membrane. TolQ and TolR are both inner membrane proteins, TolQ contains three transmembrane (TM) domains, whereas TolR contains one TM and two periplasmic domains. TolR shows the capacity to dimerise and the 3rd transmembrane domain of TolQ appears to be able to interact with both TolR and the TolR dimer. The two proteins interact with each other and with TolA, which also contains a TM domain. TolA contains three domains, TolA I is the inner membrane domain interacting with TolQ and TolR whereas Tol A II and III are periplasmic. The TolA III domain appears to regulate interaction with the periplasmic TolB protein and both TolA and TolB have also been shown to interact with Pal and with porins (164). The interaction between TolA and Pal shows that TolA must cross both the periplasm and the peptidoglycan layer (22). Pal interacts at the N-terminal glyceride moiety with the outer membrane and at the C-terminal end with peptidoglycan. Pal dimerises both *in*

vitro and *in vivo* and interacts with several other OMPs including major lipoprotein (Lpp) and outer membrane protein A (OmpA). Interactions with Lpp and OmpA are independent of the presence of the Tol proteins, however TolB interacts with Lpp and OmpA in a Pal dependent manner (21). The interaction between Pal and TolA appears to form two complexes, a major TolA/Pal heterodimer and a minor TolA/Pal multimer. Interaction also appears to be driven by a proton motive force (PMF), treatment with carbonyl cyanide *m*-chlorophenylhydrazone (CCCP) which blocks the production of membrane potentials, inhibits the TolA/Pal interaction. Homology with the TonB system in *E. coli* suggests that TolQ and TolR may be responsible for the production of the PMF and complexes of TolA/TolQ and TolA/TolR are observed with or without CCCP treatment (22). Overproduction of TolQ and TolR drives the co-precipitation of Pal with overproduced TolA. It is therefore hypothesised that TolQ TM helices II and III and the TolR TM helix form an ion pore which produces the proton motive force to drive the TolA/Pal interaction. As the ratio of TolQ to TolR has been estimated to be 3:1 the construction of the pore is likely to be more than a simple heterodimer (23). A diagram of the Tol-Pal complex is shown in figure 3.

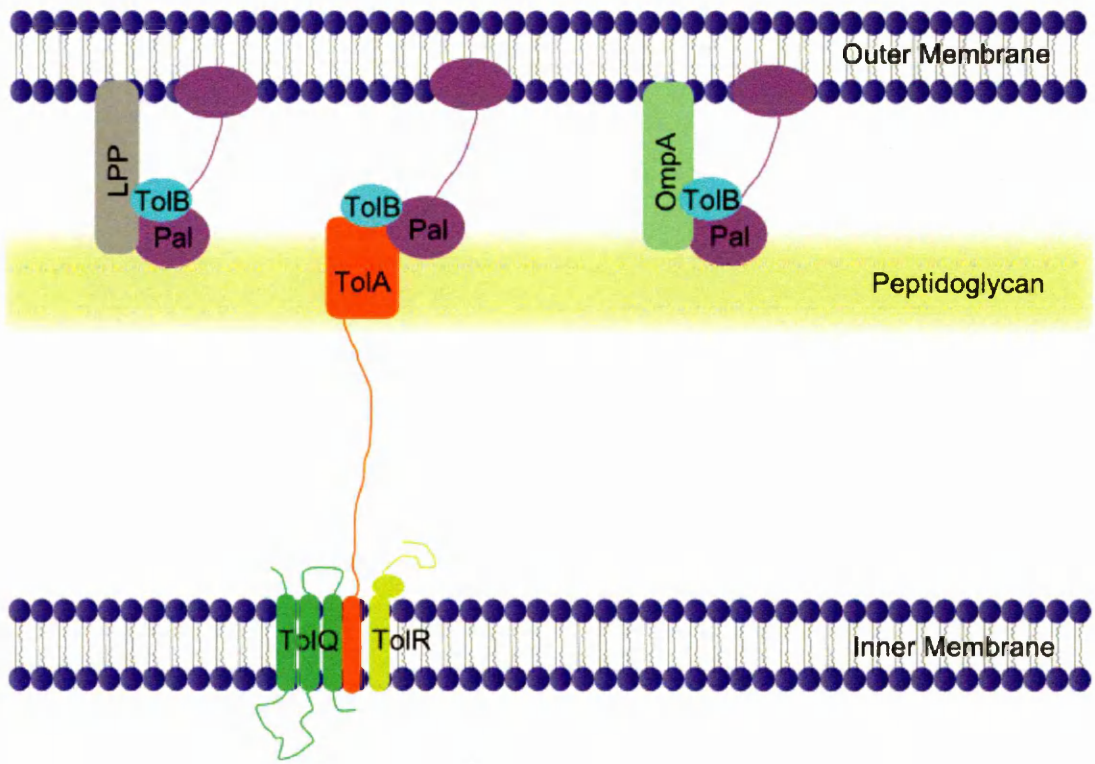

Figure 3: The arrangement of the Tol-Pal complex in the *E. coli* cell wall. The IM proteins TolQ and TolR provide a proton motive force allowing TolA to interact with Pal. TolB interacts with both proteins. Pal also interacts with other proteins in the OM including Lpp and OmpA. TolB interacts with these proteins in a Pal dependent manner.

1.6.3 Functions of the Tol-Pal complex

The mutation of several genes of the *tol-pal* complex affects both the membrane integrity and production of vesicles from *E. coli* cells. Deletion of *tolA, tolQR, tolBPal, tolB* and *pal* produce a vesicle releasing phenotype; however *tolQR* and *tolA* mutants release a greater amount of vesicles than *tolB* and *pal* mutant strains. Mutants of *tol-pal* express low levels of the OMPs, OmpF and LamB (7) and demonstrate other indicators of outer membrane defects, including susceptibility to vancomycin and detergents and the release of RNase I. It is possible to restore the TolA phenotype by plasmid complementation of the Δ*tolA* mutant. A plasmid carrying *tolA* will also reduce susceptibility to sodium dodecyl sulphate (SDS) and vancomycin and reduce the level of OMV release in Δ*lpp* mutants; however this effect is not be seen if *pal* is also mutated. Similarly, overproducing Pal in an Δ*lpp* mutant complements the mutation, but not if there is also a Δ*tolA* mutation. Lpp is not capable of complementing a Δ*pal* mutant (21,22). The interaction between TolA and Pal is vital for the

maintenance of membrane integrity by the Tol-Pal complex. The interaction between TolA and Pal is abolished if the TolA III domain is deleted; this is also the domain that governs the interaction between TolA and TolB. The TolA/TolB interaction is also important for maintaining membrane integrity and both TolA and TolB interact with porins. The Tol-Pal complex may affect porin biogenesis or help to regulate porin activity (164).

The importance of *tol-pal* operon is highlighted as it is highly conserved among Gram negative bacteria, even though the complex also allows the entry of some bacteriophages and bacteriocins into the cell. Tol-Pal certainly appears to perform an important structural role in anchoring the peptidoglycan to the outer membrane as is evidenced by the membrane instability seen in Tol-Pal mutants. The role of the Tol-Pal complex is not purely structural. Experiments have indicated that the Tol-Pal complex may be involved in the transport of macromolecules through the outer membrane. In *E. coli, Pseudomonas putida* and *P. aeruginosa* mutation of genes in the *tol-pal* complex resulted in bacteria defective in the utilisation of several carbon sources due to a failure to uptake these carbon sources at the cytoplasmic membrane (80). Mutants of *tolA* and *pal* have defects in the polymerisation of the O16 antigen in *E. coli,* possibly due to an extra-cytoplasmic stress response which is activated in these mutants (158) or indicating that Tol-Pal has a role in the transport of subunits through the outer membrane (49). There is evidence that apart from its structural and transport roles, the Tol-Pal system may also be important in the division of bacterial cells. Tol-Pal proteins localise to the site of cell constriction during cell division in and are involved in the proper invagination of the outer membrane by attaching the outer membrane to the inward moving peptidoglycan and inner membrane. In addition Δ*tol-pal* mutants also have a 'chaining' phenotype consistent with a failure of proper separation of the OM during cell division and the production of membrane blebs from mutant *E. coli* appears to be localised to the poles of constricting cells. The interaction between TolA and Pal in such a system would involve TolA engaging Pal before retracting back, pulling Pal and the OM inwards, this could possibly explain the requirement of a PMF

for TolA-Pal interaction (45). The Tol-Pal complex appears to have several possible physiological roles in Gram negative bacteria related to the structure and function of the bacterial cell wall, therefore its absence from *N. meningitidis* could be important in understanding the membrane dynamics and vesicle release of the organism.

1.7. RmpM

RmpM is one of the five major OMPs from *N. meningitidis* (144) and binds to both the peptidoglycan and outer membrane. Additionally, RmpM has a role in stabilising protein complexes. The RmpM protein shares 94.2% amino acid homology with the gonococcal Class III OMP (RmpG) (70) and shares 35% homology at the C-terminal end with the *E. coli* protein OmpA, known to be involved in the binding of peptidoglycan (54). RmpM has unusual electrophoretic mobility in the presence of SDS, appearing 6kDa larger than the predicted size of the protein calculated from the amino acid sequence. Similar behaviour has also been seen in gonococcal class III OMP (70). The OmpA like domain of RmpM contains a hydrophilic groove hypothesised to contain the conserved residues essential for peptidoglycan binding. The binding of RmpM to peptidoglycan has been shown both by Western blot and through computer docking analysis of a glycan strand with the putative structure of the OmpA like domain. It has been proposed that RmpM may act as a dimer to bind two glycan strands simultaneously and weak dimer/monomer equilibrium for the protein has been demonstrated, although dimer formation for RmpM has not been observed directly. Although the C-terminal end of RmpM contains as conserved motif for peptidoglycan binding, the N-terminal domain does not contain a recognized motif for binding with the outer membrane (54). RmpM interacts with several other OMPs, the iron regulated OMPs lactoferrin receptor LbpA, transferrin receptor TbpA and siderophore receptor FetA. LbpA, TbpA and FetA oligomers are decreased in an Δ*rmpM* mutant strain, indicating that RmpM has a stabilizing effect on these protein complexes. However, RmpM does not appear to be involved in iron acquisition (114). Similarly, RmpM interacts with the porins, PorA and PorB, and is important in stabilising porin complexes (88). These interactions are likely to

be responsible for anchoring RmpM to the outer membrane allowing it to act as a bridge between the peptidoglycan and outer membrane (64). RmpM is involved in heteroligomeric complexes of PorA, PorB and RmpM and also of PorA, PorB, FetA and RmpM (88,89,119). By forming linkages between the peptidoglycan and the outer membrane RmpM may be involved in maintaining the structural stability of the membrane. As well as complexes with the porins RmpM is important in the stabilisation of the Omp85 protein complex, which organises β-barrel proteins in the outer membrane (162).

1.7.1 RmpM in virulence

Analysis of neisserial strains by Southern blotting demonstrated that the *rmpM* gene was present in *N. meningitidis* but not in commensal species including *Neisseria lactamica, Neisseria mucosa* and *Neisseria sicca*. It was therefore hypothesised that RmpM could be used as a marker of virulence (169). However, later analysis by of chromosomal DNA and detection of RmpM protein in OMVs showed that RmpM was present in strains of *N. lactamica* and *N. sicca* (143). It was also hypothesised that antibodies to RmpM protein may be blocking the bactericidal response to OMV vaccines, analogous to the effect of gonococcal protein III (70). Subsequent work showed that anti-RmpM antibodies were immunogenic although not bactericidal and that inclusion of RmpM in an OMV vaccine made no difference to the bactericidal response (116).

1.7.2 Deletion of *rmpM*

The apparent importance of RmpM as a structural protein means that a knockout mutant would be expected to exhibit phenotypic changes similar to those seen in mutants of other proteins linking the outer membrane to the peptidoglycan. However the Δ*rmpM* mutant strain is similar to the parent strain in terms of growth curves, colony morphology and the overall profile of OMPs (70). The decrease of protein complexes which usually contain RmpM in a mutant strain indicates that deletion of *rmpM* does destabilise these complexes. However in OMV preparations that have been freeze-

dried the presence of RmpM does not increase the stability of PorA trimers and may in fact destabilise them (5). There has been little research into the effect of *rmpM* deletion on the structure and release of OMVs. There is no difference in the quantity of OMVs produced when extracted by detergent, but *ΔrmpM* mutants release more vesicles naturally than the wild-type strain (5,150). The lack of obvious phenotypic features (other than OMV release) like those observed in *Δgna33* and *Δtol-pal* mutants may indicate functional redundancy of the structural role of RmpM with other OMPs such as GNA33 fulfilling its role. The importance of RmpM in a variety of outer membrane interactions, between both proteins and peptidoglycan and in the formation of oligomeric complexes means that the protein may be very important in the structure and antigenicity of OMV vaccines. The interaction of RmpM with PorA and porin complexes is likely to be particularly important for vaccine production as the presentation of PorA on the cell surface may be affected.

1.8. Aims of thesis

The release of membrane vesicles from *N. meningitidis* is an important part of the biology of the organism; however the factors governing the release of vesicles are poorly understood. The process of vesiculation has been studied in other Gram negative bacteria such as *E. coli* and several hypotheses have been proposed for the mechanisms of membrane vesicle release, but the relevance of these hypotheses to vesiculation in *N. meningitidis* has not been examined. The aim of this thesis is to investigate the factors affecting vesicle release in *N. meningitidis*, by elucidating the role of proteins that have been previously shown to affect vesicle production. The *N. meningitidis* lytic transglycosylase GNA33 and the OMP RmpM will be studied, as well as investigating the effect of expression of the *E. coli* protein complex Tol-Pal. Examination of the effects of these proteins on both the phenotype of the organism and the vesicles produced by the bacteria will provide insights into both the mechanisms of vesiculation in *N. meningitidis* and the best methods for the adaption of the bacteria to produce native OMVs for vaccine production.

Chapter 2- Materials and Methods

2.1 Materials

All chemicals were obtained from either Sigma-Aldrich Chemicals (St Louis, MO, USA) or BDH AnalR grade (Surrey, UK) unless otherwise stated. All restriction enzymes and restriction enzyme buffers were obtained from New England Biolabs (Ipswich, MA, USA) unless otherwise stated. EDTA used was the disodium salt. All water was purified using a Milli-Q purification system (Millepore, Billerica, MA, USA).

2.1.1 Solutions

Common buffers and broth used in the study and their formulations are given in table 1 below:

Table 1. Formulations of commonly used solutions.

Name	Formulation
Phosphate buffered saline (PBS)	137mM sodium chloride 2.7mM potassium chloride 10mM Disodium hydrogen phosphate 1.8mM potassium dihydrogen phosphate pH 7.4 adjusted with Hydrochloric acid
Tris(hydroxymethyl)aminomethane (Tris) buffered saline (TBS)	137mM sodium chloride Tris 24.8mM pH 7.4 adjusted with Hydrochloric acid
Tris-acetate EDTA buffer (TAE)	40mM Tris 1mM EDTA 0.1% (v/v) Glacial acetic acid
Tris-EDTA buffer (TE)	10mM Tris 1mM EDTA pH 7.5 adjusted with Hydrochloric acid
Saline-sodium citrate buffer (SSC) 20X	3M sodium chloride 0.3M sodium citrate pH 7 adjusted with Hydrochloric acid
Luria Lysogeny Broth (LB) Broth/Agar (8)	10g/L Tryptone (Oxoid, Cambridge, UK) 8g/L sodium Chloride 5g/L Yeast Extract (Oxoid) pH 7.5 adjusted with sodium Hydroxide For agar: 15g/L Agar Flakes (Sigma-Aldrich)

2.1.2 *N. meningitidis* strains

The strains of *N. meningitidis* used in this work are listed in table 2 below. The sources of the strains were Health Protection Agency Manchester Laboratory Services (HPA-MLS), Oxford University (OU) and the Norwegian Institute of Public Health (NIPH).

Table 2. *N. meningitidis* strains.

Strain name	Serogroup	PorA variable regions	FetA variable region	PorB type	ST	Clonal complex	Source
H44/76	B	P1.7,16	F3-3	15	ST-32	cc32	HPA-MLS
MC58	B	P1.7,16-2	F1-5	15	ST-74	cc32	OU

Name	**Background strain**	**Mutation**	**Source**
gna33 Downstream single crossover	H44/76	Insertion of linearised plasmid downstream of *gna33*	This study
gna33 Upstream single crossover	H44/76	Insertion of linearised plasmid upstream of *gna33*	This study
Δ*gna33*	H44/76	Δ*gna33*	This study
Δ*gna33*	MC58	Δ*gna33*	This study
H44/76::*tolF1*	H44/76	Strain containing the pMIDGTolF1 plasmid	This study
gna33 single crossover::*tol-pal*	*gna33* downstream single crossover	Strain containing the pMIDGTol-Pal plasmid	This study
gna33 single crossover::*tolF1*	*gna33* downstream single crossover	Strain containing the pMIDGTolF1 plasmid	This study
Δ*siaD*	MC58	Δ*siaD*	C. Tang (36)
Δ*rmpM*	H44/76	Δ*rmpM*	NIPH (70)
RmpM C-term	H44/76	Deletion of the final 207 bases of the *rmpM* gene	This study

2.1.3 *E. coli* strains

The strains of *E. coli* used in this study are listed in table 3.

Table 3. *E. coli* strains.

Strain	Genotype	Source
Oneshot Top10	F- *mcr*A Δ(*mrr-hsd*RMS-*mcr*BC) ϕ80*lacZ*ΔM15 Δ*lac*X74 *rec*A1 *ara*D139 Δ(*araleu*)7697 *gal*U *gal*K *rps*L (Str^R) *end*A1 *nup*G	Invitrogen , Carlsbard, CA, USA
5-alpha F' I^q	F' *proA*$^+$*B*$^+$ *laqI*^{q} *Δ(LacZ)*M15 *zzf::tTn10* (Tet^R)/*fhuA2Δ(argF-lacZ)U169 phoA glnV44 Φ80Δ(lacZ)*M15 *gyrA96 recA1 relA1 endA1 thi-1 hsdR17*	New England Biolabs
TB28TolQ-Pal (Δ*tol-pal*)	*rph*1 *ilvG rfb*-50 *lacIZYA* <>*frttolQ-pal*<>	Gerding et al. (45)

2.1.4 Plasmids

Plasmids used in this study are listed in table 4.

Table 4. Plasmids used in this study.

Plasmid Name	Description	Source
pCR2.1 Topo	Topo cloning vector. Contained complementary 5'-thymidine overhangs bound to topoisomerase enzyme, *lacZα* gene and *ampR* and *kanR* antibiotic resistance genes.	Invitrogen
pUC19	Cloning vector. Contained *lacZα* gene and *ampR* resistance gene.	Invitrogen
pBSUDGNA33ERM	For deletion of *gna33* gene by homologous recombination. Contained *ermC* antibiotic resistance gene flanked by sequences homologous to the flanking sequences of the *gna33* gene. Also contained *ampR* resistance gene.	Adu-Bobie et al. (2)
pMIDG201	Shuttle vector for *E. coli* and *N. meningitidis*. Contained constitutive meningococcal promoter *ner*, *kanR* resistance gene and the RepA origin of replication.	J.S. Kroll (103,104)
TopoTF1	pCR2.1 Topo cloning vector. Contained the *E. coli* genes *ybgC*, *tolQ*, *tolR* and partial *tolA* and promoter P_1.	This study
TopoTF2	pCR2.1 Topo cloning vector. Contained the *E. coli* genes partial *tolA*, *tolB* and *pal* and promoter P_B.	This study
TopoTF3	pCR2.1 Topo cloning vector. Contained the *E. coli* genes *tolQ*, *tolR* and *tolA*.	This study

TopoTF4	pCR2.1 Topo cloning vector. Contained the *E. coli* genes *tolB* and *pal*.	This study
pMIDGTolF1	pMIDG201 vector. Contained *E.coli* genes *ybgC, tolQ, tolR* and partial *tolA* and promoter P_1.	This study
pMIDGTolF3	pMIDG201 vector. Contained *E.coli* genes *tolQ, tolR* and *tolA* under control of the *ner* promoter.	This study
pMIDGTol-Pal	pMIDG201 vector. Contained *E.coli* genes *ybgC, tolQ, tolR, tolA, tolB* and *pal* under control of the P_1 and P_B promoters.	This study
pMIDGTol-Palner	pMIDG201 vector. Contained *E.coli* genes *tolQ, tolR, tolA, tolB* and *pal* under control of the *ner* promoter.	This study
pMIDGTol-Pal recovered	pMIDG201 vector. pMIDGTol-Pal after recombination by *N. meningitidis,* contained *kanR* gene and RepA origin of replication.	This study
pMIDGTol-Palner recovered	pMIDG201 vector. pMIDGTol-Palner after recombination by *N. meningitidis,* contained *kanR* gene and RepA origin of replication.	This study
pMIDGTol-PalPmB	pMIDG201 vector. pMIDGTol-Pal after recombination by *N. meningitidis* strain *gna33* downstream single crossover. Addition of PmB origin of replication to pMIDGTol-Pal.	This study
TopoRmpM	pCR2.1 Topo cloning vector. Contained the *N. meningitidis* gene *rmpM*.	This study
TopoKan2	pCR2.1 Topo cloning vector. Contained a second copy of the *kanR* gene.	This study
pUCRmpM	pUC19 cloning vector. Contained the *N. meningitidis* gene *rmpM*.	This study
pRmpMC-term	pUC19 cloning vector. Contained the *N. meningitidis* gene *rmpM* truncated at 523bp. Contained *kanR* resistance gene.	This study

2.2 Microbiological methods

Microbiological techniques were carried out in a Class II microbiological safety cabinet unless otherwise stated.

2.2.1 Propagation and maintenance of *N. meningitidis* strains

N. meningitidis strains were maintained as frozen stocks at -70°C on Protect Beads (Technical Services consultants, Lancashire, England). To produce frozen stocks, single colonies were selected and inoculated onto Mueller Hinton (97) agar plates (Oxoid). A loop of the resulting culture was resuspended into the protect beads cryo-protectant media following the manufacturer's instructions. The media was then drained and the beads stored at -70°C.

For revival of frozen stocks a single bead was extracted from the vial and used to inoculate an agar plate of blood agar base No.2 (Oxoid) containing 7% v/v of defibrinated horse blood (Oxoid). After inoculation plates were incubated at 37°C in an atmosphere containing 5% carbon dioxide for approximately 15 hours (overnight).

Routine culture of *N. meningitidis* strains was carried out on Mueller Hinton agar containing the selection antibiotics kanamycin (at 75µg/ml) and erythromycin (at 7µg/ml) where appropriate. For liquid culture Mueller Hinton broth (Oxoid) was used with appropriate selection antibiotics used at the same levels as in the agar plates.

2.2.2 Propagation and maintenance of *E. coli* strains

E. coli strains were frozen on protect beads by the same methods used for the *N. meningitidis* strains. *E. coli* were revived on LB agar plates, plates were incubated at 37°C for approximately 15 hours (overnight).

Routine culture of *E. coli* strains was carried out on LB agar plates containing appropriate selection antibiotics ampicillin (at 50µg/ml), erythromycin (at 150µg/ml) and kanamycin (at 50µg/ml) as appropriate. Liquid cultures were carried out in LB broth with selection antibiotics at the same levels used in the plate culture. For the TB28TolQ-Pal strain 1% sodium chloride was added to the LB broth and LB agar used in the culture of this strain.

2.2.3 Transformation of *E. coli* OneShot Top10 and NEB 5-alphaF'I^q

Transformation of *E. coli* was carried out according to manufacturer's protocols where commercial cells were used. *E. coli* OneShot Top10 cells (Invitrogen) were thawed on ice. Once thawed DNA was added to the cells and the *E. coli* incubated on ice for 30 minutes. Cells were then heat shocked at 42°C for 30 seconds and placed back on ice. 250µl of Super Optimal broth with Catabolite repression (SOC) (Invitrogen) was added to the cells and tubes were incubated for 1 hour at 37°C with shaking.

After incubation bacteria were centrifuged at 17,000xg for one minute and the resulting pellet resuspended in 100µl of the SOC media. This suspension was inoculated onto pre-warmed LB plates containing selection antibiotics. Blue/White selection was used to identify colonies containing plasmids carrying DNA inserts. Blue/White selection used the *lacZα* gene which was present in the pCR2.1 Topo plasmid and the pUC19 plasmid. The α fragment encoded by the *lacZα* gene complements the deleted portion of the host strain's LacZ protein to allow synthesis of functional β-galactosidase. This cleaves the substrate X-gal to a blue coloured product. Cloning of an insert into the multiple cloning site of the plasmid disrupted the *LacZα* gene; when the gene was disrupted functional enzyme was no longer produced, therefore colonies that contained vector and insert were capable of growing on antibiotic containing media but appeared white rather than blue when the media also contained X-gal. For blue/white selection plates were spread with 40µl of 40mg/ml bromo-chloro-indolyl-galactopyranoside (X-Gal) in dimethylformamide (USB Corporation, Cleveland, OH, USA) and allowed to dry for one hour. Plates were incubated overnight at 37°C.

The method for 5-alpha F' I^q cells (New England Biolabs) was similar to the method for the OneShotTop10 cells, with the following amendments: Cells were incubated for five minutes on ice after heat shock and were recovered in 950µl SOC media (New England Biolabs). For blue/white selection in 5-alpha F' I^q cells plates were spread with 40µl 40mg/ml X-Gal and contained 0.3mM isopropyl β-D-1-thiogalactopyranoside (IPTG).

2.2.4 Production of competent *E. coli* from strain TB28TolQ-Pal

A single colony was inoculated into 5ml LB broth and grown overnight. 1ml of the suspension was then used to inoculate 100ml of LB broth and the culture was grown for 1-2 hours until it had reached optical density at 600nm (OD_{600}) of 0.25. Optical density was measured in a WPA biowave CO8000 cell density meter (WPA, Cambridge, UK), using polystyrene semi-micro cuvettes (VWR International, West Chester, PA, USA). After growth the culture was placed on ice for ten minutes and the bacteria

were then centrifuged at 15000xg for 10 minutes at 4°C. The cell pellet was gently resuspended in 10ml ice cold 0.1M calcium chloride and incubated on ice for 20 minutes. The suspension was then centrifuged for 5 minutes at 6000xg 4°C. The pellet was resuspended in 5ml 0.1M calcium chloride with 15% glycerol. Cells were dispensed into 100µl aliquots and frozen at -70°C.

2.2.5 Transformation of competent TB28TolQ-Pal

For competent cells produced in the lab, DNA was added to thawed cells and cells were incubated on ice for 30 minutes. Cells were then heat shocked for 2 minutes at 42°C and then placed back on ice. Bacteria were recovered in 900µl LB broth for 1 hour at 37°C with shaking. Cells were then spun down and resuspended in 100µl before being spread onto selective LB plates.

2.2.6 Growth curves

N. meningitidis were grown overnight in 3ml Mueller Hinton broth in 7ml bijou tubes (Thermo Fisher Scientific, Waltham, MA, USA) with appropriate selection antibiotics to adapt the bacteria to growth in the media. Bacteria were then resuspended from the overnight culture into 13mls of fresh Mueller Hinton broth to an OD_{600} of 0.05 in 30ml Universal tubes (Thermo Fisher Scientific) and grown at 37°C with shaking for eight hours. The OD_{600} value of the culture was tested every hour. Results were the mean of three experiments.

2.2.7 Antibiotic sensitivity assays (solid media)

The method for antibiotic sensitivity assays on solid media was adapted from the work of Jorgensen et al (67). Bacteria were grown overnight in selection antibiotics. After growth bacteria were resuspended to an OD_{600} of 0.15 in sterile 145mM sodium chloride solution. Antibiotic containing discs were produced using sterile filter paper discs (Sigma-Aldrich). Discs were soaked in antibiotic solutions of appropriate concentrations for three minutes and then air-dried for 30 minutes before use. Antibiotics used were D-cycloserine 6mg/ml, vancomycin 25mg/ml, polymyxin B 12.5mg/ml and

ampicillin 5µg/ml. Mueller Hinton plates containing 5% Defibrinated horse blood were prepared and inoculated with bacteria from the saline solution using a sterile swab. After inoculation disks were placed on the surface of the plates. Plates were incubated overnight. Zones of inhibition were measured using an Allied Vision firewire camera (Allied Vision Technologies, Stadtroda, Germany) on a Kaiser RS3 XA stand with RB 218 Light set (Kaiser Fototechnik, Buchen, Germany). Images were analysed using the ProtoCOL software (Synbiosis, Cambridge, UK). Calibration was set using the diameter of the plate and zones measured using the manual measure feature. Results were the mean of three experiments.

2.2.8 Antibiotic sensitivity assays (liquid media)

Bacteria were grown overnight in Mueller Hinton broth with selection antibiotics to adapt the bacteria to growth in the media. Bacteria were resuspended in broth with selection antibiotics and grown to an OD_{600}=1.2. Cells were split into 2ml samples and centrifuged for 1 minute at 9600xg to pellet the cells. The growth media was removed and replaced with fresh media containing 10µg/ml polymyxin B, 3µg/ml ampicillin or control media without antibiotics. Bacteria were incubated in the media for two hours and then serially diluted to a 10^{-6} dilution. 50µl of this dilution was plated out onto Mueller Hinton agar with and without selection antibiotics. Plates were grown for 24 hours and colonies were counted. Results were taken as the mean of three experiments.

2.2.9 Temperature sensitivity studies

Bacteria were grown overnight in Mueller Hinton broth to adapt them for growth in the media. Bacteria were resuspended into fresh Mueller Hinton broth at an OD_{600}= 0.05 and were grown with shaking for 7 hours at 35°C, 37°C and 39°C. After 7 hours OD_{600} readings were taken from the cultures. Results were a mean of three experiments.

2.2.10 Native OMV production

The method for native OMV production was adapted from that of Ferrari et al. (37). Bacteria were grown from frozen stocks overnight and then subcultured onto blood plates and grown for seven hours. Plates were then scraped and the bacteria resuspended into 4mls of Mueller Hinton broth which was then used to inoculate 50-150ml broth to an OD_{600}=0.15. Broth cultures were grown overnight and the bacteria were then centrifuged at 7400xg 4°C for 1 hour. After centrifugation the supernatant was removed and passed through a 0.2µm stericup filter (Millepore) by vacuum filtration. The filtrate was placed into ultracentrifuge bottles and centrifuged for 2 hours at 200000xg 4°C. The supernatant was poured off and 10ml PBS was added to each bottle to wash the pellet. The sample was centrifuged for 30 minutes at 200000xg 4°C, then the supernatant was removed and the PBS wash step repeated. Pellets were resuspended in 500µl PBS buffer containing 3% sucrose. After resuspension OMV samples were purified by fast protein liquid chromatography (FPLC) using an instrument consisting of a Pharmacia gradient programmer GP-250 Plus and a liquid chromatography controller LCC-500 Plus, driving high precision pumps P-500 (Pharmacia Biotech, St Albans, UK). Samples were first centrifuged at 8,600xg 4°C for 15 minutes to remove insoluble debris. Supernatant was diluted to 600µl with water and separation was carried out on a Superdex 200 column (Amersham biosciences, Sweden). The column was equilibrated with PBS pH7.4 and calibrated with protein standards. Flow rate was 500µl per minute for a total time of 60 minutes. Protein content was monitored by Refractive Index (RI) and Ultraviolet (UV) spectroscopy using a Lambda 600 spectrophotometer (PerkinElmer, Waltham, MA, USA). Flow through fraction containing the OMV was collected and pooled. For electron microscopy, 1500µl of flow through fraction was ultracentrifuged for 2 hours at 200000xg 4°C and OMVs resuspended in 50µl PBS.

2.2.11 Phenotype testing of the TB28TolQ-Pal strain

This method was used for testing the phenotype of the TB28TolQ-Pal strain when transformed with the pMIDGTol-Pal plasmids. The method was adapted from Gerding et al. (45). Bacterial growth on SDS and Deoxycholate (DOC) media was initially tested and it was found that 0.5% DOC gave the clearest differentiation between the wildtype and Δ*tol-pal* phenotype. LB agar plates were made containing DOC. Bacteria were grown overnight in broth culture, after growth overnight suspensions were diluted to an OD_{600}=0.02 and serially diluted to 10^{-4}. 5µl of each suspension was spotted onto the plate and the plates incubated for 24 hours at 30°C. Plates were photographed using Allied vision firewire camera and stand. Photographs were taken with the ProtoCOL software. After the first incubation, plates were incubated for a further 72 hours at room temperature and then photographed again.

2.3 Molecular biology techniques for DNA

2.3.1 Preparation of Genomic DNA

Genomic DNA extractions were carried out using the Wizard Total genomic DNA extraction kit (Promega, Fitchburg, WI, USA) according to the manufacturer's instructions. Bacteria were resuspended from plate culture in 600µl nuclei lysis buffer and incubated for 5 minutes at 80°C. After incubation the cells were cooled to room temperature and 3µl of RNase A (4mg/ml) was added. The suspension was incubated at 37°C for 15-60 minutes. After incubation 200µl protein precipitation solution was added and the suspension was vortexed for 20 seconds before being incubated on ice for 5 minutes. After incubation the suspension was centrifuged for 3 minutes at 17000xg and the supernatant mixed with 600µl of 2-propanol. After 2 minutes centrifugation at 17000xg the 2-propanol was decanted and the DNA pellet washed with 1ml of 70% (v/v) ethanol. The pellet was centrifuged for another 2 minutes at 17000xg and the ethanol was then aspirated off and the pellet

allowed to air dry for 15 minutes. The pellet was then resuspended in 100µl DNA resuspension buffer by incubating at 65°C for 1 hour.

2.3.2 Preparation of plasmid DNA

2.3.2.1 Small scale preparation of plasmid DNA from *E. coli*

Plasmid was extracted from *E. coli* using the GenElute miniprep kit (Sigma). Broths inoculated with a single colony were grown overnight at 37°C with shaking in 3-5ml of LB broth. 1.5-3ml of broth cultures were centrifuged at 17000xg for 2 minutes. Culture medium was discarded and the cell pellet was resuspended in 200µl resuspension buffer. 200µl Lysis buffer was added and the solution allowed to clear. 350µl neutralisation buffer was added and the preparations were centrifuged at 17000xg for 10 minutes. GenElute columns were prepared by eluting 500µl of column preparation solution through the column. After centrifugation, the supernatant was removed from the plasmid preparations and added to the column and centrifuged for 1 minute at 17000xg. Columns were then washed with 750µl wash solution and dried by centrifugation for 1 minute at 17000xg. Plasmid DNA was eluted from the column using 50µl elution buffer.

2.3.2.2 Large scale preparation of plasmid DNA from *E. coli*

For large scale plasmid production the Qiagen tips plasmid extraction kit was used (Qiagen, Venlo, The Netherlands). Two sizes of Qiagen tips, P100 and P500, were used and the volumes for both tip sizes are listed. Broths of 50ml or 200ml culture were inoculated from starter cultures and grown overnight. Cells were pelleted for 10 minutes at 6000xg, 4°C. Supernatant was removed and cell pellets resuspended in 4ml or 10ml Resuspension buffer P1 containing RNase. 4ml or 10ml Lysis buffer P2 was then added and the solution allowed to clear. After clearing 4ml or 10ml of chilled Neutralisation buffer P3 was added and the culture was incubated for 15-20mins on ice before being centrifuged for 30minutes at 13000xg, 4°C. Elution columns P100 and P500 were prepared by adding 4ml or 10ml equilibration buffer QTB respectively. After centrifugation supernatant was loaded on to

the tips and allowed to pass through the resin by gravity flow. Tips were washed twice with 10ml or 30ml wash buffer QC. Elution buffer QF was used to elute DNA from the columns. Eluted DNA was mixed with 0.7 volumes of 99% 2-Propanol and centrifuged for 30 minutes at 12000xg 4°C. Supernatant was decanted and the pellets washed with 1ml or 5ml 70% (v/v) ethanol. Pellets were then centrifuged for 10 minutes at 12000xg, 4°C. Ethanol was decanted and pellets allowed to air dry for 10-15 minutes before resuspension in 500µl of TE buffer.

2.3.2.3 Plasmid preparation from *N. meningitidis*

Plasmid was extracted from *N. meningitidis* using Qiagen tip P20 plasmid extraction kit (Qiagen). Method was the same as for Qiagen tips used above, with 0.3ml of the buffers P1, P2 and P3 used. 1ml QBT was used to equilibrate the columns and 2x2ml used to wash the columns. 0.8ml QF was used to elute the plasmid and 1ml of 70% (v/v) ethanol was used to wash the pellet. All centrifugation steps were carried out at 17,000xg. DNA was resuspended in 50µl TE buffer.

2.3.4 Oligonucleotide Primers

The names and sequences of desalted oligonucleotide primers (Invitrogen) used in this work are given in table 5. The lengths of the primers are given in bases.

Table 5. Oligonucleotides used in this study.

Primer	Length (bases)	Sequence
GNAUpstreamF	27	GAATTCCGAACACAATGAACAATGTCC
GNA33UpstreamR	25	GGATCCATGCTCTTGCTTTGGCAGG
GNA33DownstreamF	23	GGATCCCACGGGATATGTGTGGC
GNA33DownstreamR	24	AAGCTTTTTAGTAGGGACAACCGG
M13 Forward	16	GTAAAACGACGGCCAG
M13 Reverse	17	CAGGAAACAGCTATGAC
GNA33 UpstreamDNAF	33	ATGCCGTCTGAACGAACACAATGAACAATGTCC
T7 Forward	20	TAATACGACTCACTATAGGG
GNA33SF1	18	CTGCACAGAATCCTGAAG
GNA33FlankRev	19	CGAACGAACAAGGATGATG
GNA332F	18	GAGGGATTCGTCATGTTG
GNA333R	18	GGAACATCTGTGGTATGG
T3 Reverse	20	AATTAACCCTCACTAAAGGG

GNA33TestFor	18	GGAAAGAGCTGTATGTCG
GNA33TestRev	18	CGTCTATACCGTTGTACC
GNA33RNAF	23	GGTAGGAGCTGCCAGACATATCC
GNA33RNAR	23	GCCAAAGCAAGAGCATCCAAACC
PorARNAF	24	CAAGCCATTGATCCTTGGGACAGC
PorARNAR	25	GTCGAAACCATGGGCATAGCTGATG
gdhRNAF	23	CGAACGTTTCGCATATCTCAAAG
gdhRNAR	23	CGTTAATCACATCCAGCAGCAGG
Tol-PalF1	25	CTCGAGCTGTGCTGGTGTGATTCAC
Tol-PalR1	18	CTTACCAGAGCTTAGCTC
Tol-PalF2	19	GCAGCTGATAAGAAAGCAG
Tol-PalR2	25	CCCGGGAACCAGTAACGACAGACTC
Tol-PalnerF1	24	GGATCCTCGTGCGCTTCCCAAGTC
Tol-PalnerR1	31	CCCGGGGGTACCTCGCGATTACGGTTTGAAG
Tol-PalnerF2	24	GGTACCGCCATCGGTCCAGATAAG
T1F1	18	GTTAGCGAGAGCAACAAG
T1R1	19	CTGTTCATCAGAACGCTTC
T1F2	19	CTGCAGCTGATAAGAAAGC
T2F1	18	GTTCTATGACGCATCGTC
T2F2	19	CTACGTTGTTCAGACCAAC
T2R2	18	GAATGAAGCCACCTGACG
T2R1	18	GACCTGTCCATCAGTTGC
T2F3	19	CTGGACAAGTACGATATCC
T2R3	19	GAGTTCTGAGCAAGTACAG
SF1	18	GTAAAGGTCCAATTCTCG
SF5	18	CTGATCTGGAGTTCGTTC
SR6	18	CGCTTTCTTTCTTGCTTC
pMIDG SeqR	22	GGCTTTACACTTTATGCTTCCG
pMIDG SeqF	19	GCAGTCTCTCGAGCTCAAG
KanF	18	GTTCCACATCATAGGTGG
KanR	19	GACAAGTGGTATGACATTG
KanF2	18	CCTTAGCAGGAGACATTC
KanR2	19	GAAGAACAGTATGTCGAGC
SF7	18	CGGATGGTTCTTACAATG
SF8	19	GTAATGGTCAGCTCCAATG
SF9	18	CAGGGAGATGTTGTATTC
RmpM F	26	GAATTCGATGGTCAGGTTGACTTTCG
RmpM R	26	AAGCTTGCTCAATCGCTGCAACTGAC
RmpM DNA F	31	ATGCCGTCTGAAGTTGCTTCTGTATCTGCTG
RmpM partial R	25	TCTAGAAACAGGTACGCCGTTGCTG
RmpM partial F	25	TCTAGAATTTCTGCTGTCGGCTTGG
RmpM X2	25	CCCGGGCGTTGAGTATTGACAGTCC
RmpM X3	25	CCCGGGGTTGCTTCTGTATCTGCTG
RmpM Kan R	28	TCTAGATAAGTGTGATGGATATCTGCAG
RmpM Kan F	26	ATGCATCTTGGTACCACTCCAGCATG
RmpM long F	26	CGTTGCATTGCTCGCTTCCGGCACTG
RmpM long R	24	GTCAGGTTCGATACATGCAATCAG
RmpM short R	24	GCTGACCAGGTTGTTTGCCACTAC

2.3.5 Polymerase chain reaction

Polymerase chain reaction (PCR) was used for the amplification of DNA regions using the primers listed in table 3. For PCR the Amplitaq DNA polymerase kit (Applied Biosystems, Foster City, CA, USA) was used. Deoxynucleoside triphosphates (dNTPs): deoxyadenosine triphosphate (dATP), deoxyguanosine triphosphate (dGTP), deoxythymidine triphosphate (dTTP) and deoxycytidine triphosphate (dCTP) (Invitrogen) were used. PCR reactions were incubated in either a DNA Engine (MJ Research, Waltham, MA, USA), DNA Engine Dyad (Bio-Rad Laboratories, Hercules, CA, USA), or the Veriti 96 well thermal cycler (Applied Biosystems). Reactions were carried out in 0.2ml thin walled PCR tubes (Thermo Fisher Scientific). For multiple PCR reactions a master mix of all the components excluding the template DNA was set up and the mixture aliquoted into reaction tubes. After amplification results were examined by agarose gel electrophoresis. The reaction mixture used for PCR is detailed in table 6.

Table 6. Reaction mixture used for PCR.

Reagent	Concentration
10X Amplitaq PCR buffer I	1X
dNTPs	10mM of each dNTP
Forward Primer	1pMol/µl
Reverse Primer	1pMol/µl
Template DNA	~20ng
Amplitaq DNA Polymerase	0.05U/µl
Magnesium Chloride ($MgCl_2$) Solution 25mM	Determined by experiment
Water	To required total volume

For colony PCR the template DNA was not included and instead colonies were inoculated directly into the PCR mixture. Reactions were incubated in the thermal cycler following the programme listed in table 7:

Table 7. Thermocycler reaction conditions used for PCR.

Temperature	Time	Function	
95°C	3 minutes	Denaturation of the template DNA in colony PCR also the lysis of the bacteria	
95°C	30 seconds	Denaturation	X 30 cycles
Annealing temperature	30 seconds	Annealing of primers to template sequence	
72°C	Extension time	Extension by Taq polymerase	
72°C	10 minutes	Final extension and addition of poly-adenosine to the ends of PCR products	

The annealing temperatures, extension times and concentration of $MgCl_2$ used in each PCR reaction were determined empirically. The conditions used for the each PCR reaction are shown in table 8.

Table 8. Reaction conditions for primer pairs used in this study.

Forward primer	Reverse primer	Annealing temperature	Extension time	$MgCl_2$ concentration
GNA33UpstreamF	GNA33UpstreamR	57°C	2 minutes	2.5mM
GNA33DownstreamF	GNA33DownstreamR	57°C	2 minutes	2.5mM
GNA33TestFor	GNA33TestRev	50°C	2 minutes	1.5mM
GNA33TestFor	GNA332F	50°C	2 minutes	1.5mM
GNA333R	GNA33SF1	50°C	2 minutes	1.5mM
T3 Reverse	GNA33TestRev	50°C	2 minutes	1.5mM
GNA33RNAF	GNA33RNAR	58°C	2 minutes	1.5mM
Tol-PalnerF1	Tol-PalnerR1	63°C	3 minutes	1.5mM
Tol-PalnerF2	Tol-PalR2	63°C	3 minutes	1.5mM
Tol-PalF1	Tol-PalR1	58°C	3 minutes	1.5mM
Tol-PalF2	Tol-PalR2	58°C	3 minutes	1.5mM
Tol-PalF1	Tol-PalR2	58°C	5 minutes	2.5mM
T2F2	pMIDG SeqR	50°C	3 minutes	1.5mM
SF1	T1R1	50°C	3 minutes	1.5mM
SF1	SR6	50°C	3 minutes	1.5mM
SF5	T2R2	50°C	3 minutes	1.5mM
RmpM F	RmpM R	54°C	2 minutes	1.5mM
RmpM partial F	RmpM R	50°C	2 minutes	1.5mM
RmpM F	RmpM partial R	50°C	2 minutes	1.5mM
RmpM X2	RmpM partial R	50°C	2 minutes	1.5mM
RmpM X3	RmpM partial R	50°C	2 minutes	1.5mM
RmpM X3	RmpM R	54°C	2 minutes	1.5mM
RmpM Kan F	RmpM Kan R	58°C	2 minutes	1.5mM
RmpM X3	RmpM Kan R	54°C	2 minutes	1.5mM
RmpM DNA F	RmpM R	58°C	2 minutes	1.5mM

2.3.6 Restriction digestion

For restriction digestions of plasmid DNA the mixture shown in table 9 was used.

Table 9. Reaction mixture used for restriction digestions of plasmids

Component	Volume
Restriction enzyme	3U-20U (dependant on enzyme)
10X Bovine Serum Albumin (BSA) (New England biolabs)	1X
10X Restriction Enzyme buffer	1X
Plasmid DNA	~200-500ng
Water	To a total volume of 10µl

Reactions were incubated at 37°C for one hour. Results were examined by agarose gel electrophoresis.

To prepare DNA from plasmids for ligation a different reaction mixture was used, shown in table 10.

Table 10. Reaction mixture used for restriction digestions of plasmids for ligation.

Component	Volume
Restriction enzyme	3U-20U (dependant on enzyme)
10X BSA	1X
Restriction Enzyme buffer	1X
Plasmid DNA	~1-2µg
Water	To a total volume of 50µl

Reactions were incubated at 37°C for 2 hours. The restriction enzyme *XmaI* required incubation at 37°C for 16 hours. Results were examined by agarose gel electrophoresis.

Restriction digests for Southern blotting were carried out using the mixture detailed in table 11:

Table 11. Reaction mixture used for restriction digestion of genomic DNA for Southern blotting.

Component	Volume
Restriction enzyme 1	3U-20U (dependant on enzyme)
Restriction enzyme 2 (where used)	3U-20U (dependant on enzyme)
10X BSA	1X
Restriction Enzyme buffer	1X
Genomic DNA	~5µg
Water	To a total volume of 100µl

Digests were incubated for 16 hours (overnight) at 37°C.

2.3.7 Agarose gel electrophoresis

1% (w/v) Agarose (Invitrogen) gels were prepared by heating agarose in TAE buffer to dissolve the powder. The mixture was allowed to cool and Safeview (NBS Biologicals, Cambridgeshire, UK) was added (6µl/100ml). Gels were then poured into casting trays and allowed to set for thirty minutes. Set gels were submerged in TAE buffer in a horizontal electrophoresis tank (Bethesda research, Gaithersburg, MD, USA). DNA samples were mixed with 6X blue/orange loading dye (Promega) and the samples loaded into the wells along with a 1kilo base pair (bp) marker ladder (Invitrogen) or a λ/HindIII marker ladder (Invitrogen). Electrophoresis was performed at 100V-160V for 1-1.5 hours. Gels were visualised using a UV transilluminator and photographed in a Kodak GL1500 gel documentation system (Kodak, Rochester, NY, USA) using a 590nm band pass filter. Band sizes were estimated using the Kodak MI image analysis software (Kodak).

2.3.8 Sequencing

Sequencing reactions were prepared using the ABI prism™ BigDye™ Terminator v3.1 Cycle Sequencing kit (Applied Biosystems) using the mixture detailed in table 12:

Table 12. Reaction mixture used for DNA sequencing

Component	Concentration
Terminator Ready Reaction Mix	1X
Sequencing primer	1 pMol/µl
Sequencing template	~20ng
Sequencing buffer	0.5X
Water	To 10µl

Reaction components were combined in 0.2ml thin walled PCR tubes. After mixing reactions were placed in the thermal cycler and incubated under the conditions in table 13:

Table 13. Thermocycler reaction conditions used for DNA sequencing

Temperature	Duration	
96°C	30 seconds	X 25 cycles
50°C	15 seconds	
60°C	4 minutes	

After the incubation was complete 5µl of 125mM EDTA was added to the sequencing reactions along with 10µl of water and 80µl of 96% (v/v) ethanol. The reactions were incubated for a minimum of 15 minutes at room temperature to stop the reaction and precipitate the DNA. After incubation the reactions were centrifuged at 3000xg to pellet the samples. Pellets were washed with 200µl 70% (v/v) ethanol and incubated for five minutes at room temperature. Samples were then centrifuged at 2000xg for 15 minutes. The ethanol was discarded and pellets were dried by centrifugation of the upside down tubes for 2 minutes at 900xg. Pellets were resuspended in 10µl of Hi-Dye formamide (Applied Biosystems) and stored at -20°C prior to loading onto the sequencer. Sequencing was performed using an ABI 3130xl genetic analyser (Applied Biosystems). Sequence data was analysed using the Vector NTI version 10.1 software (Invitrogen).

2.3.9 Ligation of PCR products into pCR2.1 Topo vectors using the Topo cloning system

Topo cloning anneals PCR fragments to the Topo vector using overhanging 3'-poly-adenine tail added by Taq polymerase during the PCR reaction. The linearised topo vector contains complementary 5'-thymidine-overhangs and is bound to a topoisomerase-I enzyme. The complimentary overhangs allow the fragment to anneal to the vector and the topoisomerase enzyme ligates the fragment and vector sequences together, in the process being released from the DNA.Topo clones were produced using a pCR2.1 Topo cloning kit (Invitrogen) following the manufacturer's instructions. After PCR and agarose gel electrophoresis, 2µl of PCR product was mixed with 1µl pCR2.1 Topo plasmid, 1µl salt solution and water to 6µl. Reactions were incubated at room temperature for 5 minutes and then placed on ice. 3µl of the reaction was added to competent *E. coli* and the cells were transformed following standard protocols.

2.3.10 Ligation of DNA fragments

Ligations were carried out using T4 DNA ligase (New England biolabs) in 20µl reactions containing a 6:1 ratio of insert:vector DNA (unless otherwise stated), 1X T4 DNA ligase buffer (New England biolabs) 20U/µl T4 DNA Ligase and the required volume of water. Reactions were incubated at room temperature for two hours or at 16°C overnight before transformation. Ligation reactions were added directly to cells and *E. coli* were transformed using standard protocols.

2.3.11 Southern blot

Restriction digests were carried out as detailed in section 2.3.6. After digestion, 5µl of the digest was run on a 100ml 0.6% agarose gel containing 6µl Safeview for 8 hours at 20mV. After running, gels were imaged under UV. The gel was then placed in denaturation buffer – 0.4M sodium hydroxide, 0.6M sodium chloride for 30 minutes and then into neutralisation buffer – 0.5M Tris, 1.5M sodium chloride pH 7.5 for 30 minutes. Gels were blotted by capillary action overnight onto Hybond N+ nitrocellulose membrane (GE healthcare, Buckinghamshire, UK) with 20X SSC buffer. After blotting

was completed the blot was washed for 15 minutes in 2X SSC with gentle shaking. The blot was crosslinked by UV for five minutes in a Kodak GL1500 gel documentation system. The blot was then washed briefly in distilled water and placed between two pieces of hybridisation mesh. The blot was placed in a hybridisation bottle (Stuart Scientific, Staffordshire, UK) and incubated for two hours at 65°C with prehybridisation buffer – 5X SSC, 0.1% sodium N-lauryl sarcosine, 0.5g DIG luminescent detection kit blocking reagent (Roche, Basel, Switzerland), 0.02% SDS, 2% Salmon testes DNA (Sigma), 50% formamide and water to 25ml. Incubation was carried out in a SI30H hybridisation oven (Stuart Scientific).

The DNA probe for detection of specific DNA sequences on the Southern blot was produced using the Digoxygenin (DIG) PCR probe synthesis kit (Roche) following the manufacturer's instructions. PCR was performed with appropriate primers using a nucleotide mix containing dATP, dGTP, dCTP, dTTP and deoxyuridine triphosphate (dUTP) linked to DIG molecules (DIG-dUTP). A control reaction was also prepared containing only unlabelled dTTP. The reaction mixture is detailed in table 14:

Table 14. Reaction mixture for the production of DIG-labelled DNA probes for Southern blotting.

Reagent	Concentration in Probe synthesis reaction	Concentration in control reaction
10X PCR buffer	1X	1X
PCR DIG probe synthesis mix	200µM dATP, dCTP, dGTP, 130µM dTTP, 70µM DIG-dUTP	None
dNTP stock solution	None	200µM dATP, dCTP, dGTP, dTTP
Forward Primer	1pMol/µl	1pMol/µl
Reverse Primer	1pMol/µl	1pMol/µl
Enzyme Mix	0.05U/µl	0.05U/µl
Template DNA	50ng	50ng
Water	To 50µl	To 50µl

PCR conditions for the probe synthesis are shown in table 15:

Table 15. Thermocycler reaction conditions for the production of DIG-labelled DNA probes.

Temperature	Time	
95°C	2 minutes	
95°C	30 seconds	X 30 cycles
62°C	30 seconds	
72°C	40 seconds	
72°C	7 minutes	

The products of the PCR reaction were examined by agarose gel electrophoresis, the labelled reaction product was retarded in the gel due to the DIG molecules and labelling could therefore be confirmed by comparison to the unlabelled control reaction.

After incubation DNA probe was added to prehybridisation buffer at a concentration of 0.5µl/ml. Pre-hybridisation buffer was decanted from the hybridisation bottle and hybridisation buffer was added to the blot. 3.5ml of hybridisation buffer was used per 100cm^2 blot area. Hybridisation temperature (T_{hyb}) was calculated using the following formulae:

$$\mathbf{T_m = 16.6\log(molNa^+) + 0.41(\%GC) + 81.5}$$

$$\mathbf{T_{hyb} = (T_m - 25) - 36}$$

T_m is the theoretical melting temperature of the Probe:DNA duplex. $molNa^+$ refers to the molar concentration of sodium ions in the hybridisation buffer. %GC refers to the percentage guanosine-cytosine (GC) content of the probe sequence. -36 is the effect of adding 50% formamide to the hybridisation buffer. Hybridisation temperatures were optimised experimentally. The blot was hybridised overnight.

After hybridisation blot was washed with 2X SSC buffer containing 0.1% SDS twice for five minutes with shaking at room temperature in the hybridisation bottle. The blot was then washed twice for fifteen minutes at 68°C in 0.1X SSC 0.1% SDS buffer in the hybridisation oven.

After washing the blot was detected using the DIG luminescent detection kit (Roche) following the manufacturer's instructions. The blot was washed for five minutes with shaking in washing buffer – 0.1M maleic acid, 0.15M sodium chloride and 0.3% polyoxyethylene (20) sorbitan monolaurate (Tween20) pH 7.5. After washing the blot was then incubated with shaking in 1X blocking buffer (Roche) for 30 minutes. The blot was then incubated for 30 minutes in a 1:10000 dilution of Anti-digoxigenin alkaline phosphatase antibody (Roche) in blocking buffer. Once incubation was completed the blot was washed twice for 15 minutes with shaking in washing buffer. The blot was then equilibrated in 20ml detection buffer- 0.1M Tris-HCl, 0.1M sodium hydroxide pH9.5 for five minutes with shaking. After equilibration 2ml of chloro-5-substituted adamantyl-1,2-dioxetane phosphate (CSPD) (Roche) was diluted 1:100 in detection buffer. The blot was incubated for five minutes in the detection solution and then excess liquid was removed and blot incubated for 15 minutes at 37°C. Chemiluminescence was detected using a Kodak GL1500 gel documentation system, images were captured with 3 exposures of 15 minutes each and inverted final accumulation images were exported. Images were inverted.

2.4 Molecular biology techniques for Ribonucleic acid (RNA)

2.4.1 RNA extraction

Total RNA was extracted from *N. meningitidis* bacteria using the SV total RNA extraction kit (Promega) according to the manufacturer's instructions. Cells were either resuspended from plates or broth culture into 100µl TE buffer containing 0.4mg/ml Lysozyme (Sigma-Aldrich). 75µl of RNA lysis buffer was added to the resuspension and then 350µl RNA dilution buffer. 200µl of 96% ethanol was added and mixed by pipetting. The mixture was then transferred to a spin column and centrifuged at 17000xg for 1 minute. After centrifugation the spin column was washed with 600µl wash solution and centrifuged again under the same conditions. A mixture containing 40µl yellow core buffer, 5µl 0.0009M manganese chloride and 5µl DNase I was added to spin column and incubated for 15

minutes at room temperature. After the incubation 200µl of stop solution was added and the column centrifuged for 1 minute at 17000xg. 600µl of wash solution was added to the column and centrifuged as previously. 250µl wash solution was added and centrifuged and the RNA was eluted with 100µl nuclease free water.

2.4.2 Reverse Transcription-PCR

Reverse Transcriptase (RT) PCR was carried out using the Access RT-PCR system (Promega) according to the manufacturer's instructions. 50ng total RNA was mixed with 1X AMV/*Tfl* 5X reaction buffer, 0.2mM dNTP mix, 50pmol of both oligonucleotide primers, 1mM 25mM $MgSO_4$, 1µl AMV Reverse transcriptase and 1µl *Tfl* DNA polymerase. Reactions were incubated in the thermocycler using the conditions shown in table 16.

Table 16. Thermocycler reaction conditions for RT-PCR.

Temperature	Duration	
45°C	45 minutes	
94°C	2 minutes	
94°C	30 seconds	X 40 cycles
60°C	1 minute	
68°C	2 minutes	
68°C	7 minutes	

After incubation samples were examined by agarose gel electrophoresis.

2.5 Molecular biology techniques for proteins

2.5.1 OM preparation

Outer membranes were prepared from *N. meningitidis* by spheroplast lysis. Bacteria were grown overnight on blood agar plates and resuspended in 200µl of 200mM Tris-HCl, 1mM EDTA. 200µl of 200mM Tris-HCl, 1mM EDTA, 1M sucrose and the suspension mixed by inversion. 24µl of Lysozyme was added and then 400µl of sterile distilled water. The suspension was shaken on a rotary shaker for

30 minutes. Membranes were sedimented by centrifugation at 43000xg for 20 minutes. The pellet was resuspended in 800µl ice cold distilled water using a needle and syringe to homogenise the sample. The suspension was then centrifuged again under the same conditions and resuspended with a needle and syringe in 250µl ice cold distilled water.

2.5.2 Bicinchoninic assay

Bicinchoninic acid (BCA) assay was used to quantify the amount of protein in samples and was carried out using the BCA protein assay kit (Pierce, Rockford, IL, USA) following the manufacturer's instructions. Standards were produced by mixing BSA standard (Pierce) with the same buffer as was used for the samples to be tested in concentrations according to the manufacturer's instructions. 10µl of samples and standards as well as sample buffer were added to a 96-well microtitre plate (Nunc, Rochester, NY, USA). Protein assay reagent was made up by mixing reagent A (BCA detection reagent) with reagent B (4% copper sulphate solution) in a ratio of 50:1. 200µl of protein assay reagent was added to each of the samples and standards. The plate was shaken and then incubated a 37°C for 30 minutes. After incubation the plate was read in a Labsystems Multiskan MS spectrophotometer (Labsystems, Helsinki, Finland) at 577nm. A standard curve was plotted and the protein concentrations calculated from the curve.

2.5.3 SDS polyacrylamide gel electrophoresis

SDS polyacrylamide gel electrophoresis (SDS PAGE) gels were cast in two formats. For mini-gels the Bio-Rad mini-protean 3 system (Bio-rad, Hercules, CA, USA) was used. 12% resolving gels were cast using the recipe detailed in table 17.

Table 17. Recipe for the casting of mini-gels

Reagent	Quantity
3M Tris-HCl pH 8.8	0.65ml
30% acrylamide-bis solution (Bio-rad)	2ml
10% SDS solution	50µl
10% ammonium persulphate (APS) (Amresco, Solon, OH, USA)	50µl
N,N,N',N'-tetra-methyl-ethylenediamine (TEMED) (Bio-rad)	2µl
Water	2.25ml

Once the casting stand was assembled the gel was poured and covered in water saturated 2-butanol before being allowed to set. Once set the top of the gel was rinsed with distilled water and dried with filter paper (Millepore). The stacking gel was poured using the recipe in table 18.

Table 18. Recipe for the casting of stacking gel for mini-gels

Reagent	Quantity
0.5M Tris-HCl pH 6.8	0.65ml
30% acrylamide-bis solution	0.325ml
10% SDS solution	25µl
10% APS	25µl
TEMED	1µl
Water	1.3µl

After the gel had set the comb was removed and the wells washed with distilled water. The amount of protein in each sample was tested with the BCA assay and the samples equalised for protein content. Samples were suspended in a 2X sample buffer containing 10%w/v sucrose, 5%v/v 2-mercaptoethanol, 4ml 10% SDS , 200µl 10% APS, 15ml 1M Tris-HCl pH7.2 and 0.01g bromophenol blue (Amersham biosciences) at 1X sample buffer concentration. Samples were then boiled in sample buffer at 95°C for five minutes before loading. Gels were run in running buffer containing 0.4M glycine, 0.1M Tris and 7mM SDS at 200V for 40-60 minutes, until the dye front reached the bottom of the gel.

Large gels were cast on the Bio-rad Protean II xi system (Bio-rad). Large gels were poured using the recipe shown in table 19:

Table 19. Recipe for the casting of large gels

Reagent	Quantity
3M Tris-HCl pH 8.8	6.25ml
30% acrylamide-bis solution	20ml
10% SDS solution	0.5ml
10% APS	0.5ml
TEMED	20µl
Water	23.25ml

Gels were poured by the same method as mini-gels. The stacking gel was made up using the recipe in table 20:

Table 20. Recipe for the casting of stacking gel for the large gels.

Reagent	Quantity
0.5M Tris-HCl pH 6.8	7.5ml
30% acrylamide-bis solution	2.6ml
10% SDS solution	200µl
10% APS	200µl
TEMED	8µl
Water	7ml

Large gels were loaded and run using the same buffers as small gels. Gels were run at 10mA overnight or until the dye front reached the bottom of the gel.

After electrophoresis all gels were removed from the casting plates and placed into Coomassie blue solution. Gels were stained with Coomassie for 4-24 hours (mini gels) or 24-48 hours (large gels) incubation with gentle shaking. Once stained, the gels were destained with destain solution containing 45% v/v methanol and 10% v/v acetic acid in water. Gels were destained until bands became sufficiently clear. Gels were photographed on the Kodak 1500 gel documentation system under white light.

2.5.4 Formaldehyde crosslinking and SDS PAGE

The formaldehyde crosslinking method was adapted from Sanchez et al (119). The amount of protein in the samples was tested with the BCA assay and the protein amounts in each sample were equalised. Preparations of outer membrane were resuspended in PBS containing 1% v/v formaldehyde. Samples were incubated at room temperature for 10 minutes, 1ml of PBS was then added to preparations and the samples were centrifuged for 20 minutes at 17000xg. Supernatant was removed and the samples resuspended in PBS without formaldehyde. Control preparations were treated in the same way but formaldehyde was not included in the incubation step. For SDS PAGE samples were suspended in 2X sample buffer that did not contain 2-mercaptoethanol and were incubated for 20 minutes at 37°C before loading. Samples were loaded onto a large 8% SDS-PAGE gel and run at 10mA for 24 hours. Gels were stained with Coomassie blue and imaged following the same protocol as other SDS PAGE gels. Band identification was carried out using the Kodak MI software (Kodak) using the automated band finder tool. The conditions for the identification of bands were the same for all gel lanes.

2.6 Immunological techniques

2.6.1 Western blotting

For western blotting, SDS PAGE gels were created and electrophoresed as previously described. When electrophoresis was complete, gels were assembled into the transblotting apparatus, Bio-rad trans-blot cell (Bio-rad), with Hybond P polyvinylidine fluoride (PVDF) membrane (GE Healthcare). The trans-blot cell was filled with transblotting buffer- 25mM Tris, 0.2M glycine, 20% methanol and the blot was run at 10mA overnight. After blotting the gel was discarded and the membrane incubated in blocking buffer- TBS with 5% (w/v) Marvel milk powder (Premier International foods, Lincolnshire, UK) for one hour with gentle shaking. After incubation the membrane was incubated with primary monoclonal antibody against the P3.15 epitope of the PorB protein- National Institute of Biological

Standards and Control (NIBSC) Number 02/310 (NIBSC, Hertfordshire, UK). Antibody was diluted 1:1000 in blocking buffer and incubation was carried out for 2 hours at room temperature with gentle shaking. After incubation the membrane was washed three times for ten minutes duration each in TBS. Secondary antibody was then applied, Anti-mouse horseradish peroxidise (HRP) conjugated antibody (Sigma-Aldrich) was diluted 1:2000 in blocking buffer and incubated with the membrane for one hour at room temperature with shaking. The wash step was then repeated. 3,3 diaminobenzene (DAB) tablets were used for detection of the bands according to the manufacturer's instructions. The DAB solution was added to the membrane and allowed to incubate for 5-10 minutes until sufficient colour had appeared. The membrane was then rinsed with water to stop the reaction. The membrane was photographed under white light using the Kodak gel logic 1500 gel documentation system.

2.6.2 Slot blotting and immunoassay

Native OMVs were prepared and used for slot blotting and immunoassay for the proteins PorA (epitopes P1.7 and P1.16) and PorB. For slot blotting samples were diluted in TBS buffer. Purified PorA and PorB proteins were used as standards and diluted in the same buffer. Slot blotting was performed on the Minifold II slot blotting system (Schleider and Shuell, Dassel, Germany). 400µl of sample was blotted and the wells washed with 400µl TBS. After blotting the apparatus was disassembled and the membrane was incubated for one hour in blocking buffer- 5% Marvel milk powder in TBS. Primary antibody for PorA P1.7 (NIBSC number 01/514) (NIBSC), P1.16 (NIBSC number 01/538) (NIBSC) and PorB was diluted in blocking buffer to a concentration of 1:250. Blots were incubated with primary antibody for 1 hour and then washed for 5 minutes in TBS. The wash step was repeated three times. Anti-mouse HRP conjugated secondary antibody was diluted in blocking solution to 1:2000 and was added to the blots. After a one hour incubation with secondary antibody the blots were washed with TBS for 10 minutes and the wash step repeated three times. Blots were detected with SuperSignal west PICO chemiluminescent substrate (Pierce) according to the manufacturer's instructions. Luminol/Enhancer solution was mixed in equal parts with stable

peroxide solution. The blot was incubated with the solution for 5 minutes before being imaged in the KODAK gel logic 1500 gel documentation system. Three 5 minute exposures were taken and the final accumulation was exported. Blots were analysed using the KODAK MI analysis software (KODAK) for calculation of protein amounts. Region of interest (ROI) analysis was used to estimate brightness of standards and samples. Protein mass in the bands was calculated using mass curve analysis in the software.

2.7 Microscopy

2.7.1 Preparation of bacteria by Gram staining

Bacteria were Gram stained using a Gram stain for films kit (Sigma-Aldrich). Bacteria were grown in broth overnight under the required conditions and a 5µl drop of the resultant culture was smeared onto glass slides (BDH) using a loop. The smears were allowed to dry and the slide was then flooded with 100% methanol for two minutes to fix the bacteria. Methanol was then poured from the slide and the slide allowed to dry. Fixed films were flooded with crystal violet solution for 1 minute and then rinsed with water. Gram's iodine solution was added to the slides for 1 minute and the slide was again rinsed. Decolouriser solution was run across the slide until it ran clear and the slide was rinsed again. Carbol fuschin counterstain was then applied for 1 minute and the slide was rinsed before being air dried.

2.7.2 Light microscopy

Slides were examined with an Olympus CX41 microscope (Olympus, Tokyo, Japan) under a 100X oil immersion objective using immersion oil (Olympus). Images were captured on an Olympus U-CMAD 3 camera using the analySIS soft imaging system version 5 software (Olympus). Four images were taken on each slide at different locations. Experiments were repeated to ensure consistency.

2.7.3 Vitreous Thin Film preparation

For vitreous thin film (VTF) microscopy bacteria were prepared by two methods. In the first method bacteria were scraped from overnight plate growth and resuspended in PBS to an OD_{600}=13.2. 3-4µl of this suspension was spotted onto the grid before freezing. In the second method bacteria were scraped from overnight plate growth and resuspended in Mueller Hinton broth. 5µl drops of bacterial suspension were placed on parafilm (SPI supplies, West Chester, PA, USA). Grids were floated on these drops and incubated at 37°C for ≈ 5 minutes. After incubation the grids were taken from the drops and placed into the freezing apparatus. For both methods grids were frozen on a Leica EM CPC (Leica, Vienna, Austria) plunge freezing apparatus. Grids were blotted for 3-6 seconds and frozen in liquid ethane (BOC gases, Guilford, UK).

2.7.4 Cryo-transmission electron microscopy (Cryo-TEM)

After freezing grids were kept under liquid nitrogen and transferred to a Gatan 914 cryo specimen holder (Gatan, Pleasanton, CA, USA). Grids were examined in a Jeol JEM 2100 transmission electron microscope (JEOL, Tokyo, Japan) at 200kV. Images were taken with a Gatan 4K/4K CCD camera (Gatan) using the digital micrograph software (Gatan). Several sites were examined on each grid and experiments were repeated to ensure consistency.

2.7.5 Measurement of vesicles

Vesicle areas and perimeters were measured using the ImageJ software (http://rsb.info.nih.gov/ij, National Institutes of Health, Bethesda, MD, USA). Images were divided into grids using the grid feature of the software. Grid squares were chosen using an atmospheric noise random number generator (http://www.random.org/ Dublin, Ireland). Forty-five vesicles were selected by this method from vesicles imbedded in ice holes only. Vesicles were measured with the manual measuring tool, calibrated using the scale bar.

2.8 Statistics

2.8.1 Student's T-test

Pair wise comparison was carried out using a two tailed independent Student's t-test (T-test) (173) performed using Microsoft Excel software (Microsoft, Redmond, WA, USA). Groups contained at least three repetitions of the same experiment. Significance level was set at $P \leq 0.05$. Normal distribution of the data for the wildtype samples and the measurements of OMVs was tested using the Shapiro-Wilk test with an alpha level of P=0.05 (128). Where unequal variance of the samples was shown by F-test a Welch's T-test was used.

2.8.2 F-test for equality of two standard deviations

Comparison of variance was carried out using the F-test for equality of two standard deviations (F-test) (131) contained in the Microsoft Excel software. The test was two tailed and the level of significance for the F-statistic was set at 0.05.

Chapter 3- Investigation into phenotype and vesicle production of an H44/76 Δ*gna33* strain

3.1 Introduction

The genome derived neisserial antigen 33 (*gna33)* gene was first discovered in a genome wide search for candidate antigens for group B *N. meningitidis* vaccine, and the gene was found to be highly conserved amongst *N. meningitidis* strains (109). The *gna33* gene is 1326bp long and lies at position 32236-30911 in the *N. meningitidis* MC58 genome. Little is known about expression of *gna33* and it has not been shown to be part of any operon. The gene encodes a 441 amino acid 47kDa protein, containing an N-terminal 20 amino acid consensus lipopolypeptide signal sequence (65). The signal sequence has also been shown to be involved in gene expression by exerting a negative effect at the transcriptional/post transcriptional level through the formation of secondary structure in the mRNA (126). The *gna33* gene was shown to encode a lipoprotein that showed 41.3% amino acid homology to the *E. coli* membrane bound lytic transglycosylase enzyme MltA. Recombinantly expressed GNA33 protein has been demonstrated to have lytic transglycosylase activity (65). In addition to MltA *E. coli* contains several membrane bound lytic transglycosylases, the proteins MltB, MltC, MltD, EmtA and MltF (26,73,125). These enzymes show partial functional redundancy and *E. coli mltA* deletion mutants show no obvious phenotype (81). Sequence homologues of *mltB*, *mltC* and *mltD* have been found in the *N. meningitidis* genome (65).

A Δ*gna33* strain was created by Adu Bobie et al. in three *N. meningitidis* backgrounds, MC58, NMB and BZ232. The knockout mutant showed phenotypic changes including an attenuation of virulence in the infant rat model, decrease in growth rate and failure of the outer membrane of daughter cells to separate in cell division (2). A release of outer membrane proteins into the media was also noted, this was later shown to be caused by an increase in the release of outer membrane vesicles (37). The phenotypic changes in the Δ*gna33* strain suggest that the lytic transglycosylases of *N. meningitidis* do not show the same functional redundancy as those of *E. coli.*

The aim of this study was to investigate the phenotype of a *Δgna33* mutant in the *N. meningitidis* H44/76 strain and compare it to the phenotypes previously reported in *Δgna33* mutants in other strain backgrounds. H44/76 is an *N. meningitidis* group B strain, it has been used to manufacture an OMV vaccine and the strain and its vesicles have been extensively studied. H44/76 is also relatively easy to transform with plasmid DNA compared to other strains, justifying its use in this study. The strain was used to study the vesicle releasing phenotype of the *Δgna33* mutant in more detail, comparing the levels of vesiculation and the size and shape of the vesicles released by the wildtype and *Δgna33* mutant.

3.2 Construction of a recombination cassette to knock out *gna33*

The cloning strategy used for deleting the *gna33* gene in the H44/76 strain was adapted from the approach used to construct *Δgna33* mutant in the MC58 strain by Adu-Bobie et al (2). Homologous recombination at two sites flanking the *gna33* gene was used to replace *gna33* in the genome with an antibiotic resistance gene. Exchange of regions of identical sequence is catalysed in Gram negative bacteria by enzymes of the RecABCD pathway and the *E. coli* genes that encode these enzymes have homologues in the *N. meningitidis* genome (30,76). In the strategy used, the amplified flanking sequences were the same as those used in the construction of the MC58 *Δgna33* mutant by Adu-Bobie et al, but the cloning strategy differed in the following ways: A kanamycin antibiotic resistance gene was used in place of the erythromycin resistance gene and a pUC19 vector was used instead of a pBluescript vector. The restriction enzymes *EcoRI*, *BamHI* and *HindIII* were used in place of the enzymes *XbaI*, *SmaI* and *XhoI*.

Amplification and topo cloning of the sequences flanking the *gna33* gene were successful. Subcloning of the downstream sequence into the pUC19 vector backbone was also achieved. However, repeated subcloning of the upstream fragment only produced plasmids containing the insert in the reverse

orientation. As a contingency the plasmid pBSUDGNA33ERM used for the construction of the MC58 *Δgna33* strain by Adu-Bobie et al was obtained and used to transform H44/76.

3.3 Transformation of the *gna33* knockout cassette

The plasmid pBSUDGNA33ERM contains the erythromycin resistance gene *ermC*, flanked by sequences homologous to the sequences upstream and downstream of the *gna33* gene. A DNA uptake sequence for *N. meningitidis* was included in the downstream flanking sequence (fig. 1) (2). For the production of the MC58 *Δgna33* mutant the whole plasmid was transformed into *N. meningitidis;* this method was also used for the H44/76 strain. Transformation of whole plasmid provided several possible options for homologous recombination. A double crossover at both the upstream and downstream regions of homology would replace *gna33* with the cassette containing the *ermC* gene (fig.1b). However homologous recombination involving only one of the two regions of homology (single crossover) would result in the complete plasmid being inserted into the genome. This would be either upstream or downstream (relative to the direction of transcription) of *gna33* (fig.4 pg. 68).

A. Plasmid used for crossover

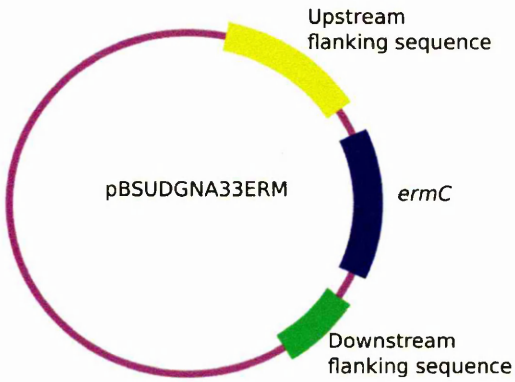

B. Double crossover

PCR reaction	Length (bp)
PCR 1 (TF-TR)	No product
PCR 2 (TF-2F)	1384bp
PCR 3 (3R-SF1)	1762bp
PCR 4 (T3-TR)	No product

Figure 1. Plasmid pBSUDGNA33ERM and map of double crossover recombination in *N. meningitidis*. (A) Map of the pBSUDGNA33ERM plasmid used for the transformation. (B) Double crossover produces a complete knock out of the *gna33* gene and replacement with the Erythromycin resistance (*ermC*) cassette. Binding sites for primers used to test for double crossover recombination are shown. The table shows bands produced by PCR reactions used to discriminate the different recombinants.

An MC58 strain was transformed with the plasmid to test the production of double crossover mutants using the transformation protocol. Successful recombinants were selected by growth on erythromycin containing media. The transformation of the MC58 strain produced many colonies and four colonies were tested using PCR. Double crossover recombination was a common event in MC58 transformation and all the colonies tested showed the correct band pattern (fig. 2).

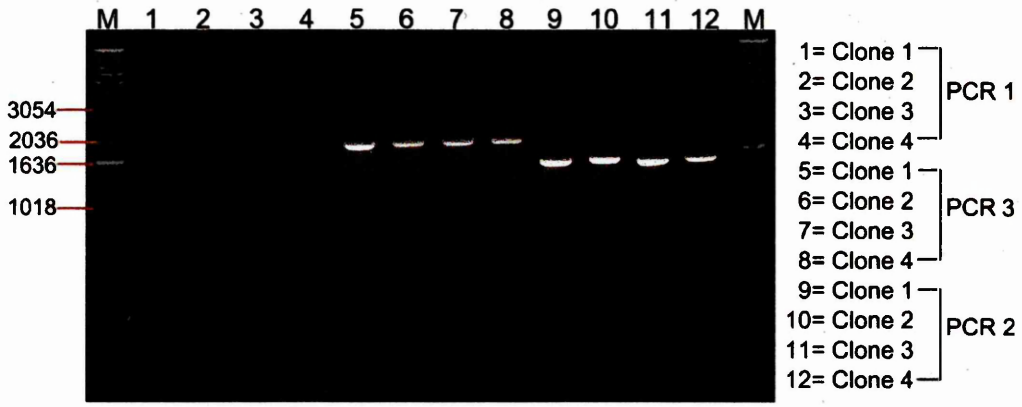

Figure 2. Colony PCR of clones from pBSUDGNA33 transformation into *N. meningitidis* MC58. Clones 1-4 were tested using PCR1 (Lanes 1-4) where no product is expected, PCR3 (Lanes 5-8) with an expected band of 1762bp and PCR2 (Lanes 9-12) with an expected band size of 1384bp.

Transformation of H44/76 strain also produced many colonies. Of three clones screened by PCR (fig.3), two clones (Clone 1 and 3) showed the correct band pattern for a double crossover in PCR 1 (no band) but in PCR 2 and PCR 4 these clones produced bands not expected in a double crossover, a band of 1.8kilo base (kb) instead of 1.4kb in PCR 2 and a band of 2kb in PCR 4 where no band was expected. PCR 3 did not produce a clear result for these clones and so was not used.

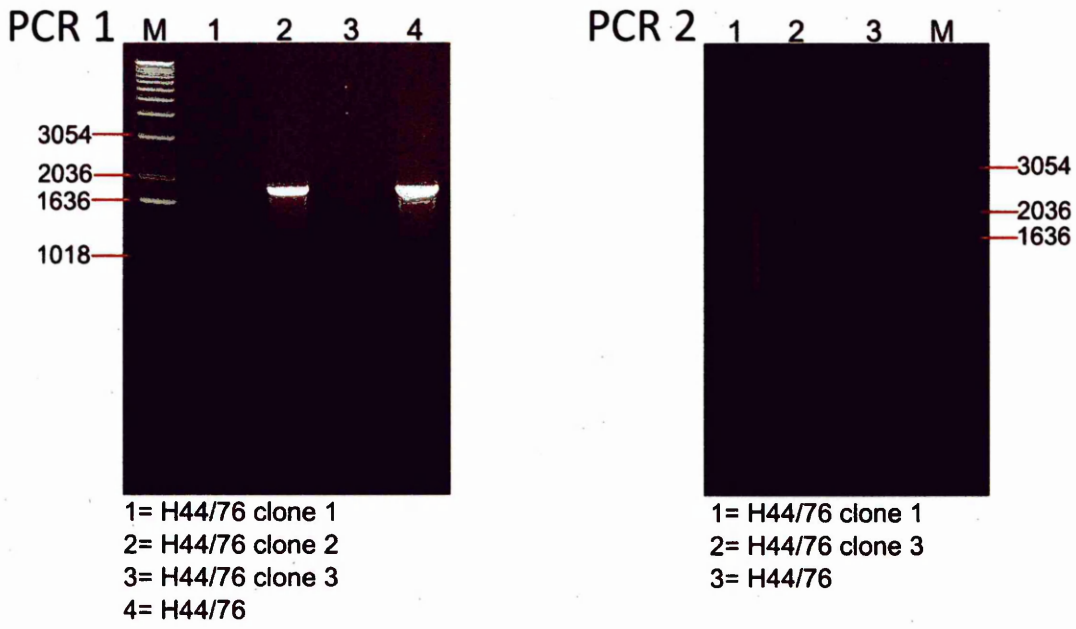

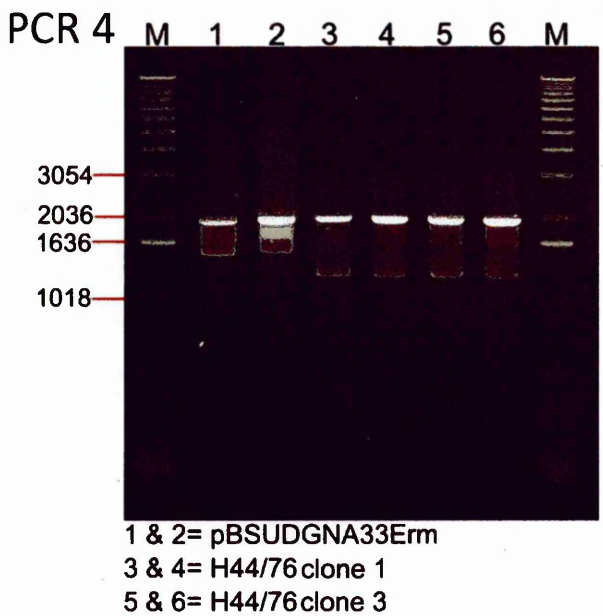

Figure 3. PCR for clones produced by transformation of pBSUDGNA33ERM into *N. meningitidis* H44/76. PCR1: PCR for three clones (lane 1-3) and wildtype H44/76 as a positive control (Lane 4) using the PCR1 primers. PCR2: PCR for clones 1 and 3 (lanes 1 and 2) and a wildtype negative control (lane 3) with PCR2 primers. PCR 4: PCR for clone 1 (lanes 3 and 4), clone 3 (lanes 5 and 6) and pBSUDGNA33ERM as a positive control (lanes 1 and 2) with the PCR 4 primers.

The results of the PCR confirmed that the H44/76 clones were not double crossover mutants but the presence of erythromycin resistance in the clones indicated that the plasmid had integrated into the genomic DNA. Maps and PCR results from the predicted single crossover options were calculated (fig. 4).

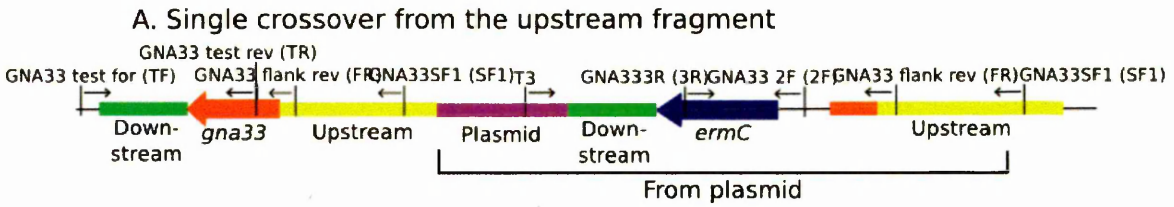

PCR reaction	Length (bp)
PCR 1 (TF-TR)	1824bp
PCR 2 (TF-2F)	7501bp
PCR 3 (3R-SF1)	2191bp
PCR 4 (T3-TR)	N/A

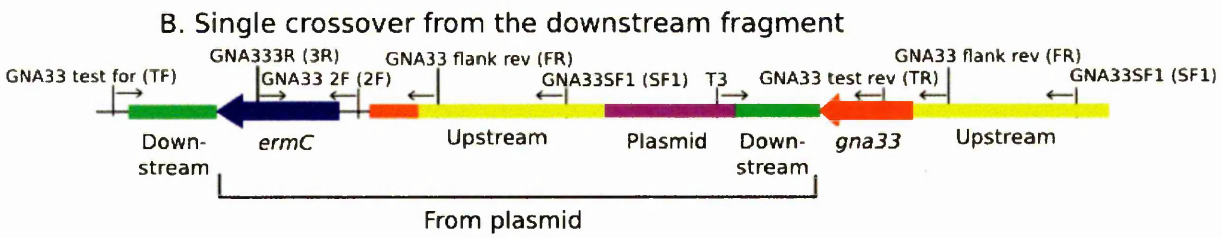

PCR reaction	Length (bp)
PCR 1 (TF-TR)	7372bp
PCR 2 (TF-2F)	1563bp
PCR 3 (3R-SF1)	2191bp
PCR 4 (T3-TR)	1979bp

Figure 4. Single crossovers of pBSUDGNA33ERM into the *N. meningitidis* genome. Single crossovers could occur at the upstream or downstream regions of homology in the *gna33* recombination cassette. (A) Single crossover recombination at the upstream region of homology. (B) Single crossover recombination at the downstream region of homology. PCR results for the PCR reactions used to discriminate the crossover types are shown in the tables.

The bands produced by PCR of clones 1 and 3 corresponded to the predicted sizes of bands in a downstream single crossover. The 2kb band in PCR4 showed the presence of a binding site for the T3 primer indicating that these clones contained linearised plasmid. The lack of a band in PCR 1 was due to the size of the band that would be amplified from a downstream single crossover (7.3kb), with an extension time of three minutes this is unlikely to be produced. However, the 1.8kb band in PCR2 was larger than the expected 1.5kb band for this crossover.

To confirm the downstream single crossover a southern blot for *gna33* was performed. Genomic DNA from a H44/76 *gna33* clone (clone 1), the *Δgna33* MC58 strain and the wildtype for both strains were

digested with *PstI* and subjected to Southern blotting. Blotted membranes were probed with a digoxigenin labelled probe for *gna33*, produced using PCR with genomic DNA from wildtype H44/76 as the template. Measurement of probe luminescence showed that *gna33* clone 1 contained a band matching the predicted size for a single downstream crossover. There was no band in the MC58 *Δgna33* mutant showing that as expected it did not contain a *gna33* gene. In the wildtype strains there were no *PstI* sites in the region of the *gna33* gene so large fragments were produced.

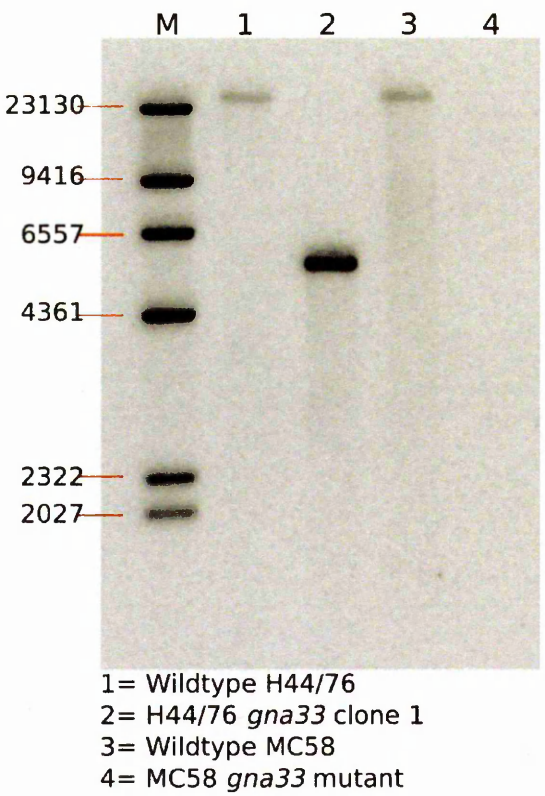

Genomic DNA	**Expected GNA33 fragment (PstI digestion)**
Wildtype (MC58/ H44/76)	31711bp
MC58 *Δgna33* (*gna33* mutant)	No fragment
gna33 upstream single crossover	35816bp
gna33 downstream single crossover	5505bp

Figure 5. Southern blot for *gna33* gene. Genomic DNA digested with *PstI* from the strains wildtype H44/76 (lane 1), H44/76 *gna33* clone 1 (lane 2), Wildtype MC58 (lane 3) and MC58 *Δgna33* (Lane 4). Blots were probed with a DNA probe for the *gna33* gene using a hybridisation temperature of 57°C.

Repeated transformations of H44/76 with the plasmid produced only single crossovers (data not shown). To increase the likelihood of a double crossover event the plasmid was linearised before transformation but this also only produced a mixture of upstream and downstream single crossovers.

Despite the ease of producing double crossover mutants in MC58 by this method, H44/76 did not produce double crossover mutants.

To generate a double crossover mutant an alternative approach was used, transforming the H44/76 wildtype strain with genomic DNA from the MC58 *Δgna33* strain. Homologous recombination between the genomic DNA of the two strains should result in the insertion of the erythromycin resistance gene into *gna33* in the H44/76 genome. Transformation produced erythromycin resistant colonies and PCR of the transformants showed that the band sizes were correct for a double crossover mutant (data not shown). Three of the clones were selected for southern blotting using the probe for the *gna33* gene. No band corresponding to *gna33* was seen, demonstrating that the *gna33* gene had been successfully knocked out (fig.6a). The clones were then backcrossed twice against wildtype H44/76 to ensure that the knockout of *gna33* was the only genetic change introduced from the MC58 genomic DNA. Finally the region across the insertion was amplified by PCR and sequenced (fig.6b); this confirmed the region was correct.

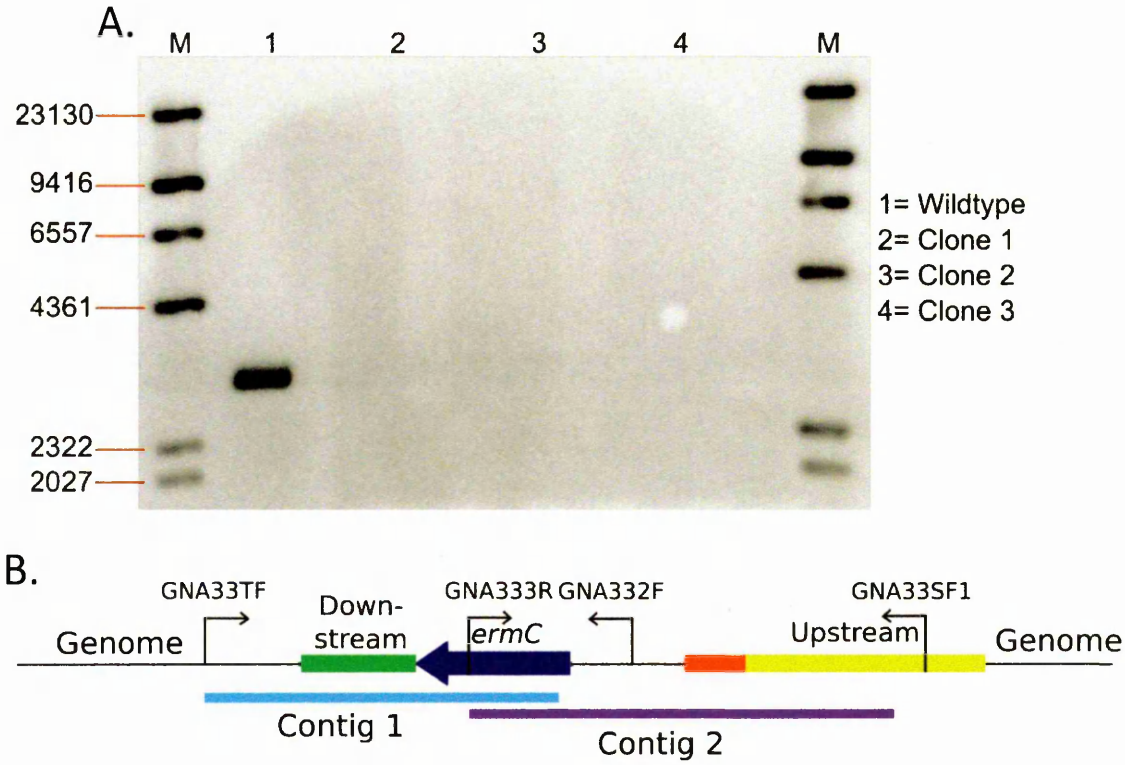

Figure 6. Backcross of genomic DNA from MC58 *Δgna33* strain into H44/76. (A) Southern blot of genomic DNA. Lane 1 Positive control Wildtype H44/76 genomic DNA digested with *PstI/AclI*. Lanes 2-4 clones 1-3 from backcross of H44/76 with MC58 *Δgna33* genomic DNA digested with *PstI*. (B) Diagram of sequencing of the *Δgna33* clone. Primers used in sequencing are marked with arrows showing direction of extension from the primers. Regions of sequencing contigs are shown by bars.

3.4 RNA production in the *gna33* mutants

To confirm that the disruption of *gna33* resulted in the loss of transcription, the *Δgna33* H44/76 strain was tested by RT-PCR for expression of *gna33* mRNA. Glucose-6-phosphate dehydrogenase (*gdh*) and *porA* mRNAs were used as controls to ensure even loading of total RNA. The Gdh protein has an important metabolic function in glucose metabolism and this should have ensured that it was consistently expressed. The *porA* gene is highly expressed and therefore easily detected, but as the PorA protein is known to have variable expression levels (152) the two control reactions were compared to each other (fig.7). Both mRNA species were expressed consistently across all the strains tested. The *porA* mRNA produced a clear band with fewer non-specific bands than the *gdh* RT-PCR and was used for the majority of further RT-PCR experiments.

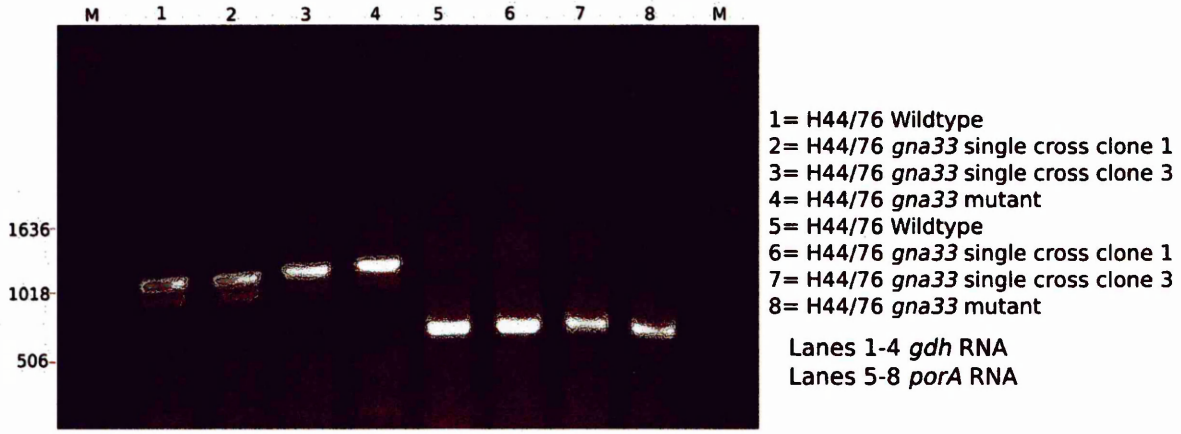

Figure 7. RT-PCR comparison of *gdh* and *porA* for use as controls. RT-PCR was performed on the *gdh* and *porA* RNA in the wildtype, *gna33* single crossover and *Δgna33* (*gna33* mutant) H44/76 strains. Lanes 1-4 show *gdh* RNA. Lanes 5-8 show *porA* RNA.

The RT-PCR for *gna33* RNA showed that the wildtype and *gna33* downstream single crossover mutants were producing *gna33* RNA as expected. The *Δgna33* mutant was not producing *gna33* mRNA, confirming that the *gna33* gene was not being expressed (fig. 8).

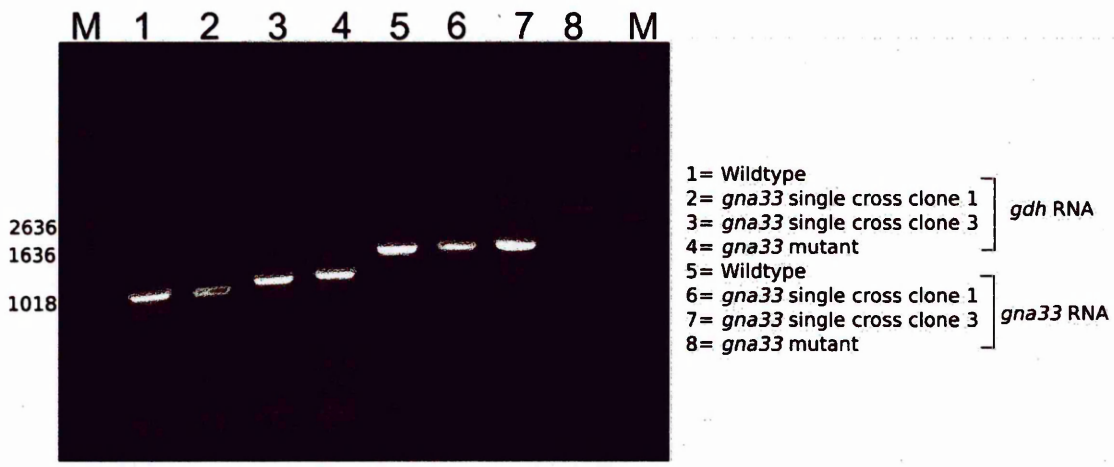

Figure 8. RT-PCR for *gna33* RNA in *gna33* mutants of H44/76. Production of control RNA from *gdh* gene is shown in lanes 1-4. Production of *gna33* RNA from wildtype and single crossover mutants is shown in lanes 5-7. Production of *gna33* RNA from the *Δgna33* mutant (*gna33* mutant) is shown in lane 8.

Previous RT-PCR experiments were performed on RNA extracted from bacteria grown in liquid culture. To test if the culture conditions changed the expression of *gna33* RNA, RT-PCR was also performed on bacteria grown on solid media (blood agar plates). Both downstream single crossover

gna33 mutants showed low or undetectable levels of RNA when grown on solid media (fig.9), despite showing normal RNA expression in liquid culture. Wildtype strain showed *gna33* expression regardless of the growth media.

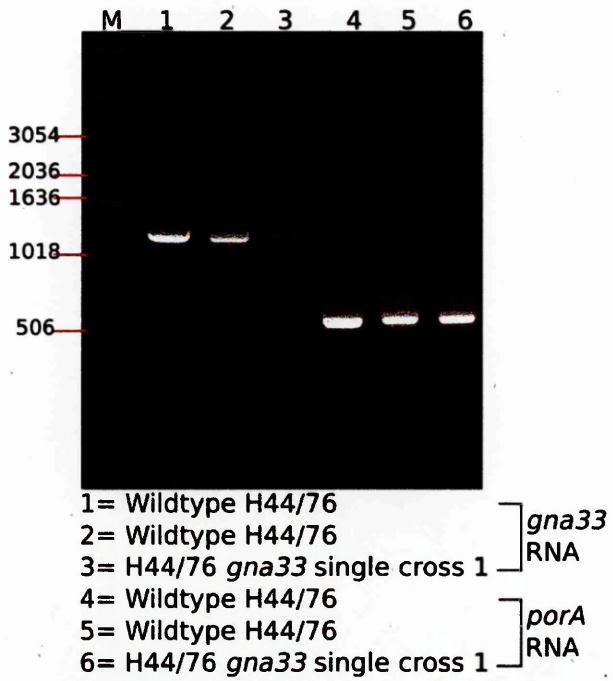

Figure 9. RT-PCR for *gna33* RNA in *gna33* single crossover 1 grown on solid media. Expression of *gna33* in wildtype bacteria grown on solid media is shown in lanes 1 and 2. Production from *gna33* single crossover mutant is shown in lane 3. Control for RNA levels (*porA*) is shown in lanes 4-6.

The result of a downstream single crossover was the introduction of the plasmid (including the *ermC* gene) into the genome and duplication of the upstream and downstream flanking regions of the *gna33* gene. Sequence beyond the downstream flanking region of *gna33* has been altered, with plasmid sequence inserted into the region. In the upstream single crossover the same sequences have been inserted and duplicated, but the plasmid sequence was inserted upstream rather than downstream of *gna33.* RNA analysis of this strain showed that it produced normal levels of *gna33* mRNA both on solid media and in liquid culture (data not shown), suggesting that it must be factors downstream of *gna33* that are affecting expression. Varying *gna33* expression levels in different

media indicates that the GNA33 protein is beneficial to the organism in liquid culture. This would be consistent with the poor growth in liquid culture observed in the MC58 *Δgna33* strain (2).

3.5 Growth of *N. meningitidis gna33* mutants

The *Δgna33* mutant has been reported to grow slower than the wildtype due to an increased doubling time when measured by optical density and colony forming units per ml (CFU/ml) (2). Growth curves were produced using the H44/76 *Δgna33* strain and the *gna33* downstream single crossover mutant (referred to as the single crossover mutant). Growth of H44/76 *Δgna33* was slow and the mutant strain reached a much lower OD_{600} after 8 hours than the wildtype (fig.10).

Increased osmotic pressure is a stress factor for organisms grown in liquid culture. A number of factors, including the increase of *gna33* expression when the single crossover was grown in liquid media, the function of GNA33 in maintaining the peptidoglycan and the slow growth of the *Δgna33* strain suggested that osmotic pressure may affect the *Δgna33* mutant more than the wildtype. Sodium chloride has been used previously to change the osmotic potential of bacterial growth media (32) and was chosen as an additive to test if changing osmotic potential could rescue the phenotype of *Δgna33* and restore growth to wildtype levels. The level of sodium chloride used was determined empirically with 0.5% v/v being found to be optimal for growth.

Addition of sodium chloride to the medium improved the growth of both the wildtype and *Δgna33* mutant strains but did not restore the growth of the *Δgna33* strain to wildtype levels (fig. 10). The mean growth rate constant in the exponential phase (μ) of both strains showed improvement; from 0.33 to 0.38 in the wildtype strain and 0.23 to 0.32 in the *Δgna33* mutant. This change was not significant in the wildtype when compared by T-test (P=>0.05) but was significant for the *Δgna33* mutant (P=<0.001). When the control and sodium chloride supplemented cultures were compared at the eight hour time point the wildtype values were not significantly different (P=>0.05), but the *Δgna33* strain did show a significant difference (P=<0.05). The improvement of the *Δgna33* mutant

was greater than that of the wildtype; indicating that the strain did suffer increased osmotic instability. However if the H44/76 *Δgna33* strain, like the MC58 *Δgna33* strain, showed a clustering phenotype then comparisons by optical density would be affected by the change in particle size. This could be the primary cause of the difference in optical density, reflecting a change in morphology rather than a difference in growth of the organisms.

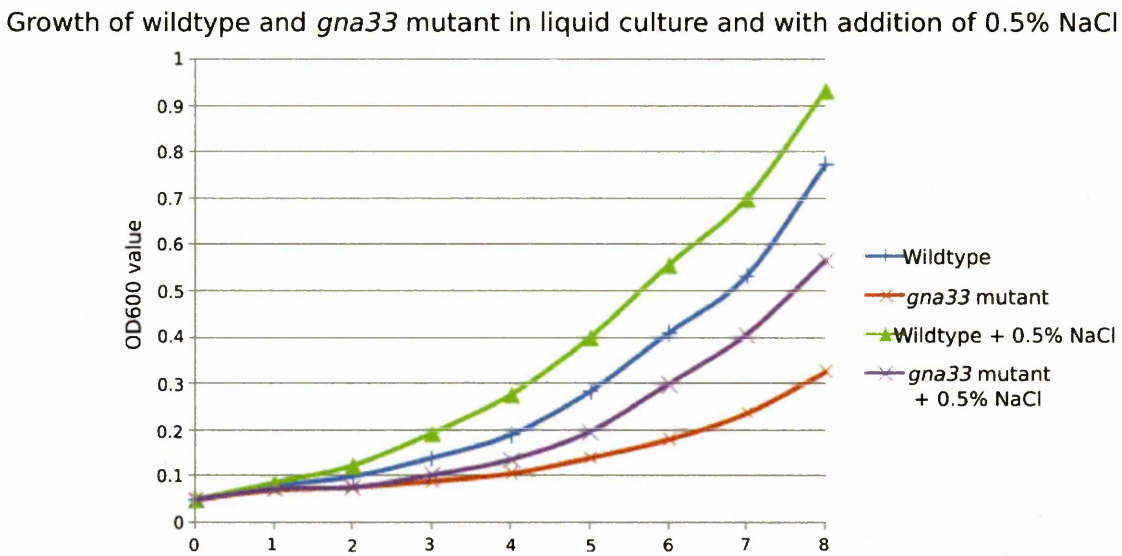

Figure 10. Growth of wildtype and *Δgna33* (*gna33* mutant) strain with and without 0.5% sodium chloride in the growth media. Bacteria were grown in liquid culture for an eight hour period in media that contained 0.5% sodium chloride or control media that did not. Measurements of OD_{600} were used as a surrogate of growth. Curves represent the mean of three experiments.

Growth of the wildtype and single crossover *gna33* mutants were similar and the OD_{600} values after eight hours growth were not significantly different (P=>0.05). The single crossover mutant produced wildtype levels of *gna33* RNA in liquid culture so was expected to grow normally (fig.11).

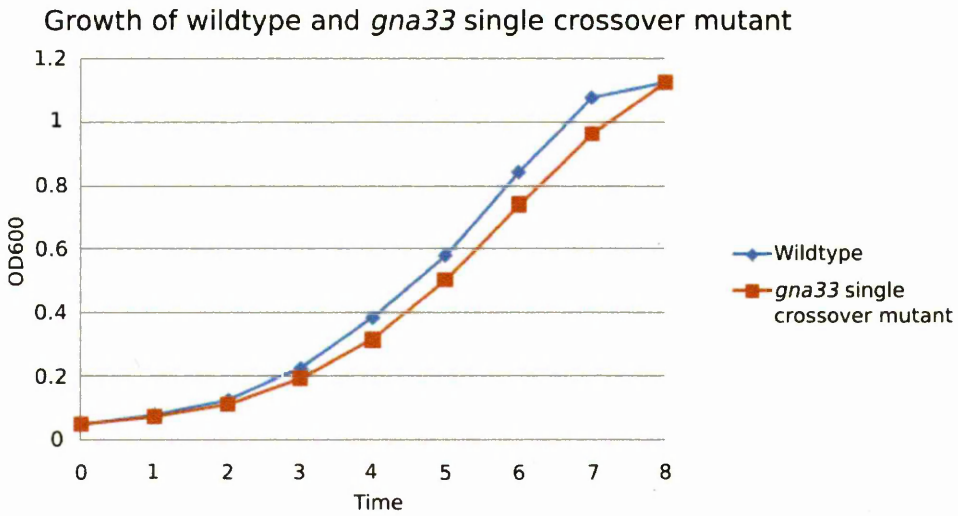

Figure 11. Growth curve of wildtype and *gna33* single crossover mutant. Growth curves taken over eight hours of growth in liquid culture. Measurements of OD_{600} were used as a surrogate of growth. Curves represent the mean of three experiments.

3.6 Cryo-Electron microscopy of whole organism wildtype and *gna33* mutants

To examine the morphology of the H44/76 *gna33* mutant strains VTF cryo-electron microscopy was used. This rapid freezing technique does not allow the water in the sample to crystallize, so structures are embedded in vitreous 'water like' ice. This preserves the bacteria in their hydrated state and reduces artifacts associated with other traditional electron microscopy techniques (3).

Wildtype bacteria were observed either as diplococcal or coccal forms (fig.12). Some distended forms (G) were observed but these were likely artefactual and caused by the position of the bacteria between the carbon film and the ice hole. The number of coccal forms observed indicated some natural variation in the shape of the bacteria. Misshapen bacteria were also observed (I and J), these were likely to be dead and degraded bacteria. The misshapen forms increased when the bacteria were left at room temperature in PBS for longer periods before freezing.

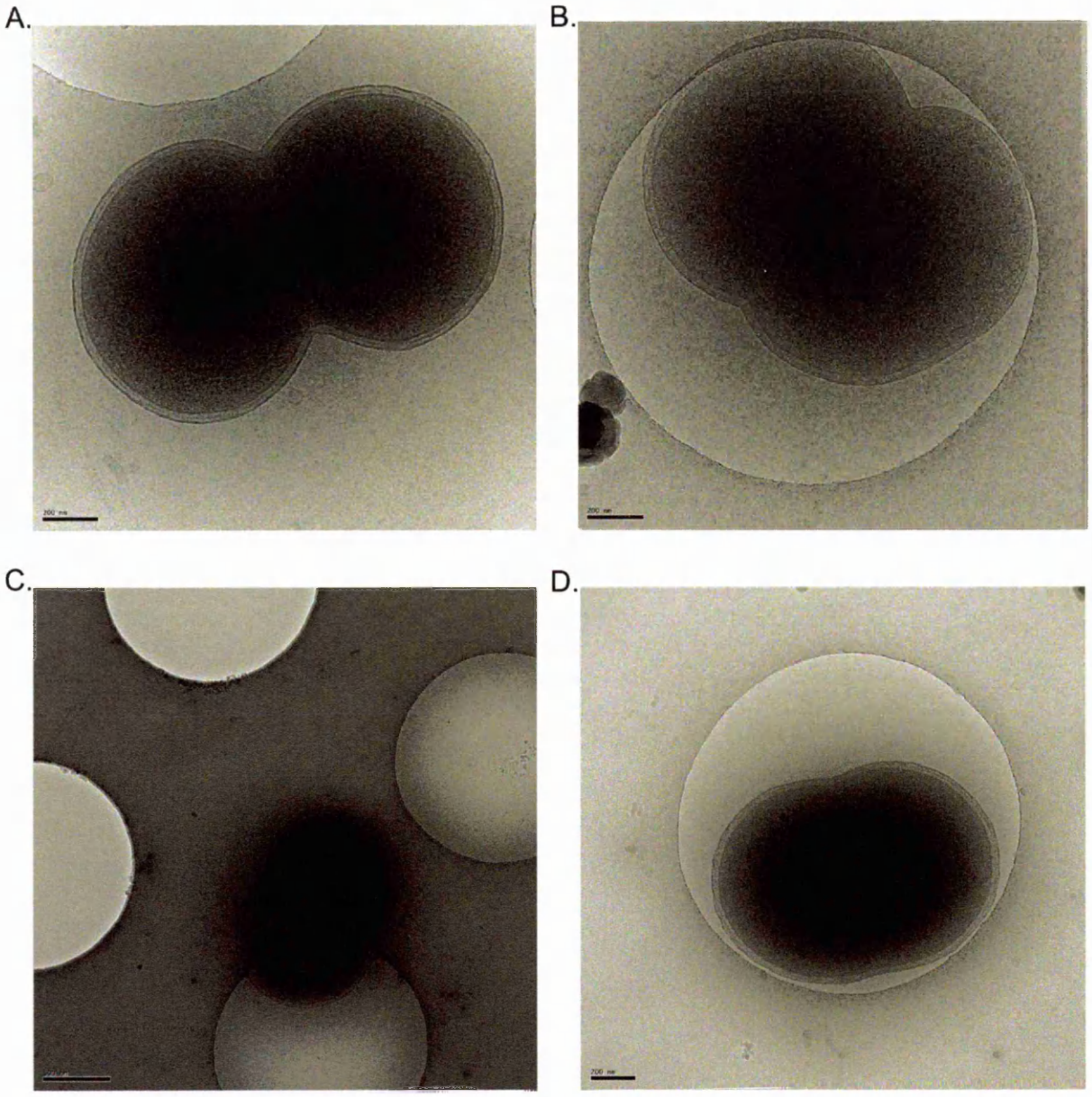

Figure 12. Cryo-electron microscopy of *N. meningitidis* H44/76. The wildtype strain was examined by VTF-Cryo-Electron microscopy for comparison to the mutant strains. (A) (C) (B) (D) Bacteria were observed in the expected diplococcal shape. Lighter circles on grid surfaces were holes in the surface carbon film to allow sample to be observed in vitreous ice without the underlying support film. (A) and (B) 25,000X 200kV (C) 12,000X 200kV (D)20,000X 200kV. (A), (B), (D) Scale bar 200nm. (C) Scale bar 500nm.

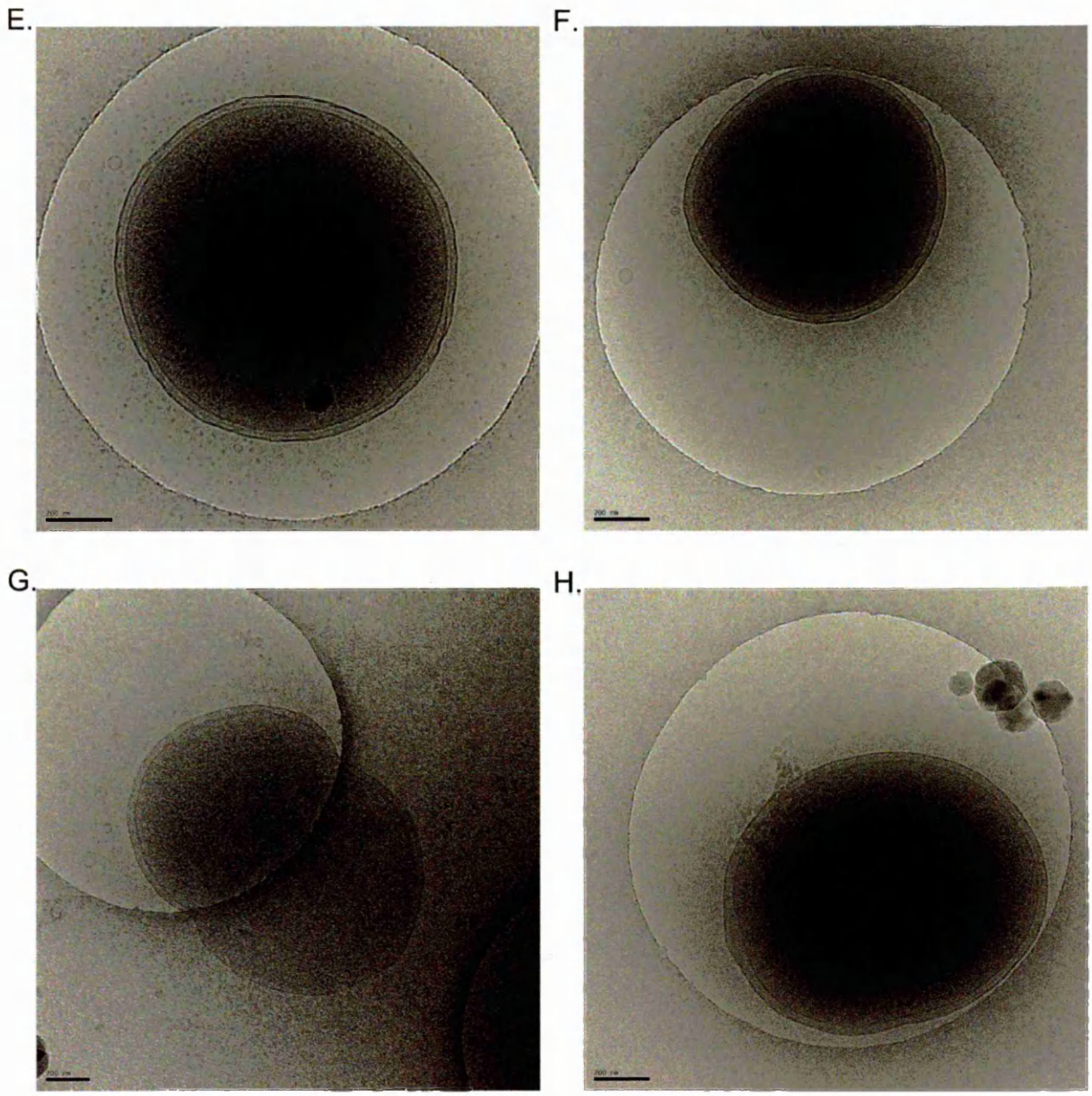

Figure 12. Cryo-electron microscopy of *N. meningitidis* H44/76 (continued). (E), (F), (H) Cocci shapes were frequently observed in the wildtype sample. (G) Oval shapes were also observed although the distension in this picture is most likely artefactual from the bacterium lying over the edge of the quantifoil hole. (E) 30,000X 200kV (F), (G) and (H) 25,000X 200kV. Scale bar 200nm.

I. J.

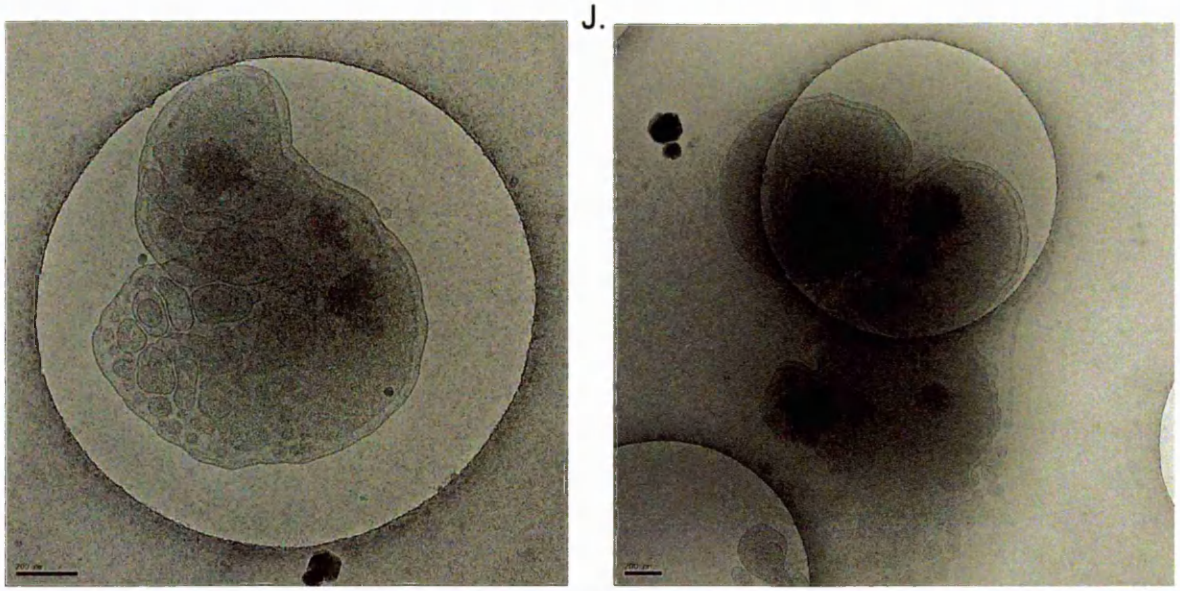

Figure 12. Cryo-electron microscopy of *N. meningitidis* H44/76 (continued). (I) and (J). Bacteria that appeared misshapen, with less electron dense cytoplasm and producing vesicles within the outer membrane envelope were observed. (I) 25,000X 200kV (J) 15,000X 200kV. Scale bar 200nm.

The *gna33* single crossover mutant was not morphologically different compared to the wildtype (fig.13).

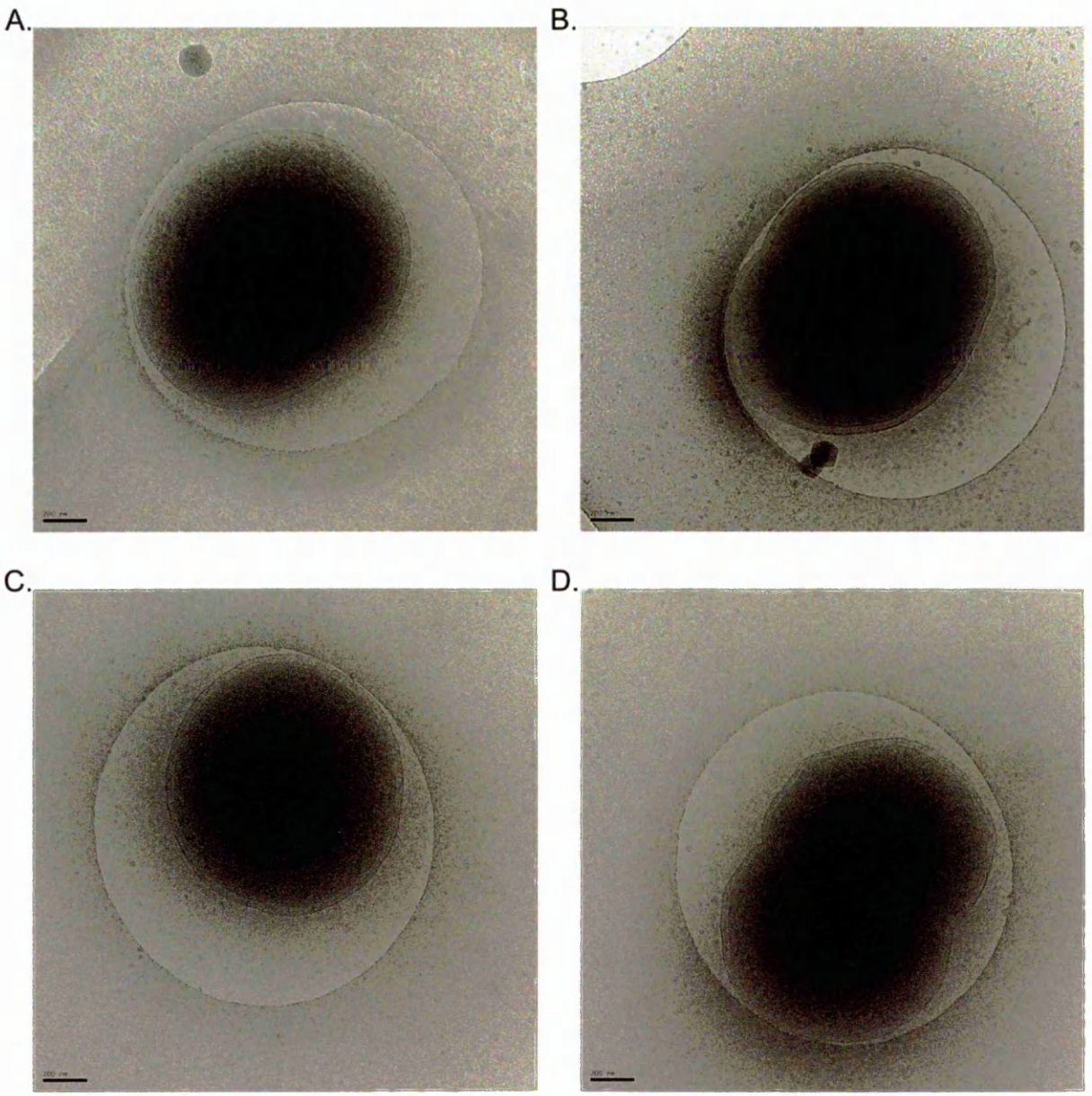

Figure 13. Cryo-Electron microscopy of *gna33* single crossover strain. The *gna33* single crossover appeared similar to the wildtype and showed no distinct phenotypic features. (A) (B) (C) (D) 20,000X 200kV. Scale bar 200nm.

The clustering described in the MC58 *Δgna33* strain was also observed in the H44/76 *Δgna33* strain (fig.14). Bacterial clusters made the formation of thin vitreous ice difficult, but this was overcome by increased blotting times for the grids before plunge freezing. Observation was only possible at the edges of clusters or in smaller clusters, as the large clusters were still too dense for the electron beam to pass through. Examination of the clusters demonstrated that the bacteria were not surrounded by a continuous outer membrane as had been previously reported (2); each bacterium had a discrete outer membrane but the cells were in contact with each other (fig.14 E,G,H). Individual bacteria were observed in the sample, but these bacteria appeared dead and degraded.

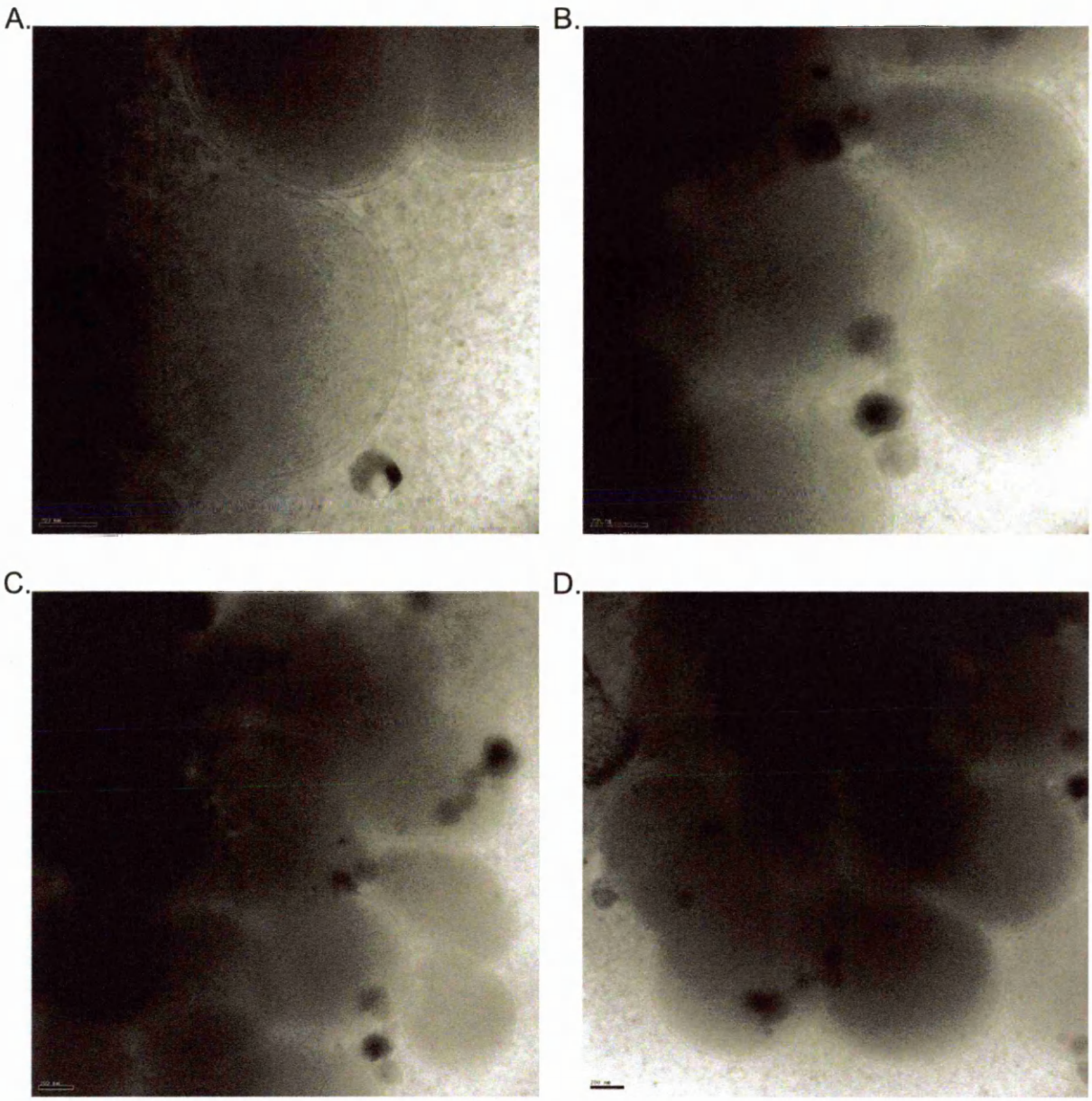

Figure 14. Cryo-Electron microscopy of the *Δgna33* strain. The clustering phenotype previously described by Abu-Bobie et al (2) was also present in the H44/76 *Δgna33* strain. Clusters were large and caused thick ice to form, making examination of the grids difficult. (A), (B), (C), (D) due to the thick ice only the edges of the clusters were easily observed. (A) (B) (C) (D) 20,000X 200kV. Scale bar 200nm.

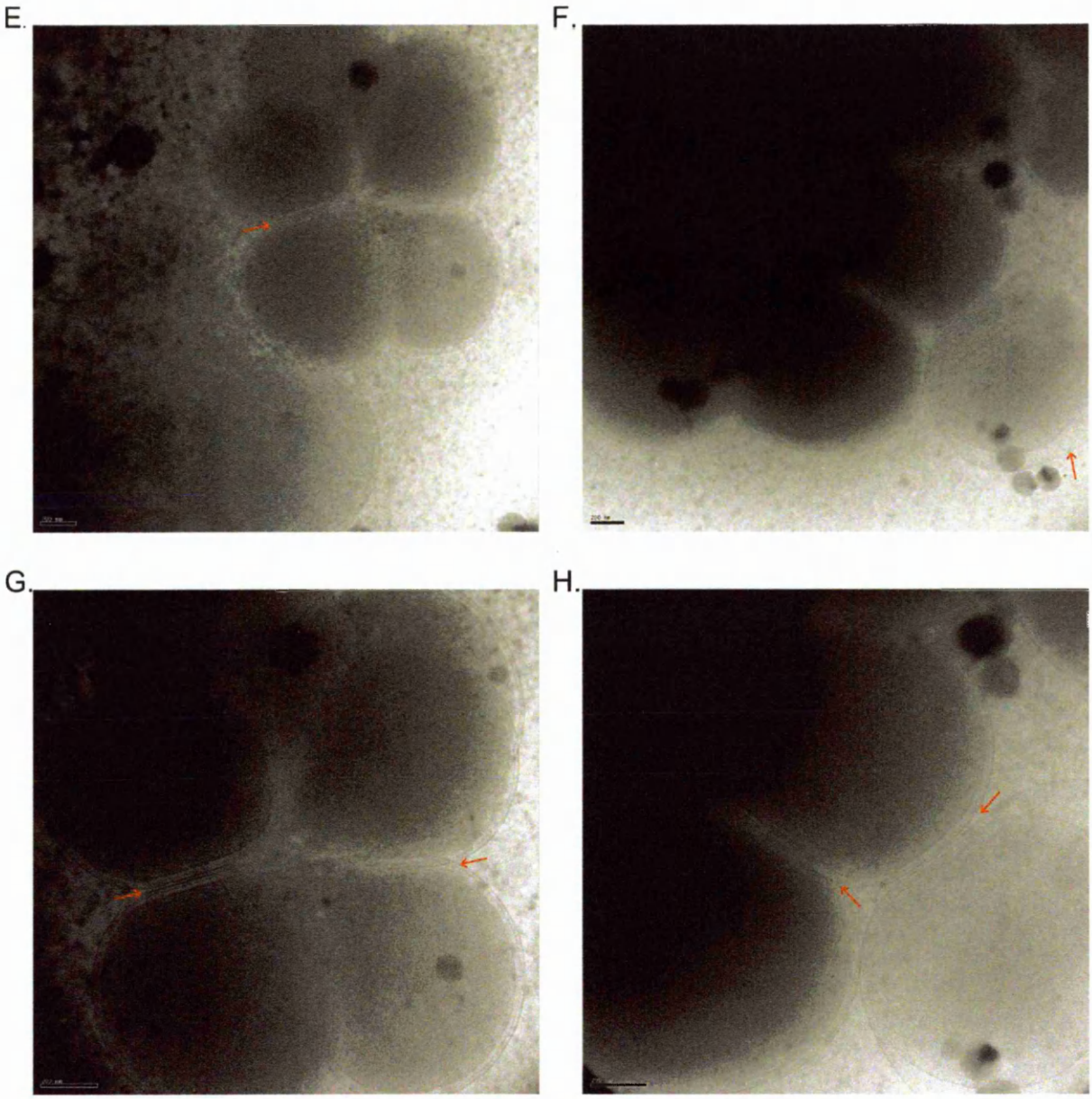

Figure 14. Cryo-Electron microscopy of the *Δgnα33* strain (continued). (E) and (F) small clusters. (G) and (H) the same clusters under higher magnification. (E), (G), (H) Close examination of the clusters showed that separate outer membranes can be seen between the bacteria within the clusters (red arrows). (E) (F) 20,000X 200kV (G) (H) 30,000X 200kV. Scale bar 200nm.

3.7 Effect of osmotic stabilizers on clustering phenotype of *Δgna33* strain

As clustering of *Δgna33* was not caused by a failure of outer membrane separation, it was hypothesized that the phenotype is caused by the osmotic instability of the *Δgna33* strain. Clustering would limit the access of water to the bacterial outer membrane and therefore reduce the osmotic pressure on the organism. Bacterial clusters could be observed under light microscopy following Gram-staining. Bacteria were grown in media containing sodium chloride, Gram stained and examined by light microscopy (fig. 15).

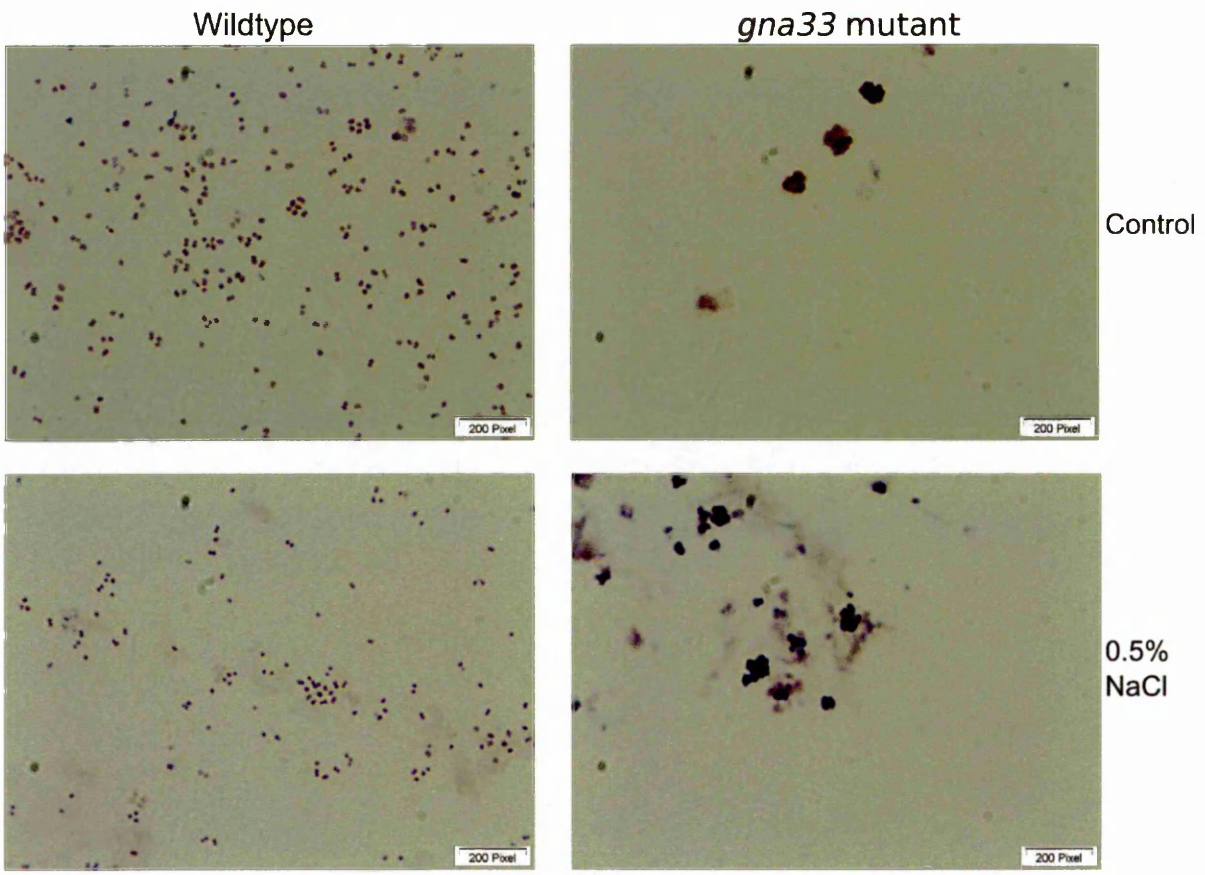

Figure 15. Light microscopy of *N. meningitidis Δgna33* (*gna33* mutant) strain grown with and without the presence of 0.5% sodium chloride in the growth media. Bacteria were Gram strained prior to imaging. Images taken at 1000X under oil immersion.

Changing in the osmotic potential of the media did not produce any observable changes in the phenotype, demonstrating that osmotic pressure was unlikely to be a factor in clustering. The results

also confirmed that the increase in growth rate caused by the addition of sodium chloride was not related to a change in clustering of the bacteria.

3.8 Antibiotic resistance of *gna33* mutants

GNA33 is an enzyme involved in the digestion and repair of peptidoglycan. The effect of GNA33 deletion on the peptidoglycan turnover and outer membrane was tested by assessing the sensitivity of the strains to antibiotics that target peptidoglycan synthesis pathways and the outer membrane. The selected antibiotics were: ampicillin which affects peptidoglycan cross-linking by the penicillin binding proteins; vancomycin which interferes with the transport of peptidoglycan across the inner membrane; D-cycloserine which blocks the formation of peptidoglycan precursors in the cytoplasm and polymyxin B which disrupts the outer membrane but does not interfere with peptidoglycan synthesis (for details see Chapter 1.3.1 pg. 4). *N. meningitidis* is naturally resistant to vancomycin, polymyxin B and D-cycloserine at clinical concentrations but high concentrations of these antibiotics killed meningococci in disc diffusion tests.

The wildtype and *gna33* single crossover mutants showed similar antibiotic susceptibility profiles. The *gna33* single crossover had a significant decrease in susceptibility (P=0.05) to ampicillin, almost certainly due to the presence of an ampicillin resistance gene in the plasmid that was incorporated into the genome. The *Δgna33* strain was significantly more susceptible to all the antibiotics (P=<0.05) (fig.16). The most significant increases in susceptibility occurred with antibiotics that disrupt peptidoglycan synthesis by interfering with the penicillin binding proteins (vancomycin and ampicillin). This suggested that the later stages of peptidoglycan synthesis were acutely sensitive to GNA33 deletion. Susceptibility to Polymyxin B indicated that *Δgna33* had an unstable outer membrane. Outer membrane instability could have potentiated the effects of the other antibiotics tested, by increasing permeability to large compounds.

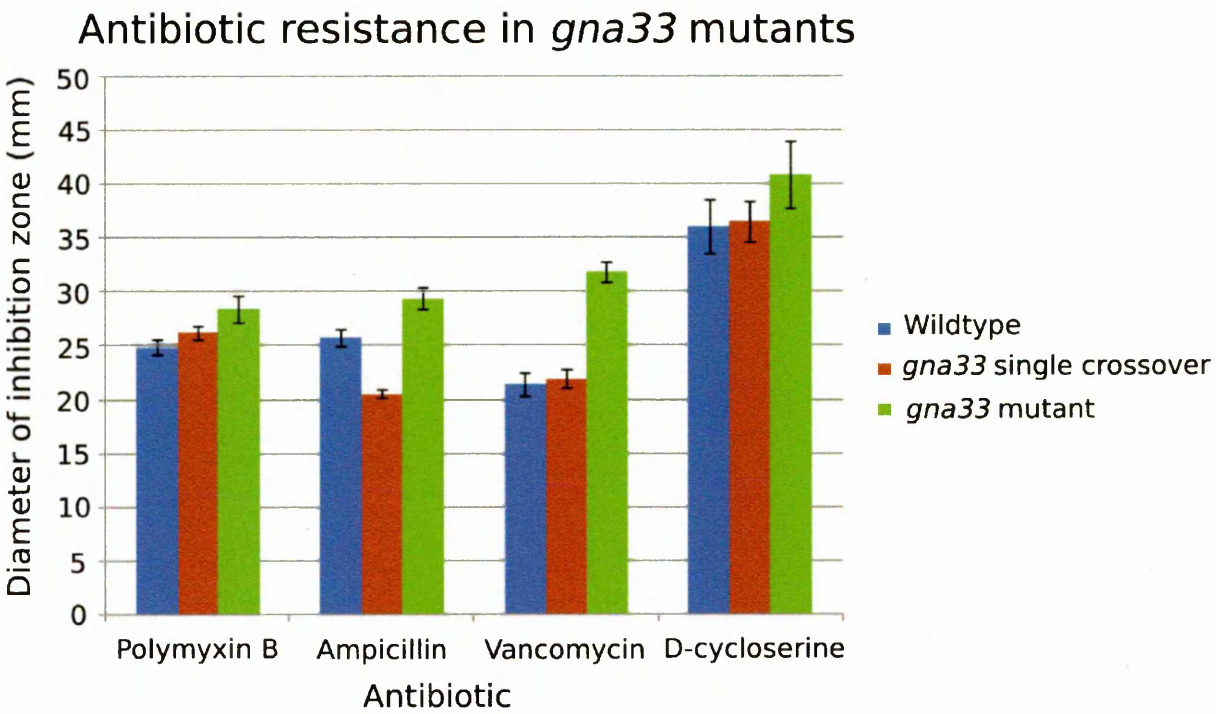

P values from T-tests

Antibiotic	Wildtype:*gna33* single crossover	Wildtype:*Δgna33*
Ampicillin	P=0.05	P=<0.01
Vancomycin	P=>0.05	P=<0.01
Polymyxin B	P=>0.05	P=<0.05
D-cycloserine	P=>0.05	P=<0.05

Figure 16. Antibiotic susceptibility in *gna33* mutants. Susceptibilities to Polymyxin B, Ampicillin, Vancomycin and D-cycloserine were tested by disc diffusion assay. Results represent mean of three replicates, error bars represent standard error of the mean (SEM). P values are given in the table. Blue cells indicate significant results. P values calculated by T-test.

3.9 Native vesicle production in wildtype and *gna33* mutants

Increased vesicle production is a known phenotype of *Δgna33* mutants. Vesicles naturally produced by the wildtype and *gna33* mutants (for method see section 2.2.10 pg. 39) were compared for the amount of the vesicles produced, the size and shape of the vesicles and the antigen content. OMV preparations from the strains were tested for the quantity of PorA and PorB by slot blotting, as

surrogate markers for the amount of vesicles. Monoclonal antibodies for the H44/76 PorA variable antigen P1.7 (NIBSC no. 01/514) and P1.16 (01/538) and for the H44/76 PorB subtype (02/310) were used and a standard curve for estimation of protein content was produced using purified PorA and PorB proteins (Fig.17).

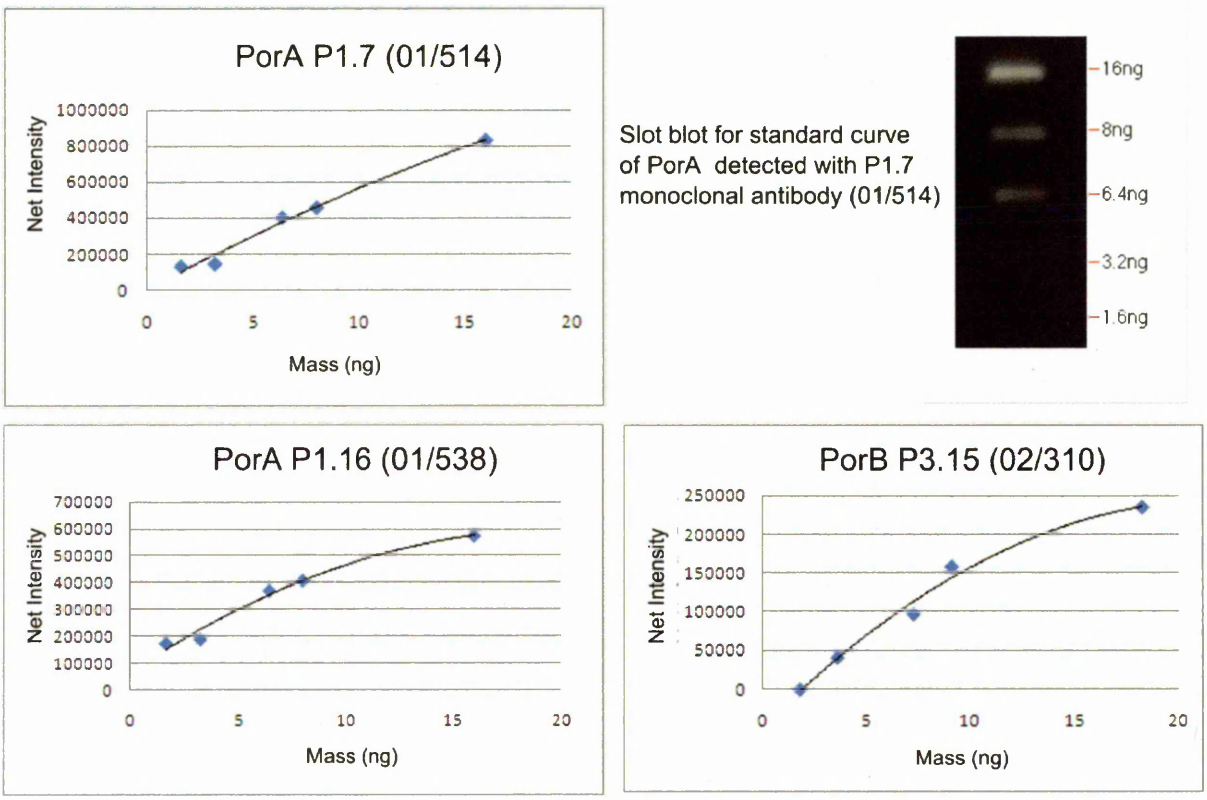

Figure 17. Standard curves for calculation of protein amounts from slot blots. Curves were prepared by using known concentrations of purified protein, the slot blot for PorA detected with monoclonal antibody 01/514 (P1.7) is shown.

The *Δgna33* strain produced more native vesicles than the equivalent wildtype strain, indicated by the increased amounts of PorA and PorB in the sample (fig.18), *Δgna33* showed a 35-fold increase in PorA compared to the wildtype. However wildtype levels of PorB were below the assay threshold of detection, so a comparison could not be made. The *gna33* single crossover also showed a mild increase in vesicle production, raising the PorB level above the threshold of detection. Compared to the *gna33* single crossover *Δgna33* showed a 16-fold increase in PorB and a 24-fold increase in PorA. The PorA (P1.7 monoclonal antibody) and PorB levels measured were similar to each other in both the *Δgna33* and *gna33* single crossover vesicles, showing that although the ratios of the two proteins

were not identical in both mutants, there was no great change in the ratio of PorA to PorB. The results of two PorA antibodies 01/514 (P.1.7) and 01/538 (P1.16) were not in agreement. This indicated differences in the avidity of the two antibodies, with the P1.16 antibody displaying lower avidity than the P1.7 antibody in all cases. The results with other mutants (see chapter 6 fig. 13 pg. 175) demonstrated that at higher concentrations of PorA the antibodies showed better accordance, which inferred a loss of accuracy of the standard curve at lower concentrations.

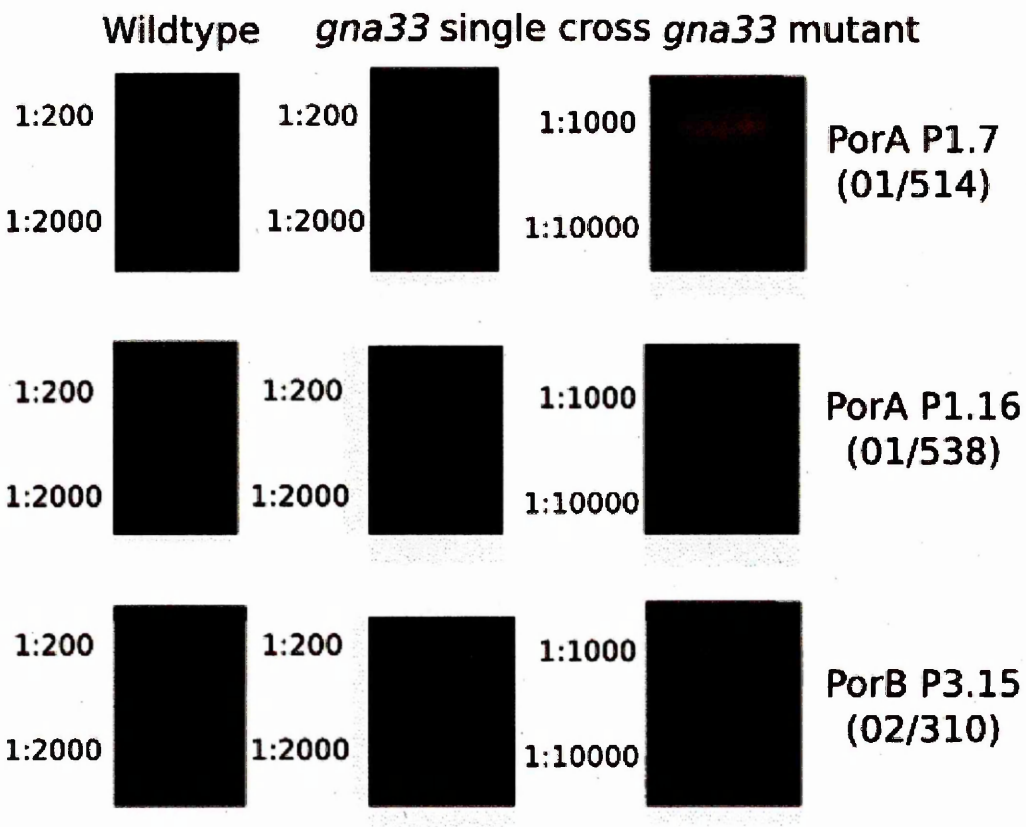

Strain	PorA P1.7 (01/514) (ng/µl)	PorA P1.16 (01/538) (ng/µl)	PorB P3.15 (02/310) (ng/µl)
Wildtype	1.0	<limit of detection	<limit of detection
gna33 single cross	1.4	<limit of detection	1.9
Δgna33 (*gna33* mutant)	33.5	4.9	29.6

Figure 18. Slot blot immunoassay of PorA and PorB in native vesicles from the wildtype and *gna33* mutants. Dilutions of native vesicle preparations were blotted with the PorA (01/514 and 01/538) and PorB (02/310) monoclonal antibodies. Dilutions of 1:200 and 1:2000 were used for the wildtype and *gna33* single crossover mutant. 1:1000 and 1:10000 was used for the *Δgna33* (*gna33* mutant) strain. Calculated protein amounts are shown in the table per µl of vesicle sample. Limit of detection was the level at which a signal above background level could not be detected by the software.

3.10 Cryo electron microscopy of OMVs of wildtype and *gna33* mutants

Morphology of vesicles from the wildtype and *gna33* mutants was examined by VTF Cryo-Electron microscopy (fig. 19, 20, 21). Wildtype vesicles (fig.19) were scarce even when samples were concentrated, as seen by low magnification views of the grid (fig.19 D). OMVs were observed both in the ice holes and present on the carbon film. Too few vesicles were present to determine if the OMVs showed a preference for either surface and vesicles were most commonly observed at the edges of ice holes.

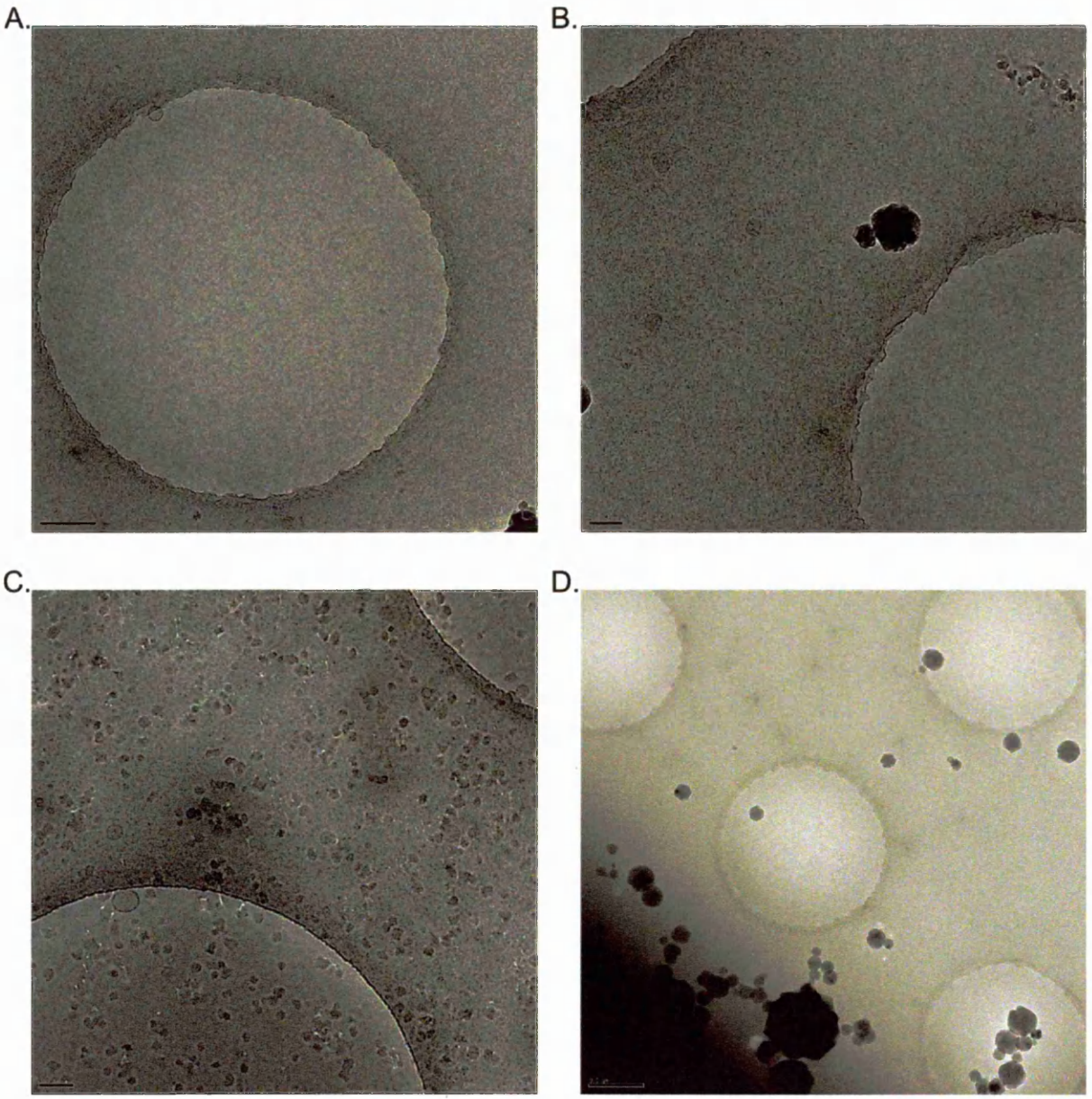

Figure 19. Cryo-Electron microscopy of wildtype vesicle samples. Wildtype vesicles were difficult to observe even in concentrated samples. (A) and (B) Vesicles were observed both in the ice and on the carbon. (C) Vesicles in ice were more commonly observed at the edges of ice holes. (D) Lower magnification view of the quantifoil showing the scarcity of vesicles in the sample. (A) 25,000X 200kV. (B) and (C) 30,000X 200kV (D) 10,000X 200kV. (A) scale bar 200nm. (B) and (C) scale bar 100nm. (D) scale bar 0.5µm.

OMVs from the *gna33* single crossover (fig.20) were also scarce, but were observed more commonly than in the wildtype sample. Vesicles were observed mainly in ice holes and were found both at the centre and edges of the ice. Anomalous vesicle morphologies were observed in the sample, such as a vesicle containing several membrane layers (fig.20 B) but these were rare.

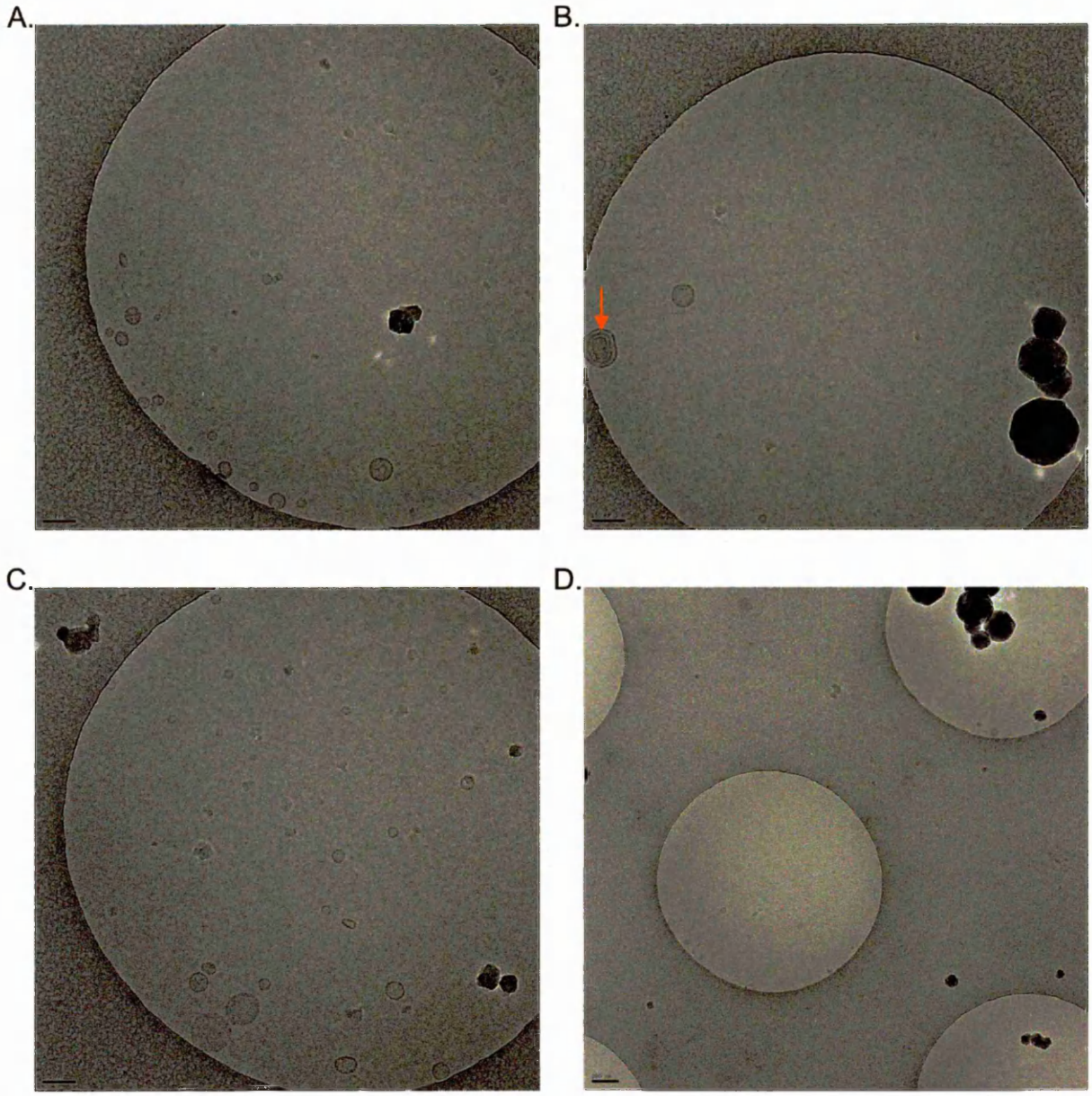

Figure 20. Cryo-Electron microscopy of OMVs from *gna33* single crossover mutant. Vesicles of the single crossover mutant were still scarce in concentrated samples but more were observed in this sample than the wildtype sample. (A) and (C) Vesicles were observed mainly in ice holes, and were found both at the edges and in the centre of ice holes. (B) Anomalous vesicles were observed such as the double membrane vesicle shown here (arrowed) but these were not common in the sample. (D) Lower magnification view shows the distribution of vesicles in the ice holes of the grid. (A) (B) (C) 30,000X 200kV. Scale bar 100nm. (D) 12,000X 200kV. Scale bar 200nm.

The *Δgna33* OMVs (fig.21) were much more abundant than the OMVs of the other strains. Vesicles were concentrated on the carbon and the edges of ice holes, although a few vesicles were observed in the centre of the ice holes (fig. 21 F and H). OMVs from *Δgna33* appeared larger than those of the other strains and anomalous vesicles that were large, oddly shaped or were double vesicles were commonly observed (fig.21 A,B and D). Vesicles on the carbon film appeared misshapen (fig.21 E), but this distortion could have been the result of interaction with the carbon film.

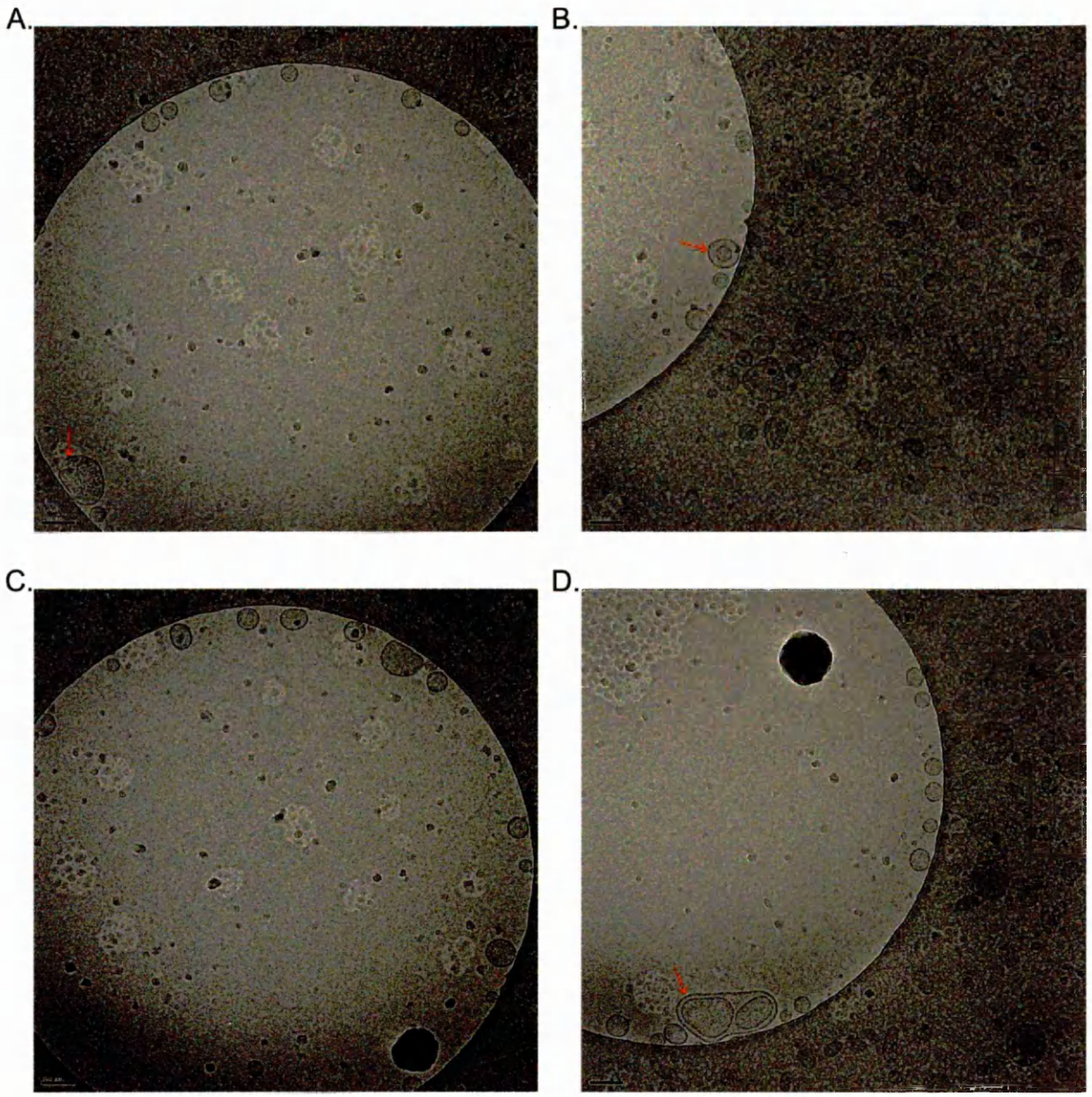

Figure 21. Cryo-Electron microscopy of OMVs from H44/76 *Δgna33* strain. A greater number of vesicles were observed in the *Δgna33* strain sample. (A) and (C) Vesicles were observed in ice holes but tended to be concentrated at the edge of the hole and on the surrounding carbon. (A) Large vesicles were observed much more commonly in the sample compared to the wildtype, both on the carbon film and in the ice (arrowed.) (B) and (D) Anomalous vesicles were also observed in several pictures, including vesicles contained within another layer of membrane (arrowed.). The amount of vesicle on the carbon compared to the ice holes is also shown. (A),(B),(C),(D) 30,000X 200kV. Scale bar 100nm.

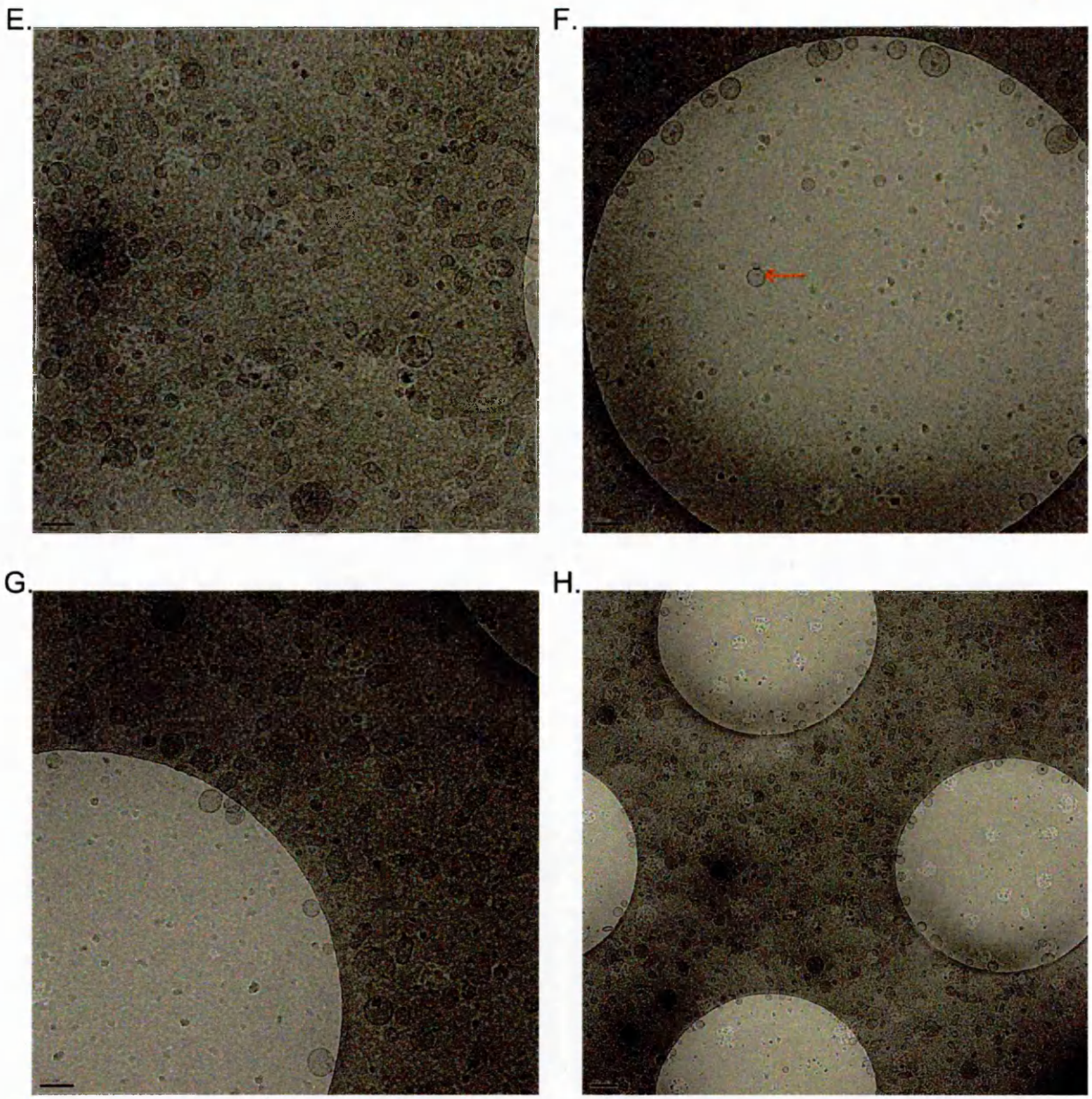

Figure 21. Cryo-Electron microscopy of OMVs from H44/76 *Δgna33* strain (continued) (E) and (G) Vesicle concentration on the carbon is shown. Many vesicles appear to be misshapen, but this may be artefactual due to the carbon film. (F) Although the majority of vesicles were observed at the edges of ice holes or on the carbon film, some were observed in the ice (arrowed). (H) Lower magnification view shows the concentration of vesicles on the carbon film and the edges of the ice holes and the variance of vesicle size and shape in the sample. (E),(F),(G) 30,000X 200kV. Scale bar 100nm. (H) 12,000X 200kV. Scale bar 200nm.

3.11 Comparison of size of OMVs from wildtype and *gna33* mutants

In order to compare the size and shape of vesicles produced by the strains, the perimeters and areas of the vesicles were measured. Only vesicles that were found in ice holes could be measured and therefore forty-five vesicle measurements were obtained in the wildtype sample. Forty-five vesicles were selected at random from the mutant samples (Table 1).

Table 1. Comparisons of vesicles from wildtype, *gna33* single crossover and *Δgna33* strains. Values are a mean of 45 vesicles chosen at random from the *gna33* single crossover and *Δgna33* strains. Significance values <0.01 are marked in blue. P values were calculated by T-test.

	Wildtype	***gna33* single crossover**	***Δgna33***
Mean perimeter (nm)	130.14	123.14	178.00
SD	41.02	51.88	59.38
Mean area (nm)	1457.42	1411.48	2707.65
SD	1064.32	1353.89	1788.41

P values from T-test

	Wildtype:*gna33* single crossover	**Wildtype:*Δgna33***	***gna33* single crossover:*Δgna33***
Perimeter	>0.1	<0.01	<0.01
Area	>0.1	<0.01	<0.01

Vesicles of the wildtype and the *gna33* single crossover were not significantly different in area or perimeter (P=>0.05). By contrast the *Δgna33* mutant were significantly larger (P=<0.01) in both area and perimeter measurements compared to the wildtype and *gna33* single crossover vesicles. *Δgna33* OMVs were more variable (by comparison of the SD values) than the vesicles of the other two strains.

The apparent increased variability of the *Δgna33* vesicles was tested using an F-test on the perimeter and area values (Table 2).

Table 2. F-test comparison of variability in the wildtype and *Δgna33* mutant. Values were calculated using a 45 vesicle sample. F-statistic was calculated using F-test; significance level was set at 0.05.

Comparison	Wildtype:*Δgna33*
Area	<0.05
Perimeter	<0.05

The *Δgna33* vesicles were also significantly more variable in area and perimeter measurements compared to the wildtype sample. The strong disparity between the strains shows that the deletion of *gna33* has disrupted vesicle release, making vesicles both larger and more variable in size than those of the wildtype and *gna33* single crossover strains.

3.12 Discussion

The aim of this study was to construct an H44/76 *Δgna33* mutant, assess the production of OMVs and compare its phenotype to a previously described MC58 *Δgna33* mutant. Comparison showed the phenotypes of the two mutant strains to be broadly similar. However, examination of the clustering showed that the hypothesis of a failure in cell separation as the cause of the phenotype was not correct. Examination of the *Δgna33* mutant phenotype also indicated links between the observed features and the lytic transglycosylase function of the GNA33 protein. Assessment of the OMVs produced by the mutant showed increased vesiculation but also a change in the vesicle characteristics, indicating different processes controlling the release of vesicles in the *Δgna33* mutant.

Although they were not examined in detail, two interesting features were demonstrated by the strains used and produced during construction of an H44/76 *Δgna33* mutant. The first was an apparent difference in recombination between the MC58 and H44/76 strains. The MC58 strain was more amenable to double crossover recombination than the H44/76 strain, despite the sequences flanking the *gna33* gene being identical in both. No differences in recombination frequency between the two strains have been reported. Therefore it was likely that the difference was specific to the *gna33* gene, possibly indicating that double crossover recombination was more strongly selected

against in the H44/76 *Δgna33* mutant. Secondly, variation of *gna33* mRNA expression in the downstream single crossover mutant, which was low on solid media and increased in liquid media, demonstrated that *gna33* transcription was affected by the insertion of the plasmid. The only factor currently known to control transcription and translation of *gna33* was the formation of mRNA secondary structure in the signal sequence (126). Sequencing showed that there was no change in this sequence in the downstream single crossover mutant. Therefore, it was likely that other unknown mechanisms regulating *gna33* transcription were being affected.

The close contact of the *Δgna33* mutant bacteria to each other in microscopy samples was referred to as clustering and this phenotype was strikingly different in the H44/76 *Δgna33* bacteria compared to the previously reported characteristics of the MC58 strain. Clustering was thought to be caused by a failure of the outer membrane to separate in cell division; however electron microscopy showed that the outer membranes of H44/76 *Δgna33* mutants were separated. This difference most likely resulted from the methods used for electron microscopy. Unlike the room temperature sectioning and staining technique, in VTF bacteria are examined in a hydrated state without requiring fixation and staining steps. Samples were also examined in an instrument operating at a higher voltage, increasing the resolution of the image. The separated outer membranes indicated that the clusters are being held together by an interaction occurring at or outside the outer membrane. Changes in the charge of the outer membrane would be a potential cause of clustering and electron microscopy of the membrane vesicles of the *Δgna33* mutant suggested that the vesicles showed a preference for the carbon film which holds a hydrophilic charge. However, the scarcity of vesicles in the wildtype sample makes it difficult to determine if this trait was unique to the *Δgna33* mutation. The core oligosaccharide of the LOS molecule usually provides the overall charge of the outer membrane and LOS must be passed through the cell wall to reach the outer membrane. Disruption of peptidoglycan structure caused by *gna33* mutation was likely to affect the ability of the bacteria to transport molecules to the outer membrane, resulting in disruption of LOS transport and charge of the outer

membrane. Other factors such as the capsule also warrant investigation as capsule transport through the outer membrane could also be affected by changes to the peptidoglycan structure. The effect of capsule expression on clustering could be examined by mutation of *gna33* in an acapsulate mutant; if capsule is a cause of clustering such a strain would show a reduction or abolition of the clustering phenotype. A hydrated sectioning technique, for example Cryo-electron microscopy of vitreous sections (CEMOVIS), could also be used to visualise clusters too thick to be examined by VTF.

The involvement of GNA33 in the response to osmotic stress was shown by the slow growth of the *Δgna33* strain, which was improved when osmotic pressure was reduced, and the upregulation of *gna33* mRNA in the single crossover mutant grown in liquid culture. When the enzymatic function of GNA33 is considered, there is a clear potential role for the protein in responding to osmotic pressure. Lytic transglycosylases like GNA33 are part of the enzymatic machinery responsible for the maintenance of the peptidoglycan. The enzymes break down peptidoglycan in a very specific manner that allows for repair and expansion. Loss of lytic transglycosylase enzymes leads to disruption of peptidoglycan structure, as seen following deletion of multiple functionally redundant lytic transglycosylases in *E. coli* (81). Unlike *E. coli, N. meningitidis* appears to rely on GNA33 as its main lytic transglycosylase for peptidoglycan remodeling. Disordering of the peptidoglycan scaffold has a detrimental effect on the bacteria's ability to cope with increased osmotic pressure by weakening the cell wall and making cells more prone to lysis. The most significant increases in antibiotic susceptibility in the strain were to both ampicillin and vancomycin, which target PBP proteins involved in the insertion and crosslinking of new peptidoglycan strands. This could indicate simply that disruption of the peptidoglycan is more acute when both insertion of new glycan strands and remodeling are directly affected. Also it has been hypothesized that proteins controlling synthesis, remodeling and degradation of the peptidoglycan (including lytic transglycosylases and penicillin binding proteins) act together as part of a multi-enzyme complex (62). GNA33 has been shown to interact with the meningococcal penicillin binding protein PBP2, which shares sequence homology with the *E. coli* PBP3

(65), a known target for ampicillin (168). Co-ordination between GNA33 and the PBPs affected by the antibiotics could explain the acute effects of these antibiotics on the mutant strain. The links between changes in growth and antibiotic sensitivity and the enzymatic function of the protein highlight the importance of GNA33 in maintenance of peptidoglycan.

As explained above, the VTF technique allowed the examination of vesicle samples in a hydrated state, in vitreous 'water-like' ice, without the dehydration artefacts that are often associated with traditional staining techniques such as negative staining (3). In addition, the measurement of vesicles embedded is the holes of quantifoil grids meant that there was no potential distortion of vesicles by the carbon support film. Vesicle measuring methods used in other studies included dynamic light scattering (DLS) (150). DLS measures the size and size distribution of vesicles by measuring the scattering of monochromatic light passed through the vesicle sample. By contrast, VTF allowed vesicles to be measured directly and could give more information about vesicle shape in terms of perimeter and area.

The wildtype vesicles examined in this study had a mean perimeter of 130.1 nm, which equated to a mean vesicle diameter of 41.4 nm. This was smaller than the diameter of native vesicles reported by a previous study by van de Waterbeemd et. al. which measured vesicles by DLS and calculated a vesicle diameter of 80.2 ±2.2 nm (150). This discrepancy could be due to either differences in the methodologies used to produce vesicles or to calculate vesicle size, or differences in the vesicles themselves. Both this study and the previous work used H44/76 strains and a similar methodology of filtration and ultracentrifugation to purify vesicles from the supernatant. An extra centrifugation step was used to remove bacteria from the supernatant prior to filtration in this study. However since this step has also been used in the purification of detergent derived vesicles (which are much larger than native vesicles) in the laboratory without the loss of large vesicles, it seemed unlikely that this could be the cause of the size discrepancy. It is also unlikely that freezing the samples has changed the size of the vesicles by contraction of the solvent, as vitrified liquids maintain the same volume as the

liquid state (170). Previous work has shown that differences in the composition of growth media can affect both the protein and LPS constituents of vesicles (145) and the amount of vesicles released by strains (122). In this study bacteria were grown in MH broth, in the previous work bacteria were grown in chemically defined medium. It is possible that the composition of the media used also affected the size of released vesicles in this study. To test this hypothesis, vesicles grown in both media under identical conditions would have to be measured by both VTF Cryo-TEM and DLS. Such a comparison would also show if the differences in measurements were due to the different methodologies used for measuring the vesicles.

The increased production of OMVs by the *Δgna33* strain had been previously reported (37), but results of this study showed that these vesicles were dissimilar to OMVs produced by the wildtype strain. Increased size and variability of the *Δgna33* vesicles indicated that vesicle size in the *Δgna33* mutant was not controlled by the same mechanisms as in the wildtype. GNA33 is an outer membrane bound protein which is also linked to the peptidoglycan. Deletion of the protein may lead to destabilisation of the outer membrane through the loss of this structural bond. But the presence of other proteins in the cell wall such as RmpM, which form a similar link and are much more ubiquitous, make this an unlikely cause of vesiculation. The disruption of the cell wall caused by GNA33 deletion is therefore the more probable cause of the increase in vesiculation. Sensitivity of *Δgna33* to polymyxin B showed that the outer membrane of the bacteria is disrupted. Action of the antibiotic requires it to pass through the outer membrane and entry into *N. meningitidis* is prevented in normal cells by modifications to Lipid A and the action of porins and efflux pumps. Bending or thinning of the peptidoglycan will lead to changes in the turgor pressure in the cell wall. Such pressure changes could disrupt the outer membrane and cause vesicle release by forcing the outer membrane to bulge and eventually bleb. Vesiculation caused by increased stresses on the outer membrane and cell wall has been reported in other Gram negative bacteria (93) and this could be the cause of vesicle release in *Δgna33*. However the strikingly different morphology of *Δgna33* vesicles would suggest that vesicle

release in the wildtype is not governed solely by outer membrane stress. Structural studies on the peptidoglycan of *Δgna33* mutants would provide more information on the precise nature of peptidoglycan disruption when *gna33* is deleted.

The phenotype of the *Δgna33* mutant can be linked to the role of the protein as the primary lytic transglycosylase in *N. meningitidis*. Disorganised peptidoglycan and loss of structural strength of the cell wall is likely to cause the phenotype of slow growth and sensitivity to peptidoglycan disrupting antibiotics. Disruption of molecule transport through the peptidoglycan could also contribute to this phenotype and be a cause of the clustering, which is likely to involve the interactions of factors at or beyond the outer membrane. Finally high level production of atypical vesicles is likely to be linked to the changes in turgor pressure in the cell wall due to disruption of the peptidoglycan. Differences in vesiculation between the wildtype and *Δgna33* also indicates that different processes are controlling vesiculation in the two strains and that GNA33 is unlikely to be involved in wildtype vesiculation.

Chapter 4- Construction of an *N. meningitidis* strain carrying the *tol-pal* genes

4.1 Introduction

The Tol-Pal complex is a group of proteins that spans the cell wall and is required for outer membrane stability in *E. coli* (156). Homologues of Tol-Pal have been identified in many other Gram negative species. Some bacteria lack the Tol-Pal complex. There is no phylogenetic relationship between these species but Tol-Pal is absent in several high vesiculating species including *N. meningitidis* (139). The complex consists of five core proteins, TolR, TolQ, TolA, TolB and Pal, and spans the cell wall from the inner membrane to the outer membrane. TolR and TolQ are bound to the inner membrane; TolA interacts with both TolR and TolQ and bridges the inner membrane and peptidoglycan. Pal interacts with TolA in the periplasm and spans the peptidoglycan and outer membrane. The interaction of TolA and Pal is dependent on a proton motive force that is produced by the inner membrane TolQ and TolR proteins. TolB interacts with TolA and Pal in the periplasmic space (see chapter 1.6.2 fig.3 pg.26) (164).

The *tol-pal* complex is located at 17 minutes on the *E. coli* K12 genome linkage map (166). The complex is arranged into two operons, which contain seven genes. The operons are transcribed from the promoters P_1 and P_B (fig. 1) (156). Promoter P_1 transcribes the genes *ybgC-tolQ-tolR-tolA* and the P_B promoter the genes *tolB-pal-ybgF*. The P_1 promoter can also produce a transcript of the region from *ybgC-ybgF*. The YbgC protein is a thioesterase involved in phospholipid synthesis and not connected to the function of the Tol-Pal complex. The YbgF protein has been shown to interact with TolA (164), but is not required for the function of the Tol-Pal complex (156).

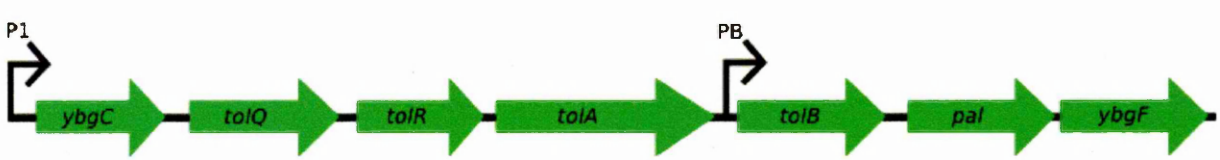

Figure 1. The *tol-pal* complex. The complex consists of seven genes expressed from two promoters P_1 for the genes *ybgC, tolQ, tolR* and *tolA* and P_B for the genes *tolB, pal* and *ybgF*. The genes *tolQ, tolR, tolA, tolB* and *pal* form the *tol-pal* complex.

Deletion of any of the *tol-pal* genes except *tolB* will abolish the formation of the functional complex (166). The Tol-Pal complex has been shown to have an important structural role in the cell wall; the deletion of the Pal protein produces a mutant that is prone to lysis by detergents and increased sensitivity to some antibiotics (7,21). Release of membrane vesicles is a phenotype of the Δ*tol-pal* strain (7) and the deletion mutants also show aberrant cell division leading to 'chaining' of the bacteria. The Tol-Pal complex has been shown to localise to the poles of the cell during cell constriction, implying the complex has a role in cell separation during division. In addition vesicles have been shown to be released from the poles of the cell during division (45).

The aim of this study is to test the hypothesis that production of the Tol-Pal complex in *N. meningitidis* would lead to an attenuation of the vesicle releasing phenotype of the bacteria. The lack of the Tol-Pal complex in *N. meningitidis* and other highly vesiculating species and the phenotype of Δ*tol-pal* mutants in *E. coli* suggested that the absence of the complex may be a cause of high levels of vesicle release. Expression of the *tol-pal* complex from the pMIDG201 expression vector was used to create a Tol-Pal producing mutant; the phenotype of this strain could then be tested to assess the effect of Tol-Pal on vesicle release.

4.2 Construction of the *tol-pal* expression vectors pMIDGTol-Pal and pMIDGTol-Palner

To express the Tol-Pal proteins in *N. meningitidis* the expression vector pMIDG201 was used. This vector was constructed by manipulation of the *Neisseria flavescens* cryptic plasmid pMIDG2830. A kanamycin resistance gene, constitutive meningococcal promoter *ner* and two copies of the *Neisserial* DNA uptake sequence to act as transcriptional terminators and facilitate the uptake of the plasmid into *N. meningitidis* were inserted (103,104). The plasmid replicates using the *repA* origin of replication, which is a low copy number origin of replication in *E. coli* (39,46,103).

It was not known if the *E. coli* native promoters of the *tol-pal* operon would be functional in *N. meningitidis*. Therefore two cloning strategies were pursued in tandem. The plasmid pMIDGTol-Pal

contained the *tol-pal* genes under the control of the native promoters P_1 and P_B and the plasmid pMIDGTol-Palner contained the genes under the control of the *ner* promoter.

To construct pMIDGTol-Pal the *tol-pal* genes were first amplified in two sections from the *E. coli* genome; the complex was amplified in two sections to reduce the size of the PCR product inserted into the plasmid. The first section contained the genes *ybgC, tolQ, tolR* and part of *tolA*. The second contained the rest of the *tolA* gene and the genes *tolB* and *pal*. The division point of *tolA* was a natural *EagI* site in the gene (fig. 2a). The *ybgC* gene was not removed from the complex due to the position of the P_1 promoter but the *ybgF* gene was not amplified as this gene has no effect on Tol-Pal complex assembly (49).

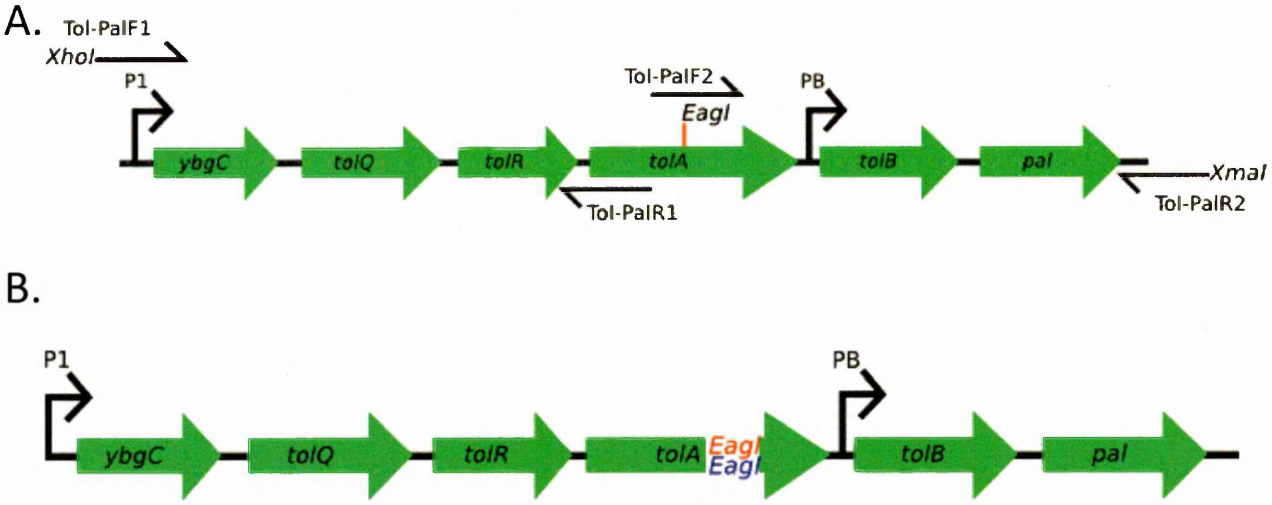

Figure 2. PCR for amplification of the *tol-pal* complex under its native promoters. (A) Two PCR amplifications were carried out from the labelled primers, overlapping at the natural *EagI* site in *tolA*. (B) The two fragments were reassembled using the natural *EagI* site.

After amplification the PCR products were ligated into Topo vectors to create plasmids TopoTF1 and TopoTF2 (fig 3.). The Topo plasmids were sequenced and the fragment TolForward1 was digested from the plasmid using the enzymes *XhoI* and *EagI*. Insertion of the fragment into pMIDG201 removed the *ner* promoter from the vector. The TolForward2 fragment was then digested from the TopoTF2 plasmid and ligated into the construct to form the pMIDGTol-Pal plasmid. Because a naturally occurring restriction site was used to ligate the two halves of the complex there was no sequence change in *tolA*.

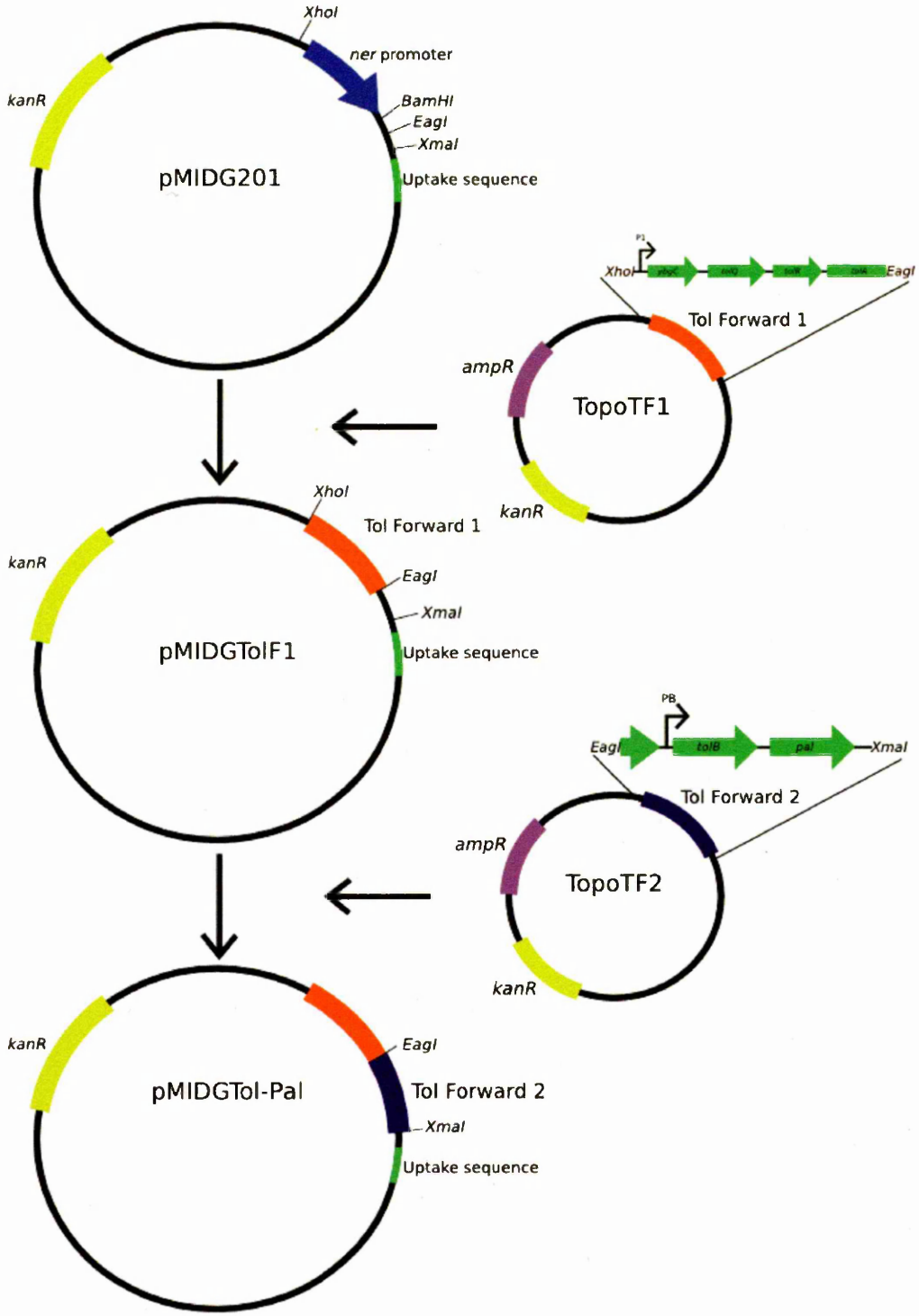

Figure 3. Construction of the pMIDGTol-Pal plasmid. The PCR amplified fragments of the *tol-pal* complex were ligated into Topo vectors (TopoF1 and TopoF2). The fragment TolForward1 was digested from the topoTF1 vector with *XhoI* and *EagI* and ligated into the pMIDG201 plasmid to form the plasmid pMIDGTolF1. The plasmid was then digested with *EagI* and *XmaI* and the second fragment TolForward2 was digested from the topoTF2 vector and ligated into the plasmid to form the construct pMIDGTol-Pal.

Construction of the plasmid containing *tol-pal* under the control of the *ner* promoter required the removal of the native promoters and *ybgC* gene. Also all the genes had to be present in the same reading frame, to be transcribed as a single polycistronic transcript. The genes were amplified in two sections, TolForward3 contained the genes *tolQ, tolR* and *tolA* and TolForward4 contained *tolB* and *pal*. The region containing the P_B promoter was not amplified in either fragment (fig 4.a).

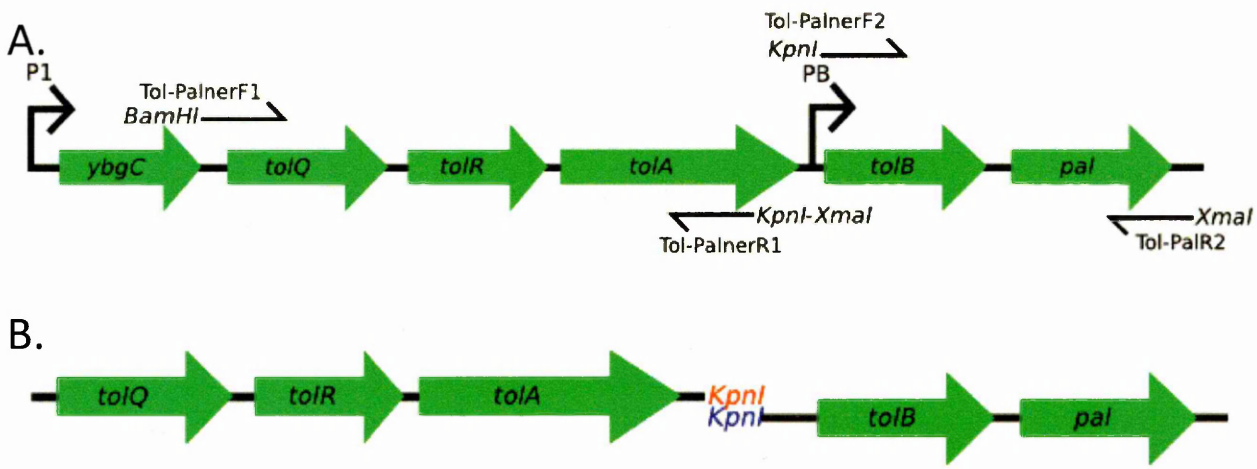

Figure 4. PCR amplification of the *tol-pal* complex for expression under the *ner* promoter. (A) PCR amplification of the *tol-pal* complex with the primers Tol-PalnerF1, Tol-PalnerR1, Tol-PalnerF2 and Tol-PalR2 removed the P_1 promoter and the *ybgC* gene. The primer Tol-PalnerR1 contains a *KpnI* site that is in frame with the *tolA* gene as well as the *XmaI* site used for cloning into pMIDG201. The primer Tol-PalnerF2 also carries a *KpnI* site. (B) When the fragments are ligated together using the *KpnI* sites inserted during PCR the P_B promoter is deleted and the *tolA* and *tolB* genes are brought into a single reading frame, allowing the complex to be transcribed from a single promoter.

A *KpnI* site was added to the 3' end of the first fragment, in the same reading frame as the *tolA* gene. The second fragment also contained a *KpnI* site at its 5' end, in frame with the start codon of the *tolB* gene. When the two fragments were ligated all the genes were in frame could be transcribed as a single transcript (fig.4b). After amplification the two fragments were inserted into Topo vectors (fig.5) resulting in the plasmids TopoTF3 and TopoTF4. After sequencing, TolForward3 was digested from the plasmid and ligated into the pMIDG201 vector downstream of the *ner* promoter to produce the plasmid pMIDGTolF3. Ligation of the Tolforward4 fragment with this plasmid resulted in the plasmid pMIDGTol-Palner (fig.5).

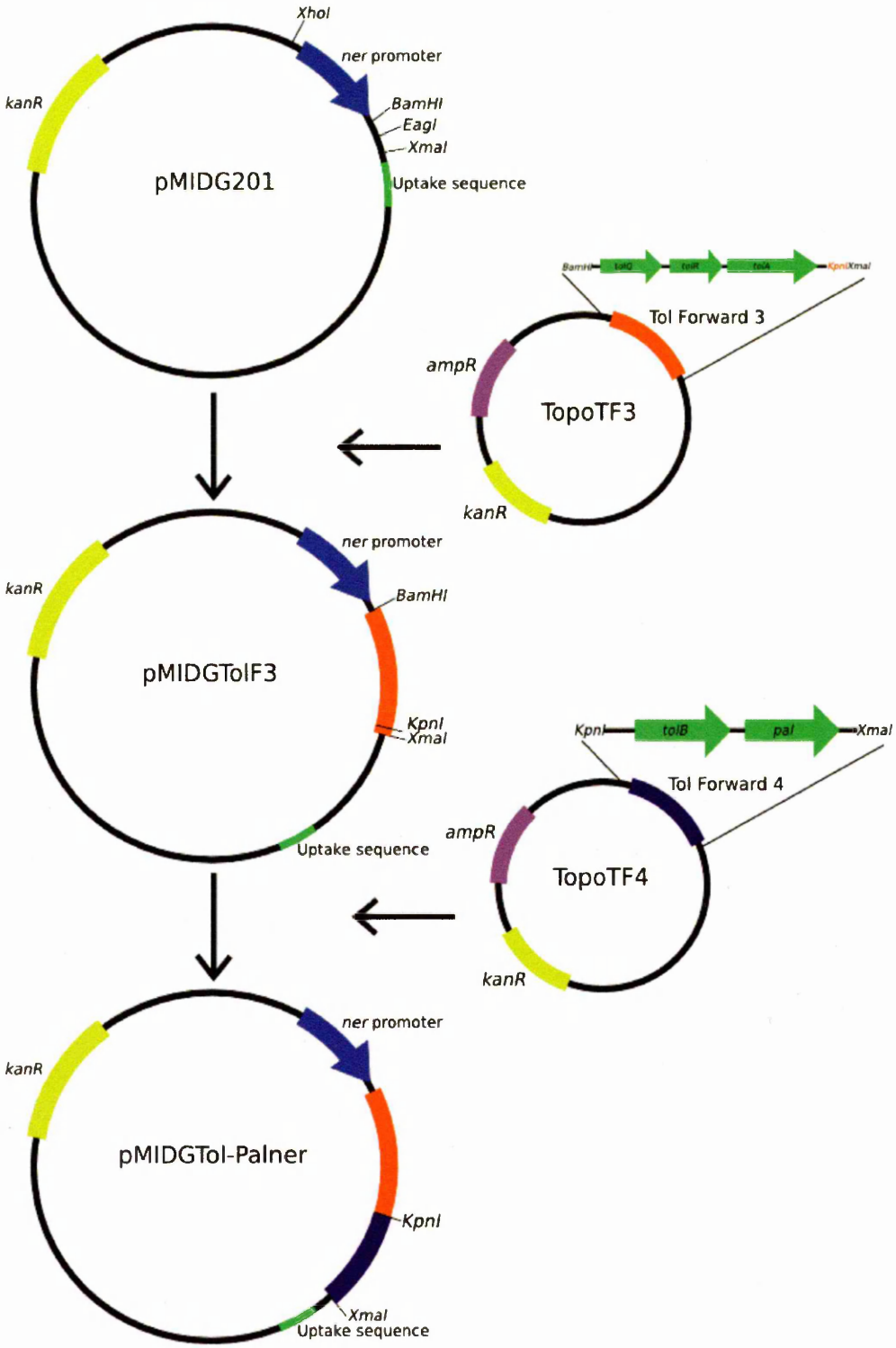

Figure 5. Construction of the pMIDGTol-Palner plasmid. The PCR amplified fragments were cloned into Topo vectors and the fragment Tol Forward 3 was digested from TopoTF3 with *BamHI* and *XmaI* for insertion into pMIDG201, creating the plasmid pMIDGTolF3. The plasmid pMIDGTolF3 was then digested with *KpnI* and *XmaI* to allow the fragment Tol Forward 4 to be inserted with the *tolA* and *tolB* genes in a single reading frame.

After construction the plasmids were sequenced to ensure the sequence of the *tol-pal* complex was correct in both plasmids. Both plasmids had some mismatches compared to the reference sequence, most of these were synonymous mutations but three mutations in the pMIDGTol-Pal sequence and two mutations in the pMIDGTol-Palner sequence caused changes to the amino acid sequence (table 1).

Table 1. Sequence mismatches in pMIDGTol-Pal and pMIDGTol-Palner. Sequencing of the *tol-pal* genes contained in the plasmids pMIDGTol-Pal and pMIDGTol-Palner showing non-synonymous changes. Sequencing was compared to the *E. coli* K12 genomic sequence. Mismatches were confirmed by sequencing on both strands of the plasmid sequence.

Plasmid	Mutation and position	Effect	Gene
pMIDGTol-Pal	A10359G	Gly/Asp	*tolR*
	C9504T	Ser/Pro	*tolQ*
	C10814T	Ala/Val	*tolA*
pMIDGTol-Palner	T6703C	Leu/Ser	*tolQ*
	C8363T	Ala/Val	*tolA*

Mismatch errors are not the same between the two plasmids, showing that the mismatches were not changes in the template sequence used to amplify the *tol-pal* genes. These errors were not seen in the sequencing of the Topo plasmids, indicating that the errors occurred during replication of the plasmids in *E. coli*. As these mutations could have affected the function of the Tol-Pal proteins, a *tol-pal* knockout *E. coli* strain was used to test the ability of the plasmids to complement the *Δtol-pal* phenotype.

4.3 Phenotype complementation of the *E. coli Δtol-pal* strain by pMIDGTol-Pal and pMIDGTol-Palner

The *Δtol-pal* strain has reduced growth on detergent containing media (45). Competent *E. coli Δtol-pal* bacteria were prepared and transformed with pMIDGTol-Pal and pMIDGTol-Palner and the presence of the plasmids was confirmed by plasmid preparation and restriction digests. Successfully transformed strains were tested for detergent sensitivity by growth on LB agar containing 0.5% DOC (fig.6).

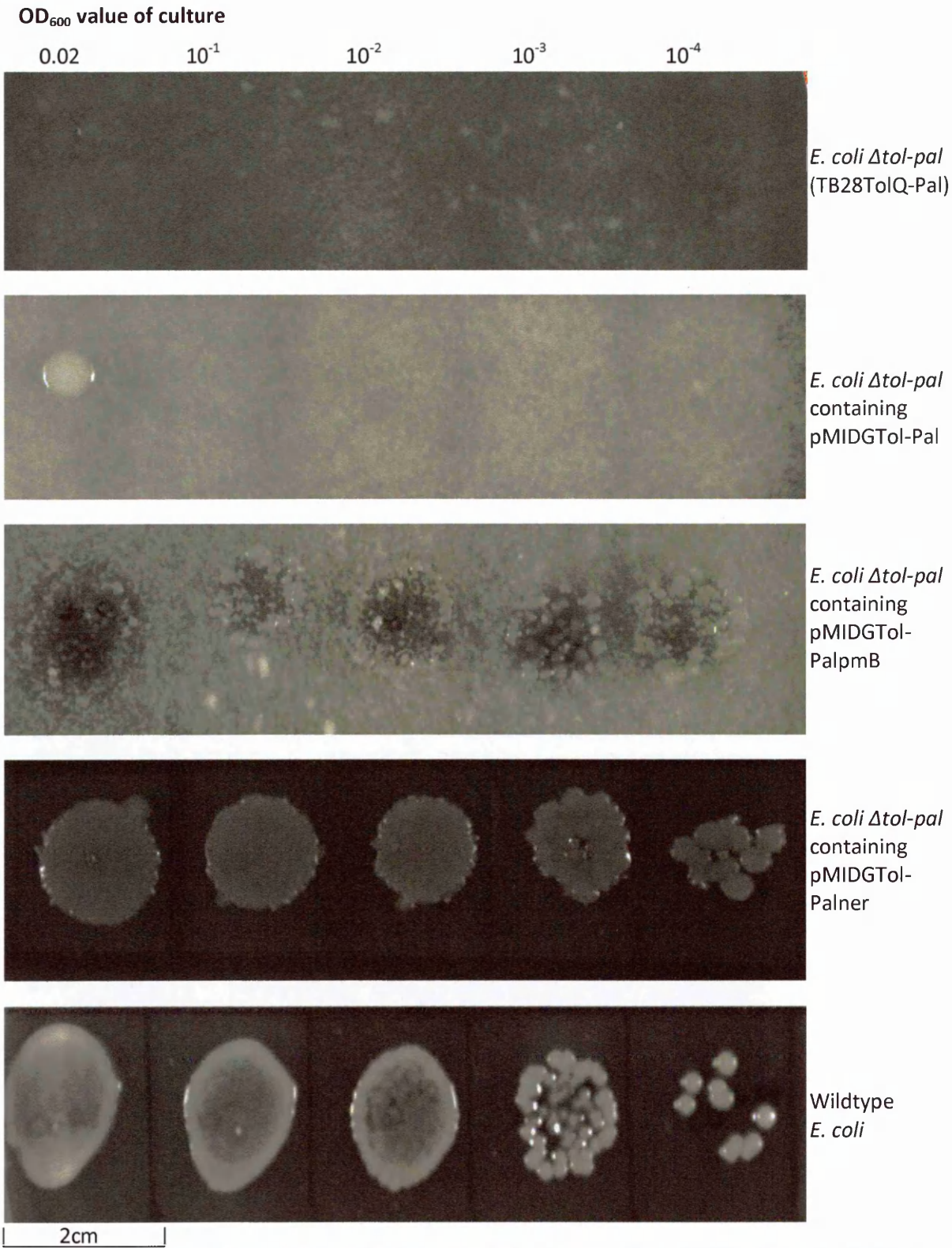

Figure 6. Phenotype complementation of *Δtol-pal* mutant *E. coli* strain with pMIDGTol-Pal and pMIDGTol-Palner plasmids. Phenotype complementation of the *Δtol-pal* strain was tested by growth on media containing 0.5% Deoxycholate. 5µl drops of Serial dilutions of a starting culture OD_{600} value of 0.02 are shown left to right. Size marker is shown below image. Clearance of opaque plate (panels 3, 4 and 5) indicated that bacteria were metabolizing deoxycholate. pMIDGTol-PalPmB was a pMIDGTol-Pal plasmid that also contained the high copy number origin of replication PmB (see section 5.3 pg. 125).

The wildtype strain grew at all the dilutions and also produced zones of clearance of the opaque plate, indicating that the bacteria were metabolizing the deoxycholate. By contrast the *Δtol-pal* mutant did not grow at any of the dilutions. The pMIDGTol-Palner plasmid, with the constitutive *ner* promoter, complemented the *Δtol-pal* strain demonstrating that the plasmid encoded a functional Tol-Pal complex and that transcription of functional single polycistronic mRNA occurred from the Neisserial *ner* promoter in *E. coli*. When the pMIDGTol-Palner plasmid was transformed into wildtype *E. coli* bacteria, it increased the detergent sensitivity of the strain (data not shown). The strain that contained pMIDGTol-Pal (*tol-pal* under the native *E. coli* promoters) only grew at the strongest concentration of bacterial suspension and produced only a mild change in the phenotype of the *Δtol-pal* strain. The proteins encoded by this plasmid could have either not been functional or had reduced functionality, possibly due to the point mutations acquired during cloning. A high copy number variant of the pMIDGTol-Pal plasmid (pMIDGTol-PalPmB) that contained the same *tol-pal* genes restored growth at all dilutions in the *Δtol-pal* strain and the bacteria cleared some deoxycholate from the plate. However, the phenotype was not completely returned to that of the wildtype. Therefore the pMIDGTol-Pal plasmid was producing Tol-Pal proteins capable of complementing the *Δtol-pal* phenotype, but not in sufficient quantities. Either the native promoters did not act as efficiently when present on a plasmid as they do when in the *E. coli* genome or the mutations in the *tol-pal* genes have reduced the efficiency of the complex, so more proteins must be produced to complement the phenotype.

4.4 Transformation of *N. meningitidis* with pMIDGTol-Pal and pMIDGTol-Palner

Following transformation of the *tol-pal* expression plasmids into *N. meningitidis* strain H44/76, kanamycin was used to select for successful transformants. The *tol-pal* insert reduced transformation frequency for both expression vectors compared to the empty vector. There would have been approximately half the number of the large *tol-pal* expression vectors (11kb) than the empty vector (6.6kb) in the 1μg of DNA used and this may have accounted for the reduced transformation

frequency. Primers for PCR were designed to amplify the *tol-pal* genes at the two ends of the operon (fig.7).

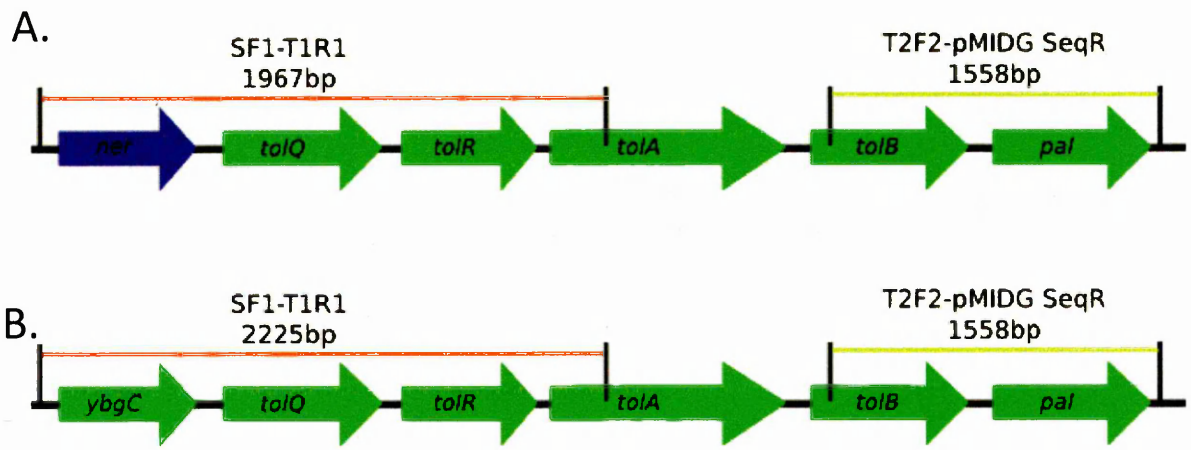

Figure 7. PCR products used to identify successful *N. meningitidis tol-pal* transformants. Bacteria carrying the plasmids were identified from transformation plates by PCR. (A) pMIDGTol-Palner PCR products. (B) pMIDGTol-Pal PCR products.

The reaction T2F2-pMIDG SeqR which amplifies *tolB* and *pal* was used to confirm the presence of the plasmid after transformation (fig. 8).

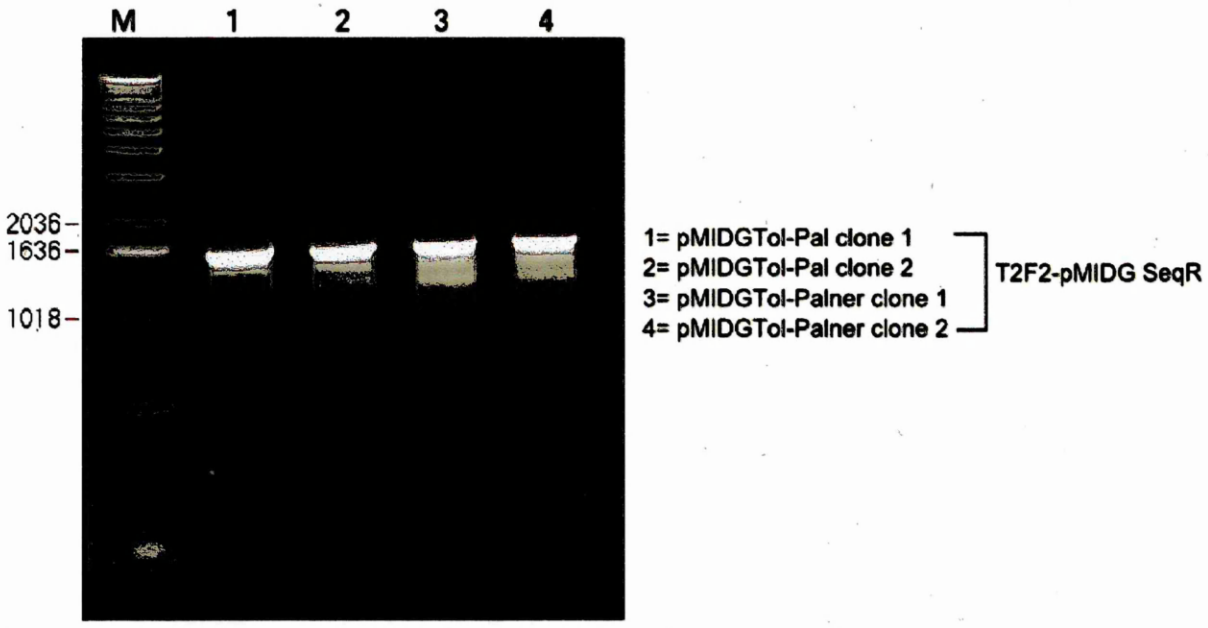

Figure 8. Transformation of pMIDGTol-Pal and pMIDGTol-Palner into wildtype H44/76 *N. meningitidis*. Colony PCR from a transformation of pMIDGTol-Pal and pMIDGTol-Palner using the primers T2F2-pMIDG SeqR. Clones from pMIDGTol-Pal transformation are in lanes 1 and 2, clones from pMIDGTol-Palner transformation are in lanes 3 and 4. Expected band size was 1558bp.

Following transformation with pMIDGTol-Palner or pMIDGTol-Pal all the colonies tested were positive for the *tol-pal* region. Colonies were sub-cultured for 24 hours after transformation and the presence of the *tol-pal* genes was tested using the PCRs at the 5' and 3' ends end of the region (SF1-T1R1 and T2F2-pMIDG SeqR) (fig.9).

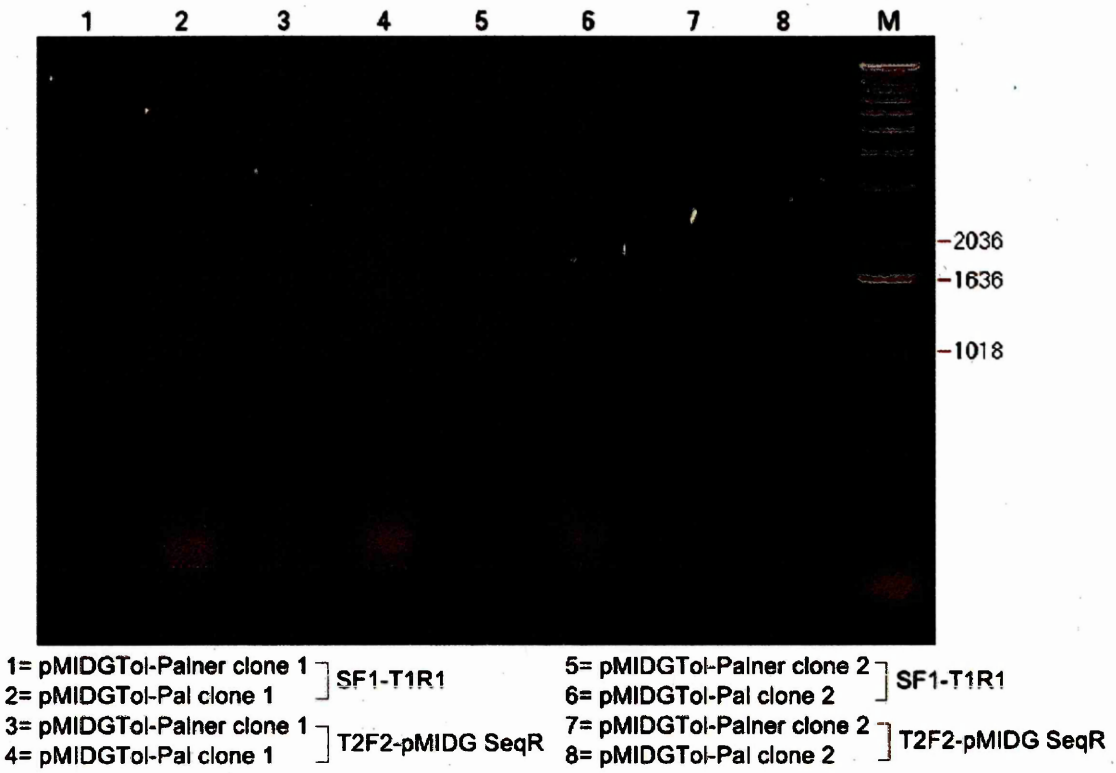

Figure 9. Colony PCR from pMIDGTol-Palner and pMIDGTol-Pal clones after twenty-four hour incubation. Colony PCR with the primers SF1-T1R1 and T2F2-pMIDG SeqR. Lanes 1 and 3 and 5 and 7 show pMIDGTol-Palner clones 1 and 2. Lanes 2 and 4 and 6 and 8 show pMIDGTol-Pal clones 1 and 2.

After 24 hours the *tol-pal* DNA could not be detected in the colonies, but the clones had maintained kanamycin resistance. Therefore it was likely that the plasmid had undergone recombination to excise the *tol-pal* genes but had not been eliminated from the bacteria. Multiple transformations of both *tol-pal* containing plasmids produced the same result; initially positive clones lost the *tol-pal* region after 24 hours further growth.

4.5 Recombination of the *tol-pal* containing plasmids by *N. meningitidis*

Potential recombination of the *tol-pal* containing plasmids was examined by isolating plasmids from transformants that maintained antibiotic resistance but became PCR negative for the *tol-pal* region. To amplify the plasmids for sequencing *E. coli* Top10 cells were transformed with plasmid recovered from two pMIDGTol-Pal and two pMIDGTol-Palner *N. meningitidis* transformants. The *E. coli* were *RecA*$^-$ and therefore recombination deficient, preventing alteration of the plasmids. Plasmid prepared in this way was sequenced to identify the regions of DNA that were lost and to locate the sites of

recombination. Because the clones remained kanamycin resistant, sequencing was performed from within the *kanR* gene in both upstream and downstream directions (fig. 10).

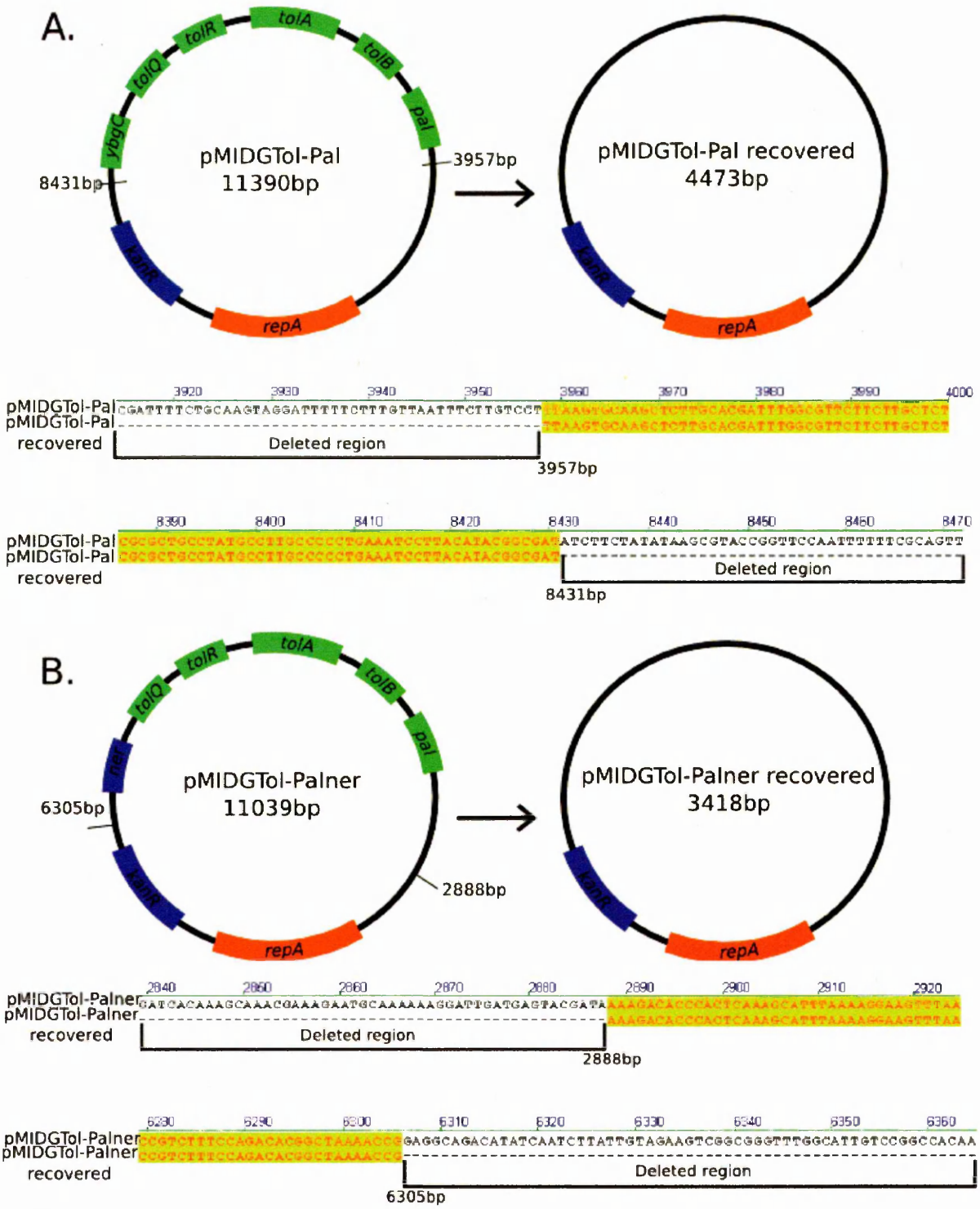

Figure 10. Recombination of the pMIDGTol-Pal and pMIDGTol-Palner plasmids by *N. meningitidis*. Plasmid recovered from the *N. meningitidis tol-pal* clones was sequenced to find the sites of recombination. (A) The pMIDGTol-Pal plasmid was shown to have lost the region between 8431bp-3957bp. (B) pMIDGTol-Palner had lost the region between 6305bp-2888bp. The two plasmids did not show common recombination sites, both maintained the Kanamycin resistance gene, the *repA* gene and the *repA* origin of replication.

Recombination had occurred to remove the *tol-pal* complex from both plasmids whilst maintaining the antibiotic resistance and origin of replication. The pMIDGTol-Pal plasmid had recombined to lose 6917bp, deleting the entire *tol-pal* region. The pMIDGTol-Palner plasmid lost 7621bp, removing the *tol-pal* region and the *ner* promoter. The sites of recombination in the two plasmids were not common and recombination was not the result of homologous sequences at the ends of the deleted regions, also no known sequences prone to recombination were identified. Loss of the *tol-pal* genes occurred in all *N. meningitidis* transformants tested; the lack of obvious motifs promoting recombination in the plasmid implied that there was a strong selection pressure on the bacterium to remove the *tol-pal* complex.

4.6 Transformation of *N. meningitidis* with pMIDGTolF1

The selection pressure against *tol-pal* could be due to either the functional Tol-Pal complex or its individual proteins. To test if the assembled complex was responsible, *N. meningitidis* was transformed with a plasmid (pMIDGTolF1) containing the first genes of the *tol-pal* operon *ybgC, tolQ, tolR* and a large portion of *tolA* under the control of the native P_1 promoter. The pMIDGTolF1 plasmid produced colonies and the presence of the partial *tol-pal* region was tested by a PCR that amplified the region between *tolQ* and *tolA*. The presence of the plasmid in the transformants was assayed following transformation and after a further twenty four hours growth (Fig.11).

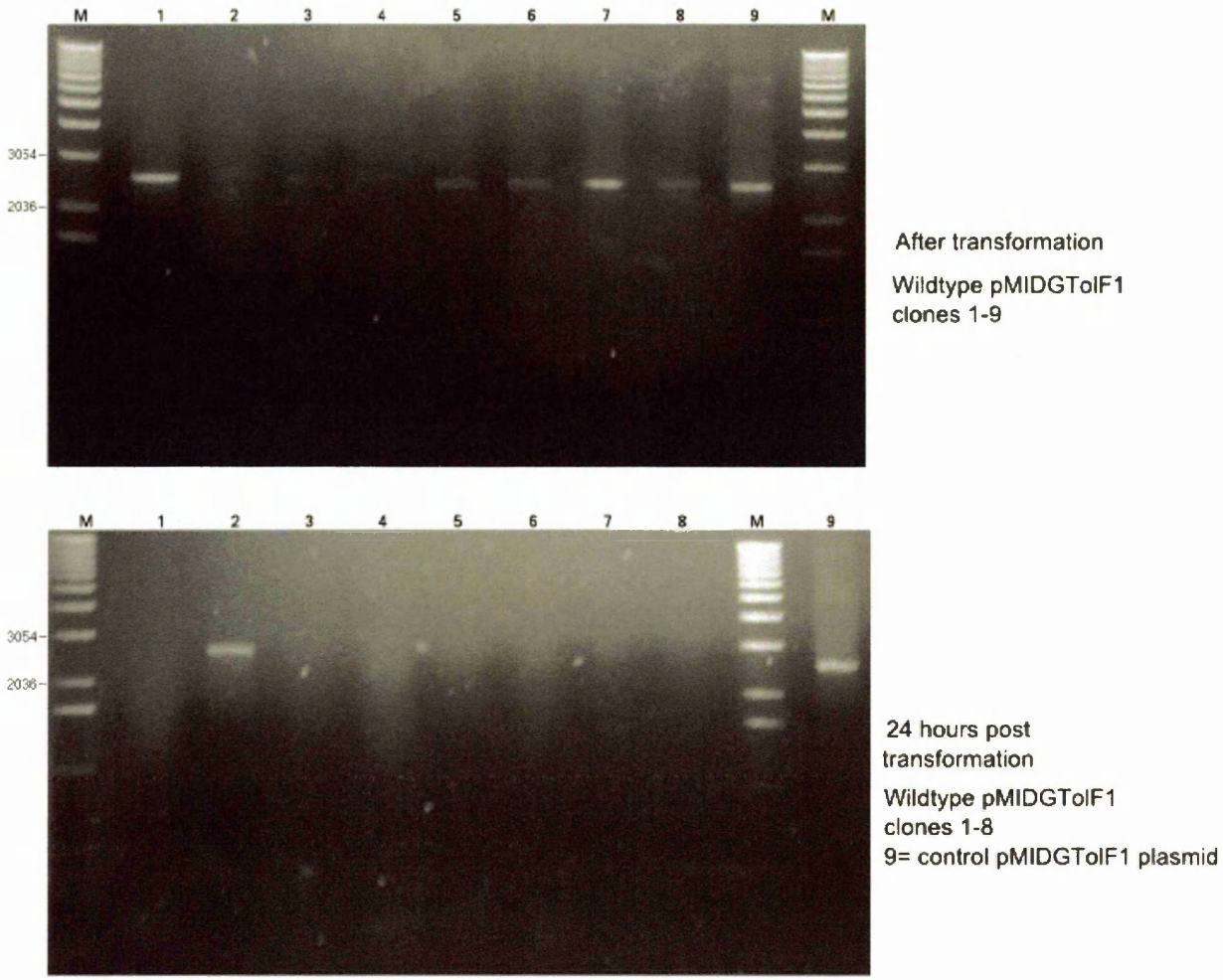

Figure 11. Transformation of the pMIDGTolF1 plasmid into wildtype *N. meningitidis*. The transformation was tested with PCR using primers SF1-SR6 to produce a product 2618bp in length. The top gel shows nine clones tested after transformation. The bottom gel shows eight of the clones tested after 24 hours further incubation.

Following transformation all of the clones were PCR positive and showed a faint band at 2.5kb. After 24 hours however, most of the clones had become negative for the *tolQ-tolA* region but maintained the antibiotic resistance. One clone (clone 9) did not grow when subcultured, probably the result of losing the kanamycin resistance gene. A single colony (lane 2) maintained the plasmid after repeated subcultures of the strain and the presence of the partial *tol-pal* region could be confirmed by PCR (data not shown). The plasmid could have contained a point mutation or small loss of sequence, but it did not show the deletion of the *tol-pal* genes that was seen in all of the other plasmids.

4.7 Discussion

The original hypothesis underlying this work was that the expression of the Tol-Pal complex in *N. meningitidis* would reduce the production of membrane vesicles. However expression of the complex in wildtype *N. meningitidis* could not be achieved, because the plasmids containing the genes were lethal to the meningococcus. Cloning of the *tol-pal* genes into the expression vector presented no problems and expression of the Tol-Pal proteins from the plasmids was tolerated in *E. coli,* complementing the detergent sensitivity of the *Δtol-pal* strain. However, when the plasmids were introduced into *N. meningitidis* the bacteria were under a strong selection pressure against the *tol-pal* genes and the plasmids underwent recombination that deleted the five *tol-pal* genes in every surviving clone. Deletion of any of the genes *tolQ, tolR, tolA, tolB* or *pal* will prevent the function of the Tol-Pal complex. In the case of the pMIDGTol-Palner plasmid, removal of the *ner* promoter would also prevent transcription and therefore function. The consistent deletion of all the genes indicated that the selection pressure operating against *tol-pal* in *N. meningitidis* was against the expression of the individual Tol-Pal proteins and not the formation of a functional multi-protein complex. Later work (Chapter 5 fig. 5 pg. 127) confirmed that mRNA was transcribed from the *tol-pal* genes in *N. meningitidis* demonstrating that the proteins were likely to be expressed in the bacteria.

The genes *tolQ*, *tolR* and the portion of *tolA* were not tolerated even without the rest of the *tol-pal* region present. However if the intolerance of the complex was due simply to these proteins, constructs containing the other *tol-pal* genes (the complete *tolA, tolB* and *pal*) would have been expected to be recovered from the bacteria. As there were no obvious motifs in *tol-pal* or the vector backbone sequence to indicate another reason why the complete complex was removed in every clone, it is likely that at least one of the genes *tolA, tolB* and *pal* is also partially responsible for the selection pressure against meningococcal strains expressing *tol-pal.* To establish the toxicity of the *tol-pal* genes individually, plasmids could be constructed containing each gene under a constitutive or inducible promoter but this was beyond the scope of this project.

The structure and biology of the Tol-Pal proteins indicates that they could potentially interfere with the normal cellular functions of *N. meningitidis*, leading to the selection pressure against the expression of these genes. TolQ and TolR show sequence homology to the *E. coli* inner membrane proteins ExbB and ExbD of the TonB system and can partially complement an ExbB ExbD null phenotype (111). Both TolQ and TolR and ExbB and ExbD are thought to produce a proton motive force to drive the interactions of their respective complexes. The TonB system is also present in *N. meningitidis*; it is involved with the translocation of iron and other molecules across the cell wall and provides a link between the inner and outer membranes. The *N. meningitidis* ExbB and ExbD proteins share 30% sequence similarity with the *E. coli* TolQ and TolR proteins (138) so it is possible that the TolQ and TolR proteins may disrupt the normal functioning of the TonB system. It has been demonstrated that disruption of TonB affects nutrient uptake, but at least some of these uptake processes can be complemented by other proteins (111,138). Disruption of TonB in *N. meningitidis* is not lethal. Therefore, although disruption of the TonB system could be part of the cause, it is not on its own sufficient to lead to such a strong negative selection pressure against the Tol-Pal proteins.

In *E. coli* Tol-Pal is important in cell division and a chaining phenotype is present in *Δtol-pal* strains (45). In order to function in cell division the Tol-Pal complex must be assembled, however it is still possible that individual proteins may interfere with cell division if they were properly folded and transported to the correct locations in the cell wall. The only targeting mechanism identified for the Tol-Pal complex is the targeting of the Pal protein by the LolABCDE system (21). A putative homologue of the LolA protein has been identified in the *N. meningitidis* MC58 genome (NMB0622) and some outer membrane proteins in *N. meningitidis* contain signal sequences consistent with transport by the Lol system (14). Therefore it is possible that Pal may interfere in cell division.

Although the individual Tol-Pal proteins could potentially interfere with the cellular functions of *N. meningitidis*, it is difficult to identify a mechanism of disruption that would produce such a strong negative selection pressure. Accumulation of misfolded or misdirected Tol-Pal proteins could itself

become a severe stress to the bacteria. Protein accumulation could lead to disruption of the outer membrane due to increased pressure in the periplasmic space, in turn increasing the likelihood of cell lysis. The overproduction of Tol-Pal in a wildtype *E. coli* clone produced a phenotype of increased detergent sensitivity, indicating that an increase in Tol-Pal proteins in the cell wall causes outer membrane disruption. If accumulation of Tol-Pal proteins in the cell wall were lethal in *N. meningitidis*, it would explain the deletion of all the *tol-pal* genes in the clones and the presence of the selection pressure against the Tol-Pal proteins regardless of whether all or some of the *tol-pal* genes are expressed. Although the interference with *N. meningitidis* cellular processes by functional proteins such as TolQ, TolR and Pal could be contributing to the selection pressure against the genes, it seems likely that a mechanism based on misfolded or misdirected protein is the most likely explanation for the selection against the expression of *tol-pal*.

Both disruption by accumulation of protein and the potential interference of Tol-Pal proteins in cellular processes, such as the functioning of the TonB system and cell division, would affect the cell wall and particularly the outer membrane. Increased vesiculation could allow for greater tolerance of the Tol-Pal proteins. It has been indicated in *E. coli* that vesicles are used to remove misfolded protein from the cell (93). Mutants of *N. meningitidis* outer membrane proteins that show high vesiculation could therefore show tolerance of the *tol-pal* genes. In addition to their increased vesicle release, changes in the structure of the outer membrane and cell wall could lessen the interference of the Tol-Pal proteins or allow the Tol-Pal proteins to compensate for the outer membrane protein mutations.

Chapter 5- Investigation of the phenotype of an *N. meningitidis* strain containing the *tol-pal* genes

5.1 Introduction

The *tol-pal* complex is commonly found in the genomes of Gram negative bacteria, but is absent in *N. meningitidis* (139). As described in the previous chapter, attempts to express *tol-pal* in the wildtype H44/76 *N. meningitidis* strain demonstrated that the *tol-pal* genes were not tolerated. It was subsequently hypothesized that the intolerance of the *tol-pal* genes was due to the Tol-Pal proteins disrupting the structure of the cell wall, either because of interference by functional proteins or accumulation of misfolded protein.

In *E. coli Δtol-pal* mutants have been shown to have phenotypes of vesicle release, membrane instability and aberrant cell division (7,21,45). A similar phenotype of high vesicle release, membrane instability and a failure of cells to separate has been shown for the *Δgna33* mutant of *N. meningitidis* (Chapter 3 pg. 82 and (2,37). The *ΔrmpM* mutant also released a high level of outer membrane vesicles compared to the wildtype (Chapter 6 pg. 175 and (150)). Selection pressure against the Tol-Pal complex may be less stringent in these mutants, the Tol-Pal proteins may be able to compensate for the mutated meningococcal proteins by stabilizing the outer membrane or, if accumulation of misfolded protein is the cause of the intolerance, increased vesiculation in both strains could allow this to be removed. Although such mutants would not be expressing the Tol-Pal proteins in a wildtype background, strains would provide evidence of the effects of the Tol-Pal proteins on *N. meningitidis* and information on the reasons why the Tol-Pal proteins are not tolerated in the wildtype.

The aim of this study was to assess the stability of the *tol-pal* genes in the mutant strains *Δgna33* and *ΔrmpM* by transforming these strains with the *tol-pal* expression vector pMIDGTol-Pal. If stable Tol-Pal expressing strains could be produced, the phenotypes of these stains would provide evidence of the effects of the Tol-Pal proteins on *N. meningitidis*.

5.2 Transformation of *N. meningitidis* outer membrane protein mutants with pMIDGTol-Pal

The plasmid pMIDGTol-Pal which contained the gene operon under the transcription control of the native *E. coli* promoters was transformed into *N. meningitidis ΔrmpM* and *Δgna33* strains (fig.1).

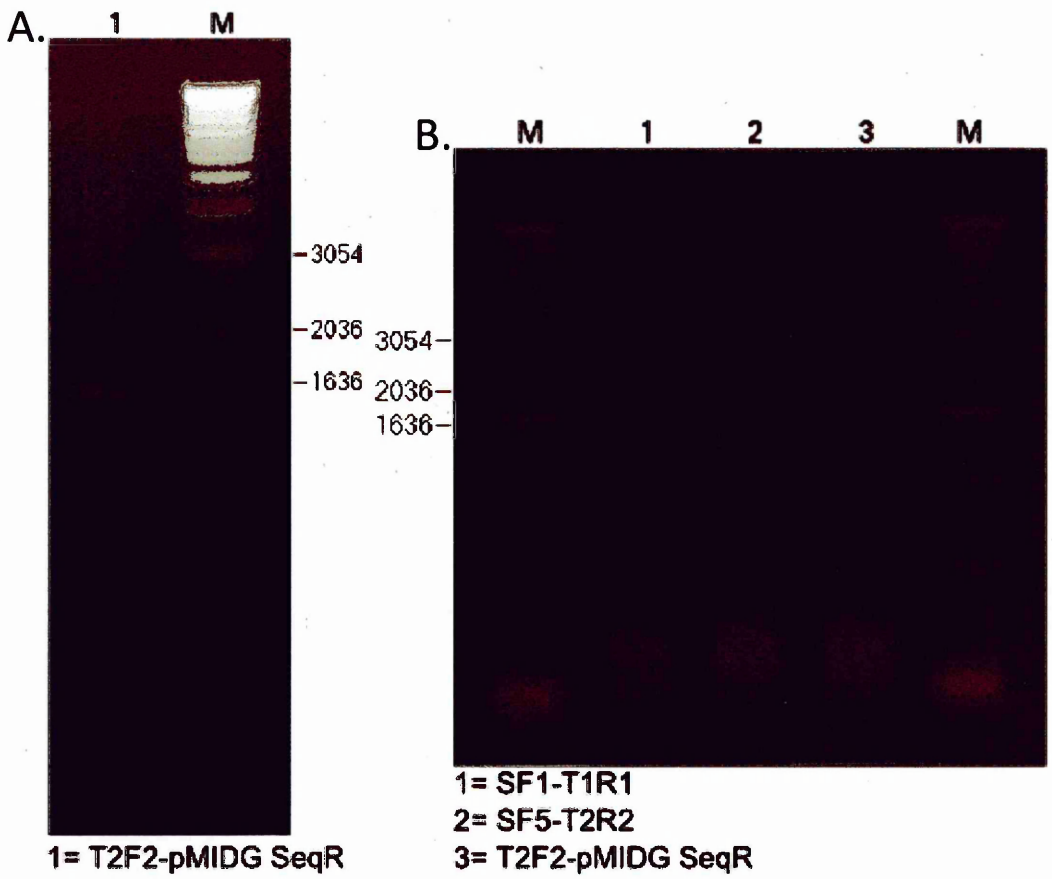

Figure 1. Transformation of an H44/76 *ΔrmpM* mutant with pMIDGTol-Pal. (A) Colony PCR with the primers T2F2-pMIDG SeqR for a colony produced by transformation of *ΔrmpM* with pMIDGTol-Pal (B) Colony PCR with primers SF1-T1R1, SF5-T2R2 and T2F2 – pMIDG SeqR (lanes 1-3) for the same colony after 24 hours incubation.

Transformation of the *ΔrmpM* strain produced a single colony containing the pMIDGTol-Pal plasmid, confirmed by colony PCR. After a further twenty four hours of growth the Tol-Pal complex had been lost from the plasmid, indicating that expression of the Tol-Pal proteins was lethal for this mutant as it was in the wildtype.

Transformation of the *Δgna33* strain did not produce any colonies with the pMIDGTol-Pal plasmid despite repeated transformations. As the *Δgna33* strain would not produce transformants, the *gna33*

single crossover strain was also transformed. This strain contained a linearised *gna33* knockout plasmid integrated downstream of the *gna33* gene and showed slightly increased vesiculation and variable levels of *gna33* mRNA expression; low on solid media and higher in liquid culture (chapter 3 fig. 9 pg.73). Transformation with pMIDGTol-Pal produced eight colonies that were positive for the Tol-Pal complex by PCR. After 24 hours further incubation two colonies were still positive for both the 5' and 3' ends of the Tol-Pal complex (fig.2).

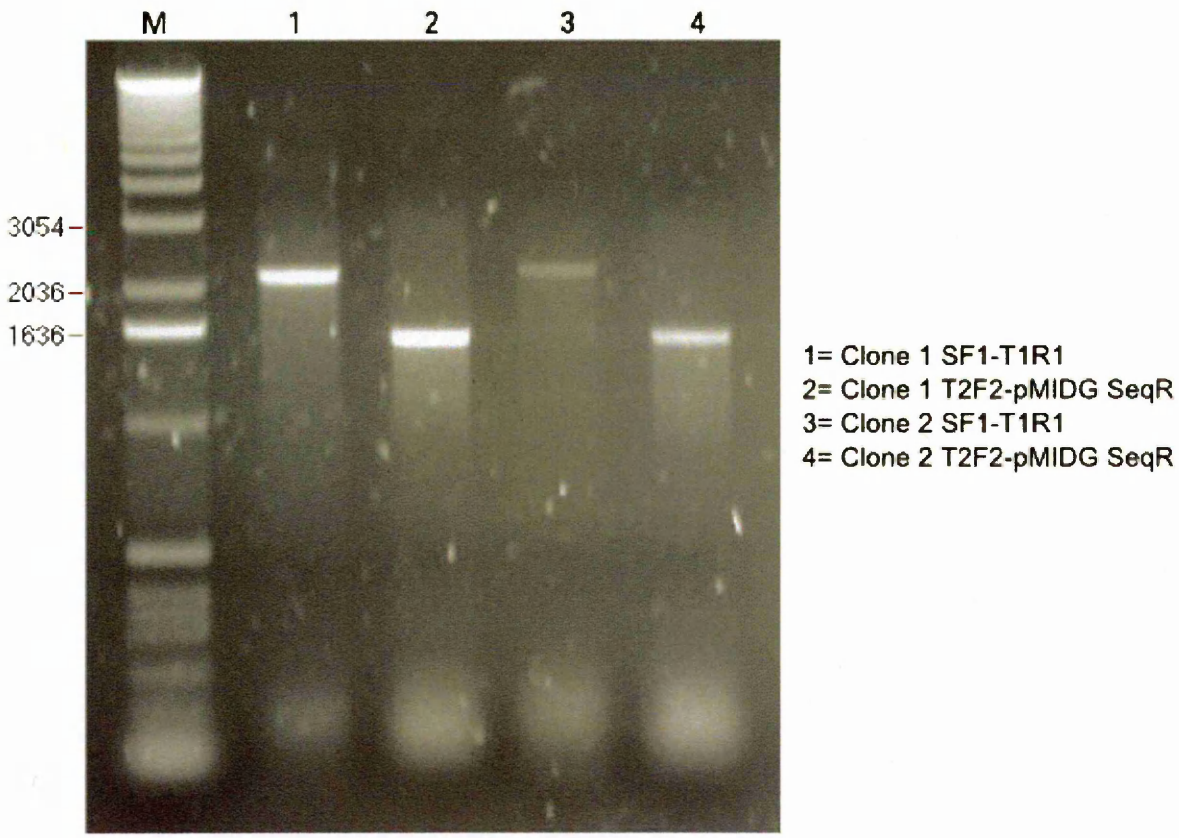

Figure 2. Transformation of the *gna33* single crossover strain with pMIDGTol-Pal. Colony PCR for two clones produced by transformation of *gna33* single crossover strain with pMIDGTol-Pal. Lanes 1 and 3, colony PCR with the primers SF1-T1R1. Lanes 2 and 4, colony PCR with the primers T2F2-pMIDG SeqR.

The pMIDGTol-Pal plasmid was stable in these colonies after repeated subcultures, but to ensure that no point mutations or small recombinations had occurred, plasmid recovered from the strains was analysed by restriction digestion and sequencing (fig.3).

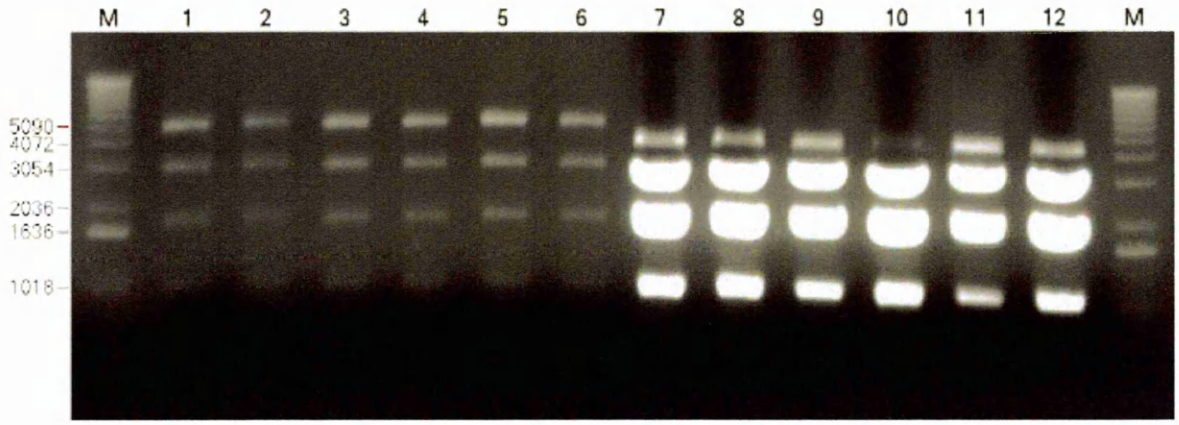

1= Clone 1 C1
2= Clone 1 C2
3= Clone 1 C3
4= Clone 1 C4
5= Clone 1 C5
6= Clone 1 C6

EcoRV

7= Clone 2 C1
8= Clone 2 C2
9= Clone 2 C3
10= Clone 2 C4
11= Clone 2 C5
12= Clone 2 C6

EcoRV

Expected fragments
5312
3099
1831
1025
123

Figure 3. Restriction digest of plasmid recovered from *N. meningitidis gna33* single crossover*::tol-pal* strains. Recovered plasmid from the *N. meningitidis* strains was transformed into *E. coli*. 6 transformants (C1-6) from each strain were tested. Lanes 1-6: *gna33* single crossover*::tol-pal* clone 1. Lanes 7-12: *gna33* single crossover*::tol-pal* clone 2.

Restriction digestion with *EcoRV* demonstrated that the plasmid from the first *gna33* single crossover*::tol-pal* clone had the expected band pattern for the pMIDGTol-Pal plasmid. The plasmid from clone 2 however showed a loss of approximately 1kb from the 5312bp band. The plasmid was also overloaded compared to the plasmid from clone 1, despite the two plasmids being prepared from the same volume of *E. coli* culture and the same amount being added to the restriction digests. This suggested that the copy number of the plasmid had changed. A *BamHI* digest performed on the plasmid (not shown) also exhibited overloading and a band 1kb smaller than the expected size. The *tol-pal* regions of both plasmids were sequenced and shown to be identical to the sequence of the pMIDGTol-Pal plasmid, confirming that no recombination or point mutation had occurred. The *gna33* single crossover mutant was therefore capable of maintaining the pMIDGTol-Pal plasmid. Because the strain maintained the *tol-pal* genes under the native promoters, the plasmid containing the *tol-pal*

genes under the constitutive *ner* promoter was also transformed into the *gna33* single crossover mutant. However, the strain would not maintain this plasmid (data not shown).

5.3 Recombination of the pMIDGTol-Pal plasmid by *gna33* single crossover mutant

The apparent increase in plasmid copy number in clone 2 suggested that the plasmid had undergone recombination outside the *tol-pal* sequence. A high copy number plasmid could have been produced by the insertion of a different origin of replication, most likely from the plasmid introduced into the genome of the *gna33* single crossover (see chapter 3 fig.4 pg. 68). The linearised *gna33* knockout plasmid contained the PmB origin of replication, which has a high copy number in *E. coli* (75) and a 361bp region of sequence homologous with the pMIDGTol-Pal plasmid. Sequencing of the *tol-pal* plasmid recovered from clone 2 found 1394bp of inserted sequence from the linearised plasmid, including the PmB origin of replication. This plasmid had a high copy number in *E. coli*, but not in *N. meningitidis* where the PmB origin is not functional. The plasmid was named pMIDGTol-PalPmB and was used to test the ability of the pMIDGTol-Pal plasmid to complement the *Δtol-pal E. coli* strain (Chapter 4 fig. 6 pg. 109).

5.4 Transformation of *gna33* single crossover with pMIDGTolF1

Unlike the wildtype, the *gna33* single crossover mutant was capable of maintaining the pMIDGTol-Pal plasmid in two out of eight clones. However, the mutant could not maintain a plasmid where the *tol-pal* complex under the control of the constitutive *ner* promoter (data not shown). These results indicated that the selection pressure against the Tol-Pal complex was ameliorated, but not abolished, in the *gna33* single crossover. In the wildtype, transformation with a plasmid containing only the genes *tolQ*, *tolR* and part of *tolA* under their native promoter (pMIDGTolF1) was not tolerated. To test if the amelioration of the selection pressure in the *gna33* single crossover was due to tolerance of these genes and if the selection pressure against the complex was increased by the number of *tol-pal* genes present, the strain was transformed with the pMIDGTolF1 plasmid. Colonies positive for the

tolQ, *tolR* and partial *tolA* genes by PCR after transformation were tested for the presence of the genes after a further 24 hours growth (fig.4).

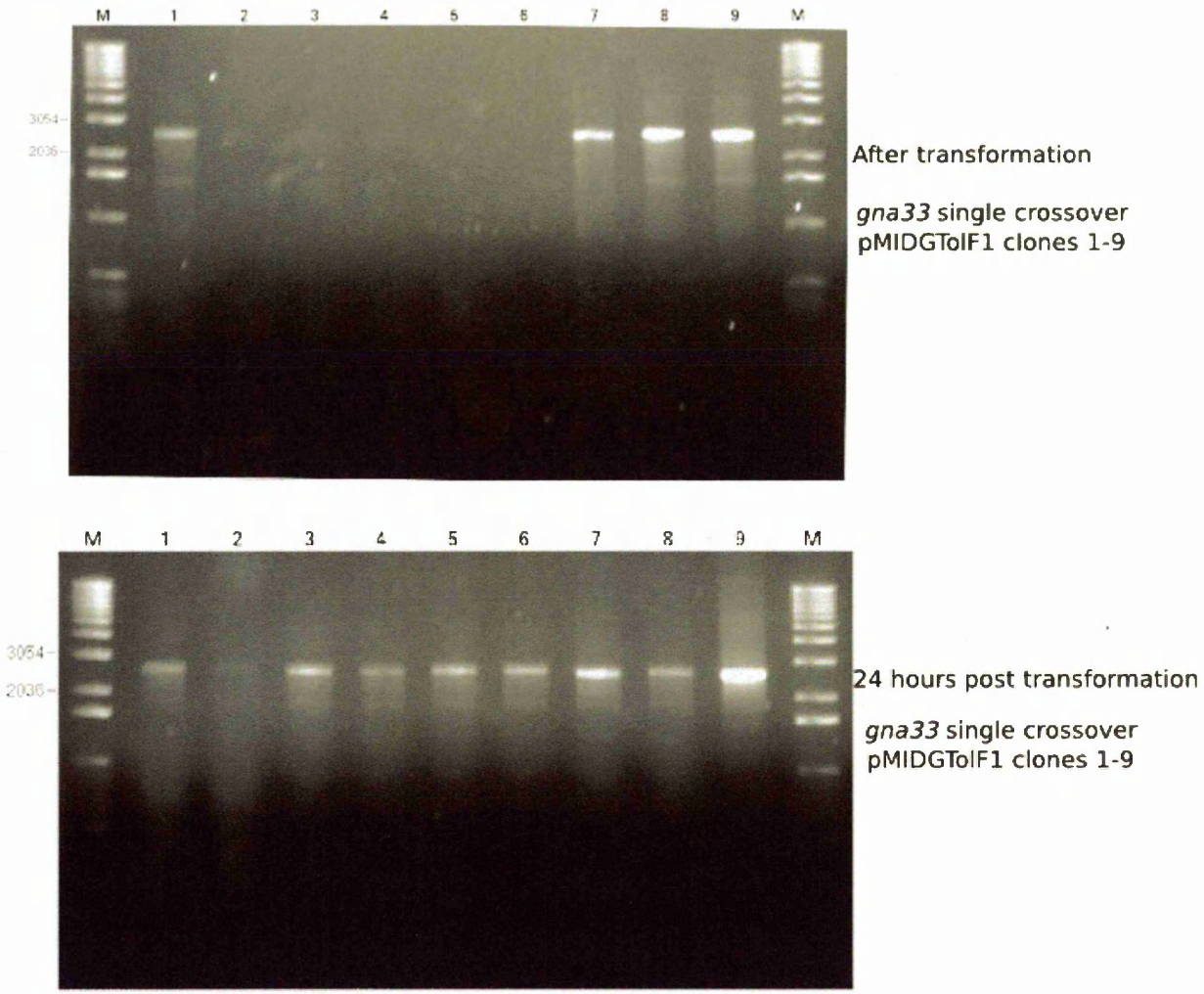

Figure 4. Transformation of the pMIDGTolF1 plasmid into *gna33* single crossover strain. The transformants were tested with colony PCR using primers SF1-SR6 producing a 2618bp product. Nine colonies were tested immediately after selection from the transformation plate and twenty four hours after subculture from the transformation plate.

The *gna33* single crossover strain tolerated the genes *tolQ, tolR* and partial *tolA* in all the clones. Although bands in the PCR after transformation were faint, eight of the nine clones were strongly positive for the *tol-pal* genes after 24 hours further growth. The clone in lane 2 was weakly positive for the construct. It is possible that the strains may contain smaller recombinations or point mutations that are not shown by the PCR, but the large loss of DNA shown in all the other strains transformed with *tol-pal* constructs was not seen. Unlike the wildtype, the *gna33* single crossover

tolerated the partial plasmid. Therefore amelioration of the selection pressure against the complete operon in the mutant was likely to result from the tolerance of the genes *tolQ*, *tolR* and partial *tolA*, but there remained a selection pressure against the expression of other *tol-pal* genes.

5.5 Transcription of *tol-pal* in the *gna33* single crossover::*tol-pal* strain

The Tol-Pal proteins were not visible on SDS-PAGE gels and monoclonal antibodies against the proteins were not available. Therefore RNA was used as an indicator of expression of the Tol-Pal proteins. To establish if the *gna33* single crossover::*tol-pal* mutant was producing mRNA from the *tol-pal* genes, total RNA from the strains was examined using RT-PCR (fig.5).

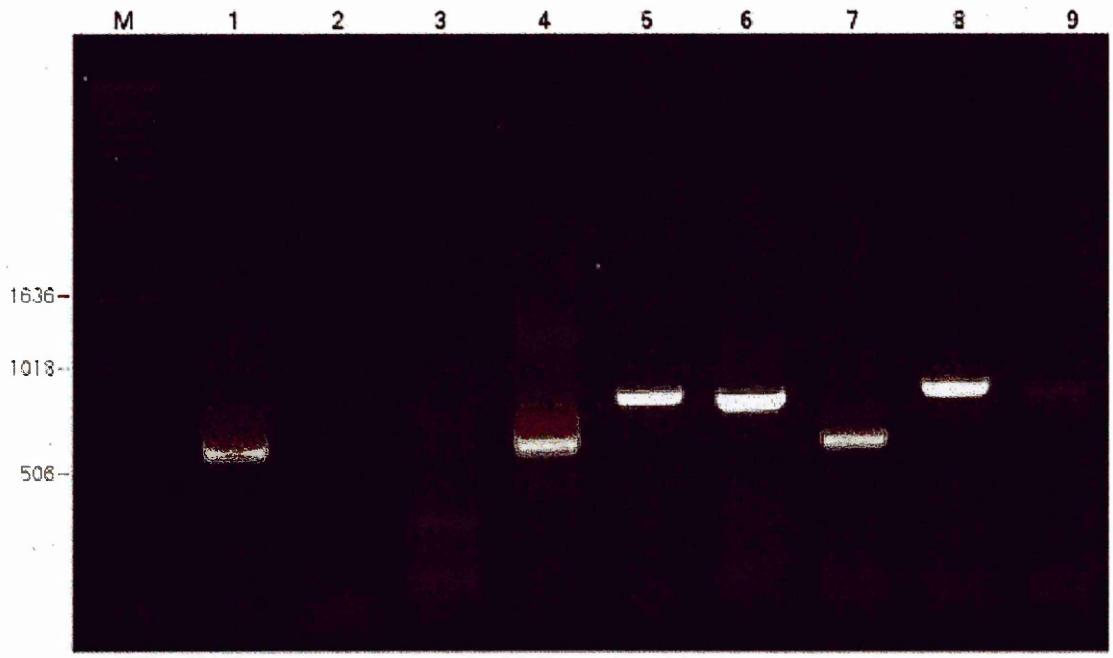

Figure 5. RNA production from *gna33* single crossover::*tol-pal* mutants. RT-PCR products of the background strain (*gna33* single crossover) and the two *tol-pal* containing mutants. *porA* mRNA production is used as a control (582bp). Lanes 1-3 contain cDNA from *porA* mRNA and the two *tol-pal* mRNA transcripts (760bp and 652bp) in the *gna33* single crossover mutant. Lanes 4-6 cDNA from the *gna33* single crossover::*tol-pal* clone 1. Lanes 7-9 cDNA from the *gna33* single crossover::*tol-pal* clone 2.

The mRNA products were detected by using two primer pairs, to test for transcripts from both promoters P_1 (lanes 5 and 8) and P_B (lanes 6 and 9). As in previous experiments, *porA* RNA was used

as a control. The background strain (*gna33* single crossover) showed no expression of either of the *tol-pal* mRNA species. The *gna33* single crossover::*tol-pal* clone 1 showed bright single bands for both transcripts, clone 2 showed a bright band for the *tolQ-tolA* transcript (from the P_1 promoter) but the band for the *tolB-pal* transcript (P_B promoter) was relatively weaker. A similar amount of total RNA was present in both reactions; therefore clone 2 was not transcribing the product from P_B as efficiently as clone 1. It is possible that the P_B promoter is non-functional in this strain; read-through expression of *tolB-pal* is known to occur from P_1. However, sequencing of this region showed no change in the P_B promoter in the plasmid. Because of this difference in expression levels, clone 1 was used for further phenotypic studies.

5.6 Production of *gna33* RNA in *gna33* single crossover::*tol-pal*

The *gna33* single crossover mutant produced low levels of *gna33* RNA when grown on solid media, but wildtype levels when the bacteria were grown in broth (chapter 3 fig.17). To see if this characteristic was also present in the *gna33* single crossover::*tol-pal* mutants the expression of *gna33* RNA from cultures grown on solid media was assayed using RT-PCR (fig.6).

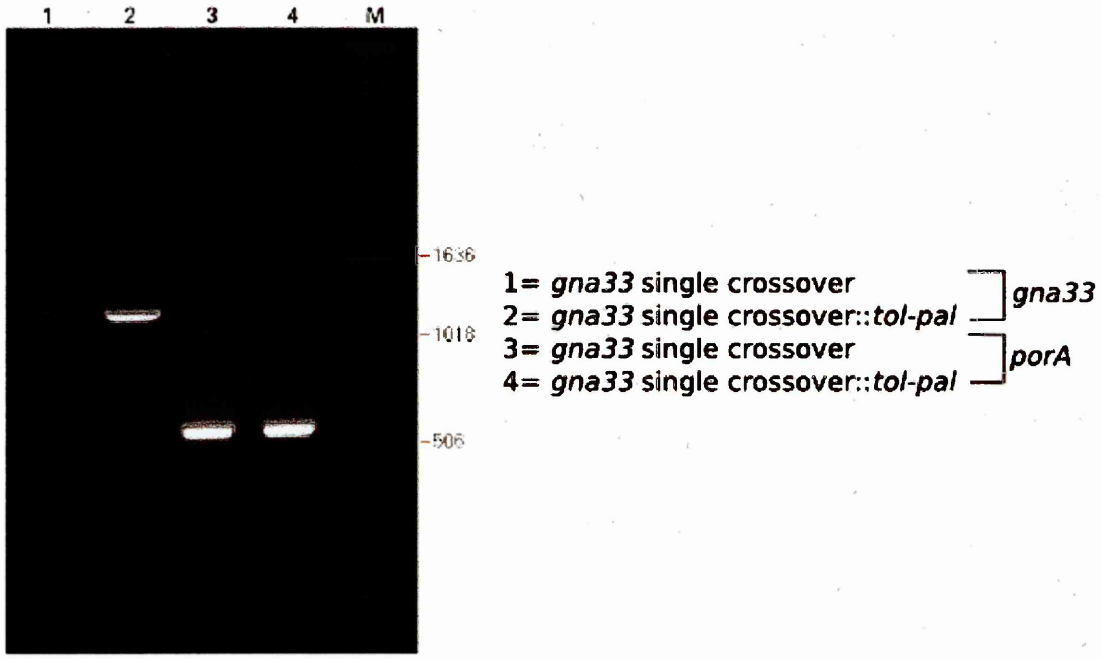

Figure 6. Changes in the transcription of *gna33* RNA in *gna33* single crossover::*tol-pal* mutants. cDNA products produced by RT-PCR from the *gna33* single crossover and *gna33* single crossover::*tol-pal* strain (clone 1) using the GNA33RNAF and GNA33RNAR primer pair. cDNA from *porA* was used as a control. *gna33* cDNA produced by RT-PCR from the two strains grown on solid media was loaded in lanes 1 and 2. *porA* cDNA was loaded in lanes 3 and 4.

As expected, the transcription of *gna33* in the *gna33* single crossover was low on solid media. However when the *tol-pal* genes are expressed the production of *gna33* mRNA was upregulated. The control of *gna33* production is influenced at both a transcriptional and post-transcriptional level by an upstream signal sequence, which has been suggested to form a GC-rich stem loop (126). This signal sequence was present twice in the *gna33* single crossover genome, due to inclusion of the linearised plasmid. Both regions were sequenced in the *gna33* single crossover and *gna33* single crossover::*tol-pal* strains (data not shown). Signal sequences were identical to the reference sequence in both the *gna33* single crossover and the *gna33* single crossover::*tol-pal* mutants. Therefore changes in transcription in the mutant strains were not the result of sequence changes to this region.

5.7 Growth of *gna33* single crossover::*tol-pal*

Growth of the *gna33* single crossover::*tol-pal* strain was compared to the background strain and the wildtype. Antibiotics were included in the growth media to maintain the *gna33* single crossover (erythromycin) and the pMIDGTol-Pal plasmid (kanamycin) (fig. 7).

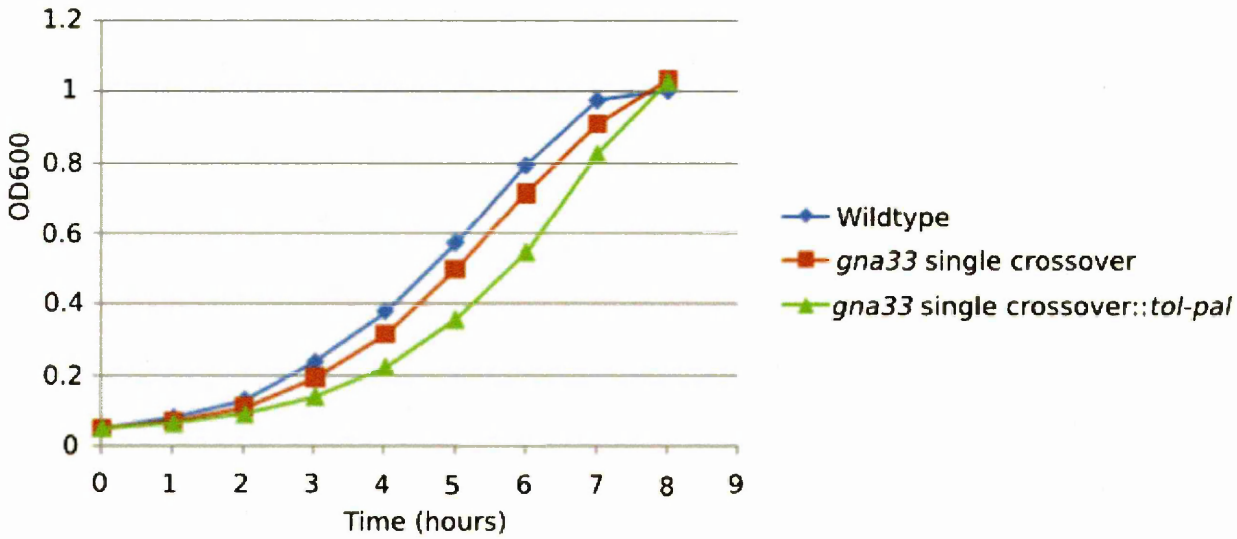

Figure 7. Growth curve of *gna33* single crossover::*tol-pal* mutant. Growth of the wildtype, *gna33* single crossover and *gna33* single crossover::*tol-pal* strains in liquid culture over an eight hour period. Measurements of OD_{600} were used as a surrogate of growth. Curves represent the mean of three experiments.

There was no significant difference between the growth of the *gna33* single crossover::*tol-pal* mutant and the background strain or wildtype when the OD_{600} values were compared at 8 hours (P=>0.05). The mutant did show a slight lag in growth compared to the background and wildtype strains. In a control experiment the *gna33* single crossover transformed with vector without Tol-Pal insert did not show any difference in growth (data not shown), so any lag was likely to be due to the expression Tol-Pal complex.

5.8 Antibiotic sensitivity phenotype of *gna33* single crossover::*tol-pal*

To examine the stability of the cell wall, bacteria were assayed for their sensitivity to a selection of antibiotics that disrupted either peptidoglycan synthesis or the outer membrane (fig.8).

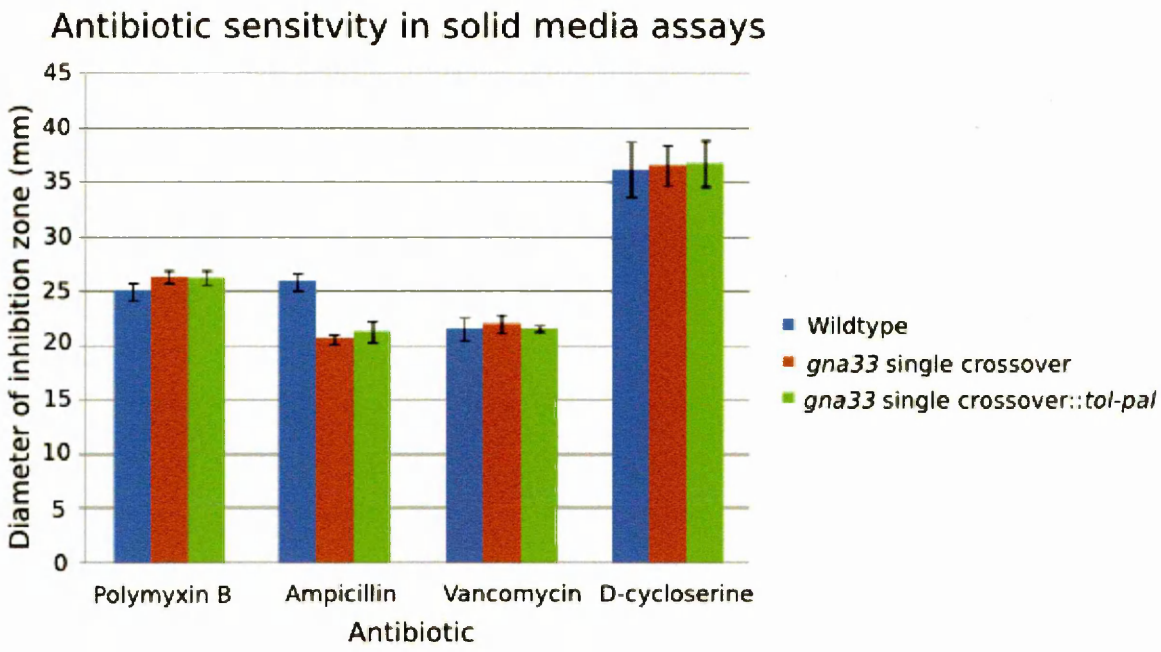

Figure 8. Antibiotic sensitivity on solid media. Sensitivity to the antibiotics polymyxin B, ampicillin, vancomycin and D-cycloserine was tested using disc diffusion assay. Bars represent mean diameter of inhibition zone of three experiments. Error bars represent SEM.

The *gna33* single crossover::*tol-pal* strain showed no significant change in susceptibility to any of the antibiotics tested compared to the background strain (P=>0.05). The *gna33* single crossover::*tol-pal* strain was not significantly different to the wildtype in susceptibility to vancomycin, D-cycloserine or polymyxin B (P=>0.05). Both the *gna33* single crossover and *gna33* single crossover::*tol-pal* were significantly less susceptible to ampicillin compared to the wildtype (P=≤0.05). This was due to the ampicillin resistance gene introduced into the genome in the production of the *gna33* single crossover strain. Expression of the Tol-Pal proteins in the *gna33* single crossover::*tol-pal* strain did not cause an increase in the susceptibility of the strain to the antibiotics tested, therefore it was unlikely that expression of the proteins significantly disrupted the cell wall when the bacteria were grown on solid media.

The growth of *N. meningitidis* in liquid culture was shown to be improved by the addition of sodium chloride (chapter 3 Fig. 11) and it was hypothesized that the bacteria were under osmotic stress. Additional osmotic stress could change the response of the *gna33* single crossover::*tol-pal* mutant to

antibiotics, so the strains were assayed for their susceptibility to the antibiotics ampicillin and polymyxin B in liquid culture. Ampicillin was used to disrupt peptidoglycan synthesis and polymyxin B because its mode of action was directly affected by disruption of the outer membrane. The survival of the bacteria was calculated by the CFU present in the treated samples compared to untreated controls and expressed as percentage survival (fig.9).

A.

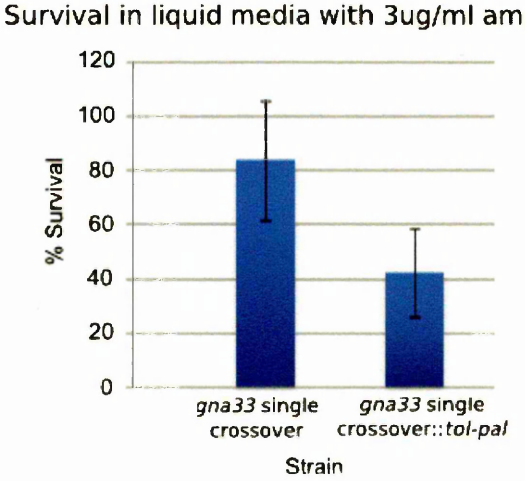

Comparison	T-test result
gna33 single crossover: *gna33* single crossover::*tol-pal*	P=0.007

B.

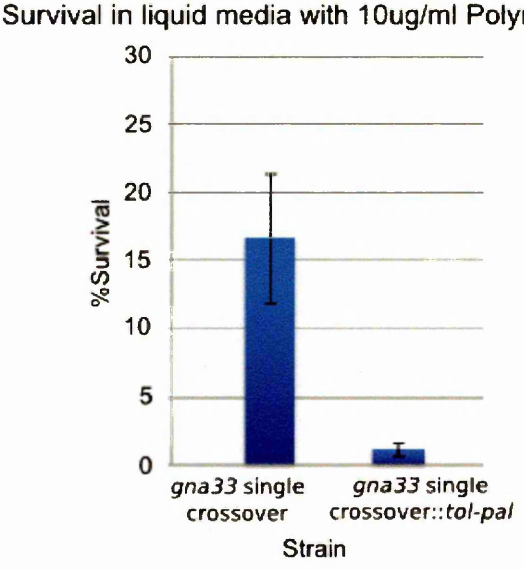

Comparison	T-test result
gna33 single crossover: *gna33* single crossover::*tol-pal*	P=0.04

Figure 9. Antibiotic sensitivity in liquid media. Antibiotic sensitivities of the *gna33* single crossover and *gna33* single crossover::*tol-pal* in liquid media were assayed. Sensitivity was assayed by changes in the number of colony forming units in samples after exposure to antibiotics. (A) Exposure to 3µg/ml ampicillin. (B) Exposure to 10µg/ml polymyxin B. Results are the mean of three experiments. Error bars represent SEM. Significance values were calculated by T-test.

The *gna33* single crossover::*tol-pal* mutant exhibited significant differences in the susceptibility to the tested antibiotics compared to the background strain. Both ampicillin and polymyxin B produced a decrease in survival in the *gna33* single crossover::*tol-pal* strain (P=0.04). To ensure the plasmid was not being lost from the *gna33* single crossover::*tol-pal* strain, cultures were also tested on plates containing kanamycin; these results were not significantly different from the cultures grown without kanamycin (P=>0.05, data not shown). The increased sensitivity to antibiotics indicated that the *gna33* single crossover::*tol-pal* mutant had a disrupted outer membrane and disrupted peptidoglycan.

5.9 Cryo-Electron microscopy of *gna33* single crossover::*tol-pal*

The effects of the Tol-Pal proteins on the outer membrane, peptidoglycan and inner membrane of the bacteria were of particular interest, due to the potential of the proteins to interact with the cell wall. Cryo-electron microscopy was used to examine the morphology of the *gna33* single crossover::*tol-pal* mutant (fig.10).

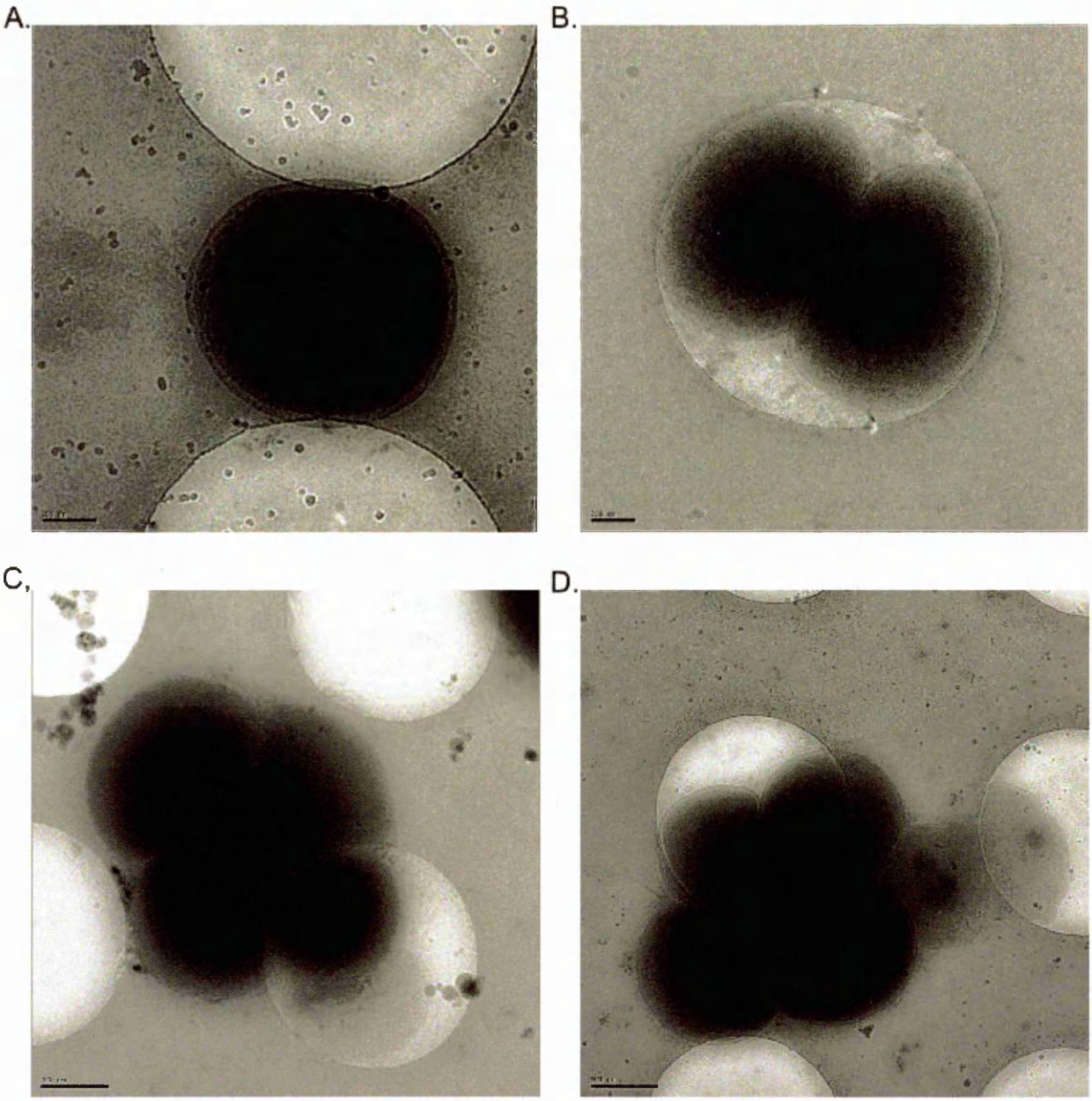

Figure 10. Cryo-electron microscopy of *gna33* single crossover*::tol-pal* strain. Bacteria were compared to the background strain (Chapter 3 fig. 13 pg.80). (A) and (B) Some bacteria were observed as single organisms or in pairs, however the majority of bacteria were observed in clusters of several organisms (C) and (D). (A) 25,000X 200kV, (B) 20,000X 200kV. Scale bar 200nm. (C) and (D) 12,000X 200kV. Scale bar 0.5µm.

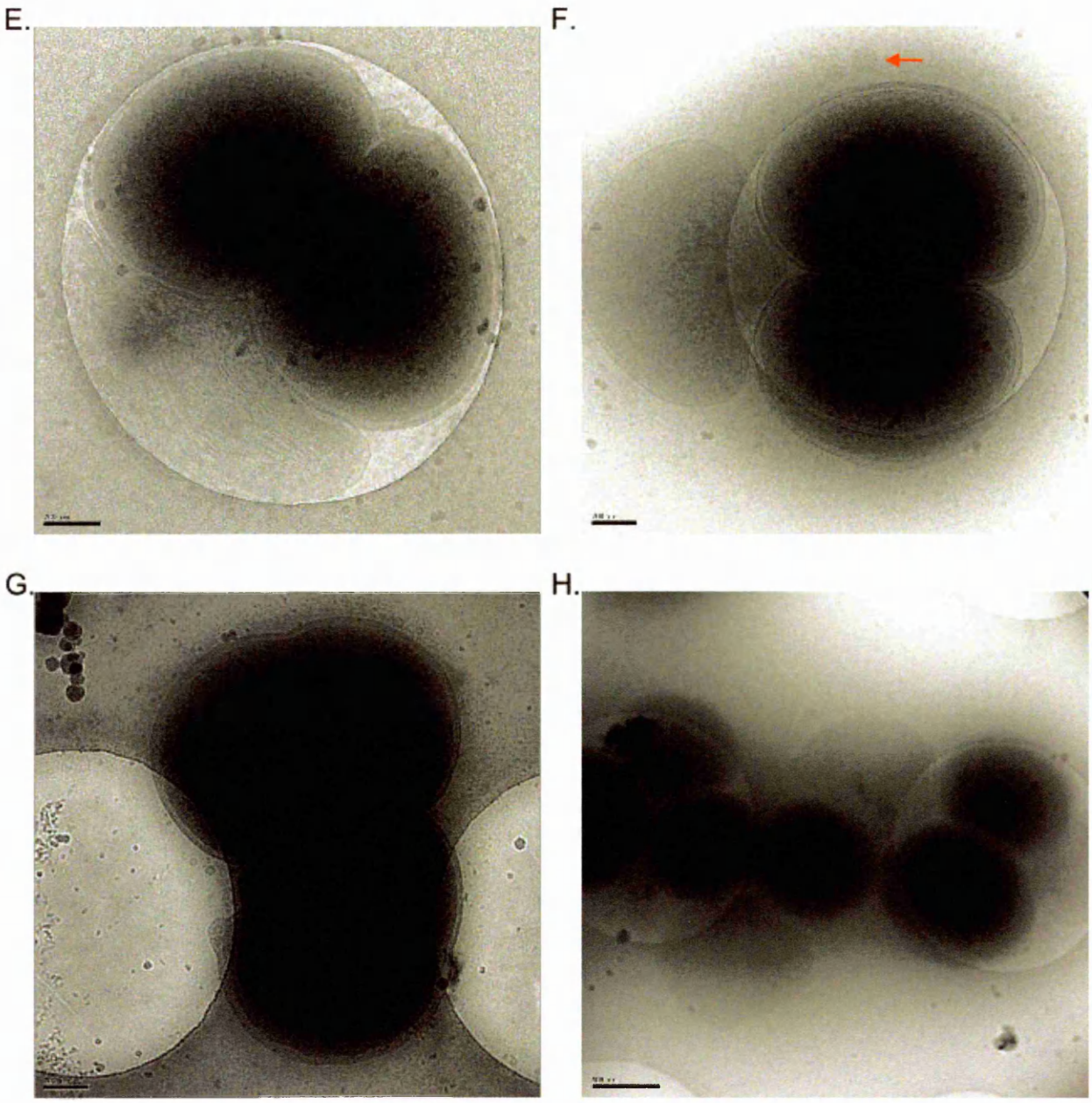

Figure 10. Cryo-electron microscopy of *gna33* single crossover::*tol-pal* strain (continued) (E) and (F) Bacteria were observed in small clusters with dead bacteria (E). Separate outer membranes were clearly visible between clustered bacteria (F). Vesicles were commonly observed (arrowed in (F)). (H) Large clusters were commonly observed. (E) 25,000X 200kV, (F) and (G) 20,000X 200kV. Scale bar 200nm. (H) 12,000X 200kV. Scale bar 0.5µm.

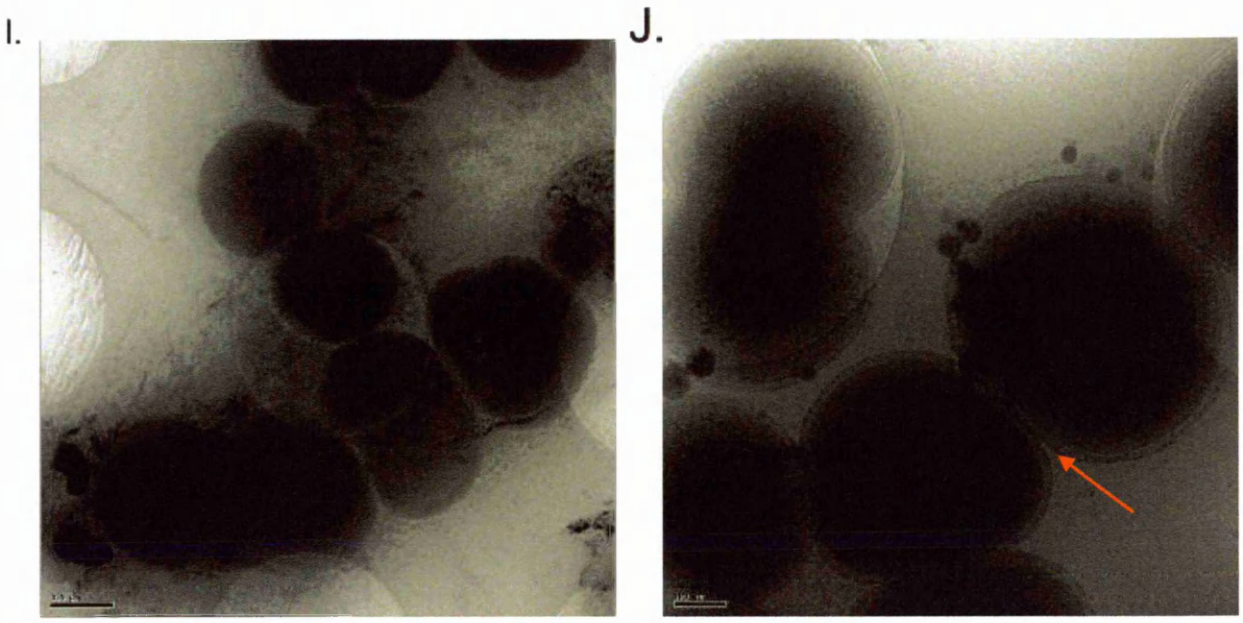

Figure 10. Cryo-electron microscopy of *gna33* single crossover*::tol-pal* strain (continued) (I) and (J) Large clusters observed seemed to show loose association between the bacteria, however bacteria were only rarely observed outside of these clusters. (J) Closer examination of the bacteria showed them to have separate outer membranes (arrowed), other than some that appear to be in the process of dividing. A normal phenotype bacterium was also observed separate from the cluster. (I) 10,000X 200kV. Scale bar 0.5µm. (J) 20,000X 200kV. Scale bar 200nm.

Morphology of the *gna33* single crossover background strain was similar to that of the wildtype (chapter 3 fig.12 and fig.13 pg.77-80). However, electron microscopy of the *gna33* single crossover*::tol-pal* mutant revealed that organisms were mainly in large clusters. Although some bacteria were observed individually (Fig. 10, panels A and J), the majority of bacteria in the sample were found in clusters of at least three cells. Large clusters of five or more bacteria were commonly observed (H), (I) and (J). Bacteria were observed in contact with both live and degraded bacteria (C), (D) and (E). Examination of these clusters showed that the bacteria had individual outer membranes and did not appear to be connected together by any visible part of the cell wall architecture, a similar clustering phenotype to the *Δgna33* mutant. Bacteria also showed no visible changes to the interior of the cells, the dark spots that appear within some of the bacteria are artefactual. The cell walls of individual bacteria also appeared morphologically normal. Other than the clustering, the morphology of the bacteria appeared similar to the background strain.

5.10 Transformation of *ΔsiaD* mutant with pMIDGTol-Pal

The clustering phenotype of the *gna33* single crossover::*tol-pal* does not occur due to an obvious defect in the separation of the outer membrane. Therefore the attraction between the bacteria must occur due to an agent on the surface of the cells or outside the outer membrane; the capsule is a candidate for such an interaction. An acapsular mutant *ΔsiaD* (147) was transformed with the plasmid containing the *tol-pal* region to test if the mutant was more tolerant than the wildtype of *tol-pal* expression (Fig.11) and if the clustering phenotype persisted in the double mutant.

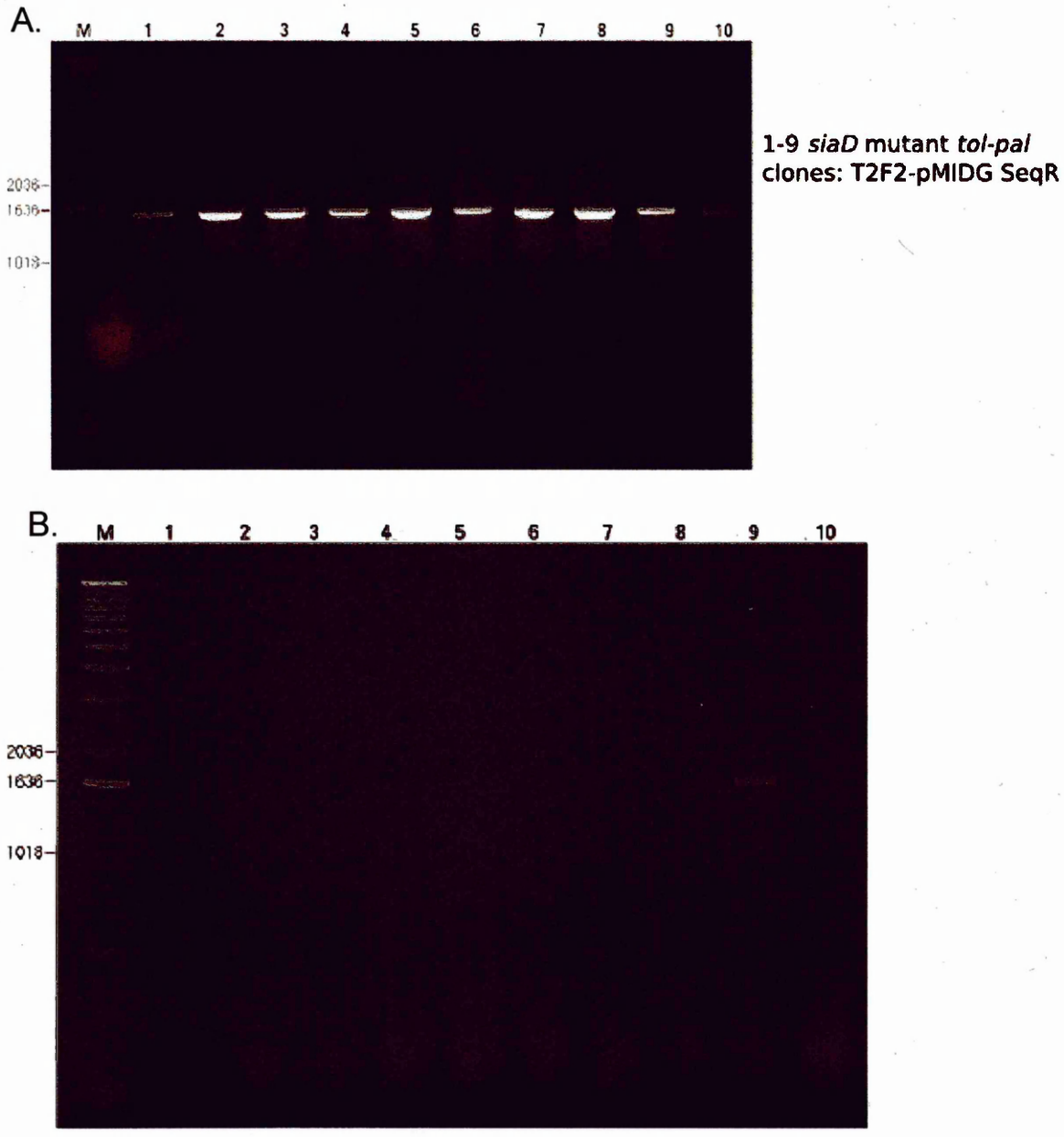

Figure 11. Transformation of a H44/76 *ΔsiaD* mutant with pMIDGTol-Pal. PCR of colonies produced by transformation of *ΔsiaD* strain with pMIDGTol-Pal. (A) Colony PCR with T2F2-pMIDG SeqR on 9 clones after selection from transformation plate. (B) Colony PCR with T2F2-pMIDG SeqR of the same 9 clones 24 hours after selection from the transformation plate.

The plasmid was unstable when transformed into the *ΔsiaD* strain. Nine of the ten colonies selected lost the plasmid within twenty four hours (Fig. 11b); the remaining the remaining colony (lane 9) lost its plasmid after forty-eight hours growth (data not shown). Therefore, although it was not possible to test whether capsule production caused the clustering of bacteria, it was not a factor affecting plasmid stability.

5.11 Native OMV production from *gna33* single crossover::*tol-pal*

In *E. coli*, absence of the Tol-Pal complex leads to increased vesicle production. To establish the effect of the presence of the Tol-Pal complex in the mutant strain preparations of vesicles produced by the bacteria were examined. First, an immunoassay was used to quantify the level of PorA and PorB in the vesicle preparations as a surrogate of vesicle quantity (fig.12).

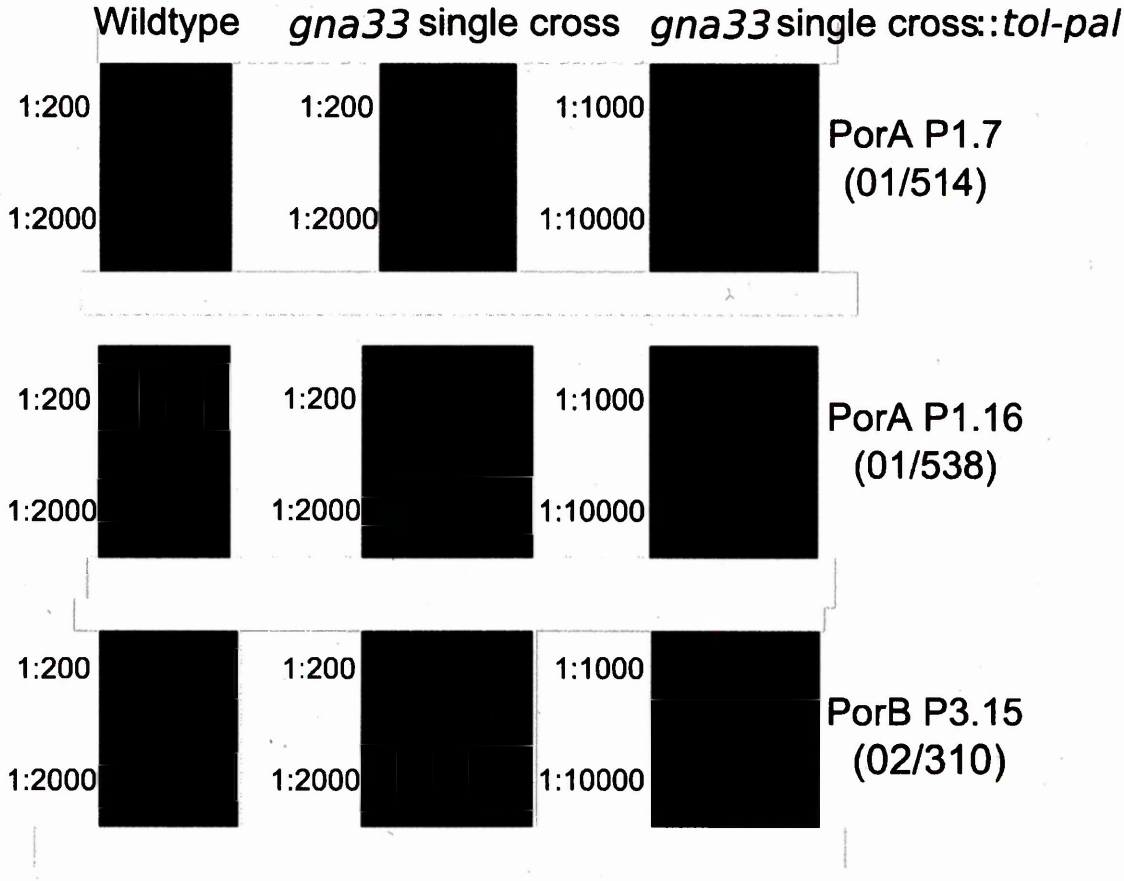

Strain	PorA P1.7 (01/514) (ng/µl)	PorA P1.16 (01/538) (ng/µl)	PorB P3.15 (02/310) (ng/µl)
Wildtype	1.0	<limit of detection	<limit of detection
gna33 single crossover	1.4	<limit of detection	1.9
gna33 single crossover::*tol-pal*	11.1	0.1	12

Figure 12. Slot blot immunoassay of PorA and PorB in native vesicles from the wildtype, *gna33* single crossover, and *gna33* single cross::*tol-pal* strain. Dilutions of the native OMV samples immunoblotted with monoclonal PorA and PorB antibodies. Dilutions of 1:200 and 1:2000 were used for the wildtype and *gna33* single crossover strains. 1:1000 and 1:10000 was used for the *gna33* single crossover::*tol-pal* strain. Calculated protein amounts per µl of vesicle sample are shown in the table. Protein amounts were calculated using the Kodak MI software by comparison to standard curves (see chapter 3 fig. 17). In samples below the limit of detection no signal above the background level could be detected by the software.

Immunoblotting showed that the *gna33* single crossover::*tol-pal* strain native OMV sample contained more PorA and PorB than the wildtype or background strain samples. The level of PorA assayed by the 01/514 and 01/538 antibodies did not correlate as was observed for the *gna33* mutants (Chapter 3 fig.18 pg.88) confirming that the PorA antibodies do not show agreement at low concentrations of antigen. The amount of PorB and PorA (from the 01/514 antibody) were approximately seven and eight times higher than in the background strain. The ratios between PorB: PorA was 1:1.1 in the *gna33* single crossover::*tol-pal* strain and 1:1.3 in the *gna33* single crossover. As both the increase in PorA and PorB and the ratio of the two proteins in both strains were consistent, this indicated an increase in vesicle size or number, but not in the protein content of the vesicles. Repeated experiments showed similar levels of increase in the samples.

5.12 Cryo-electron microscopy of native vesicles from *gna33* single crossover::*tol-pal*

The quantity and morphology of OMVs produced by the *gna33* single crossover::*tol-pal* strain was examined by Cryo-electron microscopy (fig.13) and compared to the wildtype and background strains (Chapter 3 fig.19 and fig.20 pg. 90-91)

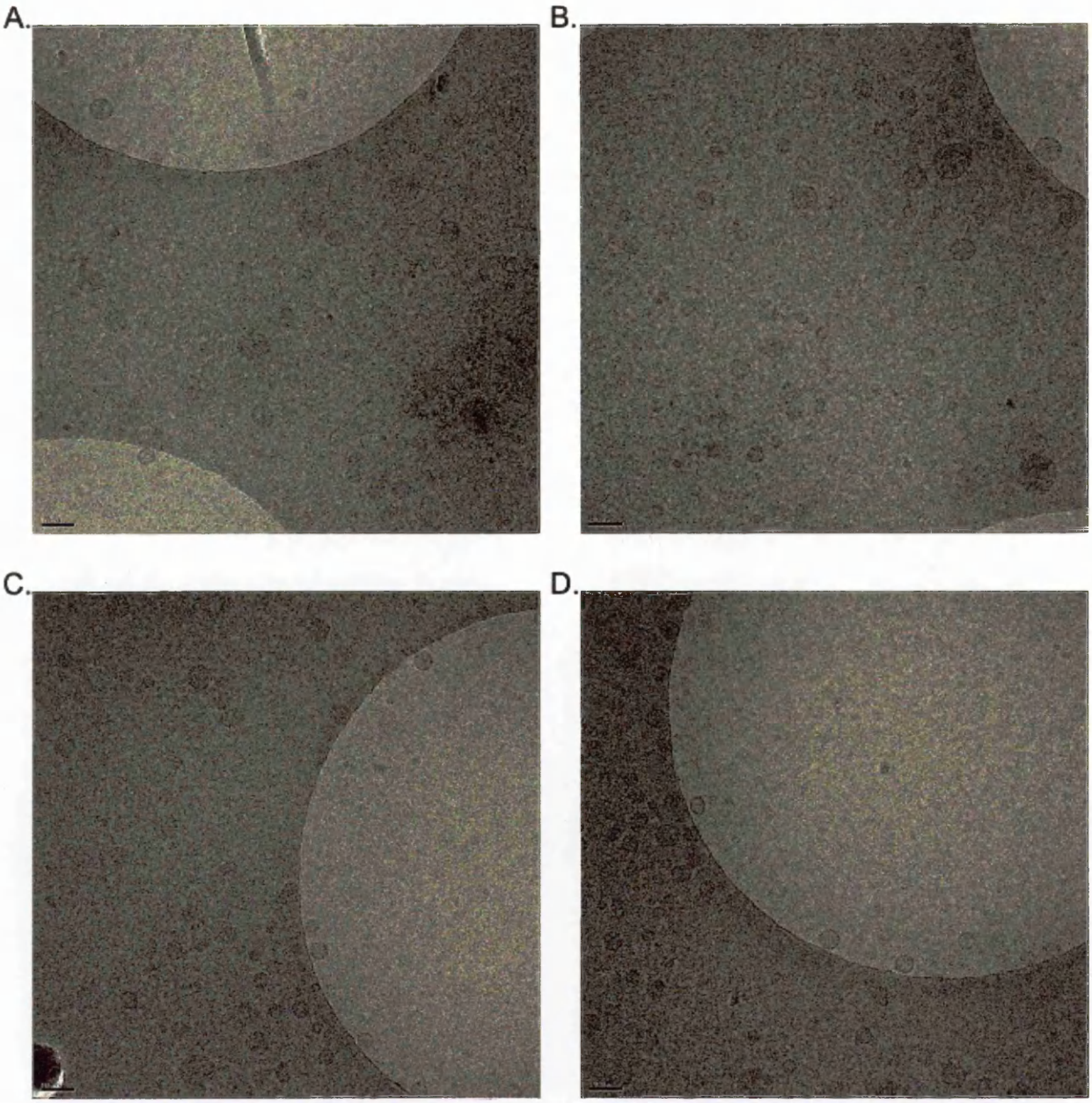

Figure 13. Cryo-Electron microscopy of native OMV produced by the *gna33* single crossover*::tol-pal* mutant. Vesicles were observed much more often in the *gna33* single crossover*::tol-pal* mutant than in the background strains (see Chapter 3 fig.20 pg.91) (A), (B), (C), (D) Vesicles were most commonly observed on the carbon film, although some vesicles were seen at the edges of ice holes. Vesicles also showed variation in size and shape. (A),(B),(C),(D) 30,000X 200kV. Scale bar 100nm.

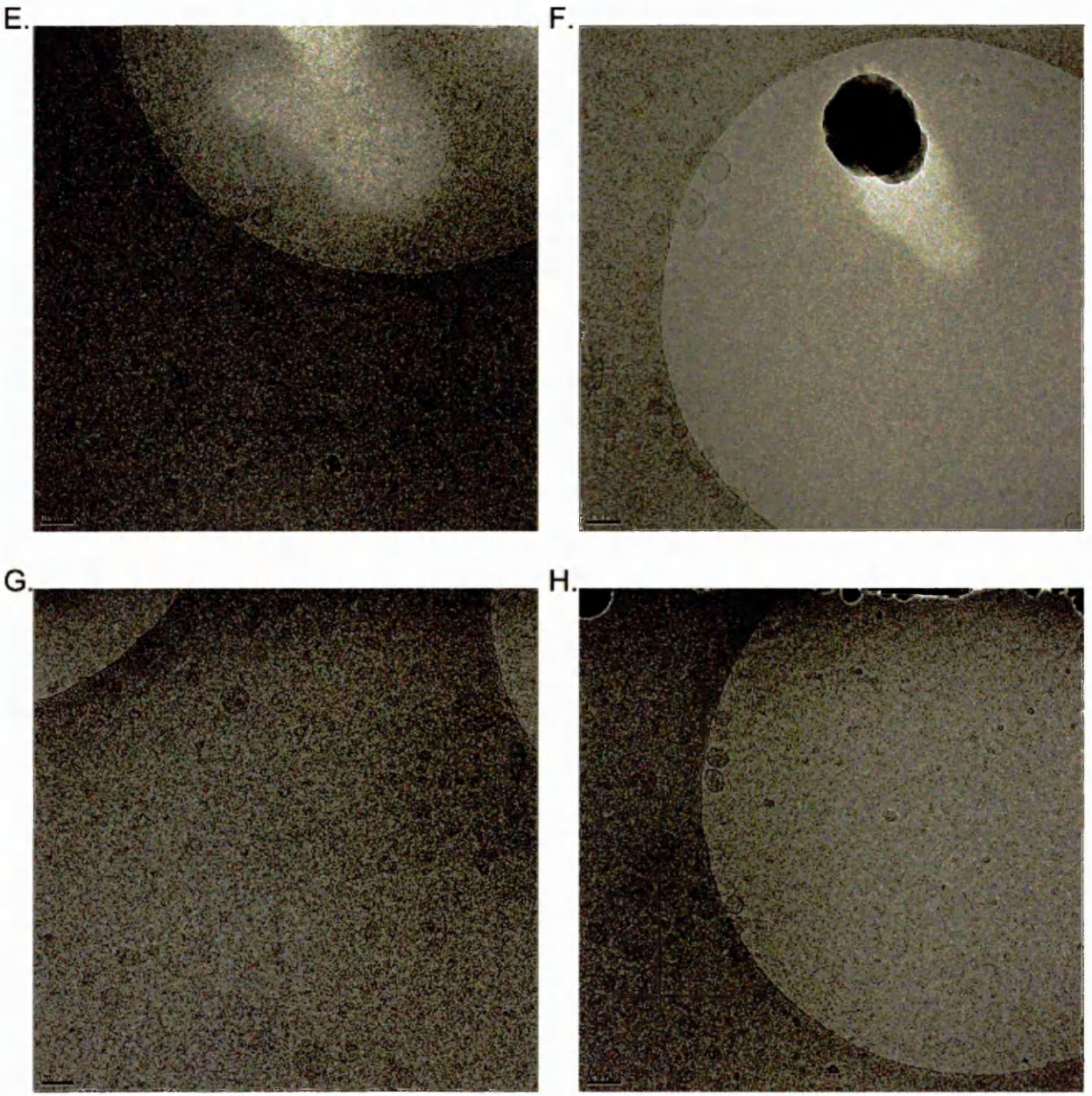

Figure 13. Cryo-Electron microscopy of native OMV produced by the *gna33* single crossover*::tol-pal* mutant (continued). (E) and (G) Vesicles were plentiful on the carbon film but were only found at the edges of the holes. (F) and (H). 30,000X 200kV. Scale bar 100nm.

Electron microscopy confirmed the results of the immunoassay; the *gna33* single crossover*::tol-pal* mutant sample contained more vesicles in the field examined than were observed in the wildtype or *gna33* single crossover strains. The vesicles in the sample were found mostly on the carbon film but were also observed at the edges of the ice holes. Vesicles appeared to vary in size and shape, those on the carbon film may have been distorted but vesicles in the ice also showed variation. Unlike

E. coli, where presence of the Tol-Pal complex decreases vesiculation, Tol-Pal increased vesiculation in *N. meningitidis*.

5.13 Morphology of native vesicles from *gna33* single crossover*::tol-pal*

Morphology of the vesicles in the electron micrographs was compared in terms of size and shape to the background strain (table 1 and 2).

Table 1. Comparison of vesicles from *gna33* single crossover and *gna33* single crossover::*tol-pal* strains. Values are a mean of 45 vesicles from *gna33* single crossover and *gna33* single crossover*::tol-pal* mutants. Vesicles were randomly selected from the samples. Significance values <P=0.01 are marked in blue. P values calculated by student's T-test.

	***gna33* single crossover**	***gna33* single crossover*::tol-pal***
Mean perimeter (nm)	121.46	166.71
SD	49.13	59.22
Mean area (nm)	1359.04	2461.9
SD	1234.51	2057.49

P values from T-test

	gna33* single crossover: *gna33* single crossover*::tol-pal
Perimeter	<0.01
Area	<0.01

Vesicles produced by the *gna33* single crossover*::tol-pal* strain had significantly larger perimeter and area measurements compared to *gna33* single crossover OMVs. Presence of the Tol-Pal complex increased both the amount and size of vesicles produced.

The change in size of the *gna33* single crossover*::tol-pal* vesicles was similar to the changes observed in the *Δgna33* mutant (Chapter 3 table 1 pg.95). Therefore *Δgna33* and *gna33* single crossover*::tol-pal* mutant vesicles were also compared and showed there was no significant difference in the perimeter and area values (P=>0.05). Standard deviations of the *gna33* single crossover*::tol-pal* vesicles suggested that the vesicles may also be more variable than those of the background strain.

The variance of the *gna33* single crossover::*tol-pal* strain was compared to both the *gna33* single crossover and the *Δgna33* strain using an F-test (Table 2).

Table 2. F-statistic values for the vesicle samples. F-statistic calculated using F-test. Significance value set at 0.05.

F-statistic values

Comparison	*gna33* single crossover:*gna33* single crossover::*tol-pal*	*Δgna33*:*gna33* single crossover::*tol-pal*
Area	<0.05	>0.05
Perimeter	>0.05	>0.05

The *gna33* single crossover::*tol-pal* strain vesicles were significantly more variable than those of the background strain in the area measurement and although it is not significantly different in the perimeter measurement, the F-test value was close to significance (F=0.06). Variability of the *Δgna33* and *gna33* single crossover::*tol-pal* strain vesicles was similar with no significant differences between the strains.

5.14 Discussion

In the previous chapter it was demonstrated that a plasmid containing the *tol-pal* genes could not be stably maintained in wildtype *N. meningitidis*. This was not due to the formation of the complete Tol-Pal complex, but was caused by some or all of the gene products of the *tol-pal* operon. It was hypothesized that this was due to either interference of the Tol-Pal proteins with the normal functioning of *N. meningitidis* proteins or accumulation of misfolded or mislocalised protein. This was sufficiently detrimental to the cell that only strains lacking the *tol-pal* genes survived. Mutants for *N. meningitidis* outer membrane proteins may have been able to maintain the *tol-pal* plasmids, due to the changes in the cell wall caused by the mutant genotype or because increased vesiculation allowed the removal of misfolded protein. The high vesiculating *ΔrmpM* strain did not stably maintain the plasmid, indicating that removal of potentially misfolded Tol-Pal protein by vesiculation did not

enhance bacterial survival. The *Δgna33* strain did not produce colonies when transformed with the *tol-pal* plasmid. As transformation into the *Δgna33* mutant could not be achieved with other plasmids or with genomic DNA, it was likely that the strain itself was not competent. However, the *gna33* single crossover strain stably maintained the plasmid in two clones. It was therefore possible to stabilize the *tol-pal* region in a mutant strain; although even this was only possible with the relatively low level of *tol-pal* expression from the native promoters.

A plasmid containing the genes *tolQ*, *tolR* and part of *tolA* was stable in the *gna33* single crossover strain, but only maintained by a single clone in the wildtype. The difference in the stability of the complete complex in the two strains was therefore most likely to be caused by a reduction in the detrimental effects of the *tolQ*, *tolR* and partial *tolA* genes on the *gna33* single crossover strain. Consequently, the recombination of the plasmid containing the complete *tol-pal* region in some *gna33* single crossover clones was due to the additional presence of the *tolA*, *tolB* and *pal* genes. This supports the hypothesis that instability of the *tol-pal* region in the wildtype was due to multiple genes and that both clusters *tolQ-tolR-partial tolA* and *tolA-tolB-pal* contained genes that caused the instability.

The effects of expressing the *tol-pal* genes included the upregulation of *gna33* transcription when the bacteria were grown on solid media. Previously the *gna33* single crossover strain had been shown to have a low level of *gna33* mRNA when grown on solid media but upregulated transcription of the gene when grown in liquid culture. It was hypothesized that this change was in some way related to an increase in membrane stress associated with growth in liquid culture. If production of the Tol-Pal proteins was also leading to membrane stress in the bacteria, this could account for the upregulation of *gna33* in the *gna33* single crossover::*tol-pal* strain on solid media. However, if the presence of GNA33 is required to maintain the *tol-pal* region stably, why was it not maintained in the wildtype where GNA33 was produced consistently at higher levels? The answer could lie in the level of *gna33* expression; it was possible that although *gna33* transcription was increased in the single crossover

mutant, expression may not have been at wildtype levels. This partial increase could have been sufficient to allow the bacteria to adapt to the increased membrane stress caused by the presence of the *tol-pal* genes, by improving peptidoglycan organization, but not enough to have caused a strong negative selection pressure due to the presence of GNA33. Further, the ability to change the expression level of *gna33* to a 'compromise' level that allowed the *tol-pal* region to be maintained could have been what differentiated clones capable of stably maintaining the *tol-pal* containing plasmid and those that did not. The maintenance of the plasmid containing the partial complex in all the clones tested would indicate that the factor requiring low GNA33 levels was most likely in the *tolQ-tolR*-partial *tolA* region. The factor requiring a higher GNA33 levels would lie in the *tolA-tolB-pal* gene cluster. Pal would seem the most likely candidate, as the protein directly interacts with the peptidoglycan. Disruption of the peptidoglycan structure was strongly indicated in the *Δgna33* mutant and has been previously recorded in lytic transglycosylase mutants in *E. coli* (81). Alternatively, GNA33 may simply allow the cell wall to adapt better to increased disruption caused by the presence of the Tol-Pal proteins, particularly disruption of the outer membrane by Pal protein in the periplasmic space. Antibiotic sensitivity results indicated that the outer membrane of the *gna33* single crossover::*tol-pal* has some slight disruption to the outer membrane. The 'compromise' level of *gna33* expression could therefore be one that allowed sufficient GNA33 to be expressed to prevent disruption of the peptidoglycan or to compensate for the outer membrane disruption caused by misfolded proteins in the periplasm. However GNA33 production would not be sufficient to enhance interference by other Tol-Pal proteins (*tolR, tolQ* or *partial tolA*) enough to cause negative selection. Examination of the *gna33* mRNA produced by the *gna33* single crossover mutant transformed with the partial plasmid could provide evidence for this hypothesis.

The hypothesis of a 'compromise' level of *gna33* expression suggests that regulation of *gna33* is complex and is likely to be affected by stress in the cell wall. Other than the effect of the signal sequence of *gna33*, little is known about the control of membrane bound lytic transglycosylases in *N.*

meningitidis or *E. coli*. However, the soluble lytic transglycosylase Slt70 has been shown to be controlled by the stringent response, a stress response pathway in *E. coli* (9). The overexpression of lytic transglycosylases has the potential to cause cell lysis; therefore it is logical that such enzymes and other murein hydrolases would be tightly controlled. Testing the levels of *gna33* mRNA after transformation with individual *tol-pal* genes and using a more accurate RNA quantitation technique such as real time PCR, would test the hypothesis of 'compromise' expression more rigorously and may provide more information on the factors affecting *gna33* mRNA expression.

The *gna33* single crossover::*tol-pal* provided a model for studying the effects of the Tol-Pal complex, even though the proteins were not expressed in a wildtype background. The phenotype of the *gna33* single crossover::*tol-pal* strain was similar but less severe than that of the *Δgna33* strain. The strain showed evidence of a mildly disrupted outer membrane and had a clustering phenotype similar to that of the *Δgna33* mutant (although clusters were smaller). It produced OMVs similar to those of the *Δgna33* mutant but significantly different from the OMVs produced by the wildtype and single crossover background strain. The OMVs were also more often observed on the hydrophilic carbon film than in the ice holes in both strains. However *gna33* single crossover::*tol-pal* did not have a significantly decreased growth rate. The similarity of the phenotypes of the two strains could be caused by reduced expression of GNA33, due to a 'compromise' expression level being reached in the *gna33* single crossover::*tol-pal* strain, leading to a milder phenotype than the complete *Δgna33* knockout. However, the strong selection pressure against the *tol-pal* region in the wildtype indicates that expression of the Tol-Pal proteins would produce phenotypic effects of their own. The phenotype of the *gna33* single crossover::*tol-pal* mutant was therefore likely to be caused by a combination of changes in GNA33 expression and the expression of Tol-Pal proteins. The similarity of the *gna33* single crossover::*tol-pal* phenotype to that of the *Δgna33* mutant indicated that the two phenotypes were caused by the same underlying processes. Cell wall disruption would be the most likely common factor between the two strains, in *Δgna33* disruption occurred due to changes in the

normal structure of peptidoglycan, in the *gna33* single crossover::*tol-pal* strain it was caused by the accumulation of Tol-Pal proteins in the cell wall and by changes to *gna33* expression. This stress led to disruption of the outer membrane and the increase in vesiculation in both strains. Stress in the cell wall and outer membrane directly related to the accumulation of misfolded protein has been shown to lead to increased vesiculation in *E. coli* (92,93). The increased detergent sensitivity observed in an *E. coli* strain that overexpressed the Tol-Pal proteins also supports the hypothesis that accumulation of Tol-Pal proteins can lead to disruption of the outer membrane. Disruption of the peptidoglycan could exacerbate the problems of misfolded proteins, by preventing correct insertion of peptidoglycan spanning proteins into the cell wall.

The *gna33* single crossover::*tol-pal* mutant does not display any defect in growth or membrane stability severe enough to indicate why the complex is so unstable in wildtype *N. meningitidis*. The genetic changes in the background strain may be ameliorating these effects, most likely by modulation of the expression of the GNA33 protein. The original aim of the Tol-Pal study was to test the hypothesis that the expression of the Tol-Pal complex in *N. meningitidis* would reduce the vesicle releasing phenotype of the bacteria. The instability of the *tol-pal* genes in the wildtype made it impossible to test this and when the genes were expressed in the *gna33* single crossover mutant they showed the opposite effect, increasing vesiculation. High vesiculation in *N. meningitidis* (and most likely in other high vesiculating Gram negative species that lack the *tol-pal* genes) is therefore not due directly to the absence of the complex. Absence of the *tol-pal* genes in so many high vesiculating species may still indicate a more complicated link with the vesiculation phenotype. For example the loss of the Tol-Pal complex may be required to develop high vesiculation, but this is likely to be the result of further evolution of the cell wall structure without Tol-Pal present rather than directly due to the gene loss.

Chapter 6- Investigation into phenotype and vesicle production of an H44/76 Δ*rmpM* strain and a strain containing a truncated *rmpM* gene

6.1 Introduction

The major outer membrane proteins of *N. meningitidis* were originally classified by size and structural analysis into five classes by Tsai et al. in 1981 (144). Of these five classes, classes 1, 2 and 3 contained the porin proteins PorA and PorB and the class 5 opacity protein Opa. The class 4 protein was found to cross-react with immune sera raised against the *N. gonorrhoeae* reduction modifiable class 3 protein RmpG (85). Sequence analysis and SDS-PAGE showed the class 4 protein to be a reduction modifiable protein that shared significant sequence similarity with the gonococcal RmpG (70,85) and the protein was named RmpM.

The *rmpM* gene (NMB0382) is 729bp long, found at position 385529-386257 in the *N. meningitidis* MC58 genome and is not known to be part of any operon. RmpM is a protein of 242 amino acids with a molecular weight (Mw) of 26.2kDa. The protein can be divided into 4 domains (Fig.1) consisting of an N and C-terminal region separated by a proline rich hinge and a 22 amino acid signal peptide which is cleaved from the mature protein (54).

A functional domain with homology to the peptidoglycan binding domain of the *E.coli* protein OmpA has been identified at the C-terminal end of RmpM (70). Although classified as an outer membrane protein and purified with outer membrane proteins, no recognised motif for incorporation into the outer membrane has been identified in the N-terminal portion (54). It has been hypothesised that outer membrane binding occurs through interactions between the N-terminal domain of RmpM and outer membrane proteins such as PorA, PorB (64) Omp85 (162) and iron acquisition proteins including FetA (114). Complexes of these proteins and RmpM have been shown to occur (64,119) supporting this hypothesis. It has also been suggested that RmpM has a role in stabilisation of outer membrane protein complexes (64).

The structure of the C-terminal OmpA like domain of the RmpM protein was determined by Grizot et al. using X-ray crystallography (54). Sequence alignments also showed conserved residues at the positions D120, Y127, R135 and R197 (fig.1). Computer docking experiments indicated that the residues Y127, R135 and R197 could form hydrogen bonds with the disaccharide moiety of the peptidoglycan, although only one conformation of protein-peptidoglycan binding was tested. This structural study also identified a disulphide bond linking two alpha helices (α-4 and α-5) to form an extended loop beneath the putative peptidoglycan binding domain. However, homology to other OmpA domains suggested that this loop was not involved in peptidoglycan binding (54).

The construction of an *ΔrmpM* strain was undertaken by Klugman *et al.* and the mutant was shown to have a similar morphology and growth to the wildtype strain (70). It has been observed that the *ΔrmpM* strain produces more vesicles more than the wildtype strain (150) but this increase has not been quantified. It has been hypothesised that RmpM forms a structural link between the peptidoglycan and outer membrane (54,71) and that the loss of this link results in separation of the outer membrane from the peptidoglycan. This allows more blebs to be formed and therefore increases the amount of vesicles released. Alternatively the increased vesiculation may be due to changes in the arrangement or stability of proteins in the outer membrane that interact with RmpM, which in turn destabilises the outer membrane. The aim of this study was to characterise the function of the RmpM protein by examining the phenotype of the *ΔrmpM* mutant strain. A mutant which is lacking the peptidoglycan binding domain of the RmpM protein, but maintains the binding to outer membrane proteins, was used to test the hypothesis that it is the loss of the linkage between the peptidoglycan and outer membrane provided by RmpM that causes the high vesiculation phenotype in the *ΔrmpM* strain.

6.2 Construction of an *rmpM* mutant lacking the C-terminal peptidoglycan binding function

The construction of a mutant lacking a peptidoglycan binding function required the deletion of part of the C-terminal domain. This domain constitutes over half of RmpM, therefore complete deletion of the region had the potential to destabilise the rest of the protein. A strategy was devised to delete the last 69 amino acids of the C-terminal domain, using a natural *XbaI* restriction site that occurred at 517bp in the C terminal region. The putative peptidoglycan binding residue R197 and the residues that form the disulphide bond between the helices α4-α5 were distal of the *XbaI* site (fig 1). The removal of these residues should have been sufficient to destroy or greatly reduce peptidoglycan binding in the mutant protein.

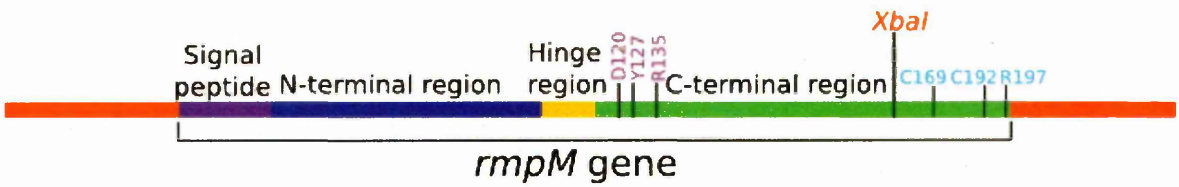

Figure 1. Structure of the *rmpM* gene The *rmpM* gene is divided into four domains. The 22 amino acid signal peptide is cleaved from the mature protein. The N-terminal region contains 40 amino acids followed by a proline rich hinge region of 20 amino acids; this is followed by the 150 amino acid C-terminal region. A disulphide bond is formed between the residues C169 and C192. Amino acids involved in peptidoglycan binding are shown in purple and blue. The *XbaI* site used in truncation is shown and the key residues removed by the truncation are shown in blue.

The cloning strategy for replacement of the RmpM protein with the truncated form is shown in figure 2.

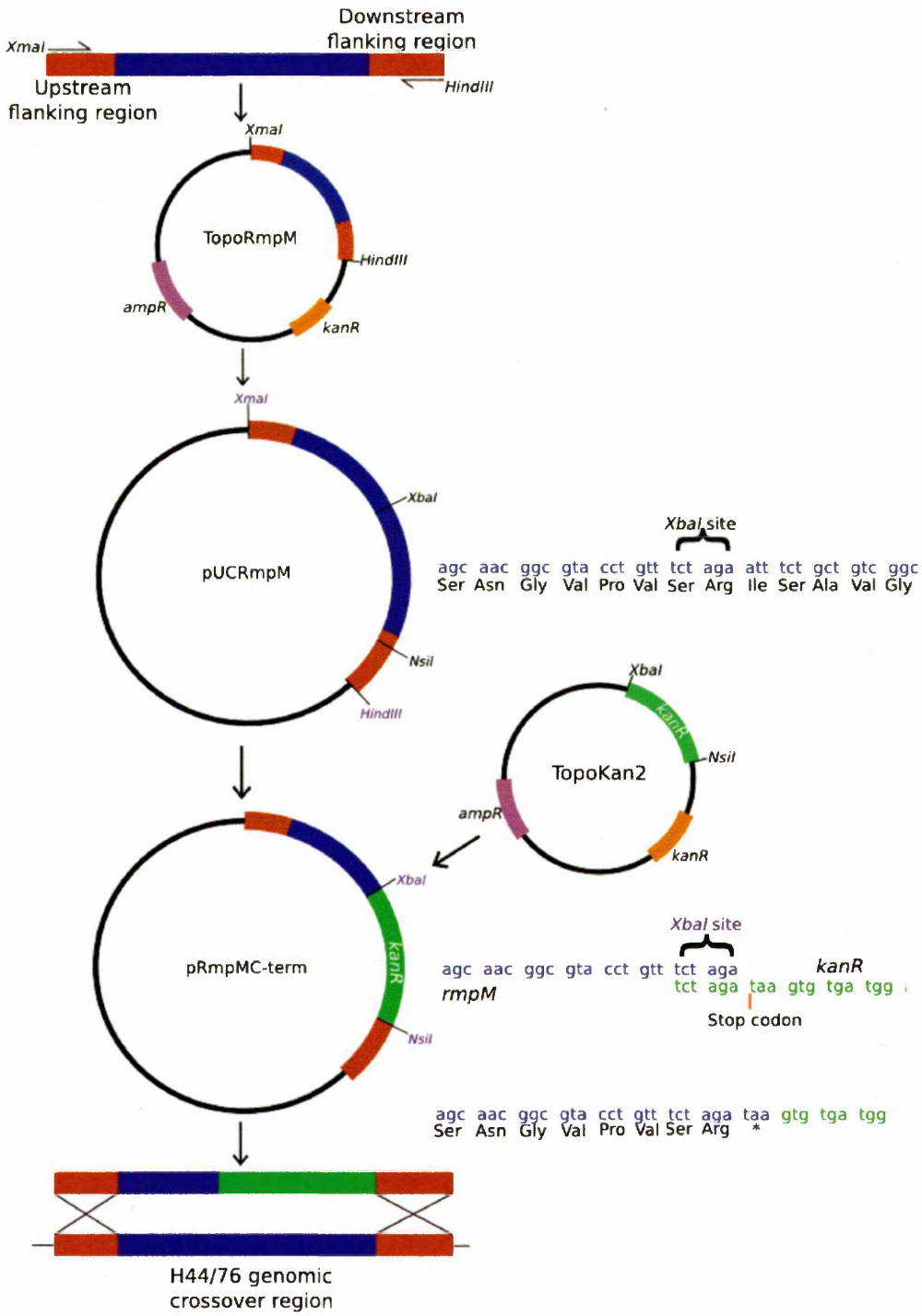

Figure 2. Cloning strategy for construction of RmpM C-term mutant. The *rmpM* gene was amplified by PCR and cloned into a topo vector to produce TopoRmpM. TopoRmpM was digested with *XmaI* and *HindIII* and the *rmpM* fragment was cloned into the pUC19 vector to produce the plasmid pUCRmpM. A Kan^{R} cassette was amplified by PCR using a primer that contains a stop codon TAA after the *XbaI* site on the 5' end. The PCR product was cloned into a topo vector to produce TopoKan2. The fragment was then digested from TopoKan2 using *XbaI* and *NsiI* and ligated into pUCRmpM to form the plasmid pUCRmpMC-term. The ligation inserted a stop codon just after the *XbaI* site in *rmpM*. The complete cassette was then amplified from pUCRmpMC-term with a 5' primer containing the neisserial DNA uptake sequence. The PCR product was then transformed into *N. meningitidis* H44/76. Homologous regions of sequence on both ends of the cassette allowed recombination with the *Neisserial* genome and clones were successfully selected on kanamycin containing medium.

The cloning strategy is described in the figure legend, although an alteration of the primer 5' of the *rmpM* gene was required to move it closer to the start codon. Transformation into *N. meningitidis* was carried out and the transformants were grown on kanamycin containing media to select colonies that had the replacement cassette inserted into the genome. A sample of colonies was tested by colony PCR for the *rmpM* truncation using the primers which amplified from sequence upstream of the *rmpM* gene to the end of the *kan*^{R} gene (fig 3a).

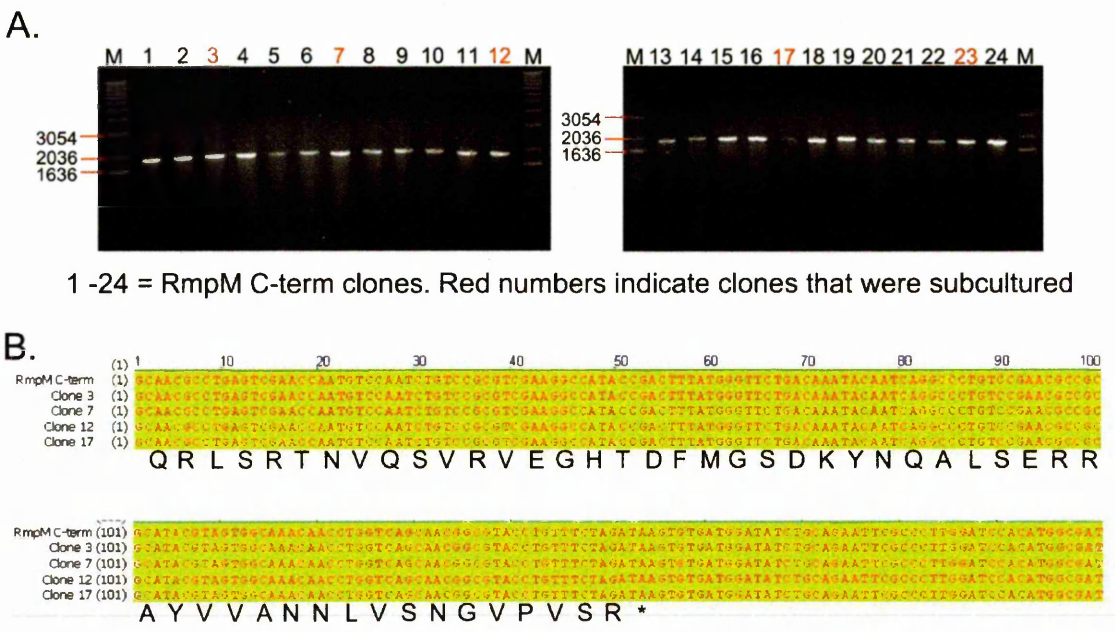

Figure 3. Transformation of RmpMC-term cassette into *N. meningitidis* (A) Colony PCR of clones produced from transformation of H44/76 with PCR product produced from pUCRmpMC-term. (B) Sequencing of four of the clones (3, 7, 12 and 17). Amino acid sequence is shown beneath the sequence alignment. Comparison was made against the theoretical sequence of the correct insertion.

All 24 transformants produced a band at the expected size of 1.7kb, although some were faint. The genomic DNA of four clones (3, 7, 12 and 17) was sequenced; all the clones contained the correct truncation (fig.3b).

6.3 *rmpM* transcription in *ΔrmpM* and RmpM C-term mutants

An RT-PCR was used to confirm both that mRNA from the truncated *rmpM* gene was being transcribed and that full length *rmpM* mRNA was no longer being expressed (fig.4).

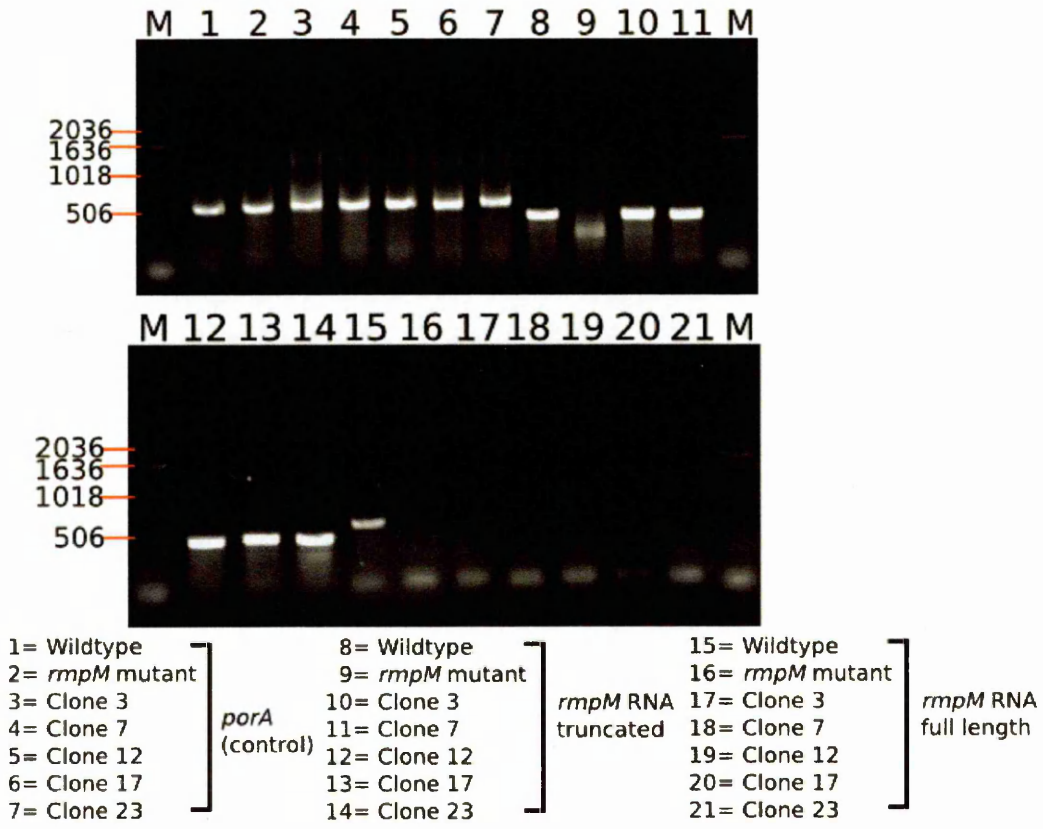

Figure 4. RT-PCR of *rmpM* RNA from wildtype, *ΔrmpM* and RmpM C-term mutants. Gel electrophoresis of RT-PCR products for full length and truncated *rmpM* RNA. *ΔrmpM* strain is labelled as *rmpM* mutant. Lanes 1-7 show control RT-PCR for PorA mRNA. Lanes 8-14 show PCR product from truncated *rmpM* gene. Lanes 15-21 show PCR product from full length *rmpM* gene.

The RmpM C-term mutant clones all showed clear bands for the truncated *rmpM* mRNA (469bp lanes 10-14) and no band for the full length *rmpM* mRNA (lanes 17-21). This showed that the full length *rmpM* gene had been successfully replaced by the truncated version and that the truncated *rmpM* gene was being transcribed (fig.4). The wildtype produced the full length *rmpM* mRNA (622bp, lane 15) and also a band for the truncated product (469bp, lane 8) amplified from the full length mRNA. The *ΔrmpM* mutant contains, as expected, no *rmpM* RNA either full length or truncated (lanes 9 and 16) although there is some non-specific amplification of the incorrect size occurring (lane 9).

6.4 RmpM protein expression in *ΔrmpM* and RmpM C-term mutants

The molecular weight (Mw) of the complete RmpM protein is 26.18kDa, however RmpM shows unusual electrophoretic mobility when reduced and the apparent molecular weight of the protein increases to 32kDa (70,85). Outer membrane of the wildtype, *ΔrmpM* and RmpM C-term mutant were prepared and subjected to SDS-PAGE under reducing conditions (fig. 5).

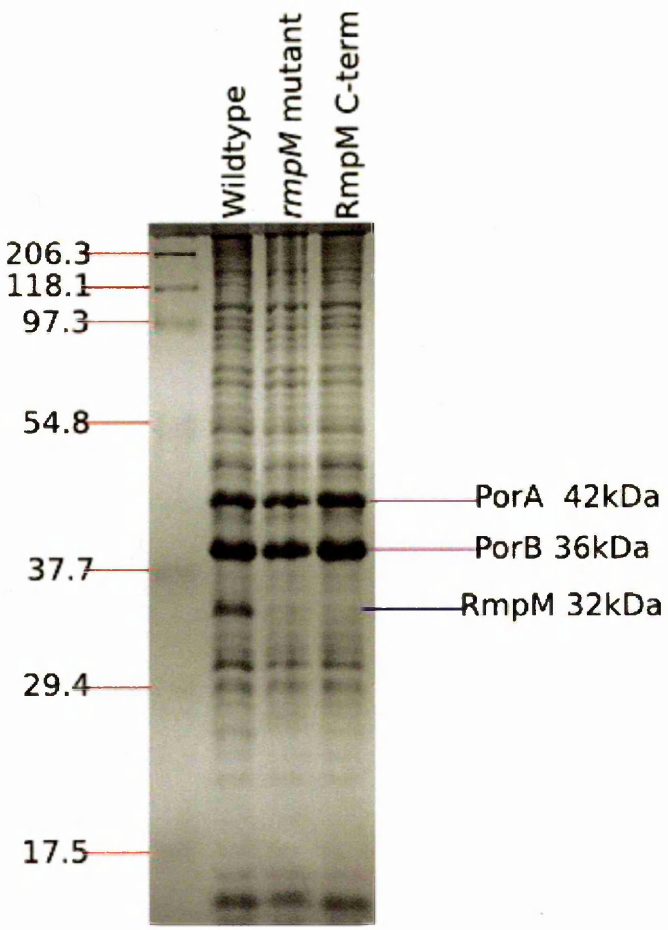

Figure 5. SDS-PAGE for RmpM Protein
Outer membrane preparations for the wildtype, *ΔrmpM* (*rmpM* mutant) and RmpM C-term mutant strains were examined on a 12% SDS-PAGE gel. Bands for PorA, PorB and RmpM proteins are marked.

The RmpM protein could be clearly seen in the wildtype preparation, a strong band was present at 32kDa. However, it was not visible in either mutant strain. The truncation of the RmpM protein removed 69 amino acids from the C-terminal portion of the protein and the Mw of the truncated protein was calculated to be 16.5kDa using the ExPASy pI/Mw tool. There was no band in the RmpM C-term preparation to correspond to the truncated protein, although as the band would run at the very bottom of this gel it may not have been visible. Gels focusing on the lower molecular weight proteins also did not show a clear band for the protein (data not shown). If the protein was being

translated it was not running at a larger size than the predicted Mw as is the case with the reduction modified complete protein. The removal of the terminal disulphide bond in the RmpM C-term mutant was likely to change the way the protein is affected by reducing conditions, as disulphide bonds would be an obvious target for reduction modification. This could have lead to the protein running at an unexpected molecular weight.

6.5 Protein complex formation in *rmpM* mutants

Complexes of RmpM and other proteins including FetA and the porins PorA and PorB have been identified in the wildtype strain (64,114,119). The presence of a functional RmpM N-terminal domain in the RmpM C-term mutant should allow the formation of complexes with other outer membrane proteins whereas the deletion of RmpM should disrupt complex formation. To investigate the outer membrane complexes, preparations of outer membrane were crosslinked with formaldehyde. Crosslinking by formaldehyde occurs by the condensation of amino groups with nearby nitrogen containing groups such as primary amides and guanidines (40). Crosslinked proteins were run against un treated controls on an 8% SDS-PAGE gel following the method of Sanchez et al. (119) (fig. 6).

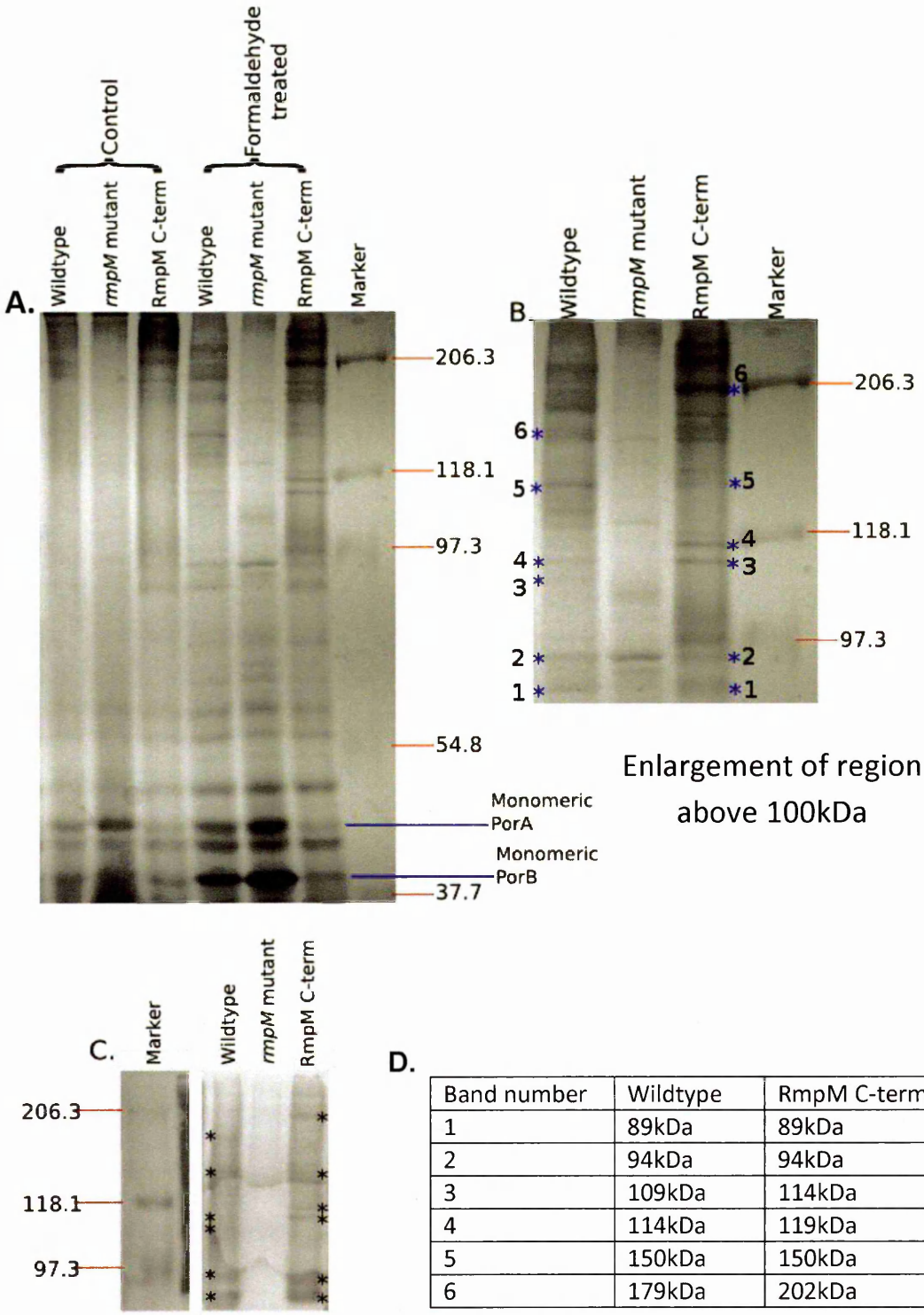

Band number	Wildtype	RmpM C-term
1	89kDa	89kDa
2	94kDa	94kDa
3	109kDa	114kDa
4	114kDa	119kDa
5	150kDa	150kDa
6	179kDa	202kDa

Figure 6. Protein complexes in the outer membrane examined by Formaldehyde crosslinking. (A) Formaldehyde cross-linked protein complex profiles for the wildtype, *ΔrmpM* (*rmpM* mutant) and RmpM C-term mutant strains. The first three lanes show non-formaldehyde treated control samples, the next three lanes contain formaldehyde treated samples. (B) Enlargement of the region above 100kDa in (A). The control lanes are not shown. Bands identified in the PorB western blot are indicated by (*) (C) Cross-linked gels Western blotted with PorB monoclonal antibody. Bands are marked with (*). (D) Estimation of band sizes for the bands marked in (B and C), bands are numbered in ascending size order.

The non-formaldehyde treated controls show very few high molecular weight bands because of the disassociation of the non crosslinked protein complexes into protein monomers. The formaldehyde treated wildtype strain shows several high molecular weight bands (greater than 100kDa) that do not appear in the non-formaldehyde control and represent protein complexes. The formaldehyde treated *ΔrmpM* strain produced few bands above or close to 100kDa with only four visible bands at 170kDa, 127kDa 105kDa and 94kDa (fig.6a + b). The wildtype strain contained bands corresponding to these sizes, suggesting that these complexes do not contain RmpM. Western blotting with PorB monoclonal antibody (02/310) showed one additional band at 150kDa that was also represented in the wildtype strain (fig.6c). The RmpM C-term also showed several bands above 100kDa and most of the bands in the wildtype sample were also present in the RmpM C-term mutant. However the two strains do not show identical band profiles; the RmpM C-term mutant showed two high molecular weight bands (above 206.3kDa) that were not present in the wildtype sample. These bands may have been caused by aggregation of protein complexes in the outer membrane. Western blotting with anti-PorB (fig.9 C and D) showed PorB containing bands in the wildtype and RmpM C-term mutants. Of the six bands shown, four (at 89kDa, 94kDa, 114kDa and 150kDa) were present at the same position in both samples. Bands at 109kDa (band 3) and 179kDa (band 6) in the wildtype strain were shifted to 119kDa (band 4) and 202kDa (band 6) in the RmpM C-term mutant. RmpM C-term containing complexes were expected to have a lower molecular weight due to the protein truncation. The shifts in molecular weight were 10kDa (band 4) and 23kDa (band 6). Neither shift was large enough to indicate the addition of PorA or PorB subunits (42kDa and 36kDa respectively) or the correct size to indicate the addition of either one or several truncated RmpM proteins (16.5kDa). This shift must have been related to the RmpM truncation, but without further analysis such as mass spectrometry to identify the constituents of the complexes this shift was difficult to explain.

Examination of the level of monomeric PorA (42kDa) and PorB (36kDa) proteins in the cross-linked samples (fig.6a) showed that the *ΔrmpM* strain contained a much higher concentration of the

monomeric forms of these proteins than the wildtype. The RmpM C-term mutant contained less monomeric PorA and PorB than both the *ΔrmpM* and the wildtype strain. Other bands in the region of the monomeric proteins showed that loading was even. Therefore the increase in monomeric PorA and PorB and the lack of high molecular weight bands in the *ΔrmpM* strain indicated that the porins were not being sequestered into high molecular weight complexes. By contrast the low levels of monomeric porins in the RmpM C-term mutant demonstrated that the porins were being efficiently sequestered into complexes.

6.6 Growth of *rmpM* mutants

To analyse the effect of the changes made to the RmpM protein, growth of the wildtype, *ΔrmpM* and RmpM C-term mutant strains was measured in liquid culture over an eight hour period (fig.7).

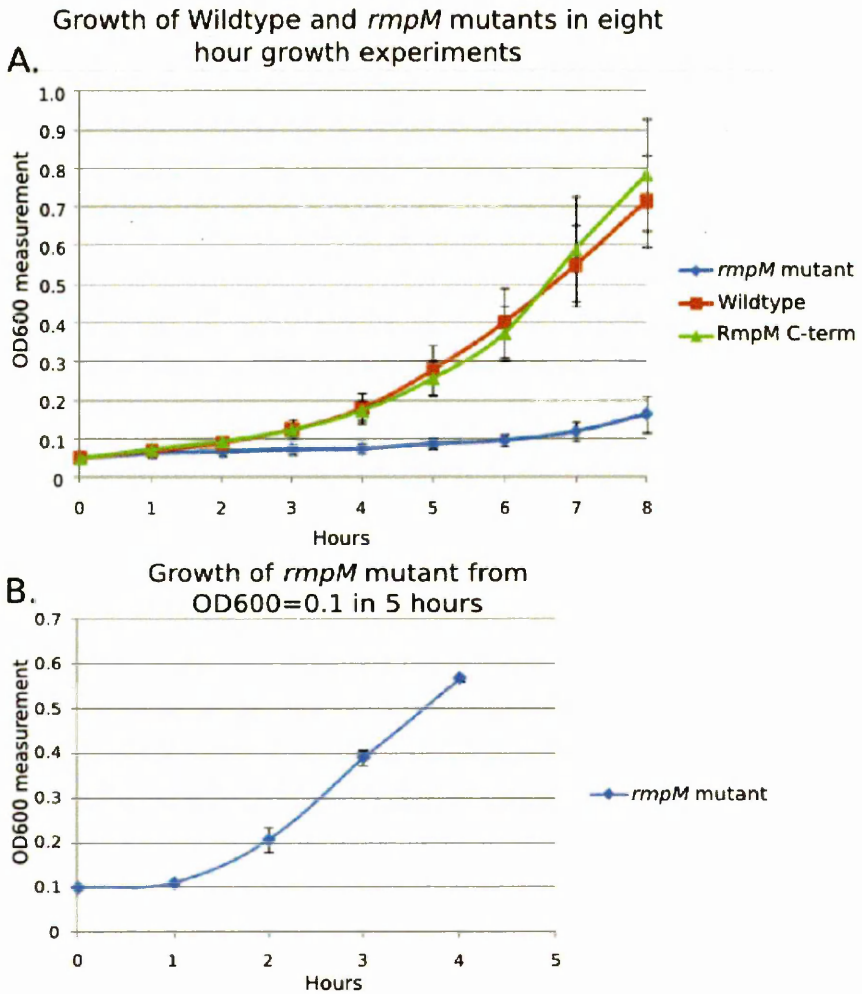

Figure 7. Growth curves for wildtype, *ΔrmpM* and RmpM C-term mutant (A) Eight hour growth curves of the wildtype and *ΔrmpM* (*rmpM* mutant) and RmpM C-term mutant grown from an OD_{600} value of 0.05 in liquid culture. Curves are the mean of three experiments. Error bars represent SEM. (B) Four hour growth curve of the *ΔrmpM* (*rmpM* mutant) strain grown from an OD_{600} value of 0.1. Error bars represent SEM. Curve is the mean of three experiments.

Wildtype growth was consistent with the rate measured in previous experiments and the RmpM C-term mutant did not show any difference in growth rate compared to the wildtype. The *ΔrmpM* strain grew poorly, despite growth curves in earlier studies reporting that the mutant grew at a similar rate to the wildtype (70). The growth curve of the *ΔrmpM* mutant only began to climb after 7 hours (Fig 7a) and the OD_{600} value after 8 hours showed that the *ΔrmpM* mutant reached 0.16 compared to the wildtype value of 0.71. However, after overnight growth little difference was seen in the OD_{600} values of wildtype and *ΔrmpM* cultures (data not shown). From a higher starting OD_{600} of 0.1 growth of *ΔrmpM* was similar to that of the wildtype (fig. 7b). These results indicated that the slow growth from

OD_{600}= 0.05 was the result of a lengthened lag phase, as bacteria started from a higher concentration of cells (with more cells able to divide) or given a longer incubation period showed normal growth. Increased lag phase in the bacteria could have been a symptom of a nutrient deficiency, in lag phase bacteria synthesise components needed for the division process and a lack of nutrients will increase the time it takes for the cell to be ready to divide.

An *N. meningitidis* group B *ΔrmpM* strain (M1080) had grown normally from an OD_{600} of 0.04 in the work of Klugman et al. The experiment used *Neisserial* typing media (140), as opposed to the Mueller Hinton media used in this study. Both media contained comparable levels of starch and animal tissue derived components. However, the typing media also contained inorganic salts and Isovitalex, an additive containing amino acids, co-factors, nucleic acids, inorganic ions (ferric nitrate) and dextrose. To test if the nutritional content of the two media were responsible for the differences observed in the growth, nutritional supplements including an inorganic ion mixture identical to that of the gonococcal typing media were added to the Mueller Hinton media. None of these supplements (either singly or in combination) altered the growth characteristics of *ΔrmpM*. Nutritional requirements did not account for the difference in growth between the *ΔrmpM* mutants in an H44/76 background in this experiment, and the previously reported growth in the M1080 strain background (70).

6.7 Temperature sensitivity of the *rmpM* mutant strains

Although the *ΔrmpM* mutant showed severe growth retardation, the RmpM C-term mutant showed wildtype like growth. The poor growth phenotype was therefore linked to the presence of the N-terminal portion of the RmpM protein, making it likely that stabilisation of outer membrane protein complexes by RmpM was a factor in the poor growth rate. If the stability of complexes was affected by the absence of RmpM, growth at a lower temperature may have ameliorated this effect. The membrane would become less fluid at lower temperatures and more fluid when the temperature is

raised and these changes in fluidity would affect the movement of proteins in the outer membrane. Interactions between proteins may also be affected directly by changes in temperature. To test this, bacteria were grown at a range of temperatures for seven hours from a starting OD_{600} of 0.05. The OD_{600} measurement at the seven hour point was taken (fig.8).

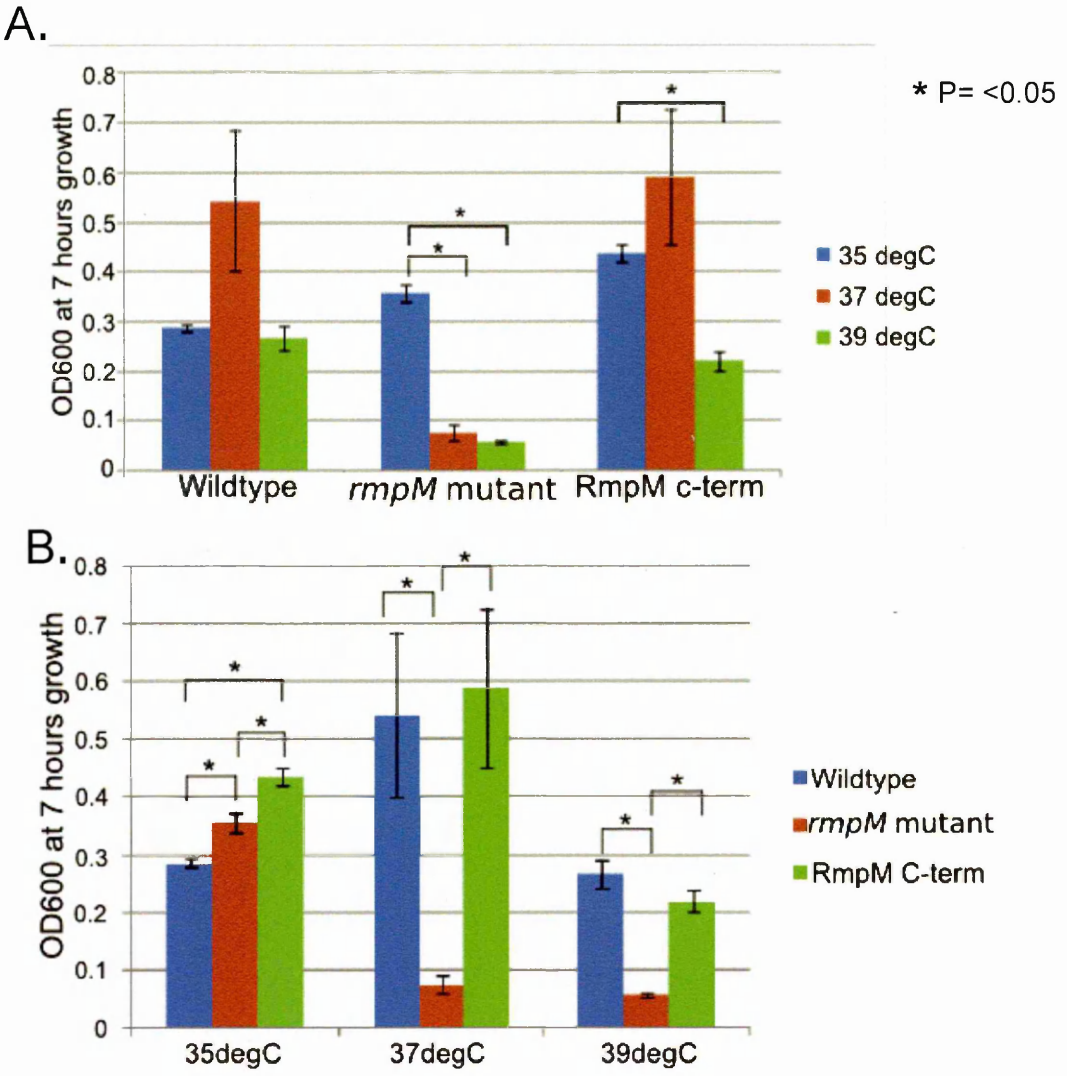

Figure 8. Growth of wildtype, *ΔrmpM* (*rmpM* mutant) and RmpM C-term mutant at different growth temperatures. Cultures were grown from OD_{600}=0.05 for seven hours at different temperatures. OD_{600} values were taken after the seventh hour of growth. (A) 7 hour OD_{600} values with strains shown on the x axis. Significant differences within strains at different temperatures are shown. (B) 7 hour OD_{600} values with temperatures shown on the x axis. Significant differences between strains at each growth temperature are shown. Results are a mean of three experiments. P values calculated by T-test. Error bars represent SEM.

The wildtype strain did not show any significant differences (P=>0.05) in growth at the three temperatures, but optimum growth occurred at 37°C. The RmpM C-term strain showed a similar

temperature sensitivity profile to the wildtype, but growth in this strain was significantly lower at 39°C compared to 35°C (P=0.001). Unlike the other two strains, the *ΔrmpM* mutant was highly temperature sensitive and grew significantly better at the lower temperature of 35°C compared to 37°C and 39°C (P=<0.001 for both) (fig.11a).

A comparison of the strains at different growth temperatures was made using the same data (fig.11b). The RmpM C-term mutant grew significantly better than both the wildtype and *ΔrmpM* strains at 35°C (P=0.02 and P=0.001 respectively). *ΔrmpM* also showed significantly improved growth compared to the wildtype at 35°C (P=0.02). Increased growth of both *ΔrmpM* and RmpM C-term at 35°C indicated that loss of the peptidoglycan binding function of the protein was beneficial for growth at lower temperatures. However the growth of *ΔrmpM* decreased sharply at both 37°C and 39°C and significantly poorer than the growth of both the wildtype (P=0.03 at 37°C and P=<0.001 at 39°C) and RmpM C-term mutant (P=0.02 at 37°C and P=0.001 at 39°C). Compared to *ΔrmpM*, the other two strains showed both a higher optimum temperature and lower sensitivity to temperature increase. This suggested that the N-terminal of RmpM was important in the growth of the organism at higher temperatures.

6.8 Antibiotic sensitivity of the *rmpM* mutant strains

Changes in protein complexes may have also affected antibiotic sensitivity in the strains, by altering the permeability of the outer membrane to antibiotic compounds. Reduction in the minimum inhibitory concentration (MIC) of some β-lactam antibiotics have been reported in porin deficient mutants of *E. coli* and it has been hypothesized that the porin channels are involved in the uptake of β-lactam antibiotics (56). The putative structural role of RmpM could also lead to defects in cell wall structure in the mutants. The *rmpM* mutants were therefore tested with the panel of antibiotics to test the integrity of peptidoglycan and the outer membrane (fig. 9).

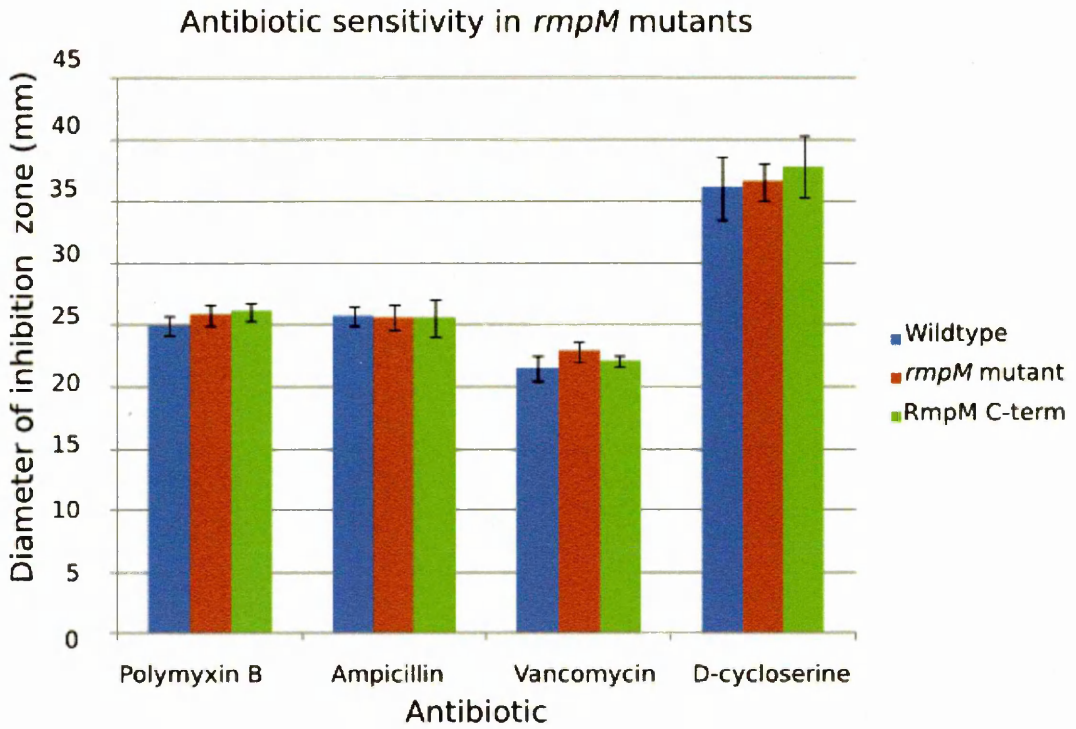

Figure 9. Antibiotic sensitivity of wildtype, *ΔrmpM* (*rmpM* mutant) and RmpM C-term mutant. Sensitivity to the antibiotics polymyxin B, ampicillin, vancomycin and D-cycloserine was tested using disc diffusion assay. Bars represent mean of three experiments. Error bars represent SEM. Significance values calculated by T-test.

The mutants and wildtype showed no significant difference in susceptibility to all the antibiotics tested (P = >0.05). Polymyxin B interacts directly with the outer membrane and equal susceptibility between the wildtype and mutant strains indicated that there was no significant disruption of the outer membrane in the *rmpM* mutant strains. The ampicillin, vancomycin and D-cycloserine antibiotics all interfere with peptidoglycan synthesis, the similarity of the *rmpM* mutants and wildtype indicated that peptidoglycan structure was also not severely affected by the deletion of *rmpM*.

6.9 Electron microscopy of *rmpM* mutant strains

The *rmpM* mutants were examined under VTF Cryo-electron microscopy (Fig. 10 and 11) and compared to the wildtype (see chapter 3 fig.12 pg.77). The *ΔrmpM* strain showed no major morphological changes, but the preparation of the bacteria for electron microscopy did highlight differences between the strains. All other strains in the study were resuspended in PBS before application to the grid by pipetting, but the *ΔrmpM* strain could not be prepared by this method.

When resuspended in PBS the suspension was too viscous to allow the formation of thin vitreous ice, even when the preparation was diluted. To overcome this problem grids were floated on a suspension of the bacteria in Mueller Hinton broth and RmpM C-term bacteria were also prepared in this way, to ensure consistency (see fig. 11 M and N). Although there were no conspicuous morphological differences between the wildtype and *ΔrmpM* strains there appeared to be a higher quantity of dead material in the *ΔrmpM* sample and some unique features were observed in the *ΔrmpM* mutant. In fig.10 A, B, E sections of the outer membrane were missing on some bacteria (indicated by arrows). This phenotype was not seen in the wildtype or the RmpM C-term mutant sample. It could have been the beginning of cell degradation, but the bacteria appeared otherwise healthy. There were also some features visible on the surface of the bacteria (fig. 10 A, B, C, E, F, H), these were common in the *rmpM* mutants but were not present in the wildtype. The features appear as thread like particles in the otherwise electron dense bacteria and may have represented alteration in either the surface membrane or cytoplasm that changed the electron density of that region. Again this could reflect cell breakdown, in the wildtype sample, dead bacteria were often observed with membranous material inside the cell (Chapter 3 fig.13 I, J). Although the *ΔrmpM* strain was observed to cluster at several sites on the grid this phenotype was not consistent, indicating that it was not a requirement for the *ΔrmpM* mutant to cluster unlike the *Δgna33* strain. In images C and H the bacteria were frozen whilst dividing. The peptidoglycan in both cases has divided to enclose both daughter cells separately; however the outer membrane has not yet separated. This order of division, with peptidoglycan separation before outer membrane invagination begins would be consistent with septal division as described in rod shaped Gram negative bacteria (47) but no sign of increased vesiculation was seen at the poles of division unlike the observations made in dividing *E. coli* (45). In image (H) vesiculation did appear to be occurring at one pole of the dividing organism but the position of these vesicles and their apparent superimposition onto each other suggested that their presence may have been co-incidental. Potential vesiculation sites were common on the surface of the bacteria and vesicles more common in the surrounding ice than in the wildtype sample. This was

not unexpected in a high vesiculating mutant but vesiculation did not appear to be confined to particular regions of the membrane and was occurring around much of the surface of the bacteria.

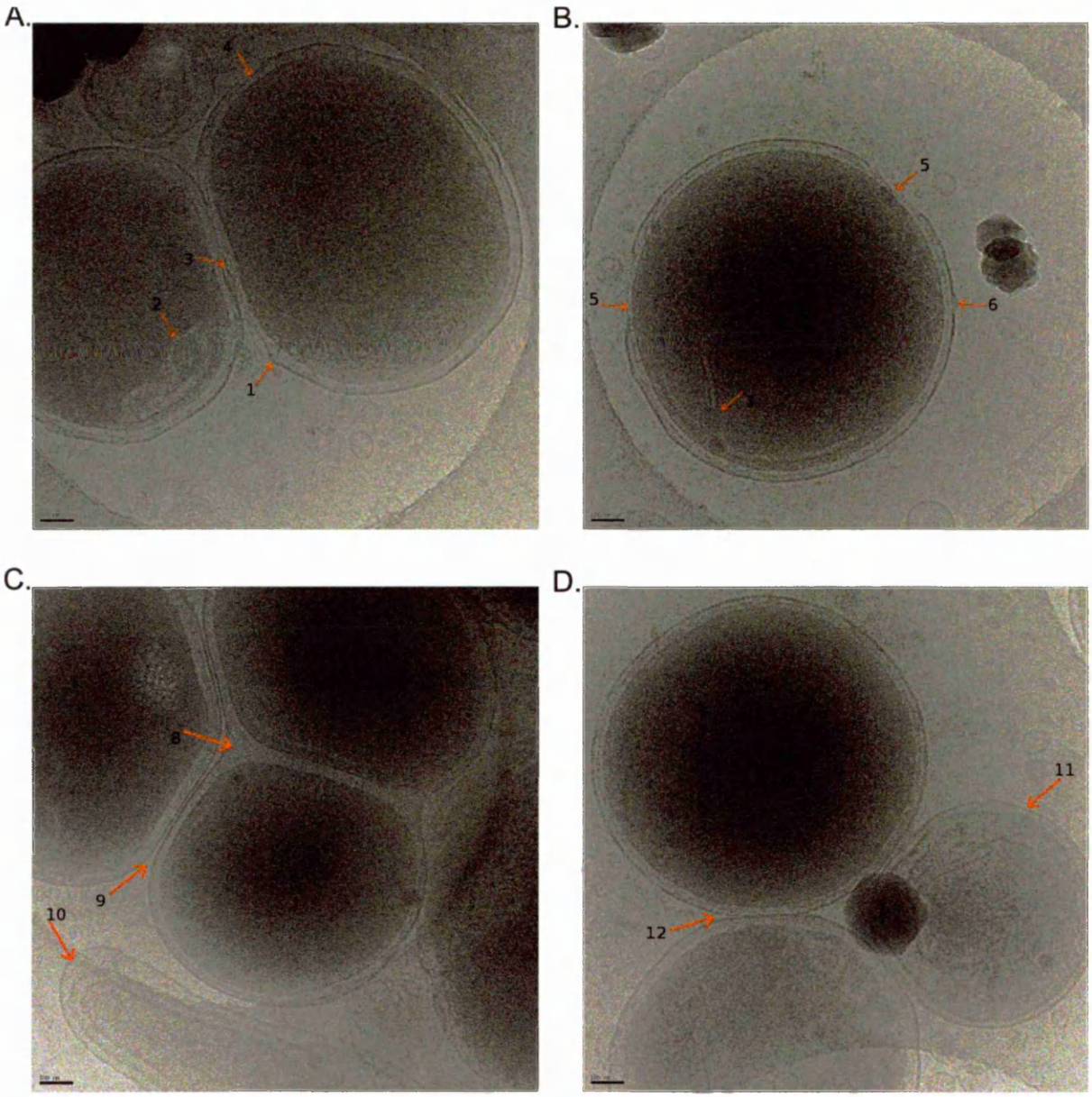

Figure 10. Cryo-electron microscopy of *N. meningitidis ΔrmpM* strain (A) Arrows indicate an area of vesiculation on the surface of the bacteria (1), features on the surface of the bacteria (2), the separation between two bacteria (3) and an area at one end of a bacterium where the outer membrane was not visible (4). (B) Further areas of missing outer membrane (5) are shown and budding vesicles (6) and surface features (7) are also marked. (C) Arrows indicate peptidoglycan separation in dividing bacteria (8). The area of light colouration in the other cell in the image is artefactual. An area of membranous material not associated with a bacteria or vesicle is also indicated (10). (D) A dead bacterium is marked on the right side of the image (11). Close contact between the bacteria is also indicated (12). (C) and (D) Bacteria were often observed in clusters although arrows indicate that the separation between the membranes of adjacent bacteria could be seen (9 & 12). All images taken at 30000X 200kV. Scale bar 100nm.

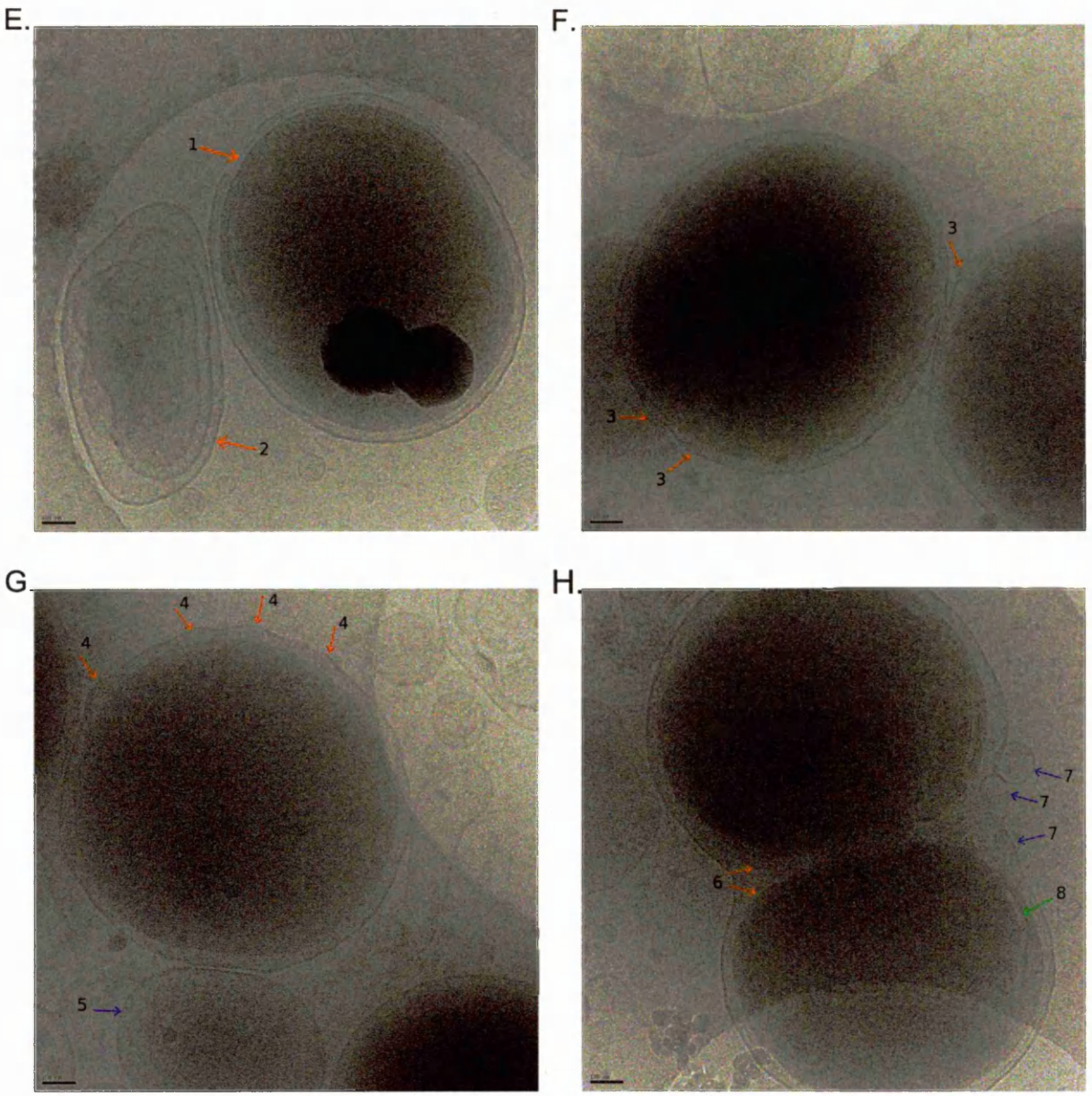

Figure 10. Cryo-electron microscopy of *N. meningitidis ΔrmpM* strain (continued) (E) Positions where outer membrane was absent are indicated (1). Also indicated is another multilayered membranous structure (2) similar to that previously observed in (C). (F) Vesiculation sites on the sides of the bacteria are marked (3). (G) Potential sites of Vesiculation are marked (4). The blue arrow indicates a large membrane bound structure which was possibly a large membrane vesicle (5). (H) Dividing cell that also showed peptidoglycan separation (6) and concentration of vesicles around one pole of the division site (7). Surface features (green arrow) can also be observed in the dividing cell (8). A similar feature was also present in the other daughter cell. All images taken at 30000X 200kV. Scale bar 100nm.

Electron microscopy of the RmpM C-term mutant showed bacteria that were morphologically similar to the wildtype strain, although like the *ΔrmpM* strain there were some minor differences. The most obvious of these was the difference in the behaviour of the outer membrane. Fig. 11 A-D showed bacteria with normal morphology, but a large number of potential vesiculation sites were visible on

the bacteria's surface in image D. Images E-M all show bacteria exhibiting a phenotype of outer membrane 'bulging', the outer membrane was expanded out from the side of the bacteria, although the peptidoglycan (indicated by purple arrows) remained continuous with the inner membrane. This phenotype indicated a disconnection between the outer membrane and peptidoglycan; as would be expected in a mutant lacking the peptidoglycan binding function of RmpM. However, the same phenotype was not observed in the *ΔrmpM* mutant. The RmpM C-term bacteria also had many vesiculation sites on the cell surface, particularly on bacteria that also exhibited bulging. Potential vesiculation sites appeared to be more common in this mutant than in the *ΔrmpM* sample. In image H and image I a large bleb can be seen separated from the bacteria, the bacteria found very near the bleb (and from which it is most likely to have been shed) has no defects in its outer membrane suggesting that release of large membrane vesicles was not detrimental to the bacteria. Large membrane bulges also did not seem to occur at any particular point of the bacterial surface, they could be observed in a range of positions and on bacteria of differing morphologies. At some vesiculation sites indicated with an arrow in images J (on a large bulge) E, I and D (on normal vesicles) the forming vesicles appeared to show a continuation of the membrane past the beginning of the vesicle bulge on one side. This raised the intriguing possibility of the re-growth of the outer membrane as the vesicle developed, the outer membrane growing from one edge of the vesicle to cover the area from where the vesicle has been released. Bacteria I and H showed some surface features similar to that observed in the *ΔrmpM* strain, suggesting that these features could be related to the loss of the C-terminal end of RmpM. Comparison of the two preparation methods for the bacteria (fig. 11 A-L are resuspended in PBS, M-N are resuspended in Mueller Hinton) showed that the same features were observable in both, including the increased vesiculation sites on the RmpM C-term (fig.11 N). However, although the membrane bulging was still present in the Mueller Hinton preparation (Fig. 11 M) it was less pronounced. Greater amounts of dead material were also seen in the Mueller Hinton preparation compared to the PBS. This indicated that the greater amount of dead material observed in the *ΔrmpM* preparation may have been due to the preparation method. Floating

the grid on the surface of the suspension would allow the least dense material to attach preferentially to the grid, which may have lead to the increase in dead material in the sample. Clustering of the bacteria was also more commonly observed in the floatation sample (data not shown) indicating that this may also be artefactual in the *ΔrmpM* preparation.

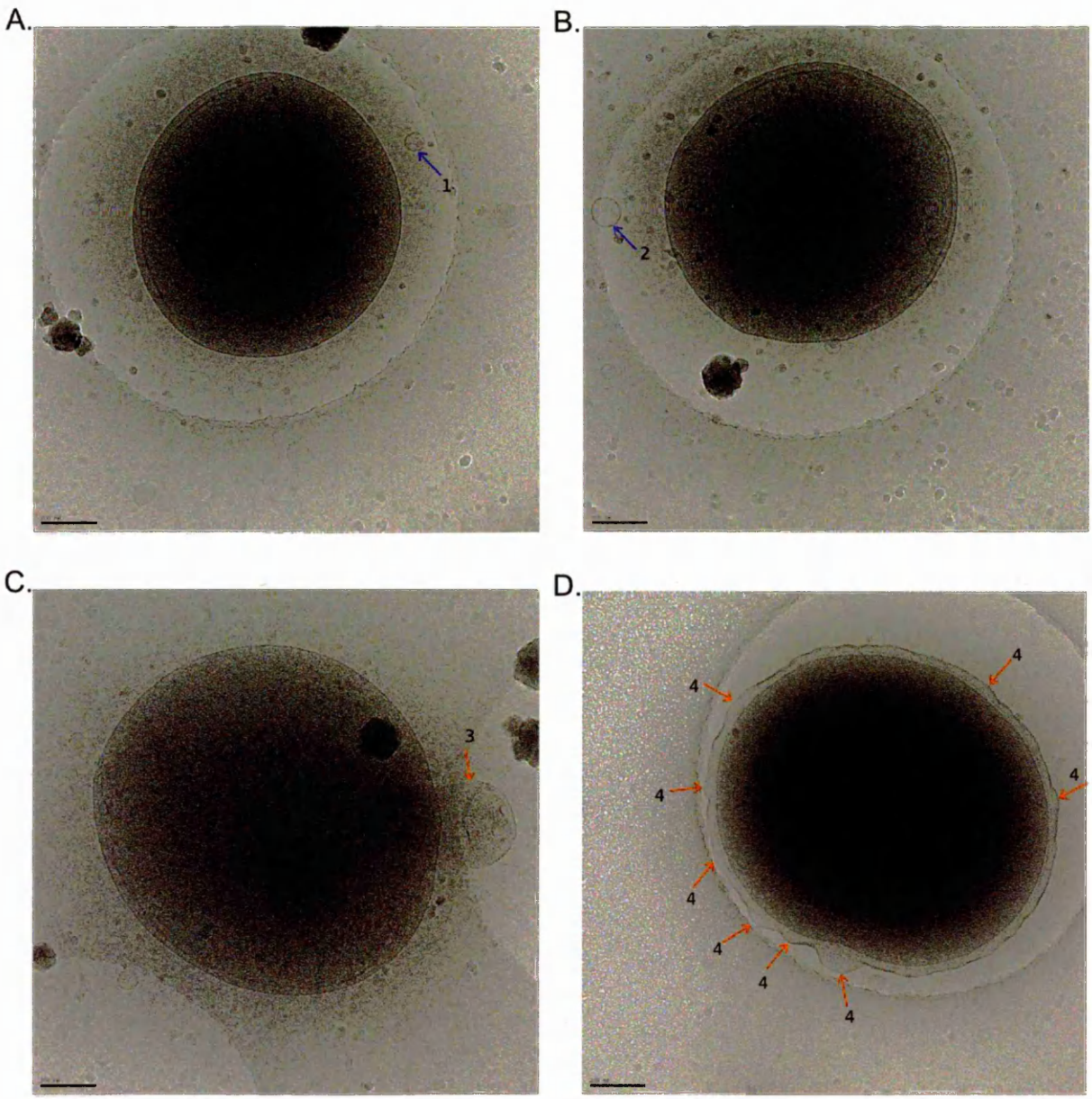

Figure 11. Cryo-electron microscopy of *N. meningitidis* RmpM C-term mutant. (A) and (B) Bacteria appeared similar to wildtype (see chapter 3 fig. 12 pg.77). A membrane vesicle is marked (blue arrow 1 & 2). (C) and (D). Some degradation products from dead bacteria were observed as arrowed in (C) (3). (D) Bacteria showed many sites of vesiculation (4). In the most developed of the vesiculation sites the outer membrane can be observed to be overlapping the edge of the vesiculation site on the right hand side. All images taken at 25000X 200kV. Scale bar 200nm.

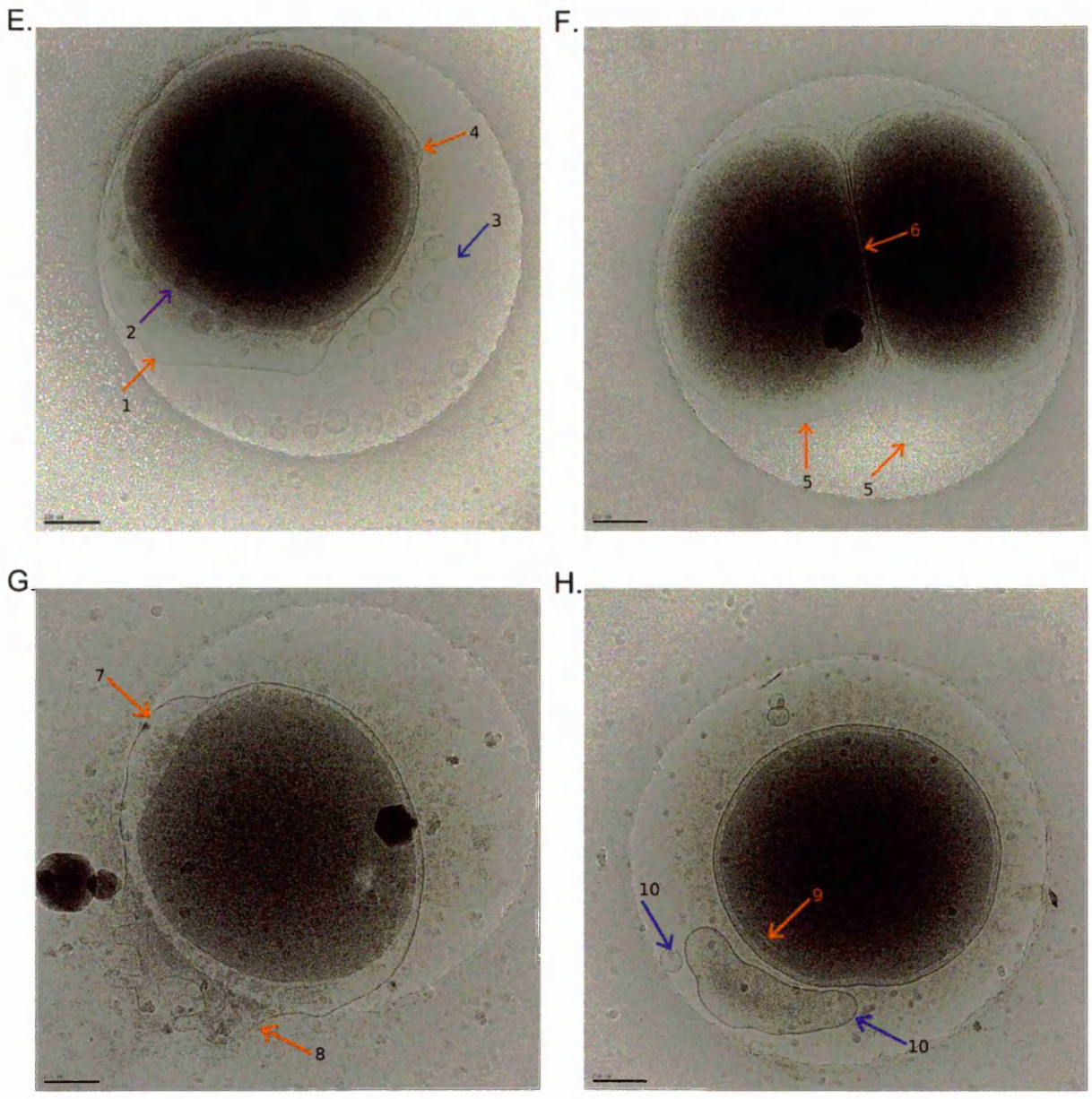

Figure 11. Cryo-electron microscopy of *N. meningitidis* RmpM C-term mutant (continued). (E) Bacteria were often found with large portions of membrane apparently detached from the peptidoglycan (1) which remains in close proximity to the inner membrane (purple arrow 2). There is also a vesiculation site present on the other side of the bacteria (4) and a large quantity of vesicles in close proximity to the bacteria (blue arrow 3). (F) Dividing bacteria, also showing detached outer membrane (5). The outer membrane has separated in this division and the division between the daughter cells can be seen (6). (G) and (H). Further bacteria showing separation of the outer membrane from the peptidoglycan. (G) The separation appears to encompass over half the membrane surface of the bacteria (7 & 8). Areas of possible separation into smaller vesicles can also be seen at the bottom edge of the separated membrane (8). (H) A very large membrane bleb as well as some smaller blebs (blue arrows) can be seen (10). An area of surface structure can also be seen (9). All images taken at 25000X 200kV. Scale bar 200nm.

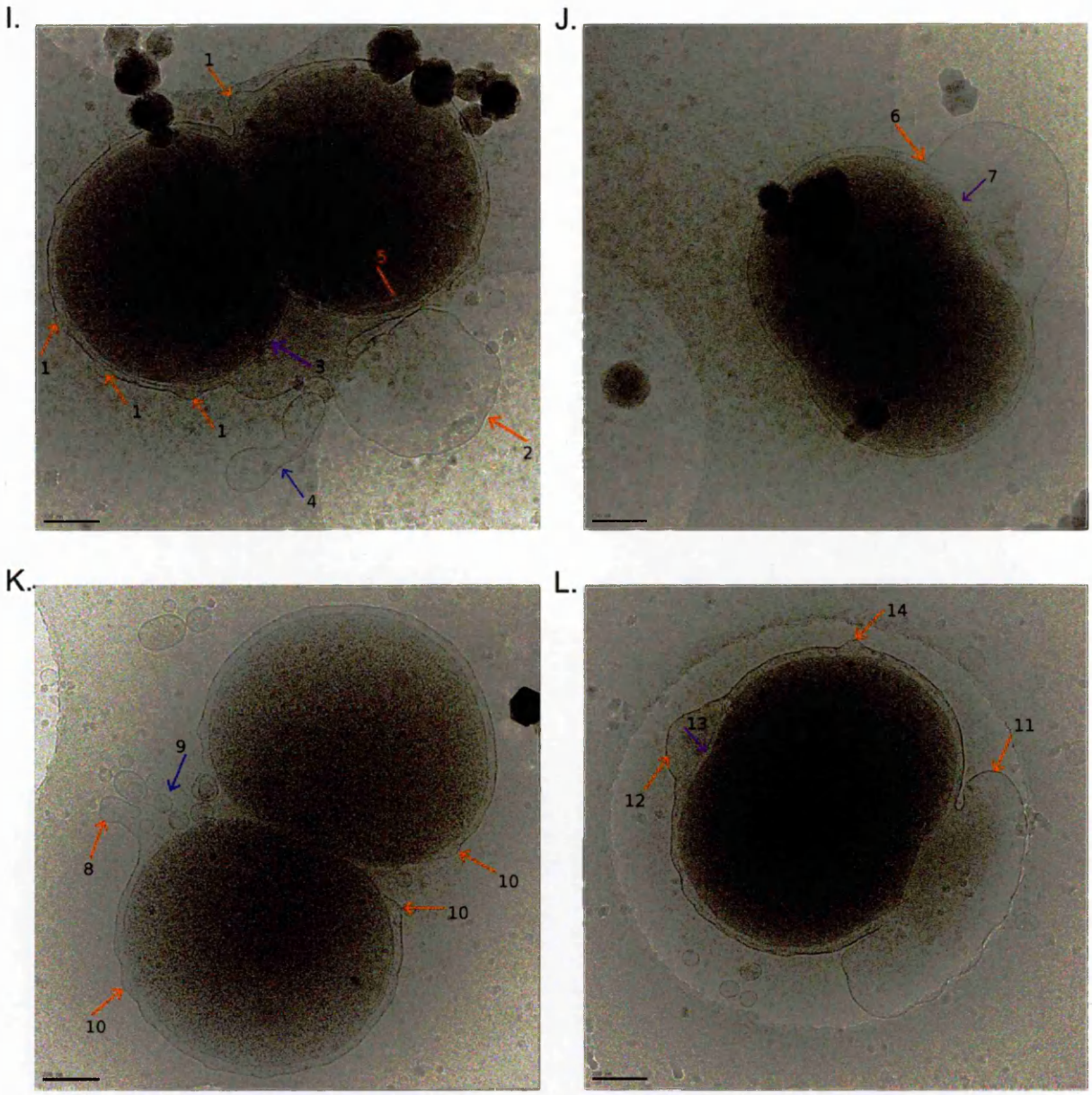

Figure 11. Cryo-electron microscopy of *N. meningitidis* RmpM C-term mutant (continued) (I) Bacterium shows areas of developing vesicles on the membrane surface (1) as well as large areas of membrane loss (2) with continuous peptidoglycan around the bacterium (purple arrow 3). A large membrane bleb can also be seen (blue arrow 4) and some areas of internal structure (5). (J) Bacteria also showing large membrane detachment. An area of overlapping membrane can be seen on the left side of the bleb (6) and continuous peptidoglycan can also be seen (purple arrow 7). (K) and (L). (K) Separating bacteria shows outer membrane being released from one pole but not the other (9). Large membrane bleb (8) and membrane vesicles are both visible (9), as well as potential sites of vesicle release (10). (L) Bacteria showing two areas of membrane detachments (11 & 12). The right side of the bug appears to have a membrane bleb that is more developed, the top edge of the bleb appears to be folding inwards (11), on the bottom edge there is an area of membrane overlapping the edge of the bleb as has been seen previously. The left hand side bleb is not as well developed (12), but the peptidoglycan layer can be seen (13). Another potential site is also indicated (14). All images taken at 25000X 200kV. Scale bar 200nm.

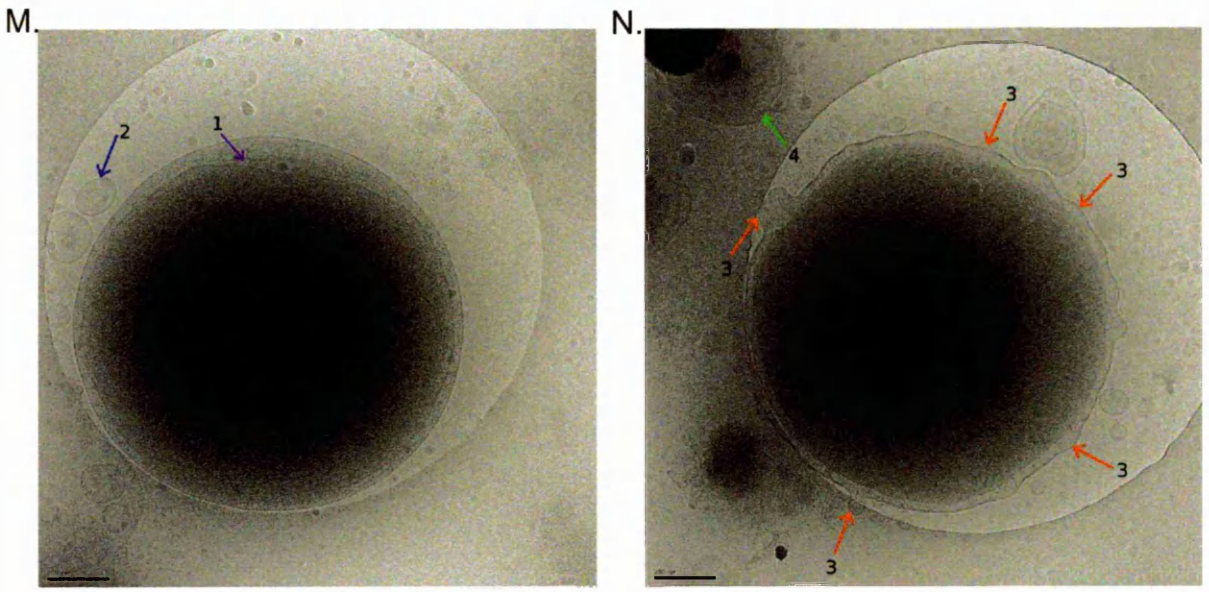

Figure 11. Cryo-Electron microscopy of *N. meningitidis* RmpM C-term mutant (continued). Bacteria were also prepared by floatation onto the grid, by the same method as the *ΔrmpM* strain for comparison. (M) The images were similar to the RmpM C-term mutant prepared by the direct application method however the membrane bulging phenotype was less pronounced in this sample (purple arrow 1), membrane vesicles were frequently observed (blue arrow 2). (N) Bacteria were still observed to have many vesiculation sites on the surface (3) a greater amount of debris was observed in this sample than was seen in the direct application grid (green arrow 4). All images taken at 25000X 200kV. Scale bar 200nm.

6.10 Native vesicles produced by the *rmpM* mutants

The disconnection of the outer membrane and the frequent sites of vesiculation displayed by the RmpM C-term mutant suggested that like the *ΔrmpM* mutant the strain would also be a high vesiculating strain. To test this hypothesis native vesicles were prepared from *ΔrmpM*, RmpM C-term and the wildtype bacteria and the preparations were run on an SDS-PAGE gel (fig.12).

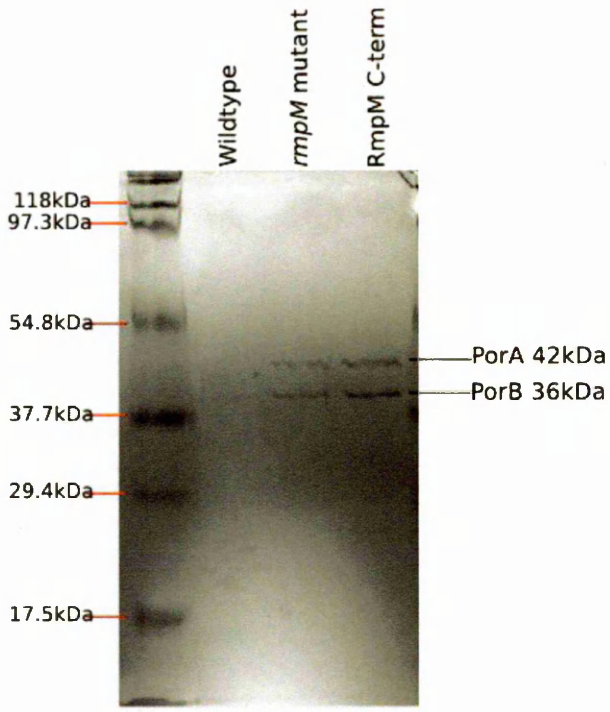

Figure 12. SDS-PAGE of native OMV for wildtype, *ΔrmpM* and RmpM C-term mutant. SDS PAGE gel showing preparations of native vesicles. Equal volumes of native vesicle preparations from the wildtype, *ΔrmpM* (*rmpM* mutant) and RmpM C-term mutants were loaded onto the gel.

Wildtype preparations of native vesicles do not usually produce enough protein to be seen by SDS-PAGE for the standard (20µl of concentrated preparation) amounts loaded. However both the *rmpM* mutants produced bands for PorA and PorB, the most abundant outer membrane proteins, at the expected sizes of 42kDa and 36kDa. Therefore both *ΔrmpM* and RmpM C-term were high vesiculating mutants. Although equal volumes of the three OMV preparations were loaded, band intensity was different between the two mutants with a greater amount of PorA and PorB in the RmpM C-term sample compared to *ΔrmpM*.

Slot blotting and immunoassay with specific monoclonal antibodies was used to produce a more accurate PorA and PorB quantification in the vesicles of the mutants (fig.13).

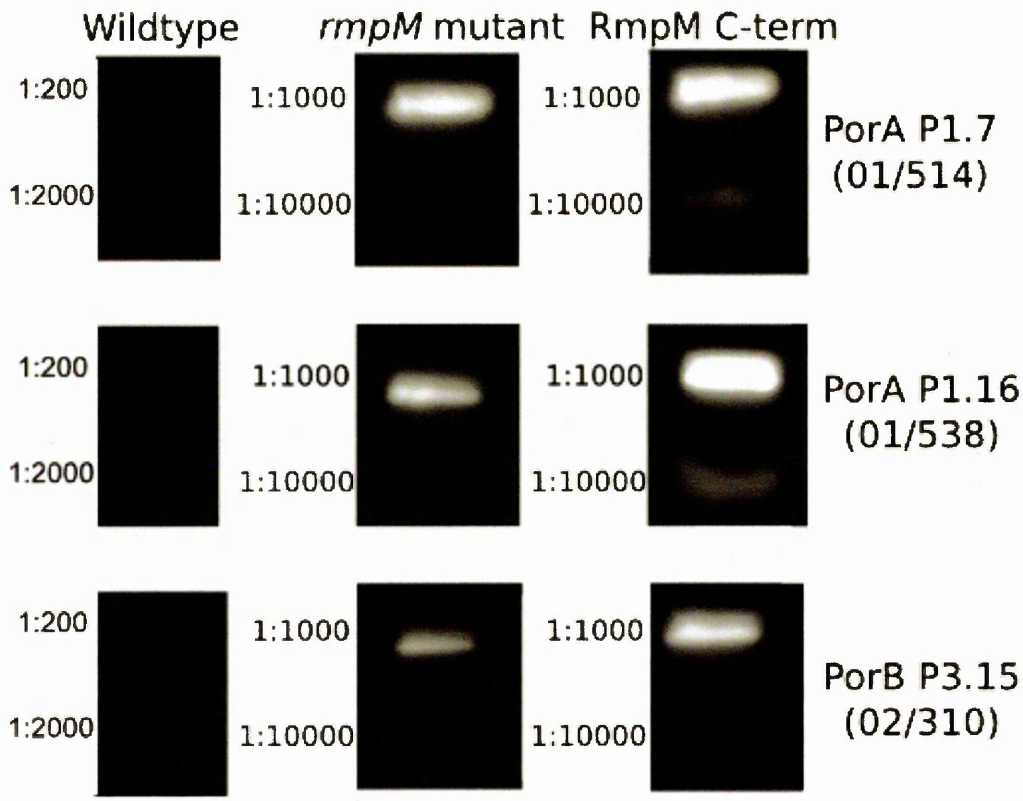

Strain	PorA P1.7 (01/514) (ng/µl)	PorA P1.16 (01/538) (ng/µl)	PorB P3.15 (02/310) (ng/µl)
Wildtype	1.0	<limit of detection	<limit of detection
ΔrmpM	68.3	64.5	140.7
RmpM C-term	213.2	205.3	156.3

Figure 13. Slot blot immunoassay of PorA and PorB in native vesicles from wildtype, *ΔrmpM* and RmpM C-term mutants. Dilutions of native OMV from wildtype, *ΔrmpM* (*rmpM* mutant) and RmpM C-term mutants were immunoblotted with monoclonal PorA and PorB antibodies. Dilutions of 1:200 and 1:2000 were used for the wildtype sample and 1:1000 and 1:10000 were used for *ΔrmpM* and RmpM C-term. Calculated protein amounts per µl of vesicle sample are shown in the table. Protein amounts were calculated using the Kodak MI software by comparison to standard curves (see chapter 3 fig. 25). In samples below the limit of detection no signal above the background level could be detected by the software.

Slot blotting with antibodies against PorA P1.7 (01/514) and P1.16 (01/538) and PorB P3.15 (02/310) showed that PorA and PorB levels were both increased in the RmpM C-term mutant compared with the wildtype and *ΔrmpM* strain. This result was also observed with other preliminary slot blot assays of vesicle preparations produced by these mutants. Densitometry was used to quantify the amount of

protein in each sample using the standard protein curves (see chapter 3 fig. 17 pg.87). Both mutants contained more of the porin proteins than the wildtype, which was only detected by one antibody in the PorA assays and was below the limit of detection in the PorB assay. There was good agreement between the two PorA antibodies for the amount of PorA present, showing that although these antibodies did not show good agreement at lower levels of PorA consistency of the two was better at higher PorA levels. Both PorA and PorB proteins were present in greater amounts in the native vesicles from RmpM C-term mutant compared to the *ΔrmpM* strain; in this assay the RmpM C-term mutant showed a 10% increase in the level of PorB protein and a ~3-fold increase in the PorA protein. An increase in vesicle number or size would have increased the levels of PorA and PorB by the same amount, so the ratios between the two proteins would have been the same in the OMVs of both strains. However, the RmpM C-term mutant vesicles contain 30% more PorA than PorB, whereas the *ΔrmpM* strain vesicles contain 100% more PorB than PorA. Therefore the change in relative proportions of porin protein was unlikely to be caused simply by an increase in the number of vesicles. Instead it indicated a change in protein expression or in the incorporation of the porins in the OMVs.

6.11 Electron microscopy of membrane vesicles from *rmpM* mutants

VTF-Cryo-electron microscopy was used to examine the vesicle preparations and *ΔrmpM* and RmpM C-term vesicles were compared to the wildtype sample (chapter 3 fig. 19 pg.90). The *ΔrmpM* strain (fig. 14) showed a large number of vesicles compared to the wildtype. Vesicles were frequently observed both in ice holes and on the carbon film, showing no preference in the vesicle sample for either surface. Some large and deformed vesicles were observed including a vesicle with a double membrane (fig. 14 F) and a broken vesicle (D), but most vesicles appeared to be intact and of similar size and shape.

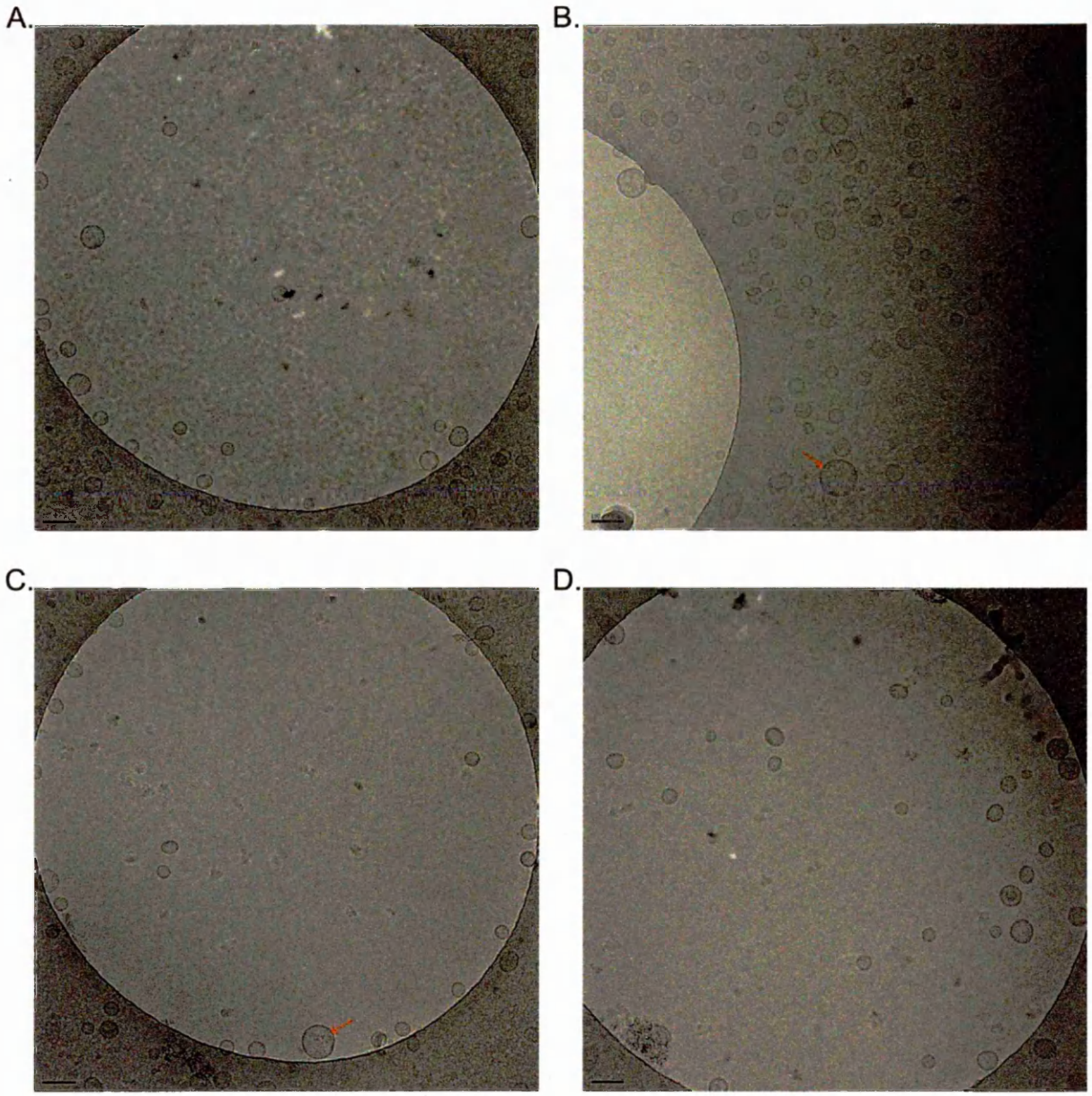

Figure 14. Cryo-electron microscopy of vesicles from the *ΔrmpM* mutant. The preparation showed many more vesicles than the equivalent wildtype (chapter 3 fig.19 pg.90) preparation. (A) and (B) Vesicles were observed in both the holes and carbon surface of the quantifoil. Most vesicles appeared of a similar size; however some larger vesicles were observed (red arrows). (C) and (D) Vesicles were distributed across the ice holes, a broken vesicle can be seen at the top left of image D. All images were recorded at 30,000X, 200kV. Scale bar 100nm.

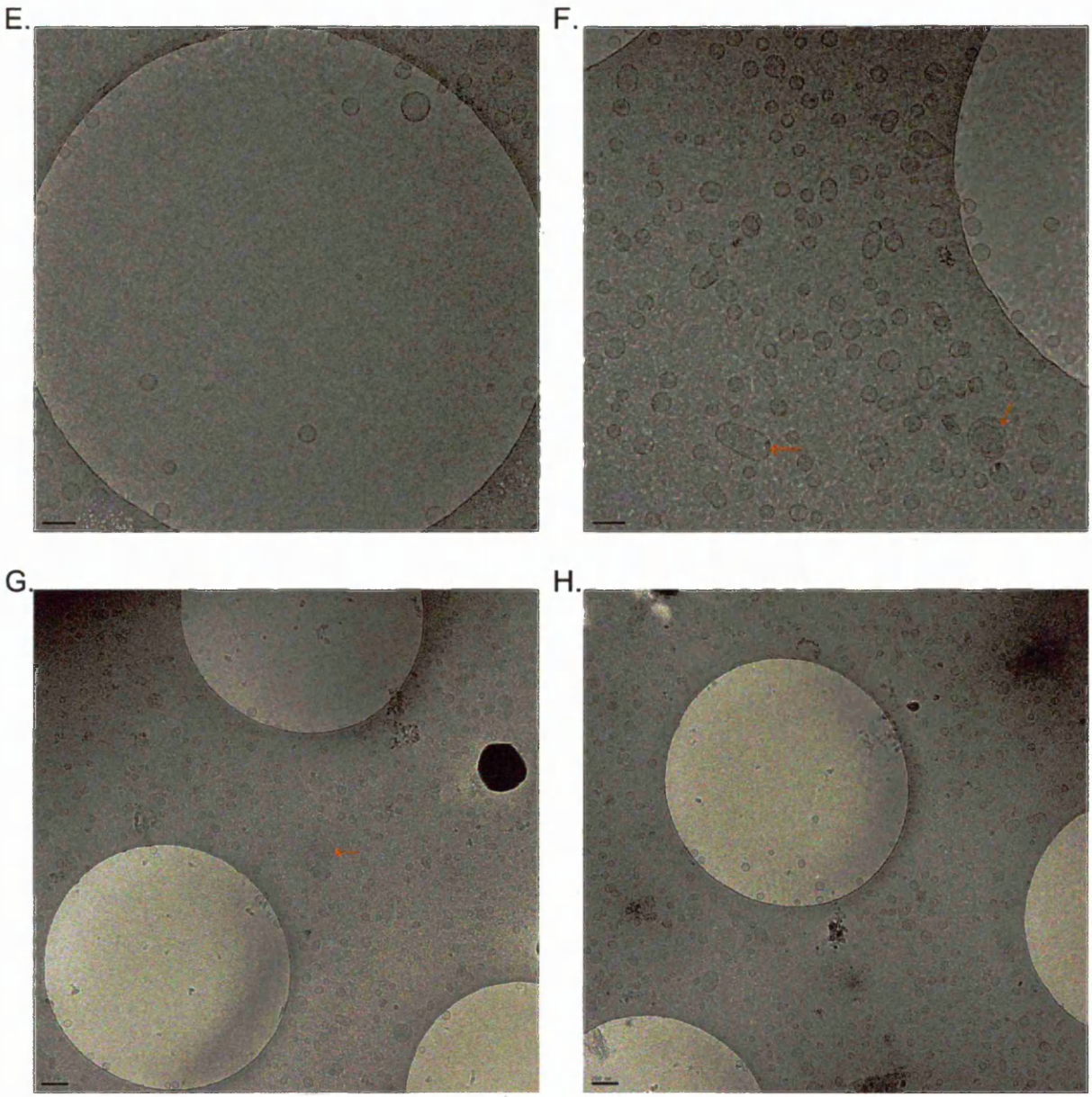

Figure 14. Cryo-electron microscopy of vesicles from the *ΔrmpM* mutant (continued). (E) and (F) Red arrows indicate deformed and double membrane vesicles, although these were not commonly observed in the sample. (G) and (H) Lower magnification showing the distribution of vesicles on the grid surface. The vesicles are mostly of similar size and shape; some larger vesicles can be seen (arrowed). (E) and (F) 30,000X 200kV. Scale bar 100nm. (G) and (H) 12,000X, 200kV. Scale bar 200nm.

The vesicles of the RmpM C-term mutant (fig. 15) appeared much more numerous than those of the *ΔrmpM* strain and the wildtype. The vesicles appeared similar in size and shape to those of the *ΔrmpM* strain. Large and double membrane vesicles were observed in (A) and (B) but these were few in number compared to the total vesicles in the preparation. High magnifications of the vesicle preparations (E and F) showed some evidence of surface features on the vesicles; however the

resolution of these images made further characterisation difficult. Low magnification images (G and H) showed the consistency of vesicle size and shape in the sample and that vesicles were spread consistently across the grid both in ice holes and on the carbon film.

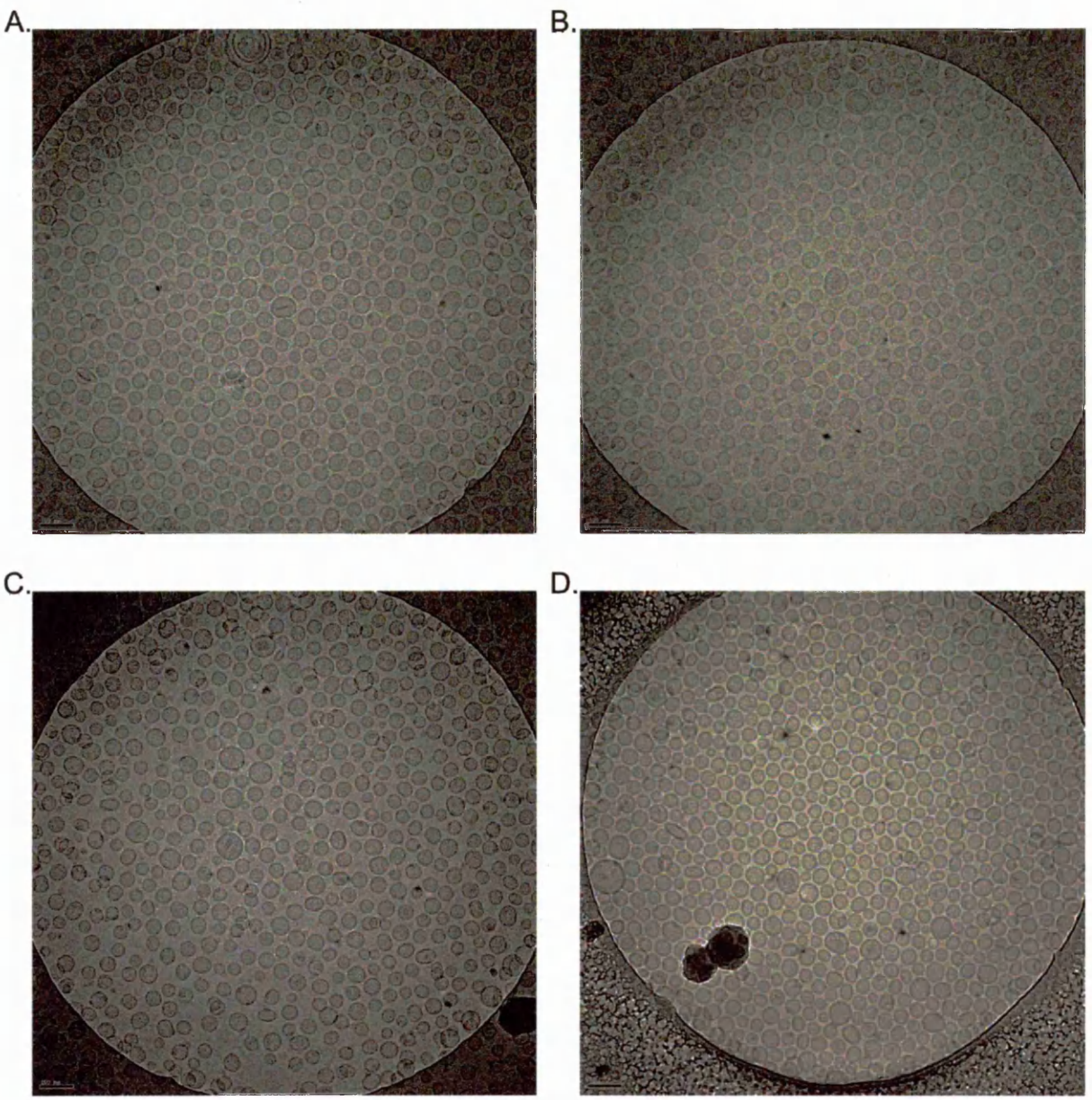

Figure 15. Cryo-electron microscopy of vesicles from RmpM C-term mutant. The mutant vesicles were much more numerous than the vesicles of the wildtype or *ΔrmpM* strain. Most vesicles appear of similar shape and size, although some larger vesicles can be observed. Some double membrane vesicles could be observed in (A) and (B). Similar levels of vesicles were observed in all the ice holes examined on the grid. Images recorded at 30,000X, 200kV. Scale bar 100nm.

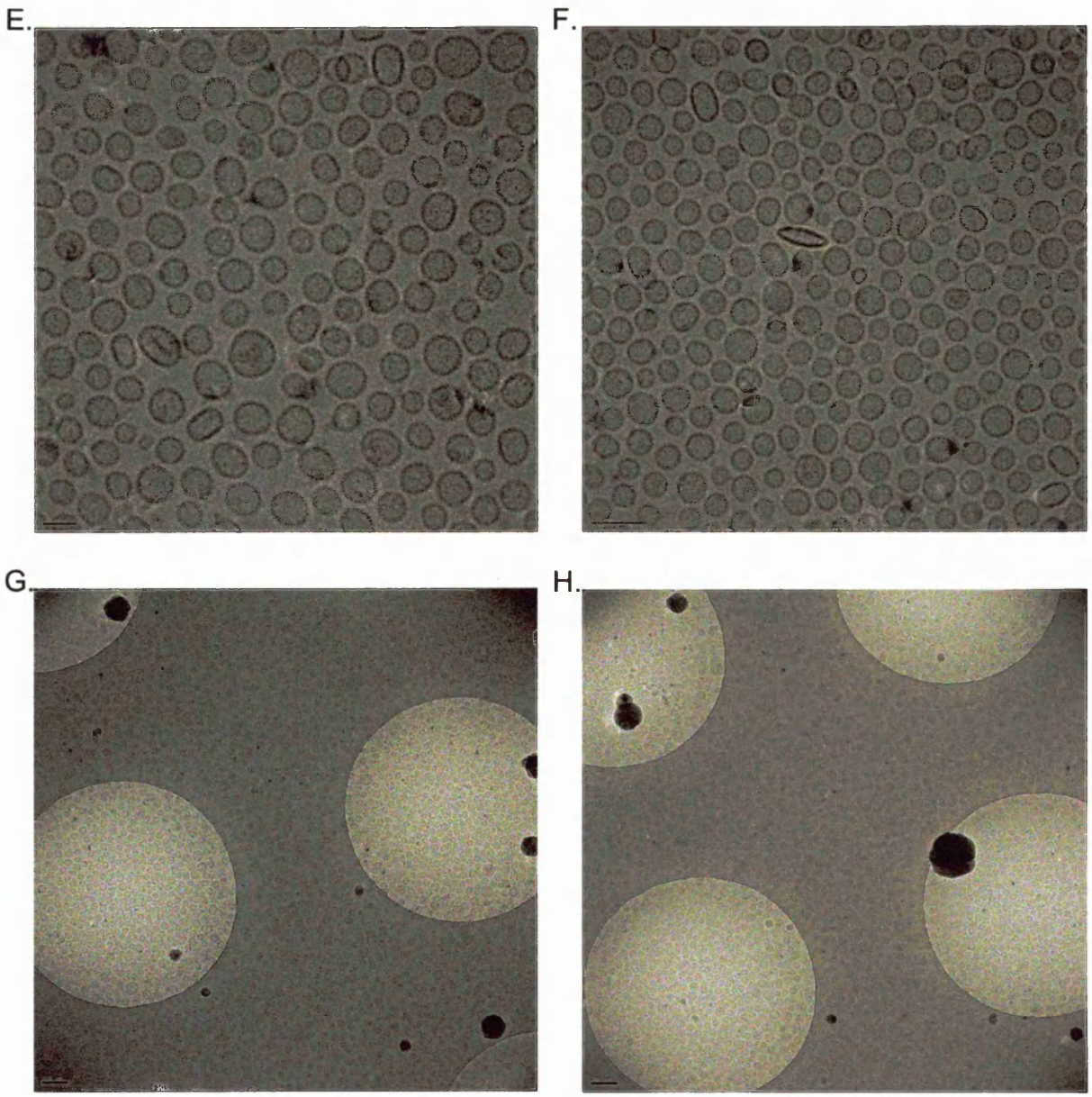

Figure 15. Cryo-electron microscopy of vesicles from RmpM C-term mutant (continued). (E) and (F) vesicles observed at a higher magnification. Although there is some variation in vesicle shape vesicles are of similar size. (G) and (H) Lower magnification images of the grid surface shows vesicles coating the entire grid. The number of vesicles appears greatly increased compared to the other mutants. (E) Image recorded at 60,000X, 200kV. Scale bar 50nm. (F) 50,000X 200kV. Scale bar 100nm. (G) and (H) 12,000X 200kV. Scale bar 200nm.

6.12 Comparison of *rmpM* mutant membrane vesicles

To test the consistency of the vesicle size and shape, vesicles were sampled from the electron micrographs and measured. As with previous strains, forty-five vesicles were randomly selected from the *ΔrmpM* and RmpM C-term mutant images for comparison to the wildtype (table 1).

Table 1. Comparison of wildtype, *ΔrmpM* and RmpM C-term native vesicles. Measurements are a mean of 45 vesicles. P values <0.05 are shown in blue. P values calculated by T-test.

	Wildtype	***ΔrmpM***	**RmpM C-term**
Mean perimeter (nm)	130.14	141.08	144.56
SD	41.02	39.27	20.48
Mean area (nm)	1457.42	1682.86	1695.04
SD	1064.32	1152.33	482.54

P values from T-test

	Wildtype:*ΔrmpM*	**Wildtype:RmpM C-term**	***ΔrmpM*:RmpM C-term**
Perimeter	>0.05	0.04	>0.05
Area	>0.05	>0.05	>0.05

There were no significant differences between the wildtype and *ΔrmpM* vesicles in terms of perimeter or area (P=>0.05). The RmpM C-term mutant showed a significant increase compared to the wildtype in terms of perimeter (P=0.04) but did not have a significantly different area measurement. The vesicles of the three strains were therefore very similar in terms of size and shape.

The standard deviation values suggested that the RmpM C-term mutant vesicles were less variable than those of the wildtype and *ΔrmpM* strains. To test the significance of this the variability of the samples were compared using an F-test (table 2.)

Table 2. Comparison of the wildtype, *ΔrmpM* and RmpM C-term samples by F-test. Wildtype, *ΔrmpM* and RmpM C-term variation was compared with a sample of 45 vesicles. F values <0.05 are indicated in blue. Values calculated by F-test. Significance level was set at 0.05

Comparison	Wildtype:*ΔrmpM*	Wildtype:RmpM C-term	*ΔrmpM*:RmpM C-term
Area	>0.05	<0.05	<0.05
Perimeter	>0.05	<0.05	<0.05

Wildtype and *ΔrmpM* vesicles were similarly variable (F=>0.05), but the RmpM C-term sample was significantly less variable than the wildtype or *ΔrmpM* strains in both area and perimeter (F=<0.05) (table 2).

6.13 Discussion

The aim of this study was to investigate the causes of increased vesiculation in *ΔrmpM* strains, the function of the RmpM protein and the characteristics of the vesicles. A mutant was constructed expressing a truncated RmpM protein, to test if loss of only the peptidoglycan binding function of the protein would increase vesiculation. Although the truncated RmpM protein was not seen on SDS-PAGE gels, data showing that the gene was transcribed together with the phenotypic characteristics of the RmpM C-term mutants provided strong evidence that a functional truncated RmpM protein was expressed. Increased vesiculation was most likely caused by the loss of the C-terminal end of RmpM, severing the link between outer membrane and cell wall peptidoglycan. Function of the N-terminal end of RmpM, which it has been suggested is involved in the stabilization of OMP complexes (121), was shown to be important for the growth of the organism. Vesicle production was increased in both *rmpM* mutant strains, but their OMVs were morphologically similar to those produced by the wildtype organism. Vesicles produced by the mutant expressing the truncated form of RmpM were enriched for the PorA protein, compared with those produced by the knockout mutant.

Cross-linked outer membranes of the *ΔrmpM* mutants contained few protein complex bands and larger amounts of the monomeric forms of PorA and PorB. This indicated that either porin complexes were not formed, or were not as stable as those of the other strains. These results differed from a

previous study by Marzoa et al. which reported no differences in high molecular weight complexes between the wildtype and mutant strains (88). This indicated that porin complexes were formed in the *ΔrmpM* strain. However Marzoa et al. used the technique of Blue Native (BN) PAGE to visualize the protein complexes. BN-PAGE uses the anionic dye Coomassie G-250, rather than SDS, to confer charge on protein complexes. It has been previously shown that the *ΔrmpM* outer membrane protein complexes have a higher sensitivity to SDS denaturation than wildtype complexes (88). Although the chemical cross-linking should prevent dissociation of complexes, this was the likely cause of the loss of some of the complexes from the *ΔrmpM* sample. Therefore, the results of these two studies indicated that the lack of complex bands was most likely due to a change in complex stability and not due to a failure of complex formation. Presence of the truncated form of RmpM improves the stability of the complexes but also affects the molecular weight of some of the complex bands observed; unexpectedly increasing the apparent molecular weight of the bands compared to the wildtype sample. A previous study by Volokhina et al. with a similar truncated RmpM protein showed a reduction in the molecular weight of complexes (162). But this study did not use a crosslinking technique, instead using a semi-native SDS PAGE method. The lack of a tether to the peptidoglycan in the truncated RmpM protein could allow protein complexes to be in closer proximity in the outer membrane, which could in turn have lead to cross linking between complexes which otherwise would not have occurred. Mass spectrometry could be used for a more accurate comparison of bands in the wildtype and RmpM C-term mutants and would show if the increase in molecular weight is an effect of the technique used to examine the OMP complex profile of the strains or an increase in the amount of the protein involved in the complexes formed. BN-PAGE may provide a better methodology for the isolation of complexes, as it does not require a cross-linking step that may introduce artefactual associations into the samples.

The loss of the N-terminal functionality of RmpM in the *ΔrmpM* strain lowered the optimum temperature for growth and extended lag times when the strain is grown at higher temperatures.

Changes in temperature can alter the fluidity of the outer membrane (99) and although gross changes in fluidity occur over a wide temperature range, changes of 10°C are sufficient to alter the fluidity of the cytoplasmic membrane in *E. coli* (157). Changes in membrane fluidity, combined with a decrease in stability of the protein complexes could explain the effects of temperature on the growth of the *ΔrmpM* strain. Lower temperatures may reduce the requirement for RmpM to stabilize the protein complexes and leading to better growth of the *ΔrmpM* strain. The unchanged antibiotic sensitivity of the *ΔrmpM* strain suggested there was no gross change in the permeability of the outer membrane. The comparison of phenotypes in the *ΔrmpM* and RmpM C-term mutants therefore showed that although the N-terminal end of the RmpM protein was important in the stability of outer membrane protein complexes, destabilization of protein complexes did not cause significant disruption to the outer membrane.

The C-terminal end of the RmpM protein contains the region hypothesized to be involved in the binding of peptidoglycan. Frequent sites of vesiculation were observed on both the *ΔrmpM* and the RmpM C-term mutant by election microscopy. This indicated that the truncation of the protein had affected the peptidoglycan binding function, leading to the outer membrane being disconnected from the peptidoglycan. It also showed that it was likely to be the loss of the C-terminal of RmpM that caused increased vesiculation in the strains. The increase in the number of vesicles produced by both strains indicated the importance of RmpM as a major structural protein. In samples prepared in PBS for cryo-EM, large areas of outer membrane disconnected from the peptidoglycan were seen in the RmpM C-term mutant. However, the lack of large areas of disconnected membrane in RmpM C-term mutants prepared in Mueller Hinton broth and the absence of unusually large vesicles in the native vesicle preparation suggested that this was an artefact of the preparation method rather than a consequence of the mutation.

Both the *ΔrmpM* and RmpM C-term mutants released large numbers of OMVs, but the differences between the two mutants offered further insights into the production of vesicles by *rmpM* mutants.

Normal growth of the RmpM C-term mutants showed that the increased production of vesicles does not affect the growth rate of the organism. In fact, the measurements of porin proteins and electron microscopy indicated that the RmpM C-term mutant was producing more vesicles than the *ΔrmpM* mutant. Although not significantly different in size and shape, the RmpM C-term vesicles appear more consistent than both the wildtype and *ΔrmpM* vesicles. However, regular packing of vesicles in the ice as can be observed in the RmpM C-term sample may cause the vesicles to appear more regular than if the sample was diluted. As well as indicating increased vesicle production, the immunoassay for the porin proteins showed a different ratio between PorA and PorB in the RmpM C-term sample compared to *ΔrmpM.* This indicated that PorA was enriched relative to the amount of PorB in the vesicles of the RmpM C-term mutant, although further experiments are required to confirm this result. Upregulation of PorA, which has variable expression levels (152), could also contribute to the increase, but no increase was seen in the levels of denatured PorA in the SDS-PAGE gels of the RmpM C-term strain or OMVs. The most likely explanation for the observed change in the amount of PorA was a difference in between the *ΔrmpM* and RmpM C-term mutants in the stability of OMP complexes. Stable OMP complexes containing RmpM C-term probably persist longer in the membrane, making the complexes more likely to be included in OMVs than monomeric forms of the proteins. RmpM has been shown to associate both with homotrimers and heteromeric complexes of the porin proteins (64,88), with the majority of complexes observed as heteromers (88,119-121). Therefore, the ratio of PorA to PorB in the heteromeric complexes may be affecting the ratio of the proteins in the vesicles. Better evidence of the *in vivo* stoichiometry of porin complexes, or high enough levels of wildtype vesicles to measure the porin content of these vesicles accurately by immunoassay, would be required to test this hypothesis.

The RmpM protein examined in this study is multifunctional. The C-terminal domain provides an anchor for the outer membrane to the peptidoglycan, stabilizing the outer membrane and preventing the bacteria from releasing high levels of OMVs. The N-terminal domain maintains the stability of the

porin complexes and other complexes such as those involving Omp85 (162). Better definition of the N-terminal domain of RmpM is needed to fully understand the effects of specific interactions on the stability of outer membrane protein complexes. The differences between the vesicles produced by the *ΔrmpM* and RmpM C-term mutants show the importance of fully understanding the role the N-terminus of RmpM plays in vesicle composition. Increased vesicle production and enrichment of the immunodominant PorA protein are both likely to be important for the production of native vesicle vaccines.

Chapter 7 - Discussion

The aim of this study was to investigate the factors involved in vesicle release from *N. meningitidis,* by elucidating the roles of two *N. meningitidis* proteins (GNA33 and RmpM) that were thought to affect the release of OMVs and have a structural function in the cell wall. The *E. coli* protein complex Tol-Pal, which is common in Gram negative bacteria but absent in *N. meningitidis* and other species with high vesicle production, was inserted to test if expression of the complex would decrease vesicle production in the strain. Wildtype vesiculation in *N. meningitidis* is known to be higher than that of other Gram negative species such as *E. coli*. The four mutants created by the study all had a phenotype of increased vesiculation. This phenotype was expected in the *Δgna33* and *ΔrmpM* mutants, but was surprising in the strain with an inserted *tol-pal* complex. In *E. coli* Tol-Pal stabilises the outer membrane and mutation of the complex leads to increased vesicle production. The mutants also showed distinct phenotypes, differing in growth and membrane stability as well as in the size and variability of the vesicles they produced.

The *Δgna33* and *gna33* single crossover::*tol-pal* mutants produced vesicles that were similar when compared to each other. However, the OMVs were significantly larger and more variable in size than those of their respective background strains. In contrast the two mutants of the RmpM protein (*ΔrmpM* and RmpM C-term) produced a much greater number of vesicles than all of the other strains and these vesicles were similar in size compared to the wildtype. The four mutants could therefore be divided into two groups; strains that produced increased levels of wildtype-like vesicles and strains that produced vesicles with an altered morphology.

7.1 Vesicles similar to the wildtype

The increase in vesiculation in the *rmpM* mutants has been shown by this study to be related to the C-terminal peptidoglycan binding function of RmpM. The other function of RmpM as a stabiliser of outer membrane protein complexes does not appear to be involved directly with vesiculation in these

strains. The production of vesicles in these strains was most likely to be due to the disconnection of the outer membrane and the peptidoglycan allowing the outer membrane to bulge and bleb more easily. This form of OMV release would be a passive process: vesicles would occur when a local build-up of turgor pressure caused the membrane to be forced outwards. The similarity of the vesicles to those produced by the wildtype suggests that a mechanism for controlling vesicle size was still present. Therefore, the control of vesicle size was not related to the RmpM protein.

7.2 Vesicles different to the wildtype

Both the *Δgna33* and *gna33* single crossover::*tol-pal* strains demonstrated a phenotype consistent with outer membrane and peptidoglycan disruption. The *Δgna33* strain was much more severely affected than the *tol-pal* strain. In both strains disruption to the peptidoglycan was likely to be caused by absence or reduction of *gna33* expression, as GNA33 is the primary lytic transglycosylase in *N. meningitidis*. Disruption of the outer membrane was probably caused by changes to peptidoglycan structure and in addition in the *gna33* single crossover::*tol-pal* by the accumulation of misfolded or mislocalised protein in the cell wall. It has been previously hypothesised by Zhou et al. that changes to peptidoglycan structure may cause vesiculation by altering the local turgor pressure in regions of the outer membrane, causing it to bulge and eventually bleb (175). Membrane disruption is also a cause of membrane vesicle release in other Gram negative species and one function of OMV release may be to remove misfolded protein from the periplasm (93). Consequently, membrane stress caused by misfolded and mislocalised Tol Pal proteins in the cell wall could have lead to vesicle release. The greater size and variability of these vesicles indicated mechanisms controlling vesicle size are disturbed, due to the disruption of the outer membrane or linked to loss of a specific protein such as GNA33.

7.3 A model of vesicle release in *N. meningitidis*

Native vesicle release in other Gram negative bacteria has been ascribed to the localised lowering of the concentration of proteins linking the peptidoglycan to the outer membrane (31). The results of this study suggest that a similar model could be applied to *N. meningitidis* and could be used to link the changes in vesicle release, size and variability in the different mutants studied.

The RmpM protein is ubiquitous in the outer membrane and is the only major outer membrane protein shown to have a peptidoglycan binding domain. The RmpM protein therefore is likely to represent the major structural linkage between the outer membrane and peptidoglycan in *N. meningitidis*. Localised disconnection of RmpM from the peptidoglycan or outer membrane would be a potential mechanism for increasing the amount of vesicles released. The GNA33 protein also binds to both the peptidoglycan and outer membrane, although it is present in the outer membrane at much lower levels than RmpM.

In this model of vesicle release, disconnection of the linkage between the outer membrane and peptidoglycan provided by RmpM produces regions of membrane more prone to bulging and forming membrane blebs. GNA33 and other proteins linking the outer membrane and peptidoglycan provide anchors in regions of the membrane. These anchor proteins would most likely include the other putative membrane bound lytic transglycosylases identified in the *N. meningitidis* genome and the TonB system. Vesiculation must occur between these protein anchors, controlling the size of the vesicles produced. The size of vesicles in the RmpM mutants remains regular because although the RmpM protein is absent or disconnected from the peptidoglycan or outer membrane, the anchoring proteins prevent large regions of the membrane from disconnecting from the peptidoglycan. When the GNA33 protein is mutated vesiculation presumably becomes irregular due to a combination of the loss of GNA33 as a protein anchor and disorganisation of the peptidoglycan affecting the distribution of other anchoring proteins. Disruption of the distribution of anchor proteins would result in the

formation of irregularly sized vesicles. Widening of the spaces between anchoring proteins will increase vesicle size. OMVs from the *Δgna33* strain showed both increased variability and an increased average size. The increased number of vesicles released by the *Δgna33* mutants is probably caused by disruption to the peptidoglycan structure, which could alter the turgor pressure between the peptidoglycan and outer membrane. Deletion of *gna33* may also cause disconnection of RmpM, as the protein may not be able to bind to the disorganised peptidoglycan. Addition of the Tol-Pal proteins also disrupts this interaction, by affecting GNA33 expression and potentially interacting with other anchoring protein complexes such as TonB. The model of vesicle release is shown in figure 1.

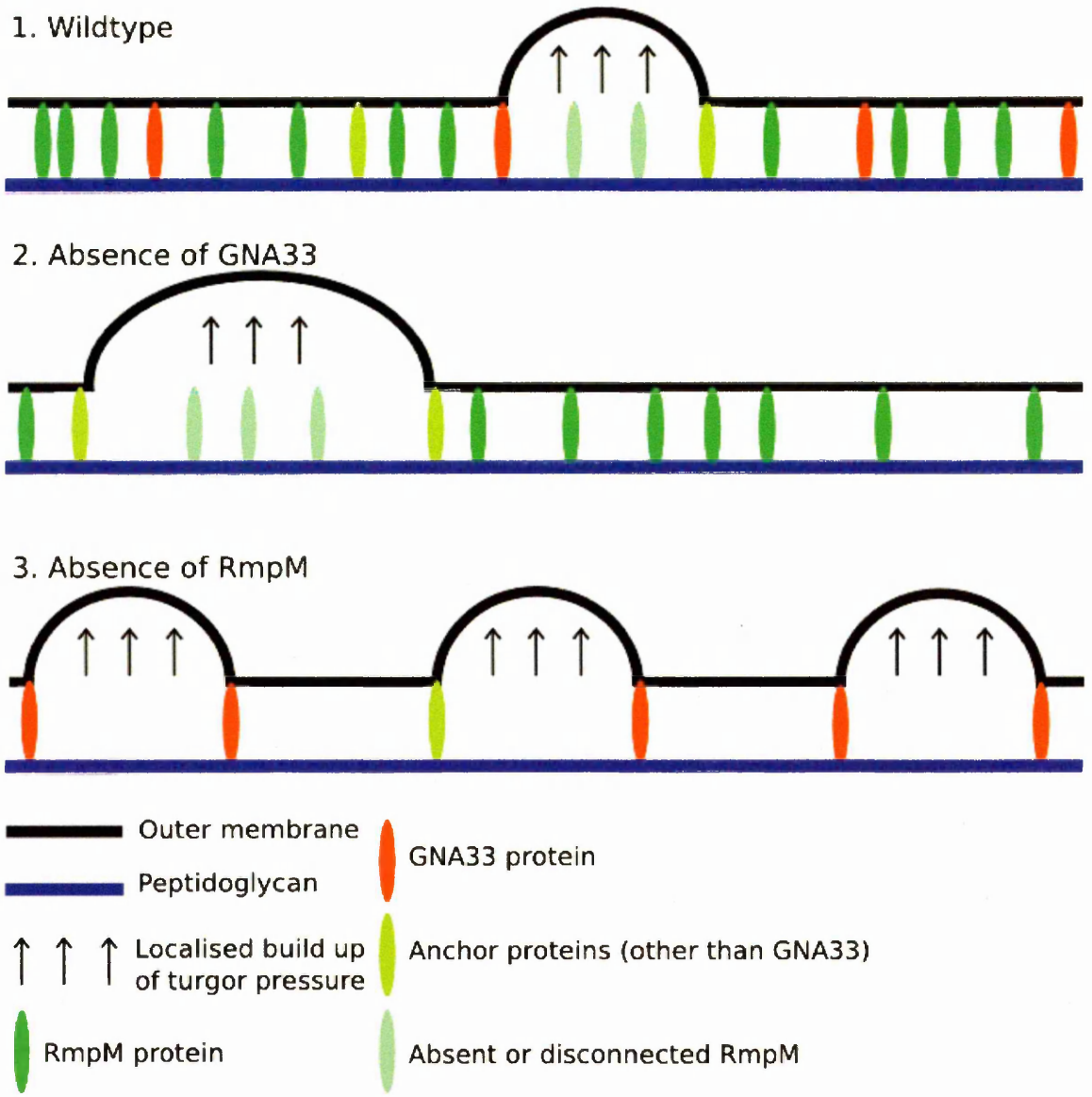

Figure 1. Model of vesicle release in *N. meningitidis*. Model of vesicle release in (1) the wildtype, where changes to the amount of RmpM connecting the outer membrane to the peptidoglycan, localised build up of turgor pressure and presence of anchor proteins with even spacing lead to controlled vesicle release. (2) A Δ*gna33* mutant, where loss of GNA33 leads to changes in the spacing of anchor proteins and release of vesicles that are larger and more variable in size. (3) A Δ*rmpM* mutant, loss of the connection between the OM and peptidoglycan made by RmpM causes increased vesiculation between anchor protein sites, leading to increased vesicle number but not increased variability in vesicle size.

Presence of the N-terminal portion of RmpM increases the stability of protein complexes in the outer membrane, improving the robustness of bacteria to changes in growth temperature and increasing the number of vesicles released. The increase in vesicle production could be due simply to improved growth of the strain. However, the model of vesicle release described above also indicates another method by which protein complexes could affect vesicle release. If turgor pressure is responsible for

the bulging of the outer membrane, then the number and position of channels that allow the passage of water and solutes through the outer membrane will be an important factor in OMV release. The N-terminal of the RmpM protein stabilises the Omp85 protein complex, which is the major machinery for insertion of β-barrel proteins into the outer membrane. In the *ΔrmpM* mutant fewer β-barrel proteins may be correctly inserted into the outer membrane, reducing the number of channels that would allow water and ionic solutes to pass through the outer membrane. This would make a build-up of turgor pressure and therefore the bulging of the membrane slower to occur in these mutants. The RmpM C-term mutant, with its functional N-terminus of RmpM, would produces bulges in the outer membrane and vesicles more frequently.

This model makes several predictions about vesiculation and the proteins involved. The first is that GNA33 and other potential anchor proteins are not randomly arranged in the membrane. The requirement for tight control of GNA33 and its known role in protein complexes to penicillin binding protein 2 (37) make it unlikely that the protein is randomly distributed in the cell wall. A second prediction of the model is that a double mutant of both *Δgna33* and *ΔrmpM* would produce large vesicles with less control over the size of the vesicles produced. It seems very likely that this mutant would not be viable if this model of vesicle release is true. As the GNA33 protein is so important to the maintenance of peptidoglycan structure, the loss of RmpM would exacerbate the effects of changes in the osmotic pressure between the peptidoglycan and outer membrane resulting in lysis. Finally, the model predicts that localised reduction of the number of RmpM protein molecules or disconnection of the protein from the outer membrane or peptidoglycan must occur for vesiculation to happen in wildtype strains. Testing of these predictions could include examining the vesicle releasing phenotypes of strains mutated for other proteins anchoring the outer membrane to the peptidoglycan, to confirm these mutants also show irregular vesicles. Monoclonal antibodies raised against the potential anchor proteins could also be used with immunogold labelling and electron

microscopy to examine if the potential anchor proteins show regular arrangements in the outer membrane.

7.4 Control of vesicle release in *N. meningitidis*

Release of large amounts of membrane vesicles does not seem to have a detrimental effect on the fitness of meningococci in *in vitro* culture, as the RmpM C-term mutant demonstrates. However, the potential of vesicles to induce an immune response against the bacterium in the host means it would be beneficial to the organism to control vesicle release during colonisation. Control of vesicle release may also play a part in additional cellular functions. In other Gram negative bacteria, for example *E. coli* and *Salmonella enterica* (93), evidence has indicated that elevated vesicle release may be a co-ordinated response to increased outer membrane stress. In *E. coli* outer membrane stress can result from accumulation of misfolded protein in the periplasm. Consequently the σ^E pathway is activated and leads to protein degradation. However when σ^E pathway is disrupted misfolded protein is preferentially packaged into OMVs and vesicle release is increased. *N. meningitidis* lacks some of the key genes of the σ^E pathway (chapter 1 table 1 pg. 16). Higher levels of vesicle release in *N. meningitidis* may provide an alternative mechanism for reducing membrane stress. This process would have to be tightly controlled in order to maintain outer membrane integrity. Use of a microarray could identify changes in gene transcription in response to conditions designed to increase stress on the outer membrane. When candidate genes have been identified, the functions of the proteins encoded by them and the effect on OMV release of the mutation of these proteins will help identify the pathways involved in response to membrane stress.

The RmpM protein would be a candidate as a method of controlling vesicle release. To increase the release of vesicles, the amount of RmpM linking the outer membrane to the peptidoglycan would have to be reduced. There are several ways in which this could be achieved. The first would be reduction of the expression of RmpM, which would increase vesicle release across the whole outer

membrane. Reduction of expression would require control of RmpM at the transcriptional or translational level, which has not been previously reported. The promoter of *rmpM* has not been identified, although a putative -10 sequence can be identified 63bp upstream of the *rmpM* start codon and a -35 sequence 87bp upstream of the start codon. However, little is known about the regulation of the *rmpM* expression. To quantify the amount of RmpM being expressed real-time PCR could be used to quantify changes to RNA expression and western blotting used to quantify the amount of protein present in the outer membrane. Alternatively, the arrangement of the RmpM protein in the outer membrane could be altered, by degradation of the protein in the outer membrane. This would lead to the reduction in the local density of RmpM molecules and the release of vesicles from specific areas of the membrane. Using a monoclonal antibody against RmpM, immunogold labelling and electron microscopy could be used to examine the positioning of RmpM in the cell wall and confirm if concentration is lower in regions of the bacteria which also show vesicle formation.

Thirdly, the link between the outer membrane and peptidoglycan formed by RmpM could also be severed by preventing the interaction of either the N-terminal domain with outer membrane proteins or the C-terminal domain with peptidoglycan. Controlling the formation or stability of either of these interactions would allow vesiculation to be initiated or prevented in specific areas of the membrane. RmpM does not bind directly to the outer membrane; instead the link is formed by the interaction of the N-terminal domain of RmpM with the inner face of outer membrane proteins including the porins. The N-terminal has not been fully characterised and the mechanism of interaction and complex formation with outer membrane proteins is unknown. Stability of the complexes could be affected either by changes to the conformation of the proteins involved in the complexes, or by addition of an accessory protein to stabilise the interaction. To date no accessory protein has been identified in mass spectrometry of complexes containing PorA, PorB and RmpM (89).The N-terminal portion of RmpM contains serine, tyrosine and threonine residues. Phosphorylation of these amino

acids is a common mechanism of controlling protein interactions and could also modulate the binding of RmpM protein. The C-terminal OmpA like domain is common amongst outer membrane proteins of Gram negative bacteria, but a mechanism to control the interaction of this domain has never been reported. RmpM has been shown to be present in outer membrane vesicles indicating that the disconnection of RmpM is more likely to occur at the C-terminal end of the protein, leaving RmpM attached to the protein complexes in the vesicles. Previous work has indicated that RmpM may bind peptidoglycan as a dimer (54), therefore control of the interaction could stem from either direct conformational changes in the peptidoglycan binding site, or by changes to the residues controlling dimerization of the protein. However, if conformational changes are responsible for control of the protein interactions at either end of the protein, then it may be possible to identify residues in the putative binding sites of the proteins by protein modelling. Site directed mutagenesis could then be used to mutate these residues and identify changes in complexes formed with RmpM or interactions of RmpM with the OMP or peptidoglycan.

Of these three potential methods of controlling RmpM linkage, the third would allow for the fastest and most sensitive response to changing conditions in the outer membrane, as it would not require changes to expression, degradation or protein transport.

7.5 Vesicle releasing mutants and vaccines

To date, the production of OMV vaccines has been based on a detergent extraction process to produce a sufficient amount of vesicles from bacterial cultures. Detergent extraction is an efficient means of vesicle production and has the additional benefit of reducing the amount of endotoxic components in the vesicles. However it has been shown that the proteomic profiles of detergent extracted vesicles differ from those of vesicles natively produced by a *Δgna33* mutant. The detergent extracted vesicles contained more cytoplasmic proteins while some lipoprotein antigens were

solubilised and therefore reduced or even lost from the vaccine preparation. Native vesicles also offered broader cross protection than detergent derived vesicles from the same strain (37).

Production of large amounts of native outer membrane vesicles is therefore an attractive method of OMV vaccine production. Deletion of the *rmpM* gene has been shown to be an effective method of increasing native vesicle release (150). An *ΔrmpM* mutant is already being used as a strain for production of the multivalent PorA vesicle vaccines known as HexaMen and NonaMen (151), although detergent is still used to extract vesicles (84). In addition to the problems of producing enough native vesicles for vaccine production, the attenuation of the endotoxic LOS component of the vesicles must also be considered. Reduction of LOS has been achieved by deletion of the *lpxA* gene (133), but if LOS is reduced, the adjuvant effect of the LOS component is also lost. By contrast, deletion of the *lpxL1* gene changes the structure of the LOS, reducing the endotoxic effect but maintaining the adjuvant activity (150,154). The ability to make these modifications to the LOS component is therefore an important consideration in any *N. meningitidis* vaccine candidate strain.

Other factors also have to be considered in the development of a potential native OMV vaccine candidate, including the content of the immunogenic proteins, such as the immunodominant PorA protein. Consistency is also key; subsequent lots of vaccine must be similar to the vaccine lots for which clinical efficacy has been established to ensure that safe, effective vaccine is always produced. Standardisation of the vaccine will be made easier if the vesicles produced by the strain are consistent in terms of size and quantities of the protein antigens. The four strains examined in this study all vesiculate at a level higher than the wildtype. However, the suitability of any of the strains for vaccine production will be affected by the tolerance of the strain to mutation to remove the endotoxic LOS component and to the culture conditions required for large scale vaccine production. The consistency of the vesicles and the level of immunogenic proteins in the vesicles produced would also be equally important.

The *Δgna33* mutant strain was originally suggested as a possible candidate for the production of a native OMV vaccine (37) and both this strain and the *gna33* single crossover::*tol-pal* strain produce increased amounts of vesicles. However, the vesicles produced are highly variable. The *Δgna33* strain exhibits poor growth, membrane instability and a clumping phenotype which are likely to make growth in large culture volumes and consistent vesicle production difficult. The *gna33* single crossover::*tol-pal* mutant grows normally and both membrane instability and clumping are much milder in this strain. However, vesiculation is lower than found in the *Δgna33* mutant and the strain has other potential problems that may make growth in large culture difficult. The change in growth conditions when the bacteria are grown on a large scale is likely to lead to changes in the stability of the *tol-pal* genes and cause recombination and loss of the plasmid. Additionally, any vaccine made from this strain may contain Tol-Pal proteins. The Pal protein in particular is known to be immunogenic, producing antibodies and inducing pro-inflammatory cytokines in mice (149). The inclusion of Pal in vesicles may therefore cause additional problems for the safety and immunogenicity of the vaccine product.

Both *rmpM* strains show good characteristics for a vaccine strain, and a *ΔrmpM* strain is already in use in the production of HexaMen (151). However, there are differences between them. The RmpM C-term mutant releases more membrane vesicles than the *ΔrmpM* strain and the size of vesicles produced appeared less variable in the RmpM C-term mutants. OMVs from the C-term mutant are also enriched for the immunodominant PorA protein. The change in the ratios of PorA and PorB in the sample suggests that the vesicles are incorporating more PorA when they are released, probably because of the inclusion of protein complexes in the vesicles. The effects of complexes in the outer membrane on immunogenicity have not been fully explored, but complexes consisting of PorA and PorB have been shown to elicit a modified immune response to the proteins, with new conformational epitopes present in the PorA/PorB complexes, when presented in liposomes (120). The incorporation of increased levels of PorA should increase the immunogenicity of the OMVs

produced from the RmpM C-term strain. Increasing the level of PorA in the vesicles also means fewer OMVs will be required for each vaccine dose. This will decrease the amount of any endotoxic components of the OMVs present, which may be useful in improving the safety and cost of any vaccine produced. Enrichment of PorA in the vesicles is an important factor to consider if the strain is used to produce vesicles for a multivalent PorA vaccine.

Of the strains tested in this study, the combination of high vesicle production, robustness of the strain, consistency in the vesicles produced and enrichment for the immunodominant PorA antigen makes the RmpM C-term mutant the most attractive candidate for the production of an outer membrane vesicle vaccine. The eventual production of a vaccine from this strain would require other genetic changes to the strain to remove the endotoxic LOS component. The vaccine may also be tailored to deliver multiple subtypes of PorA or enriched for other immunogenic proteins such as FetA, fHbp, NHBA, and NadA. A *ΔlpxA/ΔrmpM* strain has been constructed (132), as well as a strain producing modified LOS with substantially reduced endotoxin activity (*Δlpxl1*) and with a deleted *rmpM* gene (150). It is therefore likely that RmpM C-term strains could also be manipulated to remove the endotoxic LOS component.

A combination vaccine for group B *N. meningitidis*, which contains both recombinant proteins and OMVs, has recently been developed and has performed well in clinical trials. The OMV component of the vaccine has been shown to be very important for its immunogenicity (38,130). Evidence also shows that broader protection is induced by natively released OMVs (37,150). Therefore the ability to produce safe, immunogenic native OMVs in large quantities is a major part of *N. meningitidis* vaccine development. On a wider scale, OMVs are a potentially vaccine delivery system not only for *N. meningitidis*, but also other organisms through the expression of heterologous antigens in the OMVs. This methodology has already been used to express the NspA protein in OMVs from the commensal strain *N. flavescens* (104). Expression of green fluorescent protein in *E. coli* OMVs has also been achieved (24). Their natural adjuvant properties, presentation of antigens in the context of the

outer membrane and the significant work already done in their production and manipulation could make neisserial OMVs an attractive vaccine delivery system for many different antigens.

7.6 Conclusions

Native OMV provide an attractive option for the production of more broadly protective vesicle vaccines. Understanding the reasons and mechanisms underlying vesicle release is important for the production of native outer membrane vesicle vaccines, as sufficient levels of safe and consistent vesicles must be produced without the use of detergent extraction. The current study has produced a model for OMV production in *N. meningitidis* which may be useful in further developing strains and conditions to optimise vesicle production. The work has also shown that the mutation of the C-terminal peptidoglycan binding region of RmpM, whilst leaving the N-terminal protein binding region functional, creates an excellent candidate strain for vesicle production. This strain produces large quantities of membrane vesicles, which are consistent in size and enriched for the PorA protein. By expanding the understanding of the mechanisms of vesicle release and the effects of vesicle composition the best methods for production of a safe, consistent and effective OMV vaccine will be discovered.

1. **Ades, S. E.** 2008. Regulation by destruction: design of the σ^E envelope stress response. Curr. Opin. Microbiol. **11**:535-540.

2. **Adu-Bobie, J., Lupetti, P., Brunelli, B., Granoff, D., Norais, N., Ferrari, G., Grandi, G., Rappuoli, R., and Pizza, M.** 2004. GNA33 of *Neisseria meningitidis* is a lipoprotein required for cell separation, membrane architecture, and virulence. Infect. Immun. **72**:1914-1919.

3. **Al-Amoudi, A., Chang, J. J., Leforestier, A., McDowall, A., Salamin, L. M., Norlen, L. P., Richter, K., Blanc, N. S., Studer, D., and Dubochet. J.** 2004. Cryo-electron microscopy of vitreous sections. EMBO J. **23**:3583-3588.

4. **Antignac, A., Rousselle, J. C., Namane, A., Labigne, A., Taha, M. K., and Boneca, I. G.** 2003. Detailed structural analysis of the peptidoglycan of the human pathogen *Neisseria meningitidis*. J. Biol. Chem. **278**:31521-31528.

5. **Arigita, C., Jiskoot, W., Westdijk, J., van Ingen, C., Hennink, W. E., Crommelin, D. J., and Kersten, G. F.** 2004. Stability of mono- and trivalent meningococcal outer membrane vesicle vaccines. Vaccine **22**:629-642.

6. **Berlanda Scorza, F., Doro, F., Rodriguez-Ortega, M. J., Stella, M., Liberatori, S., Taddei, A. R., Serino, L., Gomes Moriel, D., Nesta, B., Fontana, M. R., Spagnuolo, A., Pizza, M., Norais, N., and Grandi, G.** 2008. Proteomics characterization of outer membrane vesicles from the extraintestinal pathogenic *Escherichia coli* Δ*tolR* IHE3034 mutant. Mol. Cell Proteomics. **7**:473-485.

7. **Bernadac, A., Gavioli, M., Lazzaroni, J. C., Raina, S., and Lloubès, R.** 1998. *Escherichia coli tol-pal* mutants form outer membrane vesicles. J. Bacteriol. **180**:4872-4878.

8. **Bertani, G.** 1951. Studies on lysogenesis. I. The mode of phage liberation by lysogenic *Escherichia coli*. J. Bacteriol. **62**:293-300.

9. **Betzner, A. S., Ferreira, L. C., Höltje, J. V., and Keck, W.** 1990. Control of the activity of the soluble lytic transglycosylase by the stringent response in *Escherichia coli*. FEMS Microbiol. Lett. **55**:161-164.

10. **Beveridge, T. J.** 1999. Structures of Gram-negative cell walls and their derived membrane vesicles. J. Bacteriol. **181**:4725-4733.

11. **Bjune, G., Hoiby, E. A., Grønnesby, J. K., Arnesen, O., Fredriksen, J.H., Halstensen, A., Holten, E., Lindbak, A. K., Nøkleby, H., Rosenqvist, E., and et al.** 1991. Effect of outer membrane vesicle vaccine against group B meningococcal disease in Norway. Lancet **338**:1093-1096.

12. **Blanco, D. R., Reimann, K., Skare, J., Champion, C. I., Foley, D., Exner, M. M., Hancock, R. E., Miller, J. N., and Lovett, M. A.** 1994. Isolation of the outer membranes from *Treponema pallidum* and *Treponema vincentii*. J. Bacteriol. **176**:6088-6099.

13. **Bomberger, J. M., Maceachran, D. P., Coutermarsh, B. A., Ye, S., O'Toole, G. A., and Stanton, B. A.** 2009. Long-distance delivery of bacterial virulence factors by *Pseudomonas aeruginosa* outer membrane vesicles. PLoS. Pathog. **5**:e1000382.

14. **Bos, M. P., and Tommassen, J.** 2004. Biogenesis of the Gram-negative bacterial outer membrane. Curr. Opin. Microbiol. **7**:610-616.

15. **Bos, M. P., Robert, V., and Tommassen, J.** 2007. Biogenesis of the Gram-negative bacterial outer membrane. Annual Review of Microbiology **61**:191-214.

16. **Bouhss, A., Trunkfield, A. E., Bugg, T. D., and Mengin-Lecreulx, D.** 2008. The biosynthesis of peptidoglycan lipid-linked intermediates. FEMS Microbiol. Rev. **32**:208-233.

17. **Boutriau, D., Poolman, J., Borrow, R., Findlow, J., Domingo, J. D., Puig-Barbera, J., Baldó, J. M., Planelles, V., Jubert, A., Colomer, J., Gil, A., Levie, K., Kervyn, A. D., Weynants, V., Dominguez, F., Barberá, R., and Sotolongo, F.** 2007. Immunogenicity and safety of three doses of a bivalent (B:4:p1.19,15 and B:4:p1.7-2,4) meningococcal outer membrane vesicle vaccine in healthy adolescents. Clin. Vaccine Immunol. **14**:65-73.

18. **Bowler, L. D., Zhang, Q. Y., Riou, J. Y., and Spratt, B. G.** 1994. Interspecies recombination between the *penA* genes of *Neisseria meningitidis* and commensal neisseria species during the emergence of penicillin resistance in *N. meningitidis*: natural events and laboratory simulation. J. Bacteriol. **176**:333-337.

19. **Braun, V.** 2006. Energy transfer between biological membranes. ACS Chem. Biol. **1**:352-354.

20. **Button, J. E., Silhavy, T. J., and Ruiz, N.** 2007. A suppressor of cell death caused by the loss of σ^E downregulates extracytoplasmic stress responses and outer membrane vesicle production in *Escherichia coli*. J. Bacteriol. **189**:1523-1530.

21. **Cascales, E., Bernadac, A., Gavioli, M., Lazzaroni, J. C., and Lloubes, R.** 2002. Pal lipoprotein of *Escherichia coli* plays a major role in outer membrane integrity. J. Bacteriol. **184**:754-759.

22. **Cascales, E., Gavioli, M., Sturgis, J. N., and Lloubes, R.** 2000. Proton motive force drives the interaction of the inner membrane TolA and outer membrane Pal proteins in *Escherichia coli*. Mol. Microbiol. **38**:904-915.

23. **Cascales, E., Lloubes, R., and Sturgis, J. N.** 2001. The TolQ-TolR proteins energize TolA and share homologies with the flagellar motor proteins MotA-MotB. Mol. Microbiol. **42**:795-807.

24. **Chen, D. J., Osterrieder, N., Metzger, S. M., Buckles, E., Doody, A. M., DeLisa, M. P., and Putnam, D.** 2010. Delivery of foreign antigens by engineered outer membrane vesicle vaccines. Proc Natl. Acad. Sci U. S. A **107(7)**:3099-3104.

25. **Cloud, K. A., and Dillard, J. P.** 2004. Mutation of a single lytic transglycosylase causes aberrant septation and inhibits cell separation of *Neisseria gonorrhoeae*. J. Bacteriol. **186**:7811-7814.

26. **Cloud-Hansen, K. A., Hackett, K. T., Garcia, D. L., and Dillard, J. P.** 2008. *Neisseria gonorrhoeae* uses two lytic transglycosylases to produce cytotoxic peptidoglycan monomers. J. Bacteriol. **190**:5989-5994.

27. **Comanducci, M., Bambini, S., Brunelli, B., Adu-Bobie, J., Arico, B., Capecchi, B., Giuliani, M. M., Masignani, V., Santini, L., Savino, S., Granoff, D. M., Caugant, D. A., Pizza, M., Rappuoli, R., and Mora, M.** 2002. NadA, a novel vaccine candidate of *Neisseria meningitidis*. J. Exp. Med. **195**:1445-1454.

28. **Councilman, W. T., Mallory, F. B., and Wright, J. H.** 1898. Epidemic cerebro-spinal meningitis and its relation to other forms of meningitis. Report of the State Board of Health, Massachusetts, Boston.

29. **Danzig, L.** 2006. Reverse vaccinology--in search of a genome-derived meningococcal vaccine. Vaccine **24 Suppl 2**:S2-11-2.

30. **Davidsen, T., Tuven, H. K., Bjørås, M., Rødland, E. A., and Tønjum, T.** 2007. Genetic interactions of DNA repair pathways in the pathogen *Neisseria meningitidis*. J. Bacteriol. **189**:5728-5737.

31. **Deatherage, B. L., Lara, J. C., Bergsbaken, T., Rassoulian Barrett, S. L., Lara, S., and Cookson, B. T.** 2009. Biogenesis of bacterial membrane vesicles. Mol. Microbiol. **72**:1395-1407.

32. **DeLisa, M. P., Valdes, J. J., and Bentley, W. E.** 2001. Mapping stress-induced changes in autoinducer AI-2 production in chemostat-cultivated *Escherichia coli* K-12. J. Bacteriol. **183**:2918-2928.

33. **Devoe, I. W.** 1982. The meningococcus and mechanisms of pathogenicity. Microbiol. Rev. **46**:162-190.

34. **Dorward, D. W., and Garon, C. F.** 1989. DNA-binding proteins in cells and membrane blebs of *Neisseria gonorrhoeae*. J. Bacteriol. **171**:4196-4201.

35. **Ellis, T. N., and Kuehn, M. J.** 2010. Virulence and immunomodulatory roles of bacterial outer membrane vesicles. Microbiol. Mol. Biol. Rev. **74**:81-94.

36. **Exley, R. M., Shaw, J., Mowe, E., Sun, Y. H., West, N. P., Williamson, M., Botto, M., Smith, H., and Tang, C. M.** 2005. Available carbon source influences the resistance of *Neisseria meningitidis* against complement. J. Exp. Med. **201**:1637-1645.

37. **Ferrari, G., Garaguso, I., Adu-Bobie, J., Doro, F., Taddei, A. R., Biolchi, A., Brunelli, B., Giuliani, M. M., Pizza, M. Norais, N. and Grandi, G.** 2006. Outer membrane vesicles from group B *Neisseria meningitidis Δgna33* mutant: proteomic and immunological comparison with detergent-derived outer membrane vesicles. Proteomics. **6**:1856-1866.

38. **Findlow, J., Borrow, R., Snape, M. D., Dawson, T., Holland, A., John, T. M., Evans, A., Telford, K. L., Ypma, E., Toneatto, D., Oster, P., Miller, E., and Pollard, A. J.** 2010. Multicenter, open-label, randomized phase II controlled trial of an investigational recombinant Meningococcal serogroup B vaccine with and without outer membrane vesicles, administered in infancy. Clin. Infect. Dis. **51**:1127-1137.

39. **Fong-Chong, J., Rodriguez-Bonano, N. M., González-Cordero, L. and Torres-Bauzá, L. J.** 2007. Functional analysis of ori1 and *repA* of the R-plasmid pSJ5.6 from *Neisseria gonorrhoeae*. Plasmid **57**:324-331.

40. **Fraenkel-Conrat, H. and Olcott, H. S.** 1948. The reaction of formaldehyde with proteins; cross-linking between amino and primary amide or guanidyl groups. J. Am. Chem. Soc. **70**:2673-2684.

41. **Frasch, C. E., Zollinger, W. D., and Poolman, J. T.** 1985. Serotype antigens of *Neisseria meningitidis* and a proposed scheme for designation of serotypes. Rev. Infect. Dis. **7(4)**:504-510.

42. **Galloway, S. M. and Raetz, C. R.** 1990. A mutant of *Escherichia coli* defective in the first step of endotoxin biosynthesis. J. Biol. Chem. **265**:6394-6402.

43. **Galloway, Y., Stehr-Green, P., McNicholas, A., and O'Hallahan, J.** 2009. Use of an observational cohort study to estimate the effectiveness of the New Zealand group B meningococcal vaccine in children aged under 5 years. Int. J. Epidemiol. **38**:413-418.

44. **Garcia, D. L. and Dillard, J. P.** 2006. AmiC functions as an N-acetylmuramyl-l-alanine amidase necessary for cell separation and can promote autolysis in *Neisseria gonorrhoeae*. J. Bacteriol. **188**:7211-7221.

45. **Gerding, M. A., Ogata, Y., Pecora, N. D., Niki, H., and de Boer, P. A.** 2007. The trans-envelope Tol-Pal complex is part of the cell division machinery and required for proper outer-membrane invagination during cell constriction in *Escherichia coli*. Mol. Microbiol. **63**:1008-1025.

46. **Gilbride, K. A. and Brunton, J. L.** 1990. Identification and characterization of a new replication region in the *Neisseria gonorrhoeae* beta-lactamase plasmid pFA3. J. Bacteriol. **172**:2439-2446.

47. **Gilleland, H. E., and Murray, R. G.** 1975. Demonstration of cell division by septation in a variety of Gram-negative rods. J. Bacteriol. **121**:721-725.

48. **Girard, M. P., Preziosi, M. P., Aguado, M. T., and Kieny, M. P.** 2006. A review of vaccine research and development: meningococcal disease. Vaccine **24**:4692-4700.

49. **Godlewska, R., Wiśniewska, K., Pietras, Z., and Jagusztyn-Krynicka, E. K.** 2009. Peptidoglycan-associated lipoprotein (Pal) of Gram-negative bacteria: function, structure, role in pathogenesis and potential application in immunoprophylaxis. FEMS Microbiol. Lett. **298**:1-11.

50. **Goldacre, M. J., Roberts, S. E., and Yeates, D.** 2003. Case fatality rates for meningococcal disease in an English population, 1963-98: database study. BMJ **327**:596-597.

51. **Gorringe, A. R., Taylor, S., Brookes, C., Matheson, M., Finney, M., Kerr, M., Hudson, M., Findlow, J., Borrow, R., Andrews, N., Kafatos, G., Evans, C. M., and Read, R. C.** 2009. Phase I safety and immunogenicity study of a candidate meningococcal disease vaccine based on *Neisseria lactamica* outer membrane vesicles. Clin. Vaccine Immunol. **16**:1113-1120.

52. **Gorringe, A., Halliwell, D., Matheson, M., Reddin, K., Finney, M., and Hudson, M.** 2005. The development of a meningococcal disease vaccine based on *Neisseria lactamica* outer membrane vesicles. Vaccine **23**:2210-2213.

53. **Granoff, D. M., Moe, G. R., Giuliani, M. M., Adu-Bobie, J., Santini, L., Brunelli, B., Piccinetti, F., Zuno-Mitchell, P., Lee, S. S., Neri, P., Bracci, L., Lozzi, L., and Rappuoli, R.** 2001. A novel mimetic antigen eliciting protective antibody to *Neisseria meningitidis*. J Immunol. **167**:6487-6496.

54. **Grizot, S., and Buchanan, S. K.** 2004. Structure of the OmpA-like domain of RmpM from *Neisseria meningitidis*. Mol. Microbiol. **51**:1027-1037.

55. **Gully, D., and Bouveret, E.** 2006. A protein network for phospholipid synthesis uncovered by a variant of the tandem affinity purification method in *Escherichia coli*. Proteomics. **6**:282-293.

56. **Hancock, R. E., and Bell, A.** 1988. Antibiotic uptake into Gram-negative bacteria. Eur. J. Clin. Microbiol. Infect. Dis. **7**:713-720.

57. **Held, K. G., and Postle, K.** 2002. ExbB and ExbD do not function independently in TonB-dependent energy transduction. J. Bacteriol. **184**:5170-5173.

58. **Henry, T., Pommier, S., Journet, L., Bernadac, A., Gorvel, J. P., and Lloubès, R.** 2004. Improved methods for producing outer membrane vesicles in Gram-negative bacteria. Res. Microbiol. **155**:437-446.

59. **Holst, J., Feiring, B., Naess, L. M., Norheim, G., Kristiansen, P., Hoiby, E. A., Bryn, K., Oster, P., Costantino, P., Taha, M. K., Alonso, J. M., Caugant, D. A., Wedege, E., Aaberge, I. S., Rappuoli, R. and Rosenqvist, E.** 2005. The concept of "tailor-made", protein-based, outer membrane vesicle vaccines against meningococcal disease. Vaccine **23**:2202-2205.

60. **Holst, J., Martin, D., Arnold, R., Huergo, C. C., Oster, P., O'Hallahan, J. and Rosenqvist, E.** 2009. Properties and clinical performance of vaccines containing outer membrane vesicles from *Neisseria meningitidis*. Vaccine **24**;27 Suppl 2:B3-12.

61. **Höltje, J. V.** 1998. Growth of the stress-bearing and shape-maintaining murein sacculus of *Escherichia coli*. Microbiol. Mol. Biol. Rev. **62**:181-203.

62. **Höltje, J. V.** 1996. A hypothetical holoenzyme involved in the replication of the murein sacculus of *Escherichia coli*. Microbiology **142 (Pt 8)**:1911-1918.

63. **Höltje, J. V., and Tuomanen, E. I.** 1991. The murein hydrolases of *Escherichia coli*: properties, functions and impact on the course of infections *in vivo*. J. Gen. Microbiol. **137**:441-454.

64. **Jansen, C., Wiese, A., Reubsaet, L., Dekker, N., de Cock, H., Seydel, U., and Tommassen, J.** 2000. Biochemical and biophysical characterization of *in vitro* folded outer membrane porin PorA of *Neisseria meningitidis*. Biochim. Biophys. Acta **1464**:284-298.

65. **Jennings, G. T., Savino, S., Marchetti, E., Aricò, B., Kast, T., Baldi, L., Ursinus, A., Höltje, J. V., Nicholas, R. A., Rappuoli, R. and Grandi, G.** 2002. *gna33* from *Neisseria meningitidis* serogroup B encodes a membrane-bound lytic transglycosylase (MltA). Eur. J. Biochem. **269**:3722-3731.

66. **Jolley, K. A., Brehony, C., and Maiden, M. C.** 2007. Molecular typing of meningococci: recommendations for target choice and nomenclature. FEMS Microbiol. Rev. **31**:89-96.

67. **Jorgensen, J. H., Crawford, S. A., Fulcher, L. C., Glennen, A., Harrington, S. M., Swenson, J., Lynfield, R., Murray P. R., and Tenover, F. C.** 2006. Multilaboratory evaluation of disk diffusion antimicrobial susceptibility testing of *Neisseria meningitidis* isolates. J. Clin. Microbiol. **44**:1744-1754.

68. **Kadurugamuwa, J. L., and Beveridge, T. J.** 1995. Virulence factors are released from *Pseudomonas aeruginosa* in association with membrane vesicles during normal growth and exposure to gentamicin: a novel mechanism of enzyme secretion. J. Bacteriol. **177**:3998-4008.

69. **Kahler, C. M., Lyons-Schindler, S., Choudhury, B., Glushka, J., Carlson, R. W., and Stephens, D. S.** 2006. O-Acetylation of the terminal N-acetylglucosamine of the lipooligosaccharide inner core in *Neisseria meningitidis*. Influence on inner core structure and assembly. J. Biol. Chem. **281**:19939-19948.

70. **Klugman, K. P., Gotschlich, E. C., and Blake, M. S.** 1989. Sequence of the structural gene (*rmpM*) for the class 4 outer membrane protein of *Neisseria meningitidis*, homology of the protein to gonococcal protein III and *Escherichia coli* OmpA, and construction of meningococcal strains that lack class 4 protein. Infect. Immun. **57**:2066-2071.

71. **Koebnik, R.** 1995. Proposal for a peptidoglycan-associating alpha-helical motif in the C-terminal regions of some bacterial cell-surface proteins. Mol. Microbiol. **16**:1269-1270.

72. **Kohler, P. L., Hamilton, H. L., Cloud-Hansen, K., and Dillard, J. P.** 2007. AtlA functions as a peptidoglycan lytic transglycosylase in the *Neisseria gonorrhoeae* type IV secretion system. J. Bacteriol. **189**:5421-5428.

73. **Kraft, A. R., Templin, M. F., and Höltje, J. V.** 1998. Membrane-bound lytic endotransglycosylase in *Escherichia coli*. J. Bacteriol. **180**:3441-3447.

74. **Kuehn, M. J., and Kesty, N. C.** 2005. Bacterial outer membrane vesicles and the host-pathogen interaction. Genes Dev. **19**:2645-2655.

75. **Kues, U., and Stahl, U.** 1989. Replication of plasmids in Gram-negative bacteria. Microbiol. Rev. **53**:491-516.

76. **Kuzminov, A.** 1999. Recombinational repair of DNA damage in *Escherichia coli* and bacteriophage λ. Microbiol. Mol. Biol. Rev. **63**:751-813, table.

77. **Kvalsvig, A. J. and Unsworth, D. J.** 2003. The immunopathogenesis of meningococcal disease. J. Clin. Pathol. **56**:417-422.

78. **Lambert, P.** 2004. Mechanism of action of antibiotics and synthetic anti-infective agents, p. 202-220. *In* Denyer S.P., Hodges N.A, and Gorman S.P. (ed.), Pharmaceutical Microbiology. Blackwell.

79. **Lee, H. S., Boulton, I. C., Reddin, K., Wong, H., Halliwell, D., Mandelboim, O., Gorringe, A. R., and Gray-Owen, S. D.** 2007. Neisserial outer membrane vesicles bind the coinhibitory receptor carcinoembryonic antigen-related cellular adhesion molecule 1 and suppress CD4+ T lymphocyte function. Infect. Immun. **75**:4449-4455.

80. **Llamas, M. A., Rodriguez-Herva, J. J., Hancock, R. E., Bitter, W., Tommassen, J., and Ramos, J. L.** 2003. Role of *Pseudomonas putida tol-oprL* gene products in uptake of solutes through the cytoplasmic membrane. J. Bacteriol. **185**:4707-4716.

81. **Lommatzsch, J., Templin, M. F., Kraft, A. R., Vollmer, W., and Höltje, J. V.** 1997. Outer membrane localization of murein hydrolases: MltA, a third lipoprotein lytic transglycosylase in *Escherichia coli*. J. Bacteriol. **179**:5465-5470.

82. **Lucidarme, J., Comanducci, M., Findlow, J., Gray, S. J., Kaczmarski, E. B., Guiver, M., Vallely, P. J., Oster, P., Pizza, M., Bambini, S., Muzzi A., and Borrow, R.** 2010. Characterization of fHBP, NHBA (GNA2132), NadA, PorA, and sequence type in group B meningococcal case isolates collected in England and Wales during January 2008 and potential coverage of an investigational group B meningococcal vaccine. Clin. Vaccine Immunol. **17**:919-929.

83. **Luijkx, T., van Dijken, H., van Els, C., and van den Dobbelsteen, G.** 2006. Heterologous prime-boost strategy to overcome weak immunogenicity of two serosubtypes in hexavalent *Neisseria meningitidis* outer membrane vesicle vaccine. Vaccine **24**:1569-1577.

84. **Luijkx, T. A., van Dijken, H., Hamstra, H. J, Kuipers, B., van der Ley, P., van Alphen, L., and van den Dobbelsteen, G.** 2003. Relative immunogenicity of PorA subtypes in a multivalent *Neisseria meningitidis* vaccine is not dependent on presentation form. Infect. Immun. **71**:6367-6371.

85. **Lytton, E. J. and Blake, M. S.** 1986. Isolation and partial characterization of the reduction-modifiable protein of *Neisseria gonorrhoeae*. J. Exp. Med. **164**:1749-1759.

86. **Maiden, M. C., Bygraves, J. A., Feil, E., Morelli, G., Russell, J. E., Urwin, R., Zhang, Q., Zhou, J., Zurth, K., Caugant, D. A., Feavers, I. M., Achtman, M., and Spratt, B. G.** 1998. Multilocus sequence typing: a portable approach to the identification of clones within populations of pathogenic microorganisms. Proc. Natl. Acad. Sci. USA. **95**:3140-3145.

87. **Martin, D. R., Ruijne, N., McCallum, L., O'Hallahan, J., and Oster, P.** 2006. The VR2 epitope on the PorA P1.7-2,4 protein is the major target for the immune response elicited by the strain-specific group B meningococcal vaccine MeNZB. Clin. Vaccine Immunol. **13**:486-491.

88. **Marzoa, J., Abel, A., Sánchez, S., Chan, H., Feavers, I., Criado, M. T., and Ferreirós, C. M.,** 2009. Analysis of outer membrane porin complexes of *Neisseria meningitidis* in wild-type and specific knock-out mutant strains. Proteomics. **9(3)**:648-656.

89. **Marzoa, J., Sánchez, S., Ferreirós, C. M., and Criado, M. T.,** 2009. Identification of *Neisseria meningitidis* outer membrane vesicle complexes using 2-D high resolution Clear Native / SDS-PAGE. J. Proteome. Res. **9(1)**:611-9.

90. **Mashburn-Warren, L. M., and Whiteley, M.** 2006. Special delivery: vesicle trafficking in prokaryotes. Mol. Microbiol. **61**:839-846.

91. **Masignani, V., Balducci, E., Di Marcello, F., Savino, S., Serruto, D., Veggi, D., Bambini, S., Scarselli, M., Aricò, B., Comanducci, M., Adu-Bobie, J., Giuliani, M. M., Rappuoli, R., and Pizza, M.** 2003. NarE: a novel ADP-ribosyltransferase from *Neisseria meningitidis*. Mol. Microbiol. **50**:1055-1067.

92. **McBroom, A. J., Johnson, A. P., Vemulapalli, S., and Kuehn, M. J.** 2006. Outer membrane vesicle production by *Escherichia coli* is independent of membrane instability. J. Bacteriol. **188**:5385-5392.

93. **McBroom, A. J. and Kuehn, M. J.** 2007. Release of outer membrane vesicles by Gram-negative bacteria is a novel envelope stress response. Mol. Microbiol. **63**:545-558.

94. **Meroueh, S. O., Bencze, K. Z., Hesek, D., Lee, M., Fisher, J. F., Stemmler, T. L., and Mobashery, S.** 2006. Three-dimensional structure of the bacterial cell wall peptidoglycan. Proc. Natl. Acad. Sci. U. S. A **103**:4404-4409.

95. **Mirlashari, M. R., Høiby, E. A., Holst, J., and Lyberg, T.** 2001. Outer membrane vesicles from *Neisseria meningitidis*: effects on cytokine production in human whole blood. Cytokine **13**:91-97.

96. **Morley, S. L., and Pollard, A. J.** 2001. Vaccine prevention of meningococcal disease, coming soon? Vaccine **20**:666-687.

97. **Mueller, J. H., and Hinton, J.** 1941. A protein-free medium for primary isolation of the Gonococcus and Meningococcus. Proc. Soc. Exp. Biol. and Med. **48**:330-333.

98. **Naess, L. M., Oftung, F., Aase, A., Wetzler, L. M., Sandin, R., and Michaelsen, T. E.** 1998. Human T-cell responses after vaccination with the Norwegian group B meningococcal outer membrane vesicle vaccine. Infect. Immun. **66**:959-965.

99. **Nichol, C. P., Davis, J. H., Weeks, G., and Bloom, M.** 1980. Quantitative study of the fluidity of *Escherichia coli* membranes using deuterium magnetic resonance. Biochemistry **19**:451-457.

100. **Nicolas, P., Norheim, G., Garnotel, E., Djibo, S., and Caugant, D. A.** 2005. Molecular epidemiology of *Neisseria meningitidis* isolated in the African Meningitis Belt between 1988 and 2003 shows dominance of sequence type 5 (ST-5) and ST-11 complexes. J. Clin. Microbiol. **43**:5129-5135.

101. **Nieves, W., Heang, J., Asakrah, S., Höner zu Bentrup, K., Roy, C. J., and Morici, L. A.** 2010. Immunospecific responses to bacterial elongation factor Tu during *Burkholderia* infection and immunization. PLoS. One. **5**:e14361.

102. **Nikaido, H.** 2003. Molecular basis of bacterial outer membrane permeability revisited. Microbiol. Mol. Biol. Rev. **67**:593-656.

103. **O' Dwyer, C. A., Langford, P. R., and Kroll, J. S.** 2005. A novel neisserial shuttle plasmid: a useful new tool for meningococcal research. FEMS Microbiol. Lett. **251**:143-147.

104. **O'Dwyer, C. A., Reddin, K., Martin, D., Taylor, S. C., Gorringe, A. R., Hudson, M. J., Brodeur, B. R., Langford, P. R. and Kroll, J. S.** 2004. Expression of heterologous antigens in commensal *Neisseria* spp.: preservation of conformational epitopes with vaccine potential. Infect. Immun. **72**:6511-6518.

105. **Patel, M. S.** 2007. Australia's century of meningococcal disease: development and the changing ecology of an accidental pathogen. Med. J. Aust. **186**:136-141.

106. **Peeters, C. C., Rümke, H. C., Sundermann, L. C., Rouppe van der Voort, E. M., Meulenbelt, J., Schuller, M., Kuipers, A.J., van der Ley, P. and Poolman, J. T.** 1996. Phase I clinical trial with a hexavalent PorA containing meningococcal outer membrane vesicle vaccine. Vaccine **14**:1009-1015.

107. **Perkins-Balding, D., Ratliff-Griffin, M., and Stojiljkovic, I.** 2004. Iron transport systems in *Neisseria meningitidis*. Microbiol. Mol. Biol. Rev. **68**:154-171.

108. **Pizza, M., Donnelly, J., and Rappuoli, R.** 2008. Factor H-binding protein, a unique meningococcal vaccine antigen. Vaccine **26 Suppl 8**:I46-I48.

109. **Pizza, M., Scarlato, V., Masignani, V., Giuliani, M. M., Aricò, B., Comanducci, M., Jennings, G. T., Baldi, L., Bartolini, E., Capecchi, B., Galeotti, C. L., Luzzi, E., Manetti, R., Marchetti, E., Mora, M., Nuti, S., Ratti, G., Santini, L., Savino, S., Scarselli, M., Storni, E., Zuo, P., Broeker, M., Hundt, E., Knapp, B., Blair, E., Mason, T., Tettelin, H., Hood, D. W., Jeffries, A. C., Saunders, N. J., Granoff, D. M., Venter, J. C., Moxon, E. R., Grandi, G., and Rappuoli, R.** 2000. Identification of vaccine candidates against serogroup B meningococcus by whole-genome sequencing. Science **287**:1816-1820.

110. **Plant, L., Sundqvist, J., Zughaier, S. Lövkvist, L., Stephens, D. S., and Jonsson, A. B.** 2006. Lipooligosaccharide structure contributes to multiple steps in the virulence of *Neisseria meningitidis*. Infect. Immun. **74**:1360-1367.

111. **Postle, K., and Kadner, R. J.** 2003. Touch and go: tying TonB to transport. Mol. Microbiol. **49**:869-882.

112. **Powell, A. J., Liu, Z. J., Nicholas, R. A., and Davies, C.** 2006. Crystal structures of the lytic transglycosylase MltA from *Neisseria gonorrhoeae* and *Escherichia coli*: insights into interdomain movements and substrate binding. J. Mol. Biol. **359**:122-136.

113. **Pridmore, A. C., Jarvis, G. A., John, C. M., Jack, D. L., Dower, S. K., and Read, R. C.** 2003. Activation of toll-like receptor 2 (TLR2) and TLR4/MD2 by *Neisseria* is independent of capsule and lipooligosaccharide (LOS) sialylation but varies widely among LOS from different strains. Infect. Immun. **71**:3901-3908.

114. **Prinz, T., and Tommassen, J.** 2000. Association of iron-regulated outer membrane proteins of *Neisseria meningitidis* with the RmpM (class 4) protein. FEMS Microbiol. Lett. **183**:49-53.

115. **Ropp, P. A., and Nicholas, R. A.** 1997. Cloning and characterization of the *ponA* gene encoding penicillin-binding protein 1 from *Neisseria gonorrhoeae* and *Neisseria meningitidis*. J. Bacteriol. **179**:2783-2787.

116. **Rosenqvist, E., Musacchio, A., Aase, A., Høiby, E. A., Namork, E., Kolberg, J., Wedege, E., Delvig, A., Dalseg, R., Michaelsen, T. E., and Tommassen, J.,** 1999. Functional activities and epitope specificity of human and murine antibodies against the class 4 outer membrane protein (Rmp) of *Neisseria meningitidis*. Infect. Immun. **67**:1267-1276.

117. **Rosenstein, N. E., Perkins, B. A., Stephens, D. S., Popovic, T., and Hughes, J. M.** 2001. Meningococcal disease. N. Engl. J Med. **344**:1378-1388.

118. **Russell, J. E., K. A. Jolley, I. M. Feavers, M. C. Maiden, and J. Suker**. 2004. PorA variable regions of Neisseria meningitidis. Emerg. Infect. Dis. **10**:674-678.

119. **Sánchez, S., Abel, A., Arenas, J., Criado, M. T., and Ferreirós, C. M.** 2006. Cross-linking analysis of antigenic outer membrane protein complexes of *Neisseria meningitidis*. Res. Microbiol. **157**:136-142.

120. **Sánchez, S., Abel, A., Marzoa, J., Gorringe, A., Criado, M. T., and Ferreirós, C. M.** 2009. Characterisation and immune responses to meningococcal recombinant porin complexes incorporated into liposomes. Vaccine **27**:5338-5343.

121. **Sánchez, S., Arenas, J., Abel, A., Criado, M. T., and Ferreirós, C. M.** 2005. Analysis of outer membrane protein complexes and heat-modifiable proteins in *Neisseria* strains using two-dimensional diagonal electrophoresis. J. Proteome. Res. **4**:91-95.

122. **Santos, S., Baruque-Ramos, J., Tanizaki, M. M., Lebrun, I., and Schenkman, R. P.**, 2006. Production of outer membrane vesicles (OMV) in batch cultivation of *Neisseria meningitidis* serogroup B. Braz. J. Microbiol. **37**:488-493.

123. **Saukkonen, K., Leinonen, M., Abdillahi, H., and Poolman, J. T.** 1989. Comparative evaluation of potential components for group B meningococcal vaccine by passive protection in the infant rat and *in vitro* bactericidal assay. Vaccine **7**:325-328.

124. **Sauvage, E., Kerff, F., Terrak, M., Ayala, J. A., and Charlier, P.** 2008. The penicillin-binding proteins: structure and role in peptidoglycan biosynthesis. FEMS Microbiol. Rev. **32**:234-258.

125. **Scheurwater, E. M. and Clarke, A. J.** 2008. The C-terminal domain of *Escherichia coli* YfhD functions as a lytic transglycosylase. J. Biol. Chem. **283**:8363-8373.

126. **Serruto, D. and Galeotti, C. L.** 2004. The signal peptide sequence of a lytic transglycosylase of *Neisseria meningitidis* is involved in regulation of gene expression. Microbiology **150**:1427-1437.

127. **Serruto, D., Spadafina, T., Ciucchi, L., Lewis, L. A., Ram, S., Tontini, M., Santini, L., Biolchi, A., Seib, K. L., Giuliani, M. M., Donnelly, J. J., Berti, F., Savino, S., Scarselli, M., Costantino, P. Kroll, J. S., O'Dwyer, C., Qiu, J., Plaut, A. G., Moxon, R., Rappuoli, R., Pizza, M., and Aricò, B.** 2010. *Neisseria meningitidis* GNA2132, a heparin-binding protein that induces protective immunity in humans. Proc. Natl. Acad. Sci. U. S. A **107**(8): 3770–3775

128. **Shapiro, S. S., and Wilk, M. B.** 1965. An analysis of variance test for normality (complete samples). Biometrika **52**:591-611.

129. **Shoberg, R. J., and Thomas, D. D.** 1993. Specific adherence of *Borrelia burgdorferi* extracellular vesicles to human endothelial cells in culture. Infect. Immun. **61**:3892-3900.

130. **Snape, M. D., Dawson, T., Oster, P., Evans, A., John, T. M., Ohene-Kena, B., Findlow, J., Yu, L. M., Borrow, R., Ypma, E., Toneatto, D., and Pollard, A. J.** 2010. Immunogenicity of two investigational serogroup B meningococcal vaccines in the first year of life: a randomized comparative trial. Pediatr. Infect. Dis. J. **29**:e71-e79.

131. **Snedecor, G. and Cochran, W.** 1989. Statistical Methods. 8th Ed. pg.223-224. Iowa State University Press.

132. **Steeghs, L., Berns, M., ten Hove, J., de Jong, A., Roholl, P., van Alphen, L., Tommassen, J. and van der Ley, P.** 2002. Expression of foreign LpxA acyltransferases in *Neisseria meningitidis*

results in modified lipid A with reduced toxicity and retained adjuvant activity. Cell Microbiol. **4**:599-611.

133. **Steeghs, L., den Hartog, R., den Boer, A., Zomer, B., Roholl, P. and P. van der Ley**. 1998. Meningitis bacterium is viable without endotoxin [letter]. Nature **392**:449-450.

134. **Stefanova, M. E., Tomberg, J., Olesky, M., Höltje, J. V., Gutheil, W. G., and Nicholas, R. A.** 2003. *Neisseria gonorrhoeae* penicillin-binding protein 3 exhibits exceptionally high carboxypeptidase and beta-lactam binding activities. Biochemistry **42**:14614-14625.

135. **Stephens, D. S.** 2009. Biology and pathogenesis of the evolutionarily successful, obligate human bacterium *Neisseria meningitidis*. Vaccine **27 Suppl 2**:B71-B77.

136. **Stephens, D. S.** 1999. Uncloaking the meningococcus: dynamics of carriage and disease. Lancet **353**:941-942.

137. **Stephens, D. S., Greenwood, B., and Brandtzaeg, P.** 2007. Epidemic meningitis, meningococcaemia, and *Neisseria meningitidis*. Lancet **369**:2196-2210.

138. **Stojiljkovic, I. and Srinivasan, N.** 1997. *Neisseria meningitidis* tonB, exbB, and exbD genes: Ton-dependent utilization of protein-bound iron in *Neisseriae*. J Bacteriol. **179**:805-812.

139. **Sturgis, J. N.** 2001. Organisation and evolution of the *tol-pal* gene cluster. J. Mol. Microbiol. Biotechnol. **3**:113-122.

140. **Swanson, J.** 1978. Studies on gonococcus infection. XII. Colony color and opacity variants of Gonococci. Infect. Immun. **19**:320-331.

141. **Tappero, J. W., Lagos, R., Ballesteros, A. M., Plikaytis, B., Williams, D., Dykes, J., Gheesling, L. L., Carlone, G. M., Høiby, E. A., Holst, J., Nøkleby, H., Rosenqvist, E., Sierra, G., Campa, C., Sotolongo, F., Vega, J., Garcia, J., Herrera, P., Poolman, J. T., and Perkins, B. A.** 1999. Immunogenicity of 2 serogroup B outer-membrane protein meningococcal vaccines: a randomized controlled trial in Chile. JAMA **281**:1520-1527.

142. **Tiwana, H., Clow, K. J., Hall, C., Feavers, I. M., and Charalambous, B. M.** 2005. The immunogenicity of a conformationally restricted peptide mimetic of meningococcal lipooligosaccharide. Scand. J Immunol. **62**:385-392.

143. **Troncoso, G., Sánchez, S., Kolberg, J., Rosenqvist, E., Veiga, M., Ferreirós, C. M., and Criado, M.** 2001. Analysis of the expression of the putatively virulence-associated neisserial protein RmpM (class 4) in commensal *Neisseria* and *Moraxella catarrhalis* strains. FEMS Microbiol. Lett. **199**:171-176.

144. **Tsai, C.M., Frasch, C. E., and Mocca, L. F.** 1981. Five structural classes of major outer membrane proteins in *Neisseria meningitidis*. J. Bacteriol. **146**:69-78.

145. **Tsolakos, N., Lie, K., Bolstad, K., Maslen, S., Kristiansen, P. A., Høiby, E. A., Wallington, A., Vipond, C., Skehel, M., Tang, C. M., Feavers, I. M., Wedege, E., and Wheeler, J. X.** 2010. Characterization of meningococcal serogroup B outer membrane vesicle vaccines from strain 44/76 after growth in different media. Vaccine **28**:3211-3218.

146. **Tzeng, Y. L., Ambrose, K. D., Zughaier, S., Zhou, X., Miller, Y. K. Shafer, W. M. and Stephens, D. S.** 2005. Cationic antimicrobial peptide resistance in *Neisseria meningitidis*. J. Bacteriol. **187**:5387-5396.

147. **Uria, M. J., Zhang, Q., Li, Y., Chan, A., Exley, R. M., Gollan, B., Chan, H., Feavers, I., Yarwood, A., Abad, R., Borrow, R., Fleck, R. A., Mulloy, B., Vazquez, J. A., and Tang, C. M.** 2008. A generic mechanism in *Neisseria meningitidis* for enhanced resistance against bactericidal antibodies. J. Exp. Med. **205**:1423-1434.

148. **Vaara, M.** 1992. Agents that increase the permeability of the outer membrane. Microbiol. Rev. **56**:395-411.

149. **Valentine, C. H., Hellman, J., Beasley-Topliffe, L. K., Bagchi, A., and Warren, H. S.** 2006. Passive immunization to outer membrane proteins MLP and Pal does not protect mice from sepsis. Mol. Med. **12**:252-258.

150. **van de Waterbeemd, B., Streefland, M., van der Ley, P., Zomer, B., van Dijken, H., Martens, D., Wijffels, R. and van der Pol, L.** 2010. Improved OMV vaccine against *Neisseria meningitidis* using genetically engineered strains and a detergent-free purification process. Vaccine **28**:4810-4816.

151. **van den Dobbelsteen, G., van Dijken, H., Hamstra, H. J., Ummels, R., van Alphen, L., and van der Ley, P.** 2004. From HexaMen to NonaMen: expanding a multivalent PorA-based meningococcal outer membrane vesicle vaccine. Abstr. p. 153. 14th Int. Pathog. *Neisseria* Conf. Milwaukee, WI.

152. **van der Ende, A., Hopman, C. T., Zaat, S., Essink, B. B., Berkhout, B., and Dankert, J.** 1995. Variable expression of class 1 outer membrane protein in *Neisseria meningitidis* is caused by variation in the spacing between the -10 and - 35 regions of the promoter. J. Bacteriol. **177**:2475-2480.

153. **van der Ley, P., van der Biezen, J., and Poolman, J. T.** 1995. Construction of *Neisseria meningitidis* strains carrying multiple chromosomal copies of the *porA* gene for use in the production of a multivalent outer membrane vesicle vaccine. Vaccine **13**:401-407.

154. **van der Ley, P., Steeghs, L., Hamstra, H. J., ten Hove, J., Zomer, B., and van Alphen, L.** 2001. Modification of lipid A biosynthesis in *Neisseria meningitidis lpxL* mutants: influence on lipopolysaccharide structure, toxicity, and adjuvant activity. Infect. Immun. **69**:5981-5990.

155. **Vermont, C. L., van Dijken, H. H., Kuipers, A. J., van Limpt, C. J., Keijzers, W. C., van der Ende, E. A., de Groot, R., van Alphen, L., and van den Dobbelsteen, G. P.** 2003. Cross-reactivity of antibodies against PorA after vaccination with a meningococcal B outer membrane vesicle vaccine. Infect. Immun. **71**:1650-1655.

156. **Vianney, A., Muller, M. M., Clavel, T., Lazzaroni, J. C., Portalier, R., and Webster, R. E.** 1996. Characterization of the *tol-pal* region of *Escherichia coli* K-12: translational control of *tolR* expression by TolQ and identification of a new open reading frame downstream of *pal* encoding a periplasmic protein. J. Bacteriol. **178**:4031-4038.

157. **Vincent, M., England, L. S., and Trevors, J. T.** 2004. Cytoplasmic membrane polarization in Gram-positive and Gram-negative bacteria grown in the absence and presence of tetracycline. Biochim. Biophys. Acta **1672**:131-134.

158. **Vinés, E. D., Marolda, C. L., Balachandran, A., and Valvano, M. A.** 2005. Defective O-antigen polymerization in *tolA* and *pal* mutants of *Escherichia coli* in response to extracytoplasmic stress. J. Bacteriol. **187**:3359-3368.

159. **Vipond, C., Wheeler, J. X., Jones, C. J., Feavers, I. M., and Suker, J.** 2005. Characterisation of the protein content of a meningococcal outer membrane vesicle vaccine by polyacrylamide gel electrophoresis and mass spectrometry. Human Vaccines **1**:80-84.

160. **Vollmer, W., and Höltje, J. V.** 2004. The architecture of the murein (peptidoglycan) in Gram-negative bacteria: vertical scaffold or horizontal layer(s)? J. Bacteriol. **186**:5978-5987.

161. **Vollmer, W., Joris, B., Charlier, P., and Foster, S.** 2008. Bacterial peptidoglycan (murein) hydrolases. FEMS Microbiol. Rev. **32**:259-286.

162. **Volokhina, E. B., Beckers, F., Tommassen, J., and Bos, M. P.** 2009. The β-barrel outer membrane protein assembly complex of *Neisseria meningitidis*. J. Bacteriol. **191**:7074-7085.

163. **Voulhoux, R., Bos, M. P., Geurtsen, J., Mols, M., and Tommassen, J.** 2003. Role of a highly conserved bacterial protein in outer membrane protein assembly. Science **299**:262-265.

164. **Walburger, A., Lazdunski, C., and Corda, Y.** 2002. The Tol/Pal system function requires an interaction between the C-terminal domain of TolA and the N-terminal domain of TolB. Mol. Microbiol. **44**:695-708.

165. **Walsh, C. T.** 1989. Enzymes in the D-alanine branch of bacterial cell wall peptidoglycan assembly. J. Biol. Chem. **264**:2393-2396.

166. **Webster, R. E.** 1991. The *tol* gene products and the import of macromolecules into *Escherichia coli*. Mol. Microbiol. **5**:1005-1011.

167. **Wedege, E., Bolstad, K., Aase, A., Herstad, T. K., McCallum, L., Rosenqvist, E., Oster, P., and Martin, D.** 2007. Functional and specific antibody responses in adult volunteers vaccinated with two different meningococcal serogroup B outer membrane vesicle vaccines in New Zealand. Clin. Vaccine Immunol. **14**(7):830-8

168. **Weigel, L. M., Belisle, J. T., Radolf, J. D., and Norgard, M. V.** 1994. Digoxigenin-ampicillin conjugate for detection of penicillin-binding proteins by chemiluminescence. Antimicrob. Agents Chemother. **38**:330-336.

169. **Wolff, K. and Stern, A.** 1995. Identification and characterization of specific sequences encoding pathogenicity associated proteins in the genome of commensal *Neisseria* species. FEMS Microbiol. Lett. **125**:255-263.

170. **Wowk, B.** 2010. Thermodynamic aspects of vitrification. Cryobiology **60**:11-22.

171. **Yakubu, D. E., Abadi, F. J., and Pennington, T. H.** 1999. Molecular typing methods for *Neisseria meningitidis*. J. Med. Microbiol. **48**:1055-1064.

172. **Yocum, R. R., Waxman, D. J., Rasmussen, J. R., and Strominger, J. L.** 1979. Mechanism of penicillin action: penicillin and substrate bind covalently to the same active site serine in two bacterial D-alanine carboxypeptidases. Proc. Natl. Acad. Sci. U. S. A **76**:2730-2734.

173. **Zabell, S. L.** 2008. On Student's 1908 article "The probable error of a mean". J. Amer. Statistical Assoc. **103**. (481) 8-11.

174. **Zarantonelli, M. L., Carlier, J. P., Alonso, J. M., and Taha, M. K.** 2003. Insertional inactivation of the *lpxA* gene involved in the biosynthesis of lipid A in *Neisseria meningitidis* resulted in *lpxA/lpxA::aph-3'* heterodiploids. FEMS Microbiol. Lett. **226**:51-56.

175. **Zhou, L., Srisatjaluk, R., Justus, D. E., and Doyle, R. J.** 1998. On the origin of membrane vesicles in Gram-negative bacteria. FEMS Microbiol. Lett. **163**:223-228.

176. **Zollinger, W. D., Donets, M. A., Schmiel, D. H., Pinto, V. B., Labrie, J. E., Moran, E. E., Brandt, B. L., Ionin, B., Marques, R., Wu, M., Chen, P., Stoddard, M. B., and Keiser, P. B.** 2010. Design and evaluation in mice of a broadly protective meningococcal group B native outer membrane vesicle vaccine. Vaccine **28**:5057-5067.